Development of New Transition Metal-Catalyzed Carbon–Fluorine, Carbon–Nitrogen, and Carbon–Carbon Bond Forming Processes

By

Yuxuan Ye

B.Sc. Chemistry
Peking University, 2013

Submitted to the Department of Chemistry in Partial Fulfillment of the Requirement for the Degree of

DOCTOR OF PHILOSOPHY IN ORGANIC CHEMISTRY

at the
Massachusetts Institute of Technology

June 2018

Signature of Author: Signature redacted
Department of Chemistry
May 11, 2018

Certified by: Signature redacted
Stephen L. Buchwald
Camille Dreyfus Professor of Chemistry
Thesis Supervisor

Accepted by: Signature redacted
Robert W. Field
Harslam and Dewey Professor of Chemistry
Chairman, Departmental Committee for Graduate Students

This doctoral thesis has been examined by a committee of the Department of Chemistry as follows:

Signature redacted

Professor Timothy F. Jamison:_____
Thesis Committee Chair

Signature redacted

Professor Stephen L. Buchwald:_____
Thesis Supervisor

Signature redacted

Professor Jeremiah A. Johnson:_____
Thesis Committee

Development of New Transition Metal-Catalyzed Carbon–Fluorine, Carbon–Nitrogen, and Carbon–Carbon Bond Forming Processes

by

Yuxuan Ye

Submitted to the department of Chemistry on May 11, 2018
In Partial Fulfillment of the Requirements for the Degree of Doctor of Philosophy
at the Massachusetts Institute of Technology

ABSTRACT

Chapter 1. Palladium-Catalyzed Fluorination of Cyclic Vinyl Triflates: Dramatic Effect of $TESCF_3$ as an Additive

A method for the synthesis of cyclic vinyl fluorides with high levels of regiochemical fidelity has been achieved by Pd-catalysis employing a new biarylphosphine ligand and $TESCF_3$ as a crucial additive. Five, six, and seven-membered vinyl triflate substrates, as well as a few acyclic substrates undergo the transformation successfully. The intriguing "$TESCF_3$ effect" provided a new tool for addressing the problem of the formation of regioisomers in Pd-catalyzed fluorination reactions.

Chapter 2. Mechanistic Studies on Pd-Catalyzed Fluorination of Cyclic Vinyl Triflates: Evidence for *in situ* Ligand Modification by $TESC_3$ as an additive.

A detailed mechanistic hypothesis for the Pd-catalyzed fluorination of cyclic vinyl triflates, and the unusual effect of $TESCF_3$ as an additive has been developed by combined experimental and computational studies. The preference of conducting β-hydrogen elimination rather than reductive elimination from the *trans*-LPd(vinyl)F complex, which is generated predominantly due to the *trans*-effect, caused the poor regioselectivity of the fluorination reaction under $TESCF_3$-free conditions. An *in situ* ligand modification by trifluoromethyl anion, leading to the generation of the *cis*-LPd(vinyl)F complex which prefers reductive elimination rather than β-hydrogen elimination, is proposed to be responsible for the improved regioselectivity of the fluorination reaction when $TESCF_3$ was used as an additive.

Chapter 3. CuH-Catalyzed Enantioselective Alkylation of Indoles with Ligand-Controlled Regiodivergence

A method for the enantioselective synthesis of either N1- and C3-chiral indoles by CuH-catalysis, depending on the choice of ligand, was developed. In contrast to conventional indole functionalization in which indoles are used as nucleophiles, hydroxyindole derivatives are employed as electrophiles in this method. DFT calculations indicated that the extent to which the Cu–P bonds of the alkylcopper intermediate distort, determines the regioselectivity of the reaction.

Thesis Supervisor: Stephen L. Buchwald
Title: Camille Dreyfus Professor of Chemistry

ACKNOWLEDGEMENT

It is not until I started writing my thesis that I realized that how fast my time at MIT has passed. As I looked back at the past five years in graduate school, I realized that this has been the most important time in my life. There have been many ups and downs during this incredible journey, and it is the choices that I made at each of those turning points that define who I am today.

First of all, I would like to thank my research advisor, Professor Stephen L. Buchwald, for his help, support, and guidance, in both chemistry and life. I was very fortunate to be accepted by MIT and able to join Steve's lab. I still remember the freezing winter morning, 18th January 2013, when I received an email from Steve asking for a phone call interview, and it was when my life changed. When I started writing the acknowledgement, I found it really difficult to express my gratitude to Steve with my poor English writing. Steve guided me by words and deeds. Steve said many words of wisdom during my stay in the lab. The one impressed me most was when he talked about the key to his success in a group meeting. He said when you get a lot of results, it is the ability to find the right direction to go that makes the difference. "Direction is more important than distance", it is not only true in scientific research, but in life as well. I will never forget the moment when he corrected us to use the term "Pd-catalyzed C–N coupling", instead of "Buchwald coupling". People fight for credits in academia, while he set a good example of what is a true scientist. Many years later, I might forget all the chemistry that he taught me, but his "obsession" with reaction reproducibility, his strict requirements for the supporting information of papers, and the freedom alone with the guidance he provided for me to explore the areas that I was interested in, will always be remembered. If I were able to achieve any accomplishments in academia in the future, it is largely due to the influence of his scientific philosophy on me and I am forever grateful.

Alone with Steve I would like to thank my thesis committee chair, Professor Timothy F. Jamison. Trough our annual meetings and informal conversations, Tim offered valuable advice and guidance for my research, and more importantly my career development. I would like to thank other committee members who have helped me during my time here. The advanced organic chemistry (5.43) taught by Professor Jeremiah A. Johnson was one of the most informative and well-organized courses that I had at MIT and I have benefited a lot from it. Professor Jeffrey Van Humbeck provided valuable scientific insights and was very helpful during my candidacy and proposal exams. I would also like to thank Professor Rick L. Danheiser, Professor Mohammad Movassaghi, and Professor Timothy M. Swager for their care and support.

I would like to convey my gratitude to my undergraduate advisor, Professor Jianbo Wang at Peking University. He enlightened me with the beauty of organic chemistry and encouraged me to pursue a career in this field. I am grateful for Professor Neil K. Garg at UCLA. His passion in Chemistry greatly inspired me, and the two-month summer research in his lab set the foundation for my further study abroad. Without the help of my previous advisors, I would not have the opportunity to come to MIT.

During my time in Steve's group, I have had the privilege to work with the most brilliant chemists all over the world. I would like to thank Christine Nguyen first for her support and help during the past few years. The day I arrived in Boston five years ago, Yang Yang took me to Zoe's Chinese restaurant for my first dinner. He has always been a friend full of valuable advice. He is one of the most knowledgeable people that I know and a model for me in academic research. Rong Zhu helped me a lot through the years and he is one of the cleverest people that I have interacted with. Shaolin Zhu was like a big brother to me when I first started in the lab. He helped me set up my Schlenk line, change my pump oil, and provided me with glassware to start with. When I went back to Nanjing two years ago, he showed me around his new laboratory. I was so impressed by his enthusiasm in developing new chemistry and I knew he would be successful. I would like to thank the fluorination team in my early days in the lab. Hong Geun Lee taught me the fluorination experimental techniques. Phil Milner shared with me his rich experience in ligand synthesis. The discussions with Aaron Sather, Joey Dennis and Bryan Ingoglia were always helpful and inspiring. I always feel lucky to be able to work next to Shiliang Shi. He had extremely good judgment on the importance of research results and I learned a great deal from him. Wenliang Huang joined the group a couple of months later than I did. All the adventures that we had together in the life outside the lab should remain as the deepest secrets forever. Special thanks to Michael Pirnot and Yiming Wang who spent considerable time proofreading the manuscript of the vinyl fluorination project. They were the most excellent proofreaders and I benefitted a lot from them. I would like to collectively thank Ye Zhu, Alex Spokoyny, Mingjuan Su, Wei Shu, Wai-Lung Ng, Bram Karsten, Nathan Jui, Nathan Park, Johannes Ernst, Yifeng Chen, Mao Chen, Katya Vinogradova, Dawen Niu, Nootaree Niljianskul, Thierry Leon Serrano, Jim Colombe, Nick Bruno, Vasudev Rhonde, Erhad Ascic, Pedro Luis Arrechea, Gen Li, Sandra King, John Nguyen, Esben Olsen, Stefan Roesner, Paula Ruiz-Castillo, Tim Senter, Zachary Wong, Renee Zhao, Min Woo Bae, Kurt Armbrust, Jeff Bandar, Emma Chant, Daniel Cohen, Ivan Sanda, Stig Friis, Joseph Macor, Mycah Uehling, Haoxuan Wang, Xueqiang Wang, Yang Zhao, Claudia Keller, Hu Zhang, Boyoung Park, Koji

Kubota, Kashif Khan and Nick White. During the time we overlapped, I benefitted a lot from the discussions with them.

It is a great honor to get to know and work with current group members Liela Bayeh, Ivan Buslov, Xijie Dai, Heemal Dhanjee, Oliver Engl, Sheng Guo, Chengxi Li, Zhaohong Lu, Scott Mccann, Klaus Speck, Andy Thomas, Liang Zhang, Spencer Shinabery, Anthony Rajas, Jeff Yang, Saki Ichikawa, Ryan King, Michael Gribble, Richard Liu, Aaron Mallek, Frieda Zhang, Joey Dennis, Bryan Ingoglia, Yujing Zhou, Erica Tsai, Sheng Feng, Azin Saebi, Jessica Xu, Priscilla Liow, Ben Nguyen and Corin Wagen. Sheng Guo, who joined the group in my fourth year, became a true friend of mine. Sheng and Shaolin are both from the Ma's group at SIOC with strong academic standings and contribution spirit, and I think it is a quirk of fate for me to get help from them, respectively, at the beginning and the end of my days here. I would like to thank Richard and Andy for proofreading my thesis in really short time. Special thanks to Yujing. When I had an emergency and was sent to hospital a few days ago, she was there for me and I am forever grateful.

Next, I would like to thank my friends who helped me tremendously over the years. Alex Mijalis (Pentelute group) and I were good friends when we first started at MIT. I still miss the fun nights when we studied together for the problem sets and exams. He once told me that I could only get better if I put myself into the uncomfortable zone. These words encouraged me to pursue a life with new challenges every day. I would like to thank Renze Wang who trained me as his successor as the president of MIT Ventrueships Club. My two-year service in the club was a valuable experience. I was exposed to a variety of MIT startups in different fields. It was extremely informative and rewarding talking to the founders and investors of these companies. Developing a career in academia is very like running a company. You need to raise money, recruit talented employees (graduate students and postdocs), and produce valuable products (scientific discoveries). At the end of the day, it is the usability of the products that determines if the company becomes a family workshop or a leading industry giant. I would like to thank Yiheng Duan who introduced me to the PC game, Overwatch. As I became good at it, I played competitively representing MIT with five other teammates in the Tespa Intercollegiate Tournament. The match we played again Emerson College was broadcast live on Twitch with thousands of viewers. Although we lost the game at the end, it is one of the most exciting moments in my life. I really want to thank Ming Yi, Tianyu Zhu (Van Voorhis group), Peng Dai (Pentelute group) and Xian Li (Nelson Group). I cannot imagine how hard it would be for me to make it through my graduate school without their support and encouragement.

I would like to save the most important acknowledgement at the end, for my parents. I could not accomplish anything without their care, support, love, and everything. My love for them is beyond words and I will always be indebted to them.

PREFACE

Parts of this thesis have been adapted from the following articles co-written by the author.

1. **Ye, Y.**; Takada, T.; Buchwald, L. S. "Palladium-Catalyzed Fluorination of Cyclic Vinyl Triflates: Effect of $TESCF_3$ as an Additive." *Angew. Chem. Int. Ed.* **2016**, *55*, 15559-15563.

2. **Ye, Y.**; Kim, S.-T.; King, R.; Baik, M.-H.; Buchwald, S. L. "Mechanistic Studies on Pd-Catalyzed Fluorination of Cyclic Vinyl Triflates: Evidence for *in situ* Ligand Modification by $TESCF_3$ as an Additive." *Manuscript in preparation.*

3. **Ye, Y.**; Kim, S.-T.; Jeong, J.; Baik, M.-H.; Buchwald, S. L. "CuH-Catalyzed Enantioselective Alkylation of Indoles with Ligand-Controlled Regiodivergence." *Manuscript in preparation.*

RESPECTIVE CONTRIBUTIONS

This thesis is the result of collaborative effort of the author and other colleagues at MIT. The specific contributions of the author are detailed below.

The author preformed all the experimental work described in Chapter 1.

The experimental work described in Chapter 2 was a collaborative effort between Ryan King and the author. The computational studies were conducted by Seoung-Tae and Prof. Mu-Hyun Baik of Korea Advanced Institute of Science and Technology (KAIST).

The author preformed all the experimental work described in Chapter 3. Seoung-Tae, Jinhoon Jeong, and Prof. Mu-Hyun Baik of Korea Advanced Institute of Science and Technology (KAIST) performed computational investigations.

TABLE OF CONTENTS

Chapter 1. Palladium-Catalyzed Fluorination of Cyclic Vinyl Triflates: Dramatic Effect of $TESCF_3$ as an Additive

1.1 Introduction.....12
1.2 Results and Discussion.....13
1.3 Conclusion.....20
1.4 Experimental.....20
1.5 Reference and Notes.....37
1.6 Spectra.....40

Chapter 2. Mechanistic Studies on Pd-Catalyzed Fluorination of Cyclic Vinyl Triflates: Evidence for *in situ* Ligand Modification by $TESCF_3$ as an Additive

2.1 Introduction.....93
2.2 Results and Discussion.....94
2.3 Conclusion.....112
2.4 Experimental.....112
2.5 Reference and Notes.....116

Chapter 3. CuH-Catalyzed Enantioselective Alkylation of Indoles with Ligand-Controlled Regiodivergence

3.1 Introduction.....121
3.2 Results and Discussion.....123
3.3 Conclusion.....135
3.4 Experimental.....136
3.5 Reference and Notes.....160
3.6 Spectra.....162

Chapter 1
Palladium-Catalyzed Fluorination of Cyclic Vinyl Triflates: Dramatic Effect of $TESCF_3$ as an Additive

1.1 Introduction

Fluorine-substituted olefins constitute a valuable class of compounds of interest for medicinal chemistry and chemical biology (Scheme 1).[1,2] The alkenyl fluoride group resembles an amide linkage in terms of both steric demand and charge distribution,[3] but fluoroalkenes exhibit substantially enhanced stability towards hydrolysis compared to amides. Moreover, in contrast to amides, which often exist as equilibrating s-*cis* and s-*trans* rotamers, fluoroalkenes are configurationally stable. As a result, they have been investigated as amide bioisosteres with improved lipophilicity and metabolic stability in pharmaceutical applications and as tools for probing the conformational properties of biologically active amides.[4]

Scheme 1. Representative fluoroalkenes as peptidomimetics.

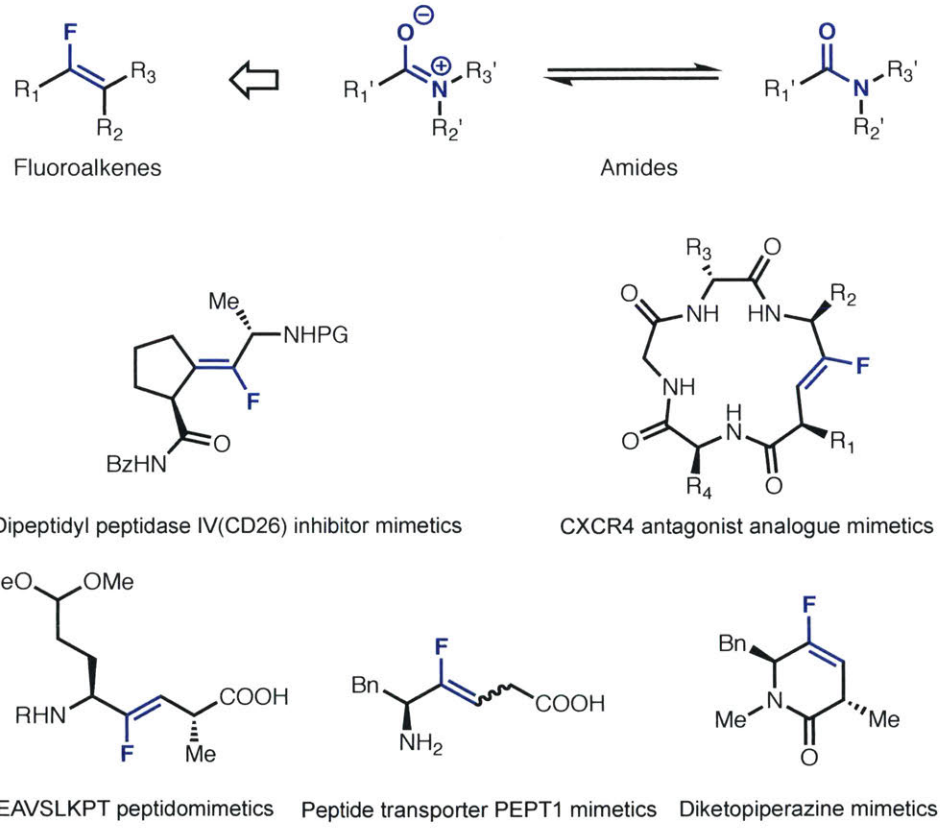

In addition to these applications, fluoroalkenes also serve as versatile starting materials for a variety of transformations, including the Diels–Alder reaction,[5a] cyclopropanation,[5b,c] and epoxidation,[5d] allowing for the construction of other classes of fluorine-containing molecules. Despite considerable potential, fluoroalkenes are underutilized due to challenges in their synthesis. Current approaches for their preparation generally require multistep functional group manipulations or the use of harsh reaction conditions, which limit the functional group

compatibility of these techniques.[6–11] The development of a mild and general method for fluoroalkene synthesis would therefore be highly desirable. Due to the challenge of preparing suitable precursors, cyclic fluoroalkenes are particularly difficult to access using existing methods, and new methods that provide access to these compounds would be especially useful.

1.2 Results and Discussion

We commenced our study using 4-phenylcyclohexenyl triflate (**1a**) as the model substrate (Table 1). Preliminary ligand evaluation showed that catalysts based on *t*-BuBrettPhos (**L1**), AdBrettPhos (**L2**), HGPhos (**L3**), or AlPhos (**L4**), which were effective ligands for the fluorination of aryl eletrophiles,[12a–c] provided low yields of the desired vinyl fluoride **2a** and a substantial amount of the undesired regioisomer **3a** (close to 1:1 ratio, entry 1–4). Replacing the 6-methoxyl group of the ligand with a methyl substituent (**L5** and **L6**) led to improved yields, indicating that ligand rigidity may be important in this transformation (entries 5, 6).[13] After further evaluation of ligands possessing a trimethylmethoxy-substituted top ring (**L7** and **L8**),[14] a novel biarylphosphine ligand **L8** was found to provide **2a** in moderate combined yield (58 %) though still with poor regioselectivity (1.8 :1; entries 7, 8).

During our investigation of the palladium-catalyzed trifluoromethylation of vinyl sulfonates,[15b] we made the serendipitous discovery that the corresponding vinyl fluoride was formed as a side product with relatively high regioselectivity (6.3:1, Scheme 2). We hypothesized that the presence of trifluoromethylsilanes, which were used as CF_3^- sources in trifluoromethylation reactions, might be responsible for the improved regioselectivity of the fluorination process. Indeed, the use of $TMSCF_3$, $TESCF_3$ or $TIPSCF_3$ as substoichiometric additives (30 mol%) drastically improved the regioselectivity (34:1, 73:1, and 4.7:1, respectively) (Table 1, entry 9–11). Although catalyst based on **L6** and **L8** gave comparable results in the absence of the trifluoromethyl silane additive, the yield and regioselectivity obtained with **L8** were considerably higher when $TESCF_3$ (30 mol%) was added (entries 6, 8, 10 and 12). Finally, performing the reaction in 2-MeTHF at 90 °C with **L8** as the supporting ligand, along with a substoichiometric amount of $TESCF_3$ afforded the desired product **2a** in 74% yield with excellent regioselectivity (>99:1) (entry 13). In addition to this significant improvement in regioselectivity, the addition of the $TESCF_3$ additive also allowed the reaction to be conducted at a lower temperature (entry 13 vs. entry 14).

Table 1. Reaction optimization studies.

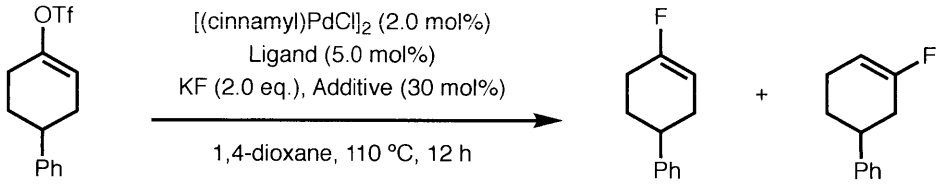

1a **2a** **3a**

Entry	Ligand	Additive	**2a** (%)	**3a** (%)	**2a/3a**
1	**L1**	–	23	21	1.1:1
2	**L2**	–	18	18	1.0:1
3	**L3**	–	11	13	0.8:1
4	**L4**	–	19	19	1.0:1
5	**L5**	–	27	20	1.4:1
6	**L6**	–	37	19	1.9:1
7	**L7**	–	23	20	1.2:1
8	**L8**	–	37	21	1.8:1
9	**L8**	$TMSCF_3$	68	2	34:1
10	**L8**	$TESCF_3$	73	1.0	73:1
11	**L8**	$TIPSCF_3$	47	10	4.7:1
12	**L6**	$TESCF_3$	57	5.0	11:1
13[b]	**L8**	$TESCF_3$	74	0.4	> 99:1
14[b]	**L8**		7	4.0	1.8:1

[a]Reactions were run at 0.1 mmol scale. Yields were determined by ^{19}F NMR analysis of the crude reaction mixture using 1-fluoronaphthanlene as an internal standard. [b]2-MeTHF, 90 °C.

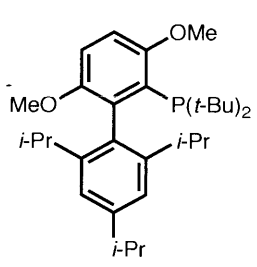

L1 (*t*-BuBrettPhos)

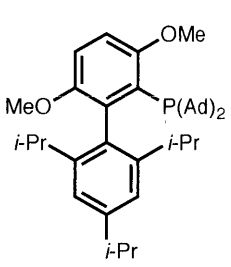

L2 (AdBrettPhos)

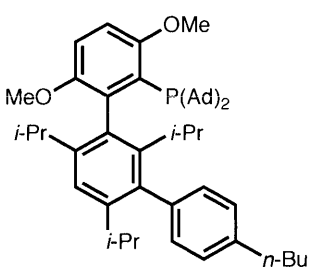

L3 (HGPhos)

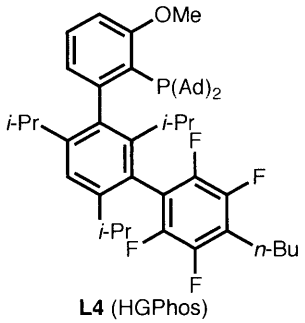

L4 (HGPhos)

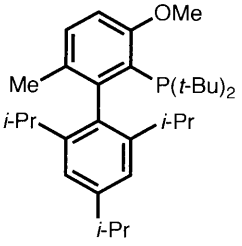

L5

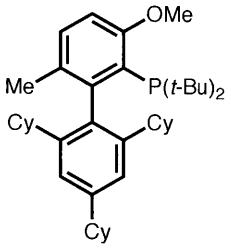

L6

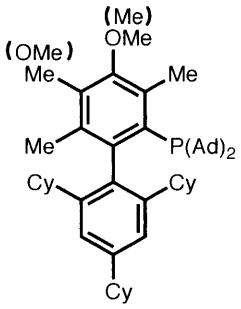

L7

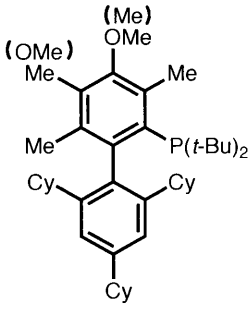

L8

Scheme 2. Fluorinated side products generated in the palladium-catalyzed trifluoromethylation reaction.

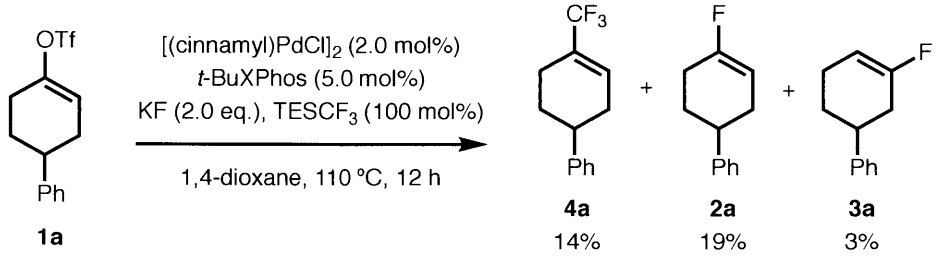

1a

4a 14%

2a 19%

3a 3%

We subsequently examined the substrate scope using these optimized reaction conditions, and found this protocol to be applicable to the fluorination of a variety of 1,2-disubstituted cyclic vinyl triflates (Table 2). In addition, the fluorination of 1,2,2-trisubstituted vinyl triflates, for which regioisomer formation is not an issue,[12d] was possible with **L3** as the ligand and CsF as the fluoride source. $TESCF_3$ was not required for these processes. Interestingly, our new ligand (**L8**) developed for vinyl triflate **1a**, did not perform well for 1,2,2-trisubstituted vinyl triflates, which likely stems from its sterically encumbered nature.

1-Cyclohexenyl triflates with substituents at the 4-(**2a** and **2c**), 3-(**2e**) or 2-(**2b**) position were all excellent substrates (Table 2, n = 1). Benzofused (**2f**) and oxygen-containing six-membered cyclic triflates (**2g**) were compatible as well. Moreover, the method could be used to access fluorinated analogues of biologically active terpene and steroid derivatives (**2h**, **2i** and **2j**).

In the case of **1j**, isomerization of the terminal double bond to the more thermodynamically stable internal position occurs under these reaction conditions.

In general, the fluorination of 1-cyclopentenyl triflates was more difficult, presumably due to the higher energy barrier for C–F reductive elimination from the respective palladium(II) complex (Table 2, $n = 0$).[16] Thus, vinyl triflate **1k** without additional substitution on the double bond provided the desired cyclopentenyl fluoride in low yield. However, substrates possessing an additional substituent at the 2-position reacted efficiently to provide the corresponding cyclic vinyl fluorides in good to excellent yields (**2l**, **2m** and **2n**).

Although 1-cycloheptenyl triflate **1o** was fully consumed under these conditions, the fluorinated product was not obtained (Table 2, $n = 2$). GC/MS analysis of the crude reaction mixture indicated the formation of the corresponding alkyne or allene product, implying that the vinyl triflate starting material decomposed through β-hydrogen elimination. Consistent with this hypothesis, seven-membered cyclic vinyl triflates without β-hydrogen atoms were fluorinated in good yields (**2p**, **2q** and **2r**).

A variety of functional groups were tolerated in this transformation, including an acetal (**2d**), a nitrile (**2l**), a trifluoromethyl group (**2m**), an amide (**2n**) and a nitro group (**2r**). Heterocycles, including an indole (**2e**), a pyrimidine (**2q**) and a pyridine (**2p**) were also compatible.

The fluorination of acyclic 1-substituted vinyl triflates **1s** was unsuccessful, presumably as a result of competitive β-hydrogen elimination. More highly substituted vinyl triflates without β-alkenyl hydrogen atoms were successfully fluorinated (**1t** and **1u**).

The formation of side-products is an important factor affecting the synthetic utility of a fluorination reaction due to the challenges often encountered during the separation of fluorinated products from side-products with similar physical properties. Thus, careful analysis of the crude reaction mixture in this fluorination protocol was performed. Generally speaking, the corresponding reduction product was formed in less than 0.5% in all cases while the corresponding vinyl chloride was formed in 2.5%-0.5%. Although the entries in Table 2 could all be purified to >99.5% purity by column chromatography, conditions that would avoid the formation of the vinyl chloride side product would significantly simplify purification of the desired vinyl fluoride.

Table 2. Palladium-catalyzed fluorination of cyclic vinyl triflates.

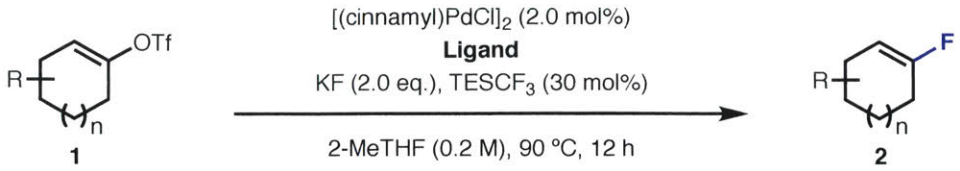

n = 1

2a
71%, **L8**

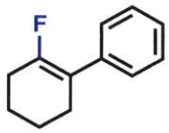

2b[b]
86%, **L8**

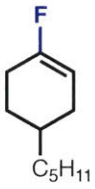

2c
74%, **L8**

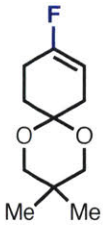

2d
76%, **L8**

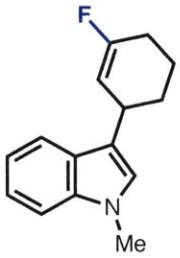

2e
72%, **L8**

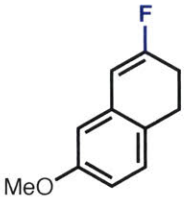

2f
73%, **L8**

2g[b,f]
72%, **L3**

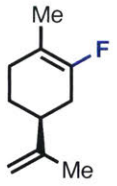

2h[b]
69%, **L1**

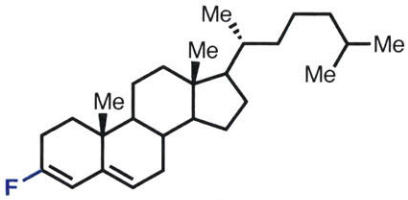

2i[f]
84%, **L8**

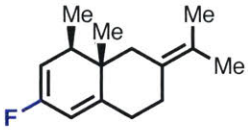

2j[d,f]
41%, **L8**

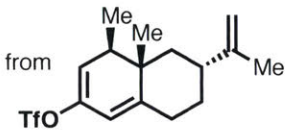

1j

n = 0

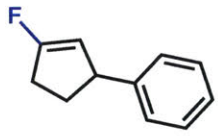

2k[g]
16%, **L8**

2l[b]
88%, **L3**

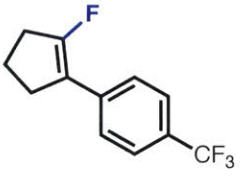

2m[b]
93%, **L3**

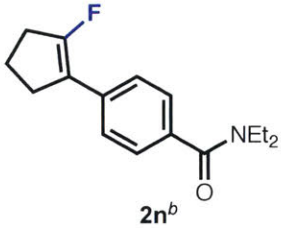

2n[b]
81%, **L3**

n = 2

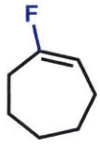

2o
0%, **L8**

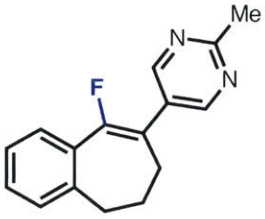

2p[b,e,f]
85%, **L3**

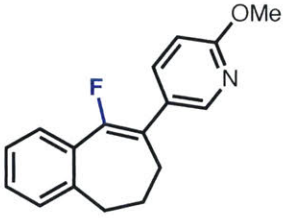

2q[b,e,f]
78%, **L3**

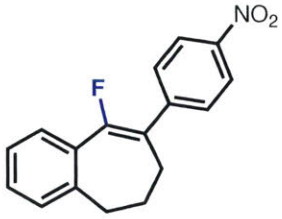

2r[b,e,f]
75%, **L3**

[a]Isolated yields are reported as an average of two runs on 1.0 mmol scale. [b]Reaction conditions: [(cinnamyl)PdCl]$_2$ (2.0 mol%), ligand (5.0 mol%), CsF (2.0 equiv), 2-MeTHF, 90 °C, 12 h. [c]*t*-BuBrettPhos as the ligand. [d]In 1,4-dioxane. [e]In toluene. [f]110 °C. [g]130 °C.

Table 3. Palladium-catalyzed fluorination of acyclic vinyl triflates.

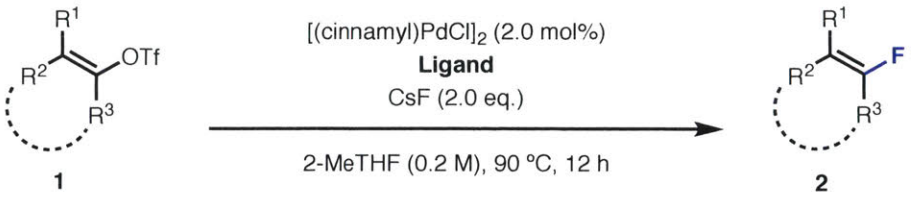

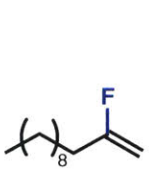

2s
0%, **L3**

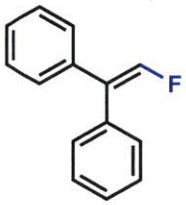

2t
72%, **L1**

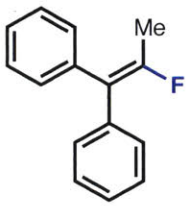

2u[b]
79%, **L3**

[a]Isolated yields are reported as an average of two runs on 1.0 mmol scale. [b]110 °C.

Towards this goal, the use of precatalysts of the form [(1,5-cyclooctadiene)(LPd)$_2$] that activate with minimal generation of reactive or other undesired byproducts were investigated. In the case of vinyl triflates for which regioisomer formation is not a concern, the use of the **L3**-derived precatalysts of this type in place of **L3**/[(cinnamyl)PdCl]$_2$ was found to provide comparable or superior yields without formation of vinyl chloride (Table 4, **2m** and **2p**). However, because of the large size of **L8**, the corresponding precatalysts based on **L8** could not be prepared. Therefore, for fluorination reactions employing **L8**, a modified reaction protocol employing a "sacrificial" vinyl triflate was developed. We found that preheating the reaction mixture with cyclohexenyl triflate (**2v**) (50 mol%) as the "sacrificial" vinyl triflate for one hour prior to the addition of the vinyl triflate starting material led to improved yields (Table 4, **2a**, **2f**, **2i**). The volatile fluorination and chlorination products derived from **2v** could be easily removed *in vacuo*. Using this protocol, the corresponding vinyl chloride coming from the vinyl triflate starting material was not detected by GC analysis of the crude reaction mixtures. Moreover, yields obtained using this protocol were generally higher than those obtained previously.

Table 4. Modified fluorination reaction protocol without the generation of chlorination side products.

Ligand = HGPhos

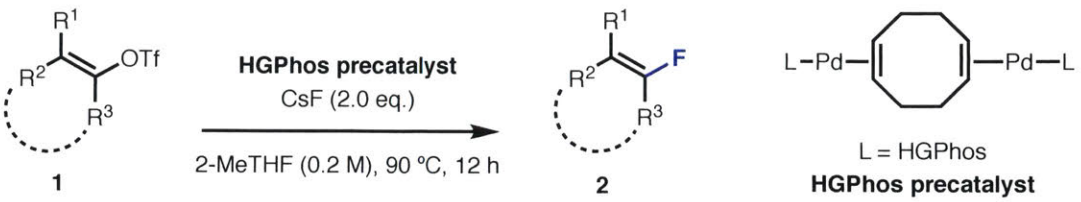

2m
92% (93%)[d]

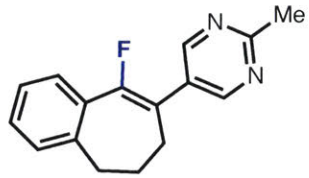

2p[b,c]
95% (85%)[d]

Ligand = L8

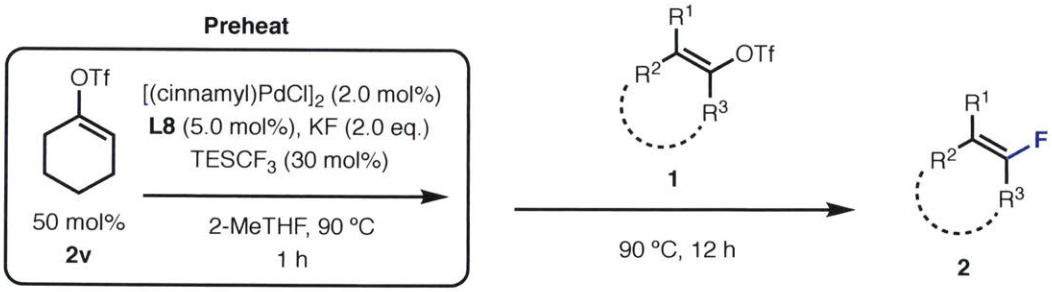

2a
85% (71%)[d]

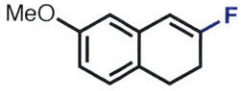

2f
79% (73%)[d]

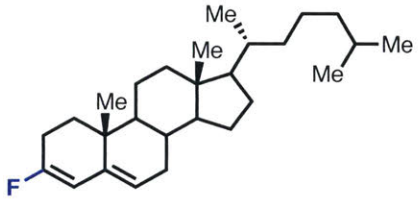

2i
88% (84%)[c,d]

[a]Isolated yields are reported as an average of two runs on 1.0 mmol scale. [b]In toluene. [c]110 °C. [d]Yield when conducted under previous reaction conditions.

1.3 Conclusion

In summary, we have developed a method for palladium-catalyzed fluorination of vinyl triflates for the synthesis of cyclic fluoroalkenes. High levels of regiochemical fidelity of this reaction were achieved by employing a new biarylphosphine ligand **L8** and $TESCF_3$ as a crucial additive. The reaction exhibited good functional group tolerance and proceeded efficiently for five, six and seven-membered vinyl triflate substrates, as well as a few acyclic substrates. As the synthesis of cyclic vinyl fluorides using existing methods is problematic due to the lack of availability of starting materials and limited functional group compatibility of the existing methods, our palladium-based protocol is complementary to these previously developed processes.[7m,7n,7o] The intriguing "$TESCF_3$ effect" has provided us with a new tool for addressing the problem of the formation of regioisomers in palladium-catalyzed fluorination reactions of vinyl triflates. Studies are undergoing to gain a detailed mechanistic understanding of this phenomenon.

1.4 Experimental

General Reagent Information: 2-Methyltetrahydrofuran (2-MeTHF) and dioxane were purchased from Sigma-Aldrich in Sure-Seal™ bottles and used as received. $CDCl_3$ and THF-d_8 were purchased from Cambridge Isotope Laboratories, Inc. Cesium fluoride (CsF) (99.9%) was purchased from Strem and dried at 180 °C under vacuum for 48 h. The dried CsF was then transferred to a nitrogen-filled glove box where it was thoroughly ground using an oven-dried mortar and pestle. The finely ground CsF was then filtered through a 45 μm stainless-steel sieve (purchased from Cole Parmer) to obtain CsF with particle size of < 45 μm.[17] Potassium fluoride (KF) (99.0%) was purchased from Sigma-Aldrich and dried using the procedure described for CsF. Silver(I) fluoride (AgF) (98%) was purchased from Strem and used as received. The preparations of *t*-BuBrettPhos (**L1**), AdBrettPhos (**L2**), HGPhos (**L3**), AlPhos (**L4**), **L5** and **L6** have been previously described.[18] All other reagents were purchased from commercial sources and used as received.

General Analytical Information: Compounds were analyzed by ^1H, ^{13}C, ^{19}F, and ^{31}P NMR, where appropriate. All ^{19}F NMR yields stated for fluorination reactions are calculated from F NMR spectra relative to an internal standard of 1- fluoronaphthalene (-124 ppm). ^1H, ^{13}C, and ^{19}F

NMR spectra were recorded on a Varian Inova-500 MHz spectrometer, a Bruker Avance-400 MHz spectrometer, and a Varian Mercury-300 MHz spectrometer. ^{1}H and ^{13}C spectra were calibrated using residual solvent as an internal reference ($CDCl_3$: δ 7.26 ppm and δ 77.16 ppm, respectively). ^{19}F NMR spectra were calibrated to an external standard of neat $CFCl_3$ (δ 0.0 ppm). ^{31}P NMR spectra were calibrated to an external standard of H_3PO_4 (δ 0.0 ppm). Elemental analyses were performed by Atlantic Microlabs Inc., Norcross, GA, USA. HRMS was recorded on a Bruker Daltonics APEXIV 4.7. Tesla Fourier transform ion cyclotron resonance mass spectrometer (FT-ICR-MS). The following abbreviations were used to explain multiplicities: s = singlet, bs = broad singlet, d = doublet, t = triplet, pt = pseudotriplet, q = quartet, p = pentet, m = multiplet. Melting points were obtained using a Stanford Research Systems EZ-Melt melting point apparatus.

1.4.1 Synthesis of L7

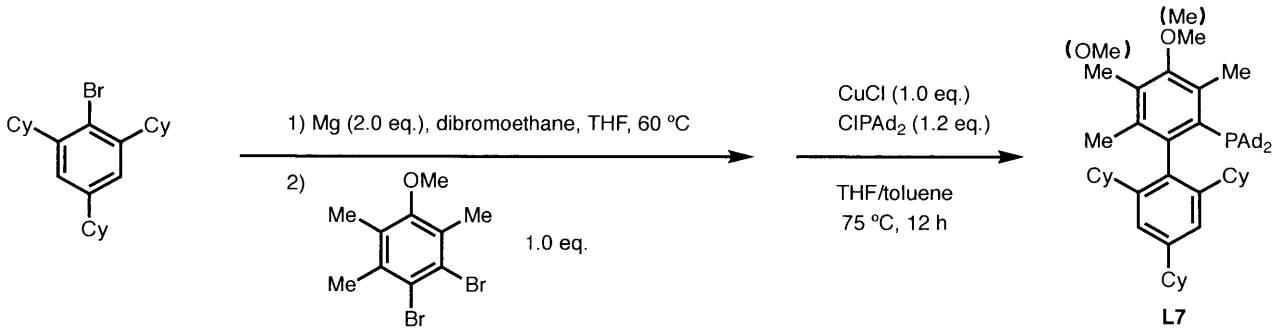

An oven-dried 100 mL three-neck round-bottom flask, was equipped with a stir bar and charged with Mg shavings (0.552 g, 23.0 mmol), then fitted with a reflux condenser, a glass stopper, and a rubber septum. The flask was purged with argon, and 2-bromo-1,3,5-tricyclohexylbenzene (4.04 g, 10.0 mmol) and anhydrous THF (20 mL) were added. The reaction mixture was heated to 60 °C, and 1,2-dibromoethane (25 μL) was added via syringe. The reaction mixture was stirred at 60 °C for an additional 1.5 h. 1,2-dibromo-4-methoxy-3,5,6-trimethylbenzene (3.08 g, 10.0 mmol) was added to the reaction mixture under a positive pressure of argon. After the addition was complete, the reaction mixture was stirred at 60 °C for an additional 1.5 h. The reaction mixture was cooled to room temperature, CuCl (0.990 g, 10.0 mmol) and $ClP(Ad)_2$ (4.04 g, 12.0 mmol) were quickly added under a stream of argon, followed by toluene (20 mL). The reaction mixture was heated at 75 °C for 24 h. The reaction mixture was cooled to room temperature, diluted with Et_2O, washed with 30% NH_4OH (50 mL × 3), dried over $MgSO_4$, filtered and concentrated under reduced pressure to give a pale yellow oil. The crude material

was triturated in MeOH with the aid of a sonication bath until a milky white suspension formed. The suspension was filtered and washed with additional MeOH to give crude **L7** as a fine white powder (~ 80% purity by ^{31}P NMR). To obtain crystalline material, the white powder was recrystallized from EtOAc/MeOH. First crop: 2.32 g. Second crop: 1.47 g. (combined 3.79 g, 49% yield, regioisomer ratio: 1:0.73). ^{1}H NMR (400 MHz, $CDCl_3$) δ 6.91/6.89 (s, 2H), 3.75/3.69 (s, 3H), 2.62/2.60 (s, 3H), 2.50 (m, 1H), 2.29/2.21 (s, 3H), 2.10 – 0.85 (m, 65H) ppm. ^{13}C NMR (101 MHz, $CDCl_3$) δ 157.1, 155.2, 150.2, 149.8, 147.1, 146.6, 146.1, 146.0, 145.5, 145.2, 141.6, 138.1, 137.9, 135.6, 134.0, 133.8, 129.4, 128.4, 126.6, 121.6, 121.5, 59.6, 59.3, 44.6, 44.5, 42.6, 42.4, 42.1, 42.0, 39.1, 38.9, 36.9, 36.2, 36.0, 34.7, 33.3, 33.2, 29.3, 29.2, 27.4, 27.3, 27.2, 27.1, 26.8, 26.6, 26.4, 22.5, 20.6, 17.3, 13.4, 13.3 ppm. (Observed complexity is due to the mixture of two isomers and C-P coupling) ^{31}P NMR (162 MHz, $CDCl_3$) δ 43.43, 43.16 ppm. IR (thin film) 2902, 2848, 1447, 1374, 1300, 1206, 1085, 904, 728, 649 cm^{-1}. m.p. 231 °C. HRMS (ESI) m/z calcd. for $C_{54}H_{78}F_3OP^+$ $[M+H]^+$: 773.5785; found 773.5771.

1.4.2 Synthesis of L8

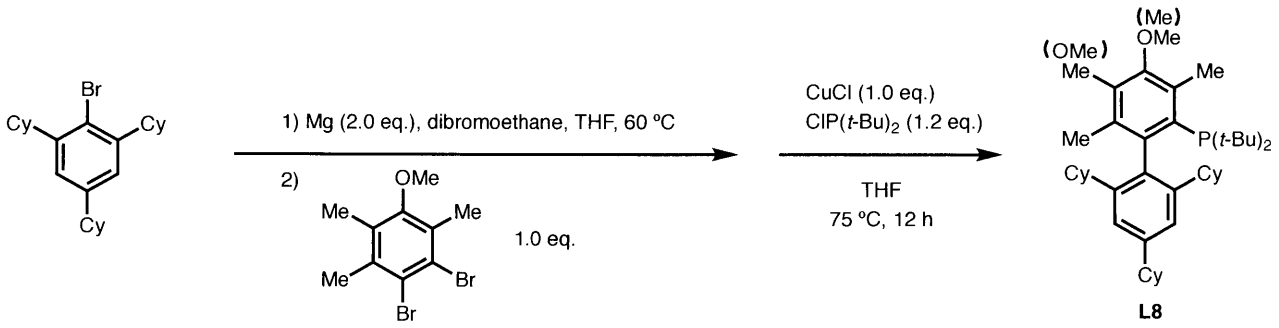

L8

An oven-dried 100 mL three-neck round-bottom flask, which was equipped with a stir bar and charged with Mg shavings (0.552 g, 23.0 mmol), then fitted with a reflux condenser, a glass stopper, and a rubber septum. The flask was purged with argon, and then 2-bromo-1,3,5-tricyclohexylbenzene (4.04 mL, 10.0 mmol) and anhydrous THF (20 mL) were added. The reaction mixture was heated to 60 °C, and 1,2-dibromoethane (25 μL) was added via syringe. The reaction mixture was stirred at 60 °C for an additional 1.5 h. 1,2-dibromo-4-methoxy-3,5,6-trimethylbenzene (3.08 g, 10.0 mmol) was added to the reaction mixture under a positive pressure of argon. After the addition of was complete, the reaction mixture was stirred at 60 °C for an additional 1.5 h. The reaction mixture was cooled to room temperature, CuCl (0.990 g, 10.0 mmol) and $ClP(t\text{-}Bu)_2$ (2.4 mL, 12.0 mmol) were added. The reaction mixture was heated to reflux at 75 °C for 12 h. The reaction mixture was cooled to room temperature, diluted with Et_2O, washed with 30% NH_4OH (50 mL × 3), dried over $MgSO_4$, filtered and concentrated under

reduced pressure to give a pale yellow oil. The crude material was triturated in MeOH with the aid of a sonication bath until a milky white suspension formed. The suspension was filtered and washed with additional MeOH to give crude **L8** as a fine white powder (~ 80% purity by ^{31}P NMR). To obtain crystalline material, the white powder was recrystallized from EtOAc/MeOH. First crop: 1.60 g. Second crop: 1.23 g. (combined 2.83 g, 46% yield, regioisomer ratio: 1:1.2). ^{1}H NMR (400 MHz, $CDCl_3$) δ 6.91/6.90, (s, 2H), 3.73/3.66 (s, 3H), 2.56/2.53 (s, 3H), 2.53 – 2.43 (m, 1H), 2.27/2.20 (s, 3H), 2.04 – 1.80 (m, 8H), 1.78/1.76 (s, 3H), 1.75 – 1.11 (m, 22H), 1.10 – 1.07 (m, 18H), 1.05 – 0.85 (m, 2H) ppm. ^{13}C NMR (101 MHz, $CDCl_3$) δ 157.4, 155.5, 149.8, 149.3, 146.5, 146.2, 146.1, 146.0, 145.3, 145.3, 145.0, 141.4, 138.0, 137.9, 137.7, 137.6, 136.1, 135.7, 135.6, 133.7, 133.6, 133.2, 129.8, 128.4, 128.3, 127.0, 121.7, 121.6, 59.5, 59.4, 44.6, 42.0, 41.9, 35.9, 35.8, 34.7, 34.2, 34.1, 33.9, 33.8, 33.4, 33.3, 32.6, 32.5, 32.4, 27.3, 27.3, 27.1, 26.9, 26.7, 26.5, 26.4, 26.0, 21.6, 20.7, 20.6, 17.2, 13.3, 13.2 ppm. (Observed complexity is due to the mixture of two isomers and C-P coupling). ^{31}P NMR (162 MHz, $CDCl_3$) δ 38.15, 37.71 ppm. IR (thin film) 2920, 2849, 1606, 1558, 1444, 1373, 1359, 1207, 1085, 1000, 861 cm^{-1}. m.p. 189-191 °C. EA Calcd. for $C_{42}H_{65}OP$: C, 81.77; H, 10.62. Found: C, 82.01; H, 10.79.

1.4.3 General procedure for the synthesis of vinyl triflates

Vinyl triflates **1a**[19], **1b**[20], **1c**[21], **1d**[19], **1e**[20], **1f**[19], **1h**[21], **1i**[19], **1j**[19], **1t**[19] and **1u**[22] have been previously described.

General procedure for the synthesis of 1g, 1l, 1m, 1n, 1p, 1q and 1r.

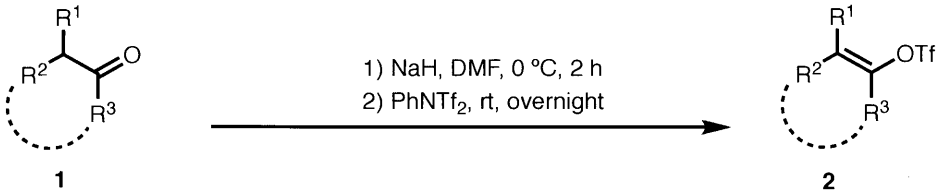

1 2

To a suspension of sodium hydride (95%, 0.32 g, 1.2 eq.) in DMF (20 mL) cooled to 0 °C in an ice/water bath, was added dropwise a solution of the corresponding ketone (10 mmol) in DMF (20 mL). The mixture was stirred for 2 h at ambient temperature. Then, *N*-phenyl-bis(trifluoromethanesulfonimide (3.9 g, 1.1 eq.) was added and the mixture was stirred overnight. The reaction mixture was extracted with Et_2O, the combined organic layers were washed with saturated NH_4Cl (aq), water, brine, dried over Mg_2SO_4, and filtered. The solvents were removed *in vacuo* and the residue purified by flash chromatography.

5-phenyl-3,6-dihydro-2*H*-pyran-4-yl triflouromethanesulfonate (1g)

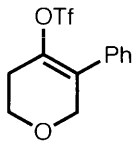

1g

The general procedure was followed using 3-phenyltetrahydro-4*H*-pyran-4-one (2.12 g, 12 mmol), NaH (0.384 g, 14.4 mmol), and *N*-phenyl-bis(trifluoromethanesulfonimide (4.71 g, 13.2 mmol). Silica gel column chromatography (10:1 Hexanes:EtOAc) yielded the title product as a colorless oil. (0.740 g, 20 %). ^{1}H NMR (400 MHz, $CDCl_3$) δ 7.50 – 7.33 (m, 3H), 7.32 – 7.23 (m, 2H), 4.42 (t, J = 2.6 Hz, 2H), 4.00 (t, J = 5.5 Hz, 2H), 2.64 (tt, J = 5.4, 2.6 Hz, 2H) ppm. ^{13}C NMR (101 MHz, $CDCl_3$) δ 140.3, 132.2, 130.1, 128.8, 128.6, 128.3, 118.1 (q, J = 321.2 Hz), 68.5 (t, J = 8.0 Hz), 64.47, 28.3 ppm. ^{19}F NMR (376 MHz, $CDCl_3$) δ -75.00 ppm. IR (thin film) 2863, 1699, 1414, 1202, 1137, 1107, 1042, 988, 870, 823, 759, 697, 598 cm^{-1}. HRMS (DART) m/z calcd. for $C_{12}H_{15}F_3NO_4S^+$ $[M+NH_4]^+$: 326.0668; found 326.0670.

2-(3-cyanophenyl)cyclopent-1-en-1-yl triflouromethanesulfonate (1l)

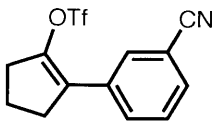

1l

The general procedure was followed using the 3-(2-oxocyclopentyl)benzonitrile[23] (0.93 g, 5.0 mmol), NaH (0.25 g, 9.5 mmol), and *N*-phenyl-bis(trifluoromethanesulfonimide (2.3 g, 6.5 mmol). Silica gel column chromatography (10:1 Hexanes:EtOAc) yielded the title product as a orange oil. (1.1 g, 70 %). ^{1}H NMR (400 MHz, $CDCl_3$) δ 7.82 – 7.66 (m, 2H), 7.63 – 7.57 (m, 1H), 7.54 – 7.46 (m, 1H), 3.00 – 2.72 (m, 4H), 2.13 (m, 2H) ppm. ^{13}C NMR (101 MHz, $CDCl_3$) δ 145.0, 133.8, 131.6, 130.3, 129.9, 127.0, 118.4, 118.3 (q, J = 322.2 Hz), 122.9, 32.4, 31.7, 19.3 ppm. ^{19}F NMR (376 MHz, $CDCl_3$) δ -74.22 ppm. IR (thin film) 2965, 2231, 1662, 1418, 1205, 1135, 958, 848, 798, 603 cm^{-1}. HRMS (DART) m/z calcd. for $C_{13}H_{14}F_3N_2O_3S^+$ $[M+NH_4]^+$: 335.0672; found 335.0687.

2-(4-(trifluoromethyl)phenyl)cyclopent-1-en-1-yl triflouromethanesulfonate (1m)

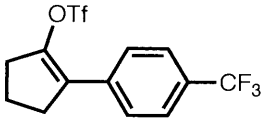

1m

The general procedure was followed using the 2-(4-(trifluoromethyl)phenyl)cyclopentan-1-one[23] (1.1 g, 5.0 mmol), NaH (0.25 g, 9.5 mmol), and *N*-phenyl-bis(trifluoromethanesulfonimide (2.3 g, 6.5 mmol). Silica gel column chromatography (10:1 Hexanes:EtOAc) yielded the title product as a orange oil. (1.5 g, 82 %). ^{1}H NMR (400 MHz, $CDCl_3$) δ 7.71 – 7.53 (m, 4H), 3.01 – 2.75 (m, 4H), 2.13 (m, 2H) ppm. ^{13}C NMR (101 MHz, $CDCl_3$) δ 144.8, 135.9, 130.1 (d, J = 32.3 Hz), 127.9, 127.6, 125.4 (q, J = 4.0 Hz), 123.9 (q, J = 272.7 Hz), 118.4, 118.2 (q, J = 321.2 Hz), 112.9, 32.4, 31.5, 19.3 ppm. ^{19}F NMR (376 MHz, $CDCl_3$) δ -62.79, -74.23 ppm. IR

(thin film) 2962, 1662, 1619, 1421, 1324, 1209, 1123, 1075, 1058, 1016, 936, 839, 604 cm^{-1}. HRMS (DART) m/z calcd. for $C_{13}H_{14}F_6NO_3S^+$ $[M+NH_4]^+$: 378.0593; found 378.0584.

2-(4-(diethylcarbamoyl)phenyl)cyclopent-1-en-1-yl triflouromethanesulfonate (1n)

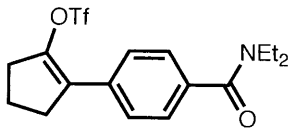

1n

The general procedure was followed using the *N*,*N*-diethyl-4-(2-oxocyclopentyl)benzamide[23] (3.6 g, 14 mmol), NaH (0.709 g, 26.6 mmol), and *N*-phenyl-bis(trifluoromethanesulfonimide (6.50 g, 18.2 mmol). Silica gel column chromatography (1:1 Hexanes:EtOAc) yielded the title product as a orange solid. (5.2 g, 94 %). ^{1}H NMR (400 MHz, $CDCl_3$) δ 7.57 – 7.45 (d, *J* = 8.0 Hz, 2H), 7.45 – 7.33 (d, *J* = 8.0 Hz, 2H), 3.79 – 3.05 (m, 4H), 3.01 – 2.66 (m, 4H), 2.16 – 2.04 (m 2H), 1.35 – 1.00 (m, 6H) ppm. ^{13}C NMR (101 MHz, $CDCl_3$) δ 170.7, 143.8, 137.0, 133.2, 128.4, 127.4, 126.6, 118.3 (q, *J* = 321.2 Hz), 43.3, 39.3, 32.3, 31.6, 19.3, 14.2, 12.9 ppm (Observed complexity is due to amide rotamers). ^{19}F NMR (376 MHz, $CDCl_3$) δ -74.31 ppm. IR (thin film) 2979, 2939, 1622, 1414, 1202, 1136, 1061, 933, 840, 764, 607 cm^{-1}. m.p. 50-52 °C. HRMS (DART) m/z calcd. for $C_{17}H_{21}F_3NO_4S^+$ $[M+H]^+$: 392.1138; found 392.1156.

8-(2-methylpyrimidin-5-yl)-6,7-dihydro-5*H*-benzo[7]annulen-9-yl triflouromethanesulfonate (1p)

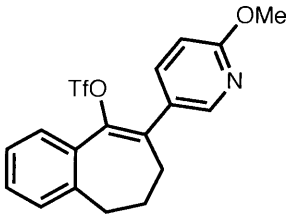

1q

The general procedure was followed using the 6-(2-methylpyrimidin-5-yl)-6,7,8,9-tetrahydro-5*H*-benzo[7]annulen-5-one[24] (2.82 g, 11.2 mmol), NaH (0.568 g, 21.3 mmol), and *N*-phenyl-bis(trifluoromethanesulfonimide (5.21 g, 14.6 mmol). Silica gel column chromatography (1:1 Hexanes:EtOAc, 1% triethylamine) yielded the title product as a white solid. (3.66 g, 85 %). ^{1}H NMR (400 MHz, $CDCl_3$) δ 8.74 (s, 2H), 7.57 – 7.52 (m, 1H), 7.41 – 7.36 (m, 2H), 7.34 – 7.29 (m, 1H), 2.87 (t, *J* = 7.1 Hz, 2H), 2.79 (s, 3H), 2.43 (p, *J* = 7.1 Hz, 2H), 2.24 (t, *J* = 7.1 Hz, 2H) ppm. ^{13}C NMR (101 MHz, $CDCl_3$) δ 167.5, 155.9, 142.6, 141.1, 133.0, 130.4 129.3, 129.0, 127.7, 127.2, 126.7, 118.0 (q, *J* = 322.2 Hz), 34.9, 31.6, 30.8, 25.9 ppm. ^{19}F NMR (376 MHz, $CDCl_3$) δ -74.35 ppm. IR (thin film) 2956, 2870, 1582, 1538, 1485, 1450, 1412, 1232, 1206, 1138, 962, 854, 803, 775, 607 cm^{-1}. m.p. 108-110 °C. HRMS (DART) m/z calcd. for $C_{17}H_{16}F_3N_2O_3S^+$ $[M+H]^+$: 385.0859; found 385.0828.

8-(4-nitrophenyl)-6,7-dihydro-5*H*-benzo[7]annulen-9-yl triflouromethanesulfonate (1r)

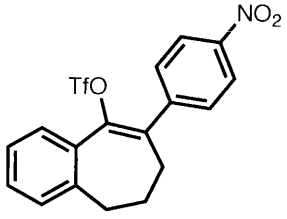

1r

The general procedure was followed using the 6-(4-nitrophenyl)-6,7,8,9-tetrahydro-5*H*-benzo[7]annulen-5-one[24] (5.6 g, 20 mmol), NaH (0.96 g, 38 mmol), and *N*-phenyl-bis(trifluoromethanesulfonimide (9.3 g, 26 mmol). Silica gel column chromatography (10:1 Hexanes:EtOAc) yielded the title product as a white solid. (7.4 g, 90 %). ^{1}H NMR (400 MHz, $CDCl_3$) δ 8.37 – 8.24 (m, 2H), 7.72 – 7.59 (m, 2H), 7.60 – 7.50 (m, 1H), 7.46 – 7.36 (m, 2H), 7.33 (m, 1H), 2.90 (t, *J* = 7.1 Hz, 2H), 2.47 (p, *J* = 7.1 Hz, 2H), 2.29 (t, *J* = 7.2 Hz, 2H) ppm. ^{13}C NMR (101 MHz, $CDCl_3$) δ 147.3, 144.7, 141.9, 141.0, 133.1, 132.3, 130.3, 129.4, 129.3, 127.2, 126.7, 123.7, 117.9 (q, *J* = 322.2 Hz), 35.2, 31.5, 31.1 ppm. ^{19}F NMR (376 MHz, $CDCl_3$) δ -74.43 ppm. IR (thin film) 2955, 2867, 1640, 1593, 1511, 1416, 1340, 1210, 1135, 1012, 998, 964, 855, 698, 601 cm^{-1}. m.p. 140 °C. HRMS (DART) m/z calcd. for $C_{18}H_{18}F_3N_2O_5S^+$ $[M+NH_4]^+$: 431.0883; found 431.0869.

1.4.4 General procedure for palladium-catalyzed fluorination of vinyl triflates

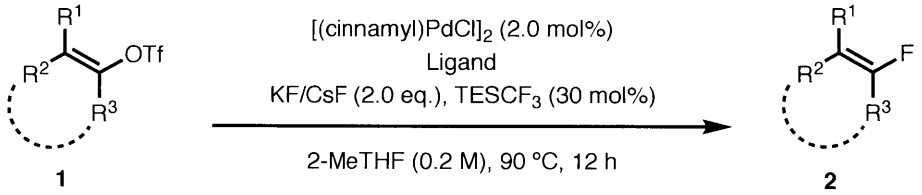

1 2

In a nitrogen-filled glovebox, an oven-dried reaction tube (Fisher 20 × 125 mm tubes – Cat. No. 1495937A) equipped with a stir bar, was charged successively with $[(cinnamyl)PdCl]_2$ (2.0 mol%, 4.0 mol% Pd), ligand (5.0 mol%), fluoride source (2.0 eq.), vinyl triflate (1.0 mmol, 1.0 eq.) and 5 mL of the reaction solvent. If the vinyl triflate was a liquid, 5 mL of the reaction solvent was added, followed by the triflate. $TESCF_3$ was then added via a micro syringe if needed. The reaction tube was sealed with a screw cap (CLOSURE OT S/T 18-400TH 14, Cat. No. 033407G) containing a Teflon septa (Thermo Scientific SPTA PTFE/SIL F/18-400 10, Cat. No. 03394B), and the reaction tube was removed from the glovebox, and vigorously stirred at 90 °C for 12 h. The reaction mixture was cooled to room temperature, filtered through a pad of silica gel, eluting with Hexanes or EtOAc and concentrated with the aid of a rotary evaporator. The crude material was purified by silica gel chromatography.

Modified reaction procedure (A) using HGPhos precatalyst:

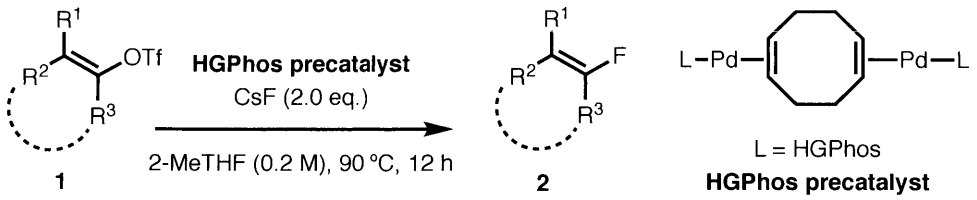

The general procedure was followed except for the use of **L3** precatalyst (4.0 mol% Pd) instead of $[(cinnamyl)PdCl]_2$ and the ligand.

Modified reaction procedure (B) using a sacrificial vinyl triflate 2v:

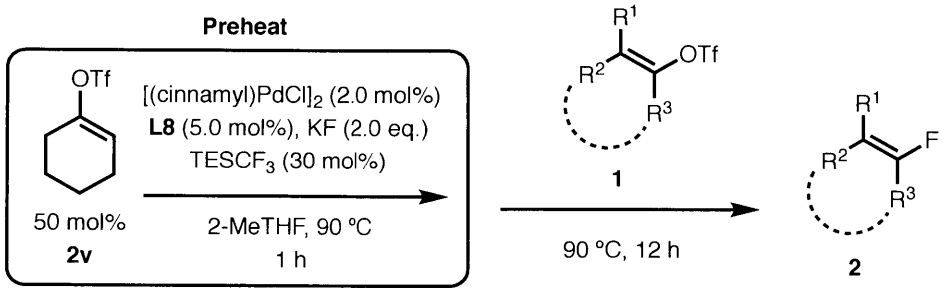

In a nitrogen-filled glovebox, an oven-dried reaction tube (Fisher 20 × 125 mm tubes – Cat. No. 1495937A) equipped with a stir bar, was charged successively with $[(cinnamyl)PdCl]_2$ (2.0 mol%), ligand (5.0 mol%), fluoride source (2.0 eq.) and 5 mL of the reaction solvent. Cyclohexenyl triflate **2v** (0.50 mmol, 0.5 eq.) and $TESCF_3$ (0.055 mL, 0.30 mmol) was then added via a micro syringe, respectively. The reaction tube was sealed with a screw cap containing a Teflon septa, removed from the glovebox, and the reaction mixture was vigorously stirred at 90 °C for 1 h. The reaction mixture was cooled to room temperature and transferred into the glovebox. The vinyl triflate (**1**, 1.0 mmol, 1.0 eq.) was added. The reaction mixture was sealed again and removed from the glovebox and vigorously stirred at 90 °C for 12 h. After completion, the reaction mixture was allowed to cool to rt, filtered through a pad of silica gel, eluting with Hexanes or EtOAc and concentrated with the aid of a rotary evaporator. The crude material was purified by silica gel chromatography.

Compounds **2a**[25], **2b**[26], racemic **2h**[27], **2m**[28] and **2u**[29] have been previously described. Compound **1v** was purchased from commercial sources and used as received.

4-fluoro-1,2,3,6-tetrahydro-1,1'-biphenyl (2a) was prepared according to general procedure using [(cinnamyl)PdCl]$_2$ (0.010 g, 0.020 mmol), **L8** (0.031 g, 0.050 mmol), 1,2,3,6-tetrahydro-[1,1'-biphenyl]-4-yl trifluoromethanesulfonate (0.31 g, 1.0 mmol), KF (0.12 g, 2.0 mmol), $TESCF_3$ (55 μL, 30 mmol%) in 2-MeTHF (5 mL) at 90 °C for 12 h. The crude material was purified by silica gel chromatography (Hexanes) to provide **2a** as a white solid (Run 1: 129 mg, 73%; Run 2: 120 mg, 68%). ^{1}H NMR (400 MHz, $CDCl_3$) δ 7.43 – 7.36 (m, 2H), 7.35 – 7.27 (m, 3H), 5.35 (m, 1H), 2.92 – 2.82 (m, 1H), 2.55 – 2.25 (m, 4H), 2.15 – 1.94 (m, 2H) ppm. ^{13}C NMR (101 MHz, $CDCl_3$) δ 159.7 (d, J = 255.5 Hz), 145.7 (d, J = 2.0 Hz), 128.5, 126.9, 126.4, 101.7 (d, J = 15.9 Hz), 39.7 (d, J = 2.0 Hz), 30.7 (d, J = 8.3 Hz), 29.6 (d, J = 9.3 Hz), 26.0 (d, J = 24.2 Hz) ppm. ^{19}F NMR (376 MHz, $CDCl_3$) δ -103.23 ppm. IR (thin film) 3027, 2922, 2845, 1704, 1495, 1373, 1126, 818, 754, 698 cm^{-1}. EA Calcd. for $C_{12}H_{13}F$: C, 81.78; H, 7.44. Found: C, 81.76; H, 7.40.

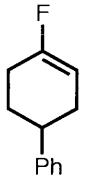

2a

6-fluoro-2,3,4,5-tetrahydro-1,1'-biphenyl (2b) was prepared according to general procedure using [(cinnamyl)PdCl]$_2$ (0.010 g, 0.020 mmol), **L3** (0.039 g, 0.050 mmol), 3,4,5,6-tetrahydro-[1,1'-biphenyl]-2-yl trifluoromethanesulfonate (0.31 g, 1.0 mmol), CsF (0.30 g, 2.0 mmol) in 2-MeTHF (5 mL) at 90 °C for 12 h. The crude material was purified by silica gel chromatography (Hexanes) to provide **2b** as a white solid (Run 1: 144 mg, 82%; Run 2: 157 mg, 89%). ^{1}H NMR (400 MHz, $CDCl_3$) δ 7.57 – 7.51 (m, 2H), 7.49 – 7.41 (m, 2H), 7.41 – 7.28 (m, 1H), 2.56 – 2.49 (m, 2H), 2.49 – 2.42 (m, 2H), 1.96 – 1.87 (m, 2H), 1.87 – 1,78 (m, 2H) ppm. EA Calcd. for $C_{12}H_{13}F$: C, 81.78; H, 7.44. Found: C, 81.75; H, 7.26.

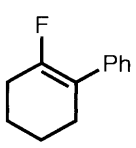

2b

1-fluoro-4-pentylcyclohex-1-ene (2c) was prepared according to general procedure using [(cinnamyl)PdCl]$_2$ (0.010 g, 0.020 mmol), **L8** (0.031 g, 0.050 mmol), 4-pentylcyclohex-1-en-1-yl trifluoromethanesulfonate (0.30 g, 1.0 mmol), KF (0.12 g, 2.0 mmol), $TESCF_3$ (55 μL, 30 mmol%) in 2-MeTHF (5 mL) at 90 °C for 12 h. The crude material was purified by silica gel chromatography (Hexanes) to provide **2c** as a colorless oil (Run 1: 117 mg, 69%; Run 2: 132 mg, 78%). ^{1}H NMR (400 MHz, $CDCl_3$) δ 5.13 (m, 1H), 2.30 – 2.05 (m, 3H), 1.89 – 1.78 (m, 1H), 1.73 – 1.63 (m, 1H), 1.55 – 1.44 (m, 1H), 1.45 – 1.20 (m, 9H), 0.90 (t, J = 6.8 Hz, 3H) ppm. ^{13}C NMR (101 MHz, $CDCl_3$) δ 159.9 (d, J = 254.5 Hz), 101.4 (d, J = 15.1 Hz), 35.8 (d, J = 2.2 Hz), 33.3 (d, J = 1.9 Hz), 32.3, 29.3 (d, J = 8.1 Hz), 28.9 (d, J = 9.1 Hz), 26.4 (d, J = 144.4 Hz), 25.4, 22.9, 14.3 ppm. ^{19}F NMR (376 MHz,

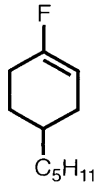

2c

$CDCl_3$) δ -103.56 ppm. IR (thin film) 2955, 2922, 2855, 1705, 1456, 1376, 1138, 1110, 815, 777, 667 cm^{-1}. HRMS (DART) m/z calcd. for $C_{11}H_{20}^{+}$ [M-F]$^+$: 151.1481; found 151.1493.

9-fluoro-3,3-dimethyl-1,5-dioxaspiro[5.5]undec-8-ene (2d) was prepared according to general procedure using [(cinnamyl)PdCl]$_2$ (0.010 g, 0.020 mmol), **L8** (0.031 g, 0.050 mmol), 3,3-dimethyl-1,5-dioxaspiro[5.5]undec-8-en-9-yl trifluoromethanesulfonate (0.33 g, 1.0 mmol), KF (0.12 g, 2.0 mmol), $TESCF_3$ (55 μL, 30 mmol%) in 2-MeTHF (5 mL) at 90 °C for 12 h. The crude material was purified by silica gel chromatography (40:1 Hexanes:EtOAc to 30:1 Hexanes:EtOAc) to provide **2d** as a yellow oil (Run 1: 146 mg, 73%; Run 2: 158 mg, 79%). ^{1}H NMR (400 MHz, $CDCl_3$) δ 5.07 – 5.00 (m, 1H), 3.55 (d, J = 12.0 Hz, 2H), 3.50 (d, J = 12.0 Hz, 2H), 2.43 – 2.36 (m, 2H), 2.31 – 2.23 (m, 2H), 2.08 – 2.03 (m, 2H), 1.01 (s, 3H), 0.94 (m, 3H) ppm. ^{13}C NMR (101 MHz, $CDCl_3$) δ 158.9 (d, J = 255.5 Hz), 98.3 (d, J = 18.7 Hz), 96.4 (d, J = 1.9 Hz), 70.5, 31.4 (d, J = 8.6 Hz), 30.2, 27.6 (d, J = 9.9 Hz), 23.4 (d, J = 26.3 Hz), 22.6 (d, J = 13.5 Hz) ppm. ^{19}F NMR (376 MHz, $CDCl_3$) δ -105.20 ppm. IR (thin film) 2954, 2868, 1708, 1473, 1379, 1247, 1112, 1039, 858, 726, 646 cm^{-1}. m.p. 34-35 °C. HRMS (DART) m/z calcd. for $C_{11}H_{18}FO_2^+$ [M+H]$^+$: 201.1285; found 201.1289.

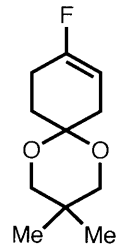

2d

3-(3-fluorocyclohex-2-en-1-yl)-1-methyl-1*H*-indole (2e) was prepared according to general procedure using [(cinnamyl)PdCl]$_2$ (0.010 g, 0.020 mmol), **L8** (0.039 g, 0.050 mmol), 3-(1-methyl-1*H*-indol-3-yl)cyclohex-1-en-1-yl trifluoromethanesulfonate (0.36 g, 1.0 mmol), KF (0.12 g, 2.0 mmol), $TESCF_3$ (55 μL, 30 mmol%) in 2-MeTHF (5 mL) at 90 °C for 12 h. The crude material was purified by silica gel chromatography (Hexanes to 5:1 Hexanes:DCM) to provide **2f** as a light yellow oil (Run 1: 156 mg, 68%; Run 2: 174 mg, 76%). ^{1}H NMR (400 MHz, $CDCl_3$) δ 7.78 – 7.72 (m, 1H), 7.43 – 7.31 (m, 2H), 7.27 – 7.21 (m, 1H), 6.92 (d, J = 0.8 Hz, 1H), 5.56 (ddt, J = 17.6, 3.7, 1.4 Hz, 1H), 4.04 – 3.90 (m, 1H), 3.81 (s, 3H), 2.49 – 2.30 (m, 2H), 2.18 – 1.76 (m, 4H) ppm. ^{13}C NMR (101 MHz, $CDCl_3$) δ 160.7 (d, J = 255.5 Hz), 137.5, 126.9, 126.6, 121.7, 119.2, 118.8, 118.7 (d, J = 2.0 Hz), 109.4, 105.7 (d, J = 14.3 Hz), 32.7, 31.1 (d, J = 8.4 Hz), 29.8 (d, J = 2.2 Hz), 25.8 (d, J = 23.3 Hz), 20.5 (d, J = 9.1 Hz) ppm. ^{19}F NMR (376 MHz, $CDCl_3$) δ -101.33 ppm. IR (thin film) 3048, 2934, 2860, 1699, 1471, 1366, 1326, 1326, 1232, 1131, 876, 735, 639 cm^{-1}. HRMS (DART) m/z calcd. for $C_{15}H_{17}FN^+$ [M+H]$^+$: 230.1340; found 230.1336.

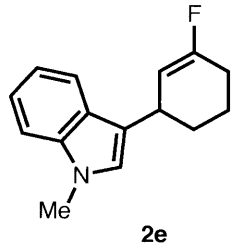

2e

3-fluoro-6-methoxy-1,2-dihydronaphthalene (2f) was prepared according to the general procedure using, [(cinnamyl)PdCl]$_2$ (0.010 g, 0.020 mmol), **L8** (0.039 g, 0.050 mmol), 7-methoxy-3,4-dihydronaphthalen-2-yl trifluoromethanesulfonate (0.33 g, 1.0 mmol), KF (0.12 g, 2.0 mmol), $TESCF_3$ (55 μL, 30 mmol%) in 2-MeTHF (5 mL) at 90 °C. The crude material was purified by silica gel chromatography (Hexanes to 10:1 Hexanes:EtOAc) to provide **2g** as a light yellow oil (Run 1: 125 mg, 70%; Run 2: 135 mg, 76%). **2f** was also prepared according to the modified procedure B (Run 1: 145 mg, 81%; Run 2: 138 mg, 77%). **Less than 5% of the product was oxidized to 2-fluoro-7-methoxynaphthalene by air during separation.** ^{1}H NMR (400 MHz, $CDCl_3$) δ 7.06 – 6.99 (m, 1H), 6.66 (dd, *J* = 8.2, 2.7 Hz, 1H), 6.58 (d, *J* = 2.7 Hz, 1H), 6.02 (m, 1H), 3.80 (s, 3H), 2.97 (tdd, *J* = 8.4, 2.7, 0.9 Hz, 2H), 2.57 (tdd, *J* = 8.4, 3.9, 1.2 Hz, 2H) ppm. ^{13}C NMR (101 MHz, $CDCl_3$) δ 163.8 (d, *J* = 269.7 Hz), 158.6, 134.4 (d, *J* = 10.3 Hz), 128.0, 124.1, 111.9 (d, *J* = 6.1 Hz), 111.0 (d, *J* = 2.4 Hz), 104.9 (d, *J* = 18.9 Hz), 55.29 , 27.8 (d, *J* = 7.4 Hz), 25.1 (d, *J* = 23.2 Hz) ppm. ^{19}F NMR (376 MHz, $CDCl_3$) δ -100.02 ppm. IR (thin film) 2940, 2835, 1675, 1607, 1499, 1308, 1256, 1217, 1125, 1037, 866, 792, 772 cm^{-1}. HRMS (DART) m/z calcd. for $C_{11}H_{12}FO^+$ [M+H]$^+$: 179.0867; found 179.0868.

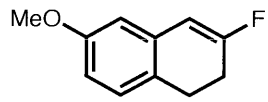

2f

4-fluoro-5-phenyl-3,6-dihydro-2*H*-pyran (2g) was prepared according to general procedure using [(cinnamyl)PdCl]$_2$ (0.0104 g, 0.020 mmol), **L3** (0.039 g, 0.050 mmol), 5-phenyl-3,6-dihydro-2*H*-pyran-4-yl trifluoromethanesulfonate (0.31 g, 1.0 mmol), CsF (0.30 g, 2.0 mmol) in 2-MeTHF (5 mL) at 110 °C for 12 h. The crude material was purified by silica gel chromatography (Hexanes to 10:1 Hexanes:EtOAc) to provide **2h** as a colorless oil (Run 1: 123 mg, 69%; Run 2: 134 mg, 75%). ^{1}H NMR (400 MHz, $CDCl_3$) δ 7.42 – 7.26 (m, 5H), 4.46 (dt, *J* = 6.7, 2.4 Hz, 2H), 3.98 (td, *J* = 5.7, 2.5 Hz, 2H), 2.51 (tq, *J* = 5.4, 2.6 Hz, 2H) ppm. ^{13}C NMR (101 MHz, $CDCl_3$) δ 152.5 (d, *J* = 265.6 Hz), 128.4, 127.5 (d, *J* = 4.0 Hz), 127.4, 112.9 (d, *J* = 4.8 Hz), 66.9 (d, *J* = 3.7 Hz), 64.8 (d, *J* = 9.3 Hz), 26.9 (d, *J* = 21.2 Hz) ppm. ^{19}F NMR (376 MHz, $CDCl_3$) δ -105.59 ppm. IR (thin film) 3057, 2933, 2837, 1695, 1495, 1348, 1178, 1132, 987, 854, 760, 693, 672 cm^{-1}. HRMS (DART) m/z calcd. for $C_{11}H_{12}O^+$ [M-F]$^+$: 159.0804; found 159.0808.

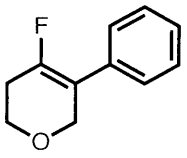

2g

4-fluoro-5-phenyl-3,6-dihydro-2*H*-pyran (2h) was prepared according to general procedure using [(cinnamyl)PdCl]$_2$ (0.010 g, 0.020 mmol), **L1** (0.024 g, 0.050 mmol), (*R*)-2-methyl-5-(prop-1-en-2-yl)cyclohex-1-en-1-yl trifluoromethanesulfonate (0.25 g, 1.0 mmol), CsF (0.30 g, 2.0 mmol) in 2-MeTHF (5 mL) at 90 °C for 12 h. The crude material was purified by silica gel chromatography (Hexanes) to provide **2i** as a colorless oil (Run 1: 99 mg, 64%; Run 2: 113 mg, 73%). ^{1}H NMR (400 MHz, $CDCl_3$) δ 4.85 – 4.65 (m, 2H), 2.35 – 1.90 (m, 5H), 1.80 – 1.35 (m, 8H) ppm.

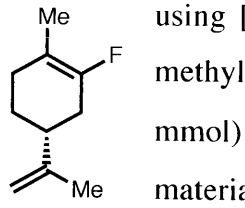

2h

(8*S*,9*S*,10*R*,13*R*,14*S*)-3-fluoro-10,13-dimethyl-17-((*R*)-6-methylheptan-2-yl)-2,7,8,9,10,11,12,13,14,15,16,17-dodecahydro-1*H*-cyclopenta[*a*]phenanthrene (2i) was prepared according to general procedure using [(cinnamyl)PdCl]$_2$ (0.010 g, 0.020 mmol), **L8** (0.031 g, 0.050 mmol), (8*S*,9*S*,10*R*,13*R*,14*S*)-10,13-dimethyl-17-((*R*)-6-methylheptan-2-yl)-2,7,8,9,10,11,12,13,14,15,16,17-dodecahydro-1*H*-cyclopenta[*a*]phenanthren-3-yl trifluoromethanesulfonate (0.52 g, 1.0 mmol), KF (0.12 g, 2.0 mmol), $TESCF_3$ (55 μL, 30 mmol%) in 2-MeTHF (5 mL) at 110 °C for 12 h. The crude material was purified by silica gel chromatography (Hexanes) to provide **2j** as a white solid (Run 1: 329 mg, 85%; Run 2: 317 mg, 82%). 2j was also prepared according to the modified procedure B (Run 1: 344 mg, 89%; Run 2: 337 mg, 87%.) ^{1}H NMR (400 MHz, $CDCl_3$) δ 5.56 (dd, *J* = 15.4, 2.1 Hz, 1H), 5.33 (dd, *J* = 5.1, 2.1 Hz, 1H), 2.46 – 2.34 (m, 1H), 2.27 – 2.09 (m, 2H), 2.02 (dt, *J* = 12.6, 3.5 Hz, 1H), 1.92 – 1.79 (m, 2H), 1.70 – 1.00 (m, 20H), 0.97 (s, 3H), 0.92 (d, *J* = 6.5 Hz, 3H), 0.87 (dd, *J* = 6.6, 1.8 Hz, 6H), 0.70 (s, 3H) ppm. ^{13}C NMR (101 MHz, $CDCl_3$) δ 159.2 (d, *J* = 260.6 Hz), 138.9 (d, *J* = 8.3 Hz), 122.4 (d, *J* = 9.4 Hz), 106.5 (d, *J* = 17.4 Hz), 100.0, 56.8, 56.2, 48.0, 42.4, 39.7, 39.5, 36.2, 35.8, 35.0, 33.6 (d, *J* = 8.8 Hz), 31.8 (d, *J* = 5.1 Hz), 28.2, 28.0, 24.2, 23.8, 23.6, 23.4, 22.8, 22.6, 21.3, 18.7 (d, *J* = 5.4 Hz), 12.0 ppm. ^{19}F NMR (376 MHz, $CDCl_3$) δ -105.56 ppm. IR (thin film) 2934, 2867, 1681, 1641, 1467, 1380, 1207, 1128, 870, 862, 650 cm^{-1}. m.p. 84-85 °C. EA Calcd. for $C_{27}H_{43}F$: C, 83.88; H, 11.21. Found: C, 83.87; H, 11.23.

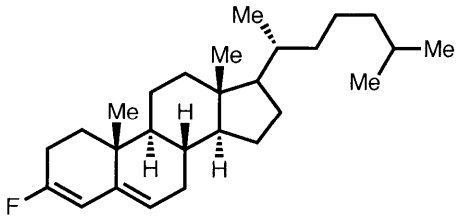

2i

(4a*S*,5*R*)-7-fluoro-4a,5-dimethyl-3-(propan-2-ylidene)-1,2,3,4,4a,5-hexahydronaphthalene

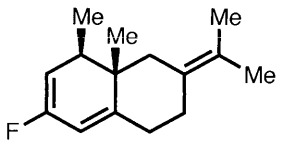

2j

(2j) was prepared according to general procedure using [(cinnamyl)PdCl]$_2$ (0.010 g, 0.020 mmol), **L8** (0.031 g, 0.050 mmol), (4*R*,4a*S*)-4,4a-dimethyl-6-(propan-2-ylidene)-4,4a,5,6,7,8-hexahydronaphthalen-2-yl trifluoromethanesulfonate (0.35 g, 1.0 mmol), KF (0.12 g, 2.0 mmol), $TESCF_3$ (55 μL, 30 mmol%) in 1,4-dioxane (5 mL) at 110 °C for 12 h. The crude material was purified by silica gel chromatography (Hexanes) to provide **2j** as an oil (Run 1: 82 mg, 37%; Run 2: 99 mg, 45%). ^{1}H NMR (400 MHz, $CDCl_3$) δ 5.51 (dt, *J* = 6.6, 1.7 Hz, 1H), 4.73 (dt, *J* = 12.3, 2.4 Hz, 1H), 2.64 – 2.49 (m, 3H), 2.35 – 2.28 (m, 2H), 1.98 – 1.78 (m, 2H), 1.68 (d, *J* = 1.2 Hz, 6H), 1.04 (dd, *J* = 7.4, 0.8 Hz, 3H), 0.78 (s, 3H) ppm. ^{13}C NMR (101 MHz, $CDCl_3$) δ 156.3 (d, *J* = 248.5 Hz), 151.6 (d, *J* = 9.5 Hz), 128.1, 124.1, 113.3 (d, *J* = 34.3 Hz), 103.3 (d, *J* = 12.4 Hz), 41.2, 40.7, 38.4 (d, *J* = 6.1 Hz), 31.6 (d, *J* = 2.0 Hz), 29.4, 20.1 (d, *J* = 4.0 Hz), 14.9, 14.3 (d, *J* = 1.3 Hz) ppm. ^{19}F NMR (376 MHz, $CDCl_3$) δ -120.20 ppm. IR (thin film) 2967, 2922, 2356, 1670, 1451, 1370, 1182, 1098, 998, 911, 838, 668 cm^{-1}. HRMS (DART) m/z calcd. for $C_{15}H_{22}F^+$ [M+H]$^+$: 221.1700; found 221.1709.

3-(2-fluorocyclopent-1-en-1-yl)benzonitrile (2l) was prepared according to general procedure using [(cinnamyl)PdCl]$_2$ (0.010 g, 0.020 mmol), **L3** (0.039 g, 0.050 mmol), 2-(3-cyanophenyl)cyclopent-1-en-1-yl trifluoromethanesulfonate (0.32 g, 1.0 mmol), CsF (0.30 g, 2.0 mmol) in 2-MeTHF (5 mL) at 90 °C for 12 h. The crude material was purified by silica gel chromatography (Hexanes to 10:1 Hexanes:EtOAc) to provide **2m** as an solid (Run 1: 161 mg, 86%; Run 2: 168 mg, 90%). ^{1}H NMR (400 MHz, $CDCl_3$) δ 7.80 – 7.68 (m, 2H), 7.53 – 7.38 (m, 2H), 2.69 (m, 4H), 2.13 – 1.96 (m, 2H) ppm. ^{13}C NMR (101 MHz, $CDCl_3$) δ 159.8 (d, *J* = 287.9 Hz), 135.0 (d, *J* = 4.9 Hz), 130.7 (d, *J* = 7.5 Hz), 130.0 (d, *J* = 8.1 Hz), 129.8 (d, *J* = 2.0 Hz), 129.1, 119.0, 112.5, 111.6 (d, *J* = 3.4 Hz), 30.9 (d, *J* = 20.2 Hz), 29.4 (d, *J* = 7.0 Hz), 18.0 (d, *J* = 9.8 Hz) ppm. ^{19}F NMR (376 MHz, $CDCl_3$) δ -112.95 ppm. IR (thin film) 2923, 2854, 2229, 1675, 1482, 1343, 1199, 796, 689 cm^{-1}. m.p. 40-42 °C. EA Calcd. for $C_{12}H_{10}FN$: C, 76.99; H, 5.38. Found: C, 76.91; H, 5.45.

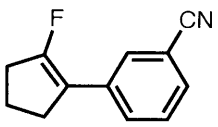

2l

1-(2-fluorocyclopent-1-en-1-yl)-4-(trifluoromethyl)benzene (2m) was prepared according to general procedure using [(cinnamyl)PdCl]$_2$ (0.010 g, 0.020 mmol), **L3** (0.039 g, 0.050 mmol), 1-(2-fluorocyclopent-1-en-1-yl)-4-(trifluoromethyl)benzene (0.360 g, 1.0 mmol), CsF (0.30 g, 2.0 mmol) in 2-MeTHF (5 mL) at 90 °C for 12 h. The crude material was purified by silica gel chromatography (Hexanes) to provide **2n** as a white solid (Run 1: 216 mg, 94%; Run 2: 212 mg, 92%). **2n** was also prepared according to the modified procedure A. Run 1: 214 mg, 93%; Run 2: 209 mg, 91%. ^{1}H NMR (400 MHz, $CDCl_3$) δ 7.65 – 7.55 (m, 4H), 2.77 – 2.66 (m, 4H), 2.09 – 1.99 (m, 1H) ppm. ^{13}C NMR (101 MHz, $CDCl_3$) δ 159.7 (d, J = 287.9 Hz), 137.3 (dd, J = 4.9, 1.5 Hz), 128.3 (qd, J = 32.3, 2.0 Hz), 126.7 (d, J = 7.1 Hz), 125.1 (q, J = 3.8 Hz), 124.4 (q, J = 272.7 Hz), 112.3 (d, J = 3.0 Hz), 30.9 (d, J = 21.2 Hz), 29.5 (d, J = 7.3 Hz), 18.0 (d, J = 9.7 Hz) ppm. ^{19}F NMR (376 MHz, $CDCl_3$) δ -62.51, -113.25 ppm. IR (thin film) 2968, 1829, 1760, 1674, 1619, 1323, 1164, 1116, 1064, 1015, 841 cm^{-1}. m.p. 56-58 °C. HRMS (DART) m/z calcd. for $C_{15}H_{22}F^+$ [M-H]$^+$: 229.0646; found 229.0632.

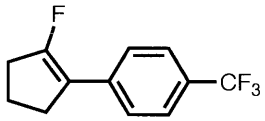

2m

***N,N*-diethyl-4-(2-fluorocyclopent-1-en-1-yl)benzamide (2n)** was prepared according to general procedure using [(cinnamyl)PdCl]$_2$ (0.010 g, 0.020 mmol), **L3** (0.039 g, 0.050 mmol), 2-(4-(diethylcarbamoyl)phenyl)cyclopent-1-en-1-yl trifluoromethanesulfonate (0.39 g, 1.0 mmol), CsF (0.30 g, 2.0 mmol) in 2-MeTHF (5 mL) at 90 °C for 12 h. The crude material was purified by silica gel chromatography (2:1:1 Hexanes:EtOAc:DCM with 1% triethylamine) to provide **2o** as a an oil (Run 1: 201 mg, 77%; Run 2: 220 mg, 84%). ^{1}H NMR (400 MHz, $CDCl_3$) δ 7.47 (d, J = 8.2 Hz, 2H), 7.31 (d, J = 8.3 Hz, 2H), 3.71 – 3.03 (m, 4H), 2.77 – 2.53 (m, 4H), 1.96 (p, J = 7.4 Hz, 2H), 1.34 – 0.95 (m, 6H) ppm. ^{13}C NMR (101 MHz, $CDCl_3$) δ 171.1, 158.6 (d, J = 286.8 Hz), 135.1 (d, J = 2.0 Hz), 134.6 (d, J = 5.1 Hz), 126.5, 126.4, 126.3, 112.7 (d, J = 3.5 Hz), 43.3, 39.3, 30.9 (d, J = 21.2 Hz), 29.6 (d, J = 7.3 Hz), 18.0 (d, J = 9.7 Hz), 14.2, 12.9 ppm (Observed complexity is due to amide rotamers). ^{19}F NMR (376 MHz, $CDCl_3$) δ -114.98 ppm. IR (thin film) 2970, 2933, 2853, 1675, 1626, 1471, 1422, 1345, 1286, 1096, 1074, 944, 841, 767 cm^{-1}. EA Calcd. for $C_{16}H_{20}FNO$: C, 73.53; H, 7.71. Found: C, 73.58; H, 7.82.

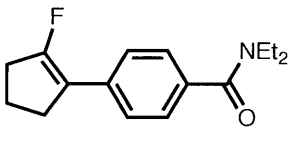

2n

5-(9-fluoro-6,7-dihydro-5*H*-benzo[7]annulen-8-yl)-2-methylpyrimidine (2p) was prepared according to general procedure using [(cinnamyl)PdCl]$_2$ (0.010 g, 0.020 mmol), **L3** (0.039 g, 0.050 mmol), 8-(2-methylpyrimidin-5-yl)-6,7-dihydro-5*H*-benzo[7]annulen-9-yl trifluoromethanesulfonate (0.38 g, 1.0 mmol), CsF (0.30 g, 2.0 mmol) in toluene (5 mL) at 110 °C for 12 h. The crude material was purified by silica gel chromatography (10:1 Hexanes:EtOAc to 1:1 Hexanes:EtOAc with 1% triethylamine) to provide **2p** as a white solid (Run 1: 209 mg, 82%; Run 2: 224 mg, 88%). **2p** was also prepared according to the modified procedure B. Run 1: 242 mg, 95%; Run 2: 242 mg, 95%. ^{1}H NMR (400 MHz, $CDCl_3$) δ 8.74 (s, 2H), 7.56 – 7.51 (m, 1H), 7.34 – 7.16 (m, 3H), 2.79 – 2.73 (m, 2H), 2.72 (s, 3H), 2.35 – 2.28 (m, 2H), 2.26 – 2.16 (m, 2H) ppm. ^{13}C NMR (101 MHz, $CDCl_3$) δ 166.1 (d, *J* = 1.5 Hz), 156.0 (d, *J* = 5.5 Hz), 154.1 (d, *J* = 256.5 Hz), 141.0 (d, *J* = 7.0 Hz), 132.4 (d, *J* = 27.3 Hz), 129.5, 129.1 (d, *J* = 3.0 Hz), 129.0, 126.6 (d, *J* = 4.4 Hz), 126.4, 113.1 (d, *J* = 12.1 Hz), 32.8, 32.6 (d, *J* = 2.0 Hz), 29.1 (d, *J* = 3.3 Hz), 25.7 ppm. ^{19}F NMR (376 MHz, $CDCl_3$) δ -101.87 ppm. IR (thin film) 3025, 2931, 2859, 1649, 1582, 1536, 1446, 1285, 1046, 760, 749, 648 cm^{-1}. m.p. 67-69 °C. EA Calcd. for $C_{16}H_{15}FN_2$: C, 75.57; H, 5.95. Found: C, 75.62; H, 6.04.

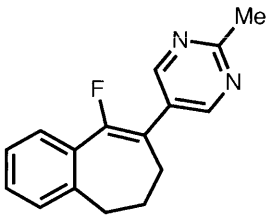

2p

5-(9-fluoro-6,7-dihydro-5*H*-benzo[7]annulen-8-yl)-2-methoxypyridine (2q) was prepared according to general procedure using [(cinnamyl)PdCl]$_2$ (0.010 g, 0.002 mmol), **L3** (0.039 g, 0.050 mmol), 8-(6-methoxypyridin-3-yl)-6,7-dihydro-5*H*-benzo[7]annulen-9-yl trifluoromethanesulfonate (0.37 g, 1.0 mmol), CsF (0.30 g, 2.0 mmol) in toluene (5 mL) at 110 °C for 12 h. The crude material was purified by silica gel chromatography (Hexanes to 10:1 Hexanes:EtOAc) to provide **2q** as a light yellow oil (Run 1: 199 mg, 74%; Run 2: 221 mg, 82%). ^{1}H NMR (400 MHz, $CDCl_3$) δ 8.36 (m, 1H), 7.74 (m, 1H), 7.61 – 7.53 (m, 1H), 7.35 – 7.21 (m, 3H), 6.78 (dd, *J* = 8.6, 0.8 Hz, 1H), 3.98 (s, 3H), 2.77 (t, *J* = 6.6 Hz, 2H), 2.36 – 2.15 (m, 4H) ppm. ^{13}C NMR (101 MHz, $CDCl_3$) δ 162.9 (d, *J* = 1.3 Hz), 152.5 (d, *J* = 254.5 Hz), 146.3 (d, *J* = 4.8 Hz), 140.9 (d, *J* = 6.9 Hz), 138.7 (d, *J* = 5.0 Hz), 133.3 (d, *J* = 28.3 Hz), 129.1 (d, *J* = 2.0 Hz), 129.0, 127.2, 126.5 (d, *J* = 3.8 Hz), 126.3, 116.2 (d, *J* = 11.7 Hz), 110.3, 53.4, 33.1 (d, *J* = 2.5 Hz), 32.8, 29.6 (d, *J* = 3.5 Hz) ppm. ^{19}F NMR (376 MHz, $CDCl_3$) δ -105.02 ppm. IR (thin film) 2942, 2858, 1598, 1563, 1492, 1375, 1283, 1254, 1024, 828, 761 cm^{-1}. HRMS (DART) m/z calcd. for $C_{17}H_{17}FNO^+$ $[M+H]^+$: 270.1289; found 270.1270.

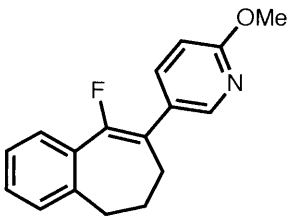

2q

9-fluoro-8-(4-nitrophenyl)-6,7-dihydro-5*H*-benzo[7]annulene (2r) was prepared according to general procedure using [(cinnamyl)PdCl]$_2$ (0.010 g, 0.020 mmol), **L3** (0.039 g, 0.05 mmol), 8-(4-nitrophenyl)-6,7-dihydro-5*H*-benzo[7]annulen-9-yl trifluoromethanesulfonate (0.41 g, 1.0 mmol), CsF (0.30 g, 2.0 mmol) in toluene (5 mL) at 110 °C for 12 h. The crude material was purified by silica gel chromatography (Hexanes to 10:1 Hexanes:EtOAc) to provide **2r** as a white solid (Run 1: 201 mg, 71%; Run 2: 224 mg, 79%). ^{1}H NMR (400 MHz, $CDCl_3$) δ 8.32 – 8.20 (m, 2H), 7.75 – 7.62 (m, 2H), 7.62 – 7.53 (m, 1H), 7.42 – 7.32 (m, 2H), 7.32 – 7.26 (m, 1H), 2.81 (t, J = 6.7 Hz, 2H), 2.45 – 2.20 (m, 4H) ppm. ^{13}C NMR (101 MHz, $CDCl_3$) δ 154.1 (d, J = 259.6 Hz), 146.4, 145.2, 141.1 (d, J = 7.0 Hz), 132.8 (d, J = 27.3 Hz), 129.6, 129.2, 129.1, 126.7 (d, J = 3.8 Hz), 126.4, 123.5, 117.7 (d, J = 10.6 Hz), 33.2 (d, J = 2.5 Hz), 32.6, 29.5 (d, J = 3.0 Hz) ppm. ^{19}F NMR (376 MHz, $CDCl_3$) δ -101.15 ppm. IR (thin film) 3070, 2933, 2837, 1695, 1496, 1348, 1178, 1132, 987, 854, 760, 693, 672 cm^{-1}. m.p. 126-128 °C. HRMS (DART) m/z calcd. for $C_{17}H_{15}FNO_2^+$ [M+H]$^+$: 284.1081; found 284.1083.

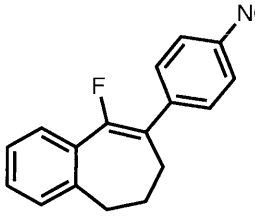

2r

(2-fluoroethene-1,1-diyl)dibenzene (2t) was prepared according to general procedure using [(cinnamyl)PdCl]$_2$ (0.010 g, 0.020 mmol), **L2** (0.032 g, 0.050 mmol), 2,2-diphenylvinyl trifluoromethanesulfonate (0.41 g, 1.0 mmol), CsF (0.30 g, 2.0 mmol) in 2-MeTHF (5 mL) at 90 °C for 12 h. The crude material was purified by silica gel chromatography (Hexanes to 30:1 Hexanes:EtOAc) to provide **2t** as a colorless oil (Run 1: 137 mg, 69%; Run 2: 149 mg, 75%). ^{1}H NMR (400 MHz, $CDCl_3$) δ 7.56 – 7.34 (m, 10H), 7.08 (d, J = 80.0 Hz, 1H). ^{13}C NMR (101 MHz, $CDCl_3$) δ 145.9 (d, J = 269.7 Hz), 137.2 (d, J = 8.1 Hz), 135.3, 129.9 (d, J = 4.2 Hz), 128.8 (d, J = 3.0 Hz), 128.7, 128.4, 128.0, 127.9, 126.4 (d, J = 5.5 Hz) ppm. ^{19}F NMR (376 MHz, $CDCl_3$) δ -127.74 (d, J = 82.7 Hz) ppm. IR (thin film) 3067, 1635, 1497, 1444, 1175, 1088, 1072, 909, 761, 728, 693, 655 cm^{-1}. HRMS (DART) m/z calcd. for $C_{14}H_{12}F^+$ [M+H]$^+$: 199.0918; found 199.0937.

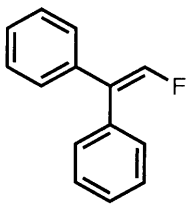

2t

(2-fluoroprop-1-ene-1,1-diyl)dibenzene (2u) was prepared according to general procedure using [(cinnamyl)PdCl]$_2$ (0.010 g, 0.020 mmol), **L3** (0.039 g, 0.050 mmol), 1,1-diphenylprop-1-en-2-yl trifluoromethanesulfonate (0.34 g, 1.0 mmol), CsF (0.30 g, 2.0 mmol) in 1,4-dioxane (5 mL) at 110 °C for 12 h. The crude material was purified by silica gel chromatography (Hexanes to 30:1 Hexanes:DCM) to provide **2u** as a white solid (Run 1: 159 mg, 75%; Run 2: 176 mg, 83%). ^{1}H NMR (400 MHz, $CDCl_3$) δ 7.49 – 7.28 (m, 10H), 2.17 (d, J = 17.9 Hz, 3H) ppm. ^{13}C NMR (101 MHz, $CDCl_3$) δ 155.1 (d, J = 285.6 Hz), 139.4 (d, J = 8.3 Hz), 137.8, 130.5 (d, J = 3.0 Hz), 129.7 (d, J = 4.8 Hz), 128.5, 128.1, 127.3, 126.9, 120.5 (d, J = 14.8 Hz), 17.2 (d, J = 30.3 Hz) ppm. ^{19}F NMR (376 MHz, $CDCl_3$) δ -96.41 (q, J = 18.0 Hz) ppm. IR (thin film) 3057, 1664, 1600, 1496, 1444, 1382, 1265, 1200, 906, 760, 730, 696, 633 cm^{-1}. m.p. 52-54 °C. EA Calcd. for $C_{15}H_{13}F$: C, 84.88; H, 6.17. Found: C, 85.02; H, 6.14.

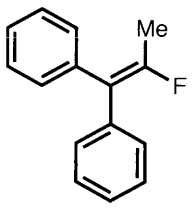

2u

1.5 References and Notes

(1) For reviews, see: (a) Purser, S.; Moore, P. R.; Swallow, S.; Gouverneur, V. *Chem. Soc. Rev.* **2008**, *37*, 320. (b) Neumann, C. N.; Ritter, T. *Angew. Chem. Int. Ed.* **2015**, *54*, 3216; *Angew. Chem.* **2015**, *127*, 3261. (c) Kirk, K. L. *Org. Process Res. Dev.* **2008**, *12*, 305. (d) Müller, K.; Faeh, C.; Diederich, F. *Science* **2007**, *317*, 1881.

(2) (a) Welch, J.; Lin, J. *Tetrahedron* **1996**, *52*, 291. (b) Narumi, T.; Hayashi, R.; Tomita, K.; Kobayashi, K.; Tanahara, N.; Ohno, H.; Naito, T.; Kodama, E.; Matsuoka, M.; Oishi, S.; Fujii, N. *Org. Biomol. Chem.* **2010**, *8*, 616. (c) Lamy, C.; Hofmann, J.; Parrot-Lopez, H.; Goekjian, P. *Tetrahedron Lett.* **2007**, *48*, 6177. (d) Niida, A.; Tomita, K.; Mizumono, M.; Tanigaki, H.; Terada, T.; Oishi, S.; Otaka, A.; Inui, K.-I.; Fuji, N. *Org. Lett.* **2006**, *8*, 613. (e) Niida, A.; Mizumoto, M.; Narumi, T.; Inokuchi, E.; Oishi, S.; Ohno, H.; Otaka, A.; Kitaura, K.; Fujii, N. *J. Org. Chem.* **2006**, *71*, 4118.

(3) (a) Abraham, R. J.; Ellison, S. L. R.; Schonholzer, ; Thomas, P. W. A. *Tetrahedron* **1986**, *42*, 2101; (b) Urban, J.; Tillman, B.; Cronin, W. A. *J. Phys. Chem. A* **2006**, *110*, 11120.

(4) Couve-Bonnaire, S.; Cahard, D.; Pannecoucke, X. *Org. Biomol. Chem.* **2007**, *5*, 1151.

(5) (a) Ernet, T.; Maulitz, A. H.; Wurthwein, E.-U.; Haufe, G. J. *Chem. Soc. Perkin Trans. 1* **2001**, 1929. (b) Meyer, O. G. J.; Frohlich, R.; Haufe, G. *Synthesis* **2000**, 1479. (c) Wong, O. A.; Shi, Y. *J. Org. Chem.* **2009**, *74*, 8377.

(6) For reviews, see: (a) Van Steenis, J. H.; Van der Gen, A. *J. Chem. Soc. Perkin Trans. 1* **2002**, 2117. (b) Landelle, G.; Bergeron, M.; Turcotte-Savard, M.- O.; Paquin, J.-F. *Chem. Soc. Rev.* **2011**, *40*, 2867. (c) Burton, D. J.; Yang, Z. Y.; Qiu, W. *Chem. Rev.* **1996**, *96*, 1641.

(7) Representative fluoroalkene synthesis from fluorinated precursors: (a) Patrick, T. B.; Nadji, S. *J. Fluorine Chem.* **1990**, *49*, 147. (b) Narumi, T.; Tomita, K.; Inokuchi, E.; Kobayashi, K.; Oishi, S.; Ohno, H.; Fujii, N. *Org. Lett.* **2007**, *9*, 3465. (c) Zhang, H.; Zhou, C.-B.; Chen, Q.-Y.; Xiao, J.-C.; Hong, R. *Org. Lett.* **2011**, *13*, 560. (d) Hassan, A.; Montgomery, T. P.; Krische, M. J. *Chem. Commun.* **2012**, *48*, 4692. (e) Prakash, G. K. S.; Chacko, S.; Vaghoo, H.; Shao, N.; Gurung, L.; Mathew, T.; Olah, G. A. *Org. Lett.* **2009**, *11*, 1127. (f) Zajc, B.; Kake, S. *Org. Lett.* **2006**, *8*, 4457. (g) Van Steenis, J. H.; Van der Gen, A. *Eur. J. Org. Chem.* **2001**, 897. (h) Asakura, N.; Usuki, Y.; Iio, H. *J. Fluorine Chem.* **2003**, *124*, 81. (i) Pigeon, X.; Bergeron, M.; BarabØ, F.; DubØ, P.; Frost, H. N.; Paquin, J. F. *Angew. Chem. Int. Ed.* **2010**, *49*, 1123; *Angew. Chem.* **2010**, *122*, 1141. (j) Ichikawa, J.; Miyazaki, S.; Fujiwara, M.; Minami, T. *J. Org. Chem.* **1995**, *60*, 2320. (k) Thornbury, R. T.; Toste, F. D. *Angew. Chem. Int. Ed.* **2016**, *55*, 11629; *Angew. Chem.* **2016**, *128*, 11801.

(8) Deoxyfluorination of ketones: (a) Sano, K.; Fukuhara, T.; Hara, S. *J. Fluorine Chem.* **2009**, *130*, 708. (b) Biedermann, D.; Sarek, J.; Klinot, J.; Hajduch, M.; Dzubak, P. *Synthesis* **2005**, 1157.

(9) Fluoroalkene synthesis by olefin metathesis: (a) Salim, S.; Bellingham, R. K.; Satcharoen, V.; Brown, R. C. D. *Org. Lett.* **2003**, *5*, 3403. (b) Marhold, M.; Buer, A.; Hiemstra, H.; Van Maarseveen, J. H.; Haufe, G. *Tetrahedron Lett.* **2004**, *45*, 57. (c) Nguyen, T. T.; Koh, M. J.; Shen, X.; Romiti, F.; Schrock, R. R.; Hoveyda, A. H. *Science* **2016**, *352*, 569.

(10) Hydrofluorination of alkynes: (a) Akana, J. A.; Bhattacharyya, K. X.; Mueller, P.; Sadighi, J. P. *J. Am. Chem. Soc.* **2007**, *129*, 7736. (b) Gorske, B. C.; Mbofana, C. T.; Miller, S. J. *Org. Lett.* **2009**, *11*, 4318. (c) Okoromoba, O.; Han, J.; Hammond, G.; Xu, B. *J. Am. Chem. Soc.* **2014**, *136*, 14381. (d) Nguyen, T.-H.; Abarbri, M.; Guilloteau, D.; Mavel, S.; Emond, P. *Tetrahedron* **2011**, *67*, 3434. (e) Alonso, P.; Pardo, P.; FaÇanμs, F. J.; Rodríguez, F. *Chem. Commun.* **2014**, *50*, 14364.

(11) Electrophilic fluorination of alkenylmetal species: M=Li, see: (a) Kerr, W. J.; Morrison, A. J.; Pazicky, M.; Weber, T. *Org. Lett.* **2012**, *14*, 2250. (b) Yang, M.-H.; Matikonda, S. S.; Altman, R. A. *Org. Lett.* **2013**, *15*, 3894. M=Sn, see: (c) Tius, M.A.; Kawakami, J. K. *Tetrahedron* **1995**, *51*, 3997. M = Si, see : (d) Greedy, B.; Gourverneur, V. *Chem. Commun.* **2001**, 233. M = B, see: (e) Petasis, N. A.; Yudin, A. K.; Zavialov, I. A.; Prakash, G. K. S.; Olah, G. A. *Synlett* **1997**, 606. (f) Furuya, T.; Ritter, T. *Org. Lett.* **2009**, *11*, 2860. (g) Ye, Y.; Schimler, S. D.; Hanley, P. S.; Sanford, M. S. *J. Am. Chem. Soc.* **2013**, *135*, 16292.

(12) (a) Watson, D. A.; Su, M.; Teverovskiy, G.; Zhang, Y.; García- Fortanet, J.; Kinzel, T.; Buchwald, S. L. *Science* **2009**, *325*, 1661. (b) Lee, H. G.; Milner, P. J.; Buchwald, S. L. *Org. Lett.* **2013**, *15*, 5602. (c) Lee, H. G.; Milner, P. J.; Buchwald, S. L. *J. Am. Chem. Soc.* **2014**, *136*, 3792. (d) Milner, P. J.; Kinzel, T.; Zhang, Y.; Buchwald, S. L. *J. Am. Chem. Soc.* **2014**, *136*, 15757. (e) Sather, A. C.; Lee, H. G.; Rose, V. Y. D. L.; Yang, Y.; Müller, P.; Buchwald, S. L. *J. Am. Chem. Soc.* **2015**, *137*, 13433.

(13) Wu, X.; Fors, B. P.; Buchwald, S. L. *Angew. Chem. Int. Ed.* **2011**, *50*, 9943; *Angew. Chem.* **2011**, *123*, 10117.

(14) Ueda, S.; Ali, S.; Fors, B. P.; Buchwald, S. L. *J. Org. Chem.* **2012**, *77*, 2543. Ligands (such as **L7** and **L8**) with the trimethylmethoxy- substituted top ring exist as two isomers in a ratio close to 1:0.97. These ligands are used as surrogates for the ligands with the tetramethyl-substituted top ring, since they can be prepared from a more readily available precursor.

(15) (a) Cho, E. J.; Senecal, T. D.; Kinzel, T.; Zhang, Y.; Watson, D. A.; Buchwald, S. L. *Science* **2010**, *328*, 1679. (b) Cho, E. J.; Buchwald, S. L. *Org. Lett.* **2011**, *13*, 6552.

(16) Milner, P. J.; Yang, Y.; Buchwald, S. L. *Organometallics* **2015**, *34*, 4775.

(17) Noël, T.; Maimone, T. J.; Buchwald, S. L. *Angew. Chem., Int. Ed.* **2011**,*50*, 8900.

(18) *t*-BuBrettPhos: Fors, B. P.; K. Dooleweerdt, K.; Zeng, Q.; Buchwald, S. L. *Tetrahedron*, **2009**, *65*, 6576; AdBrettPhos: Lee, H. G.; Milner, P. J.; Buchwald, S. L. *Org. Lett.* **2013**, *15*, 5602; **L5, L6**: Salvi, L.; Davis, N. R.; Ali, S. Z.; Buchwald, S. L. *Org. Lett.* **2012**, *14*, 170.

(19) Cho, E. J.; Buchwald, S. L. *Org. Lett.* **2011**, *13*, 6552.

(20) Grundl, M.; Kaster, A.; Beaulieu, E. D.; Trauner, D. *Org. Lett.* **2006**, 5429.

(21) Cai, X.; Snieckus, V. *Org. Lett.* **2004**, *6*, 2293.

(22) Wallace, D. J.; Klauber, D. J.; Chen, C.-Y.; Volante, R. P. *Org. Lett.* **2003**, *5*, 4749.

(23) Xu, Y.; Su, T.; Huang, Z.; Dong, G. *Angew. Chem., Int. Ed.* **2016**, *55*, 2559.

(24) Fox, J. M.; Huang, X.; Chieffi, A.; Buchwald, S. L. *J. Am. Chem. Soc.* **2000**, *122*, 1360.

(25) Tius, M.; Kawakami, J. K. *Tetrahedron* **1995**, *51*, 3997.

(26) Yang, M.-H.; Matikonda, S. S.; Altman, R. A. *Org. Lett.* **2013**, *15*, 3894.

(27) Zhang, Q.; Tiefenbacher, K. *Nature chem.* **2015**, *7*, 197.

(28) Ichikawa, J.; Wada, Y.; Fujiwara, M.; Sakoda, K. *Synthesis* **2002**, 1917.

(29) Wenz, J.; Rettenmeier, C. A.; Wadepohl, H.; Gade, L. H. *Chem. Commun.* **2016**, *52*, 202

Copies of NMR Spectra

L8

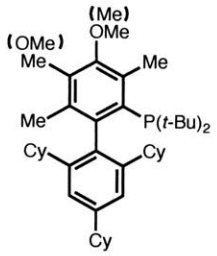

L8

^{1}H NMR, 400 MHz, $CDCl_3$

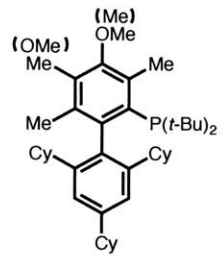

L8

^{13}C NMR, 101 MHz, $CDCl_3$

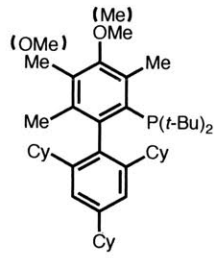

L8

^{31}P NMR, 162 MHz, $CDCl_3$

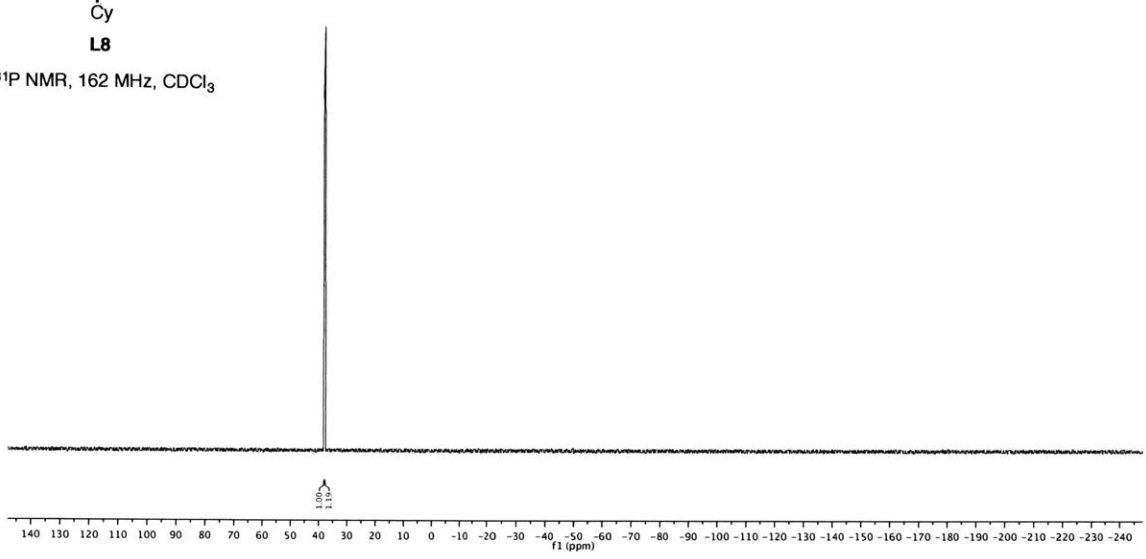

L7

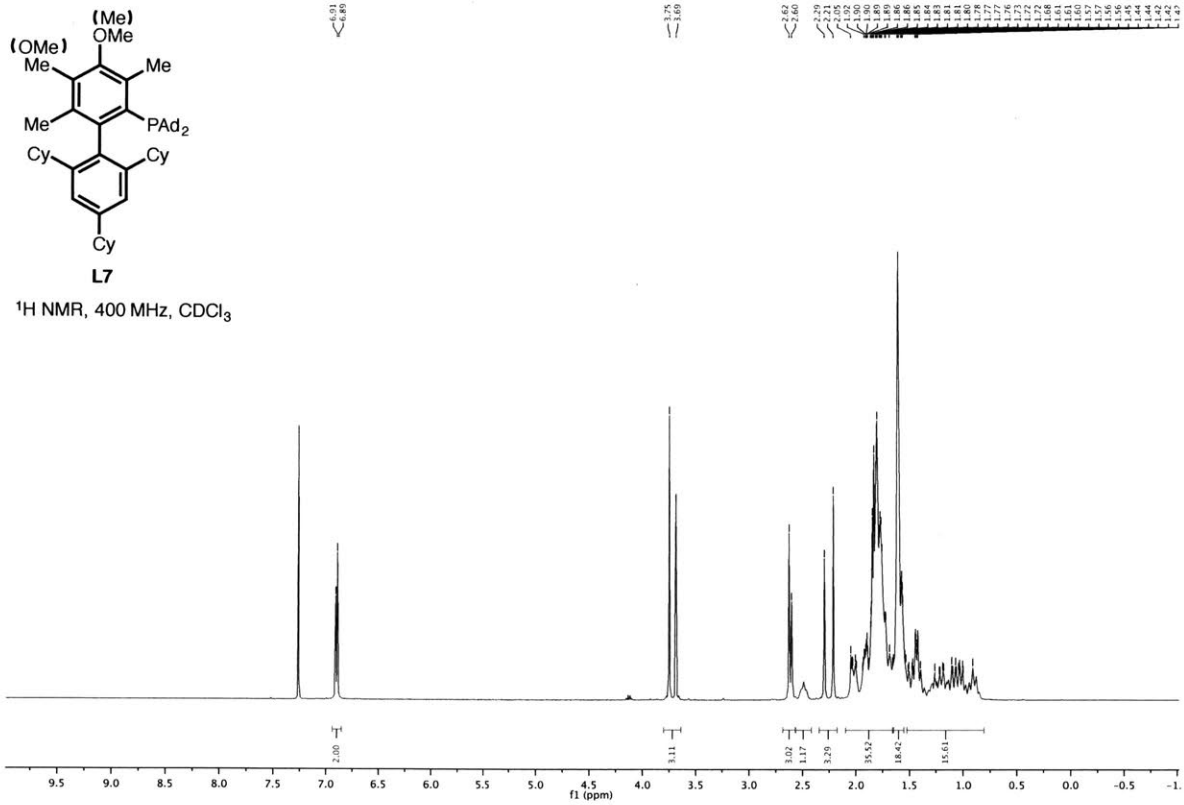
(Me)
OMe
(OMe)
Me
Me
Me
PAd2
Cy
Cy
Cy
L7
1H NMR, 400 MHz, CDCl3
f1 (ppm)

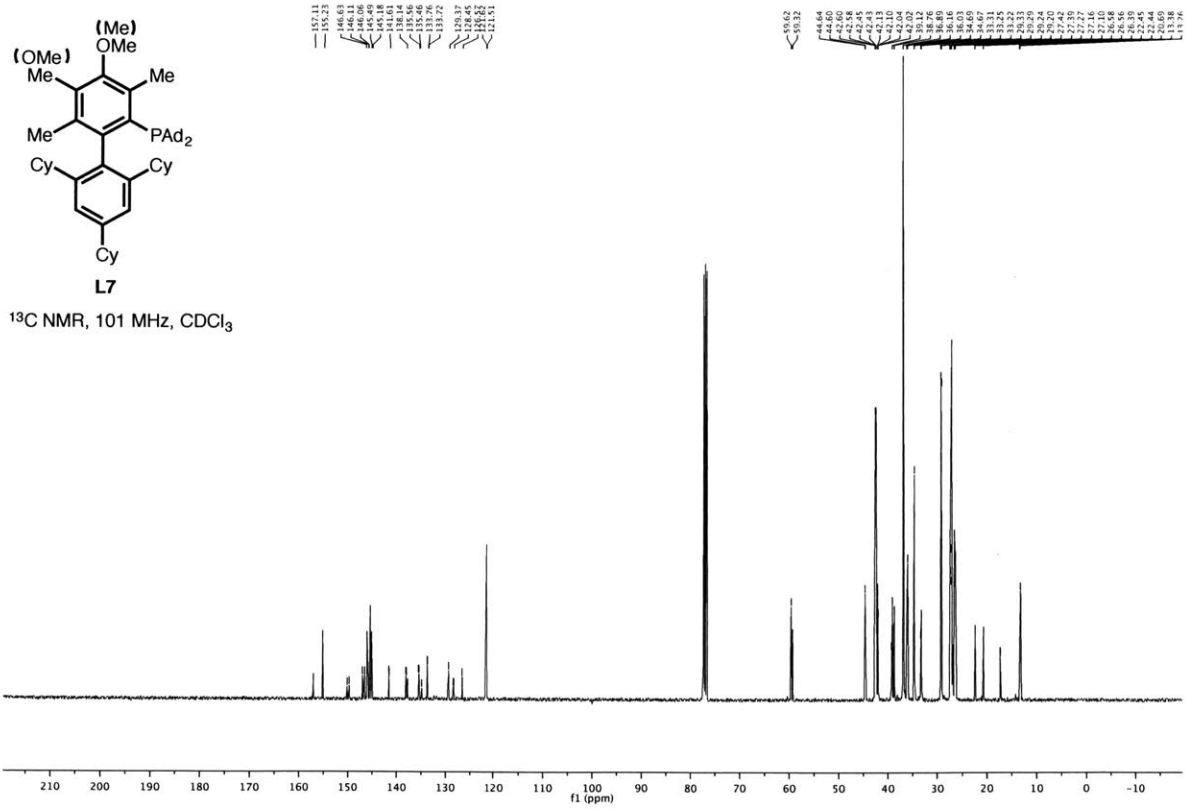
(Me)
OMe
(OMe)
Me
Me
Me
PAd2
Cy
Cy
Cy
L7
13C NMR, 101 MHz, CDCl3
f1 (ppm)

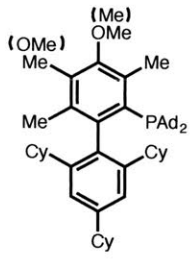

L7

^{31}P NMR, 162 MHz, $CDCl_3$

5-phenyl-3,6-dihydro-2*H*-pyran-4-yl triflouromethanesulfonate (1g)

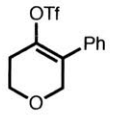

1g

^{1}H NMR, 400 MHz, $CDCl_3$

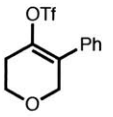

1g

^{13}C NMR, 101 MHz, $CDCl_3$

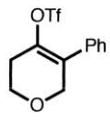

1g

^{19}F NMR, 376 MHz, $CDCl_3$

2-(3-cyanophenyl)cyclopent-1-en-1-yl triflouromethanesulfonate (1l)

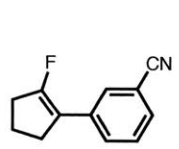

1l

^{1}H NMR, 400 MHz, $CDCl_3$

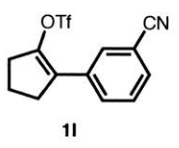

1l

^{13}C NMR, 101 MHz, $CDCl_3$

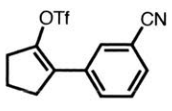

1l

^{19}F NMR, 376 MHz, $CDCl_3$

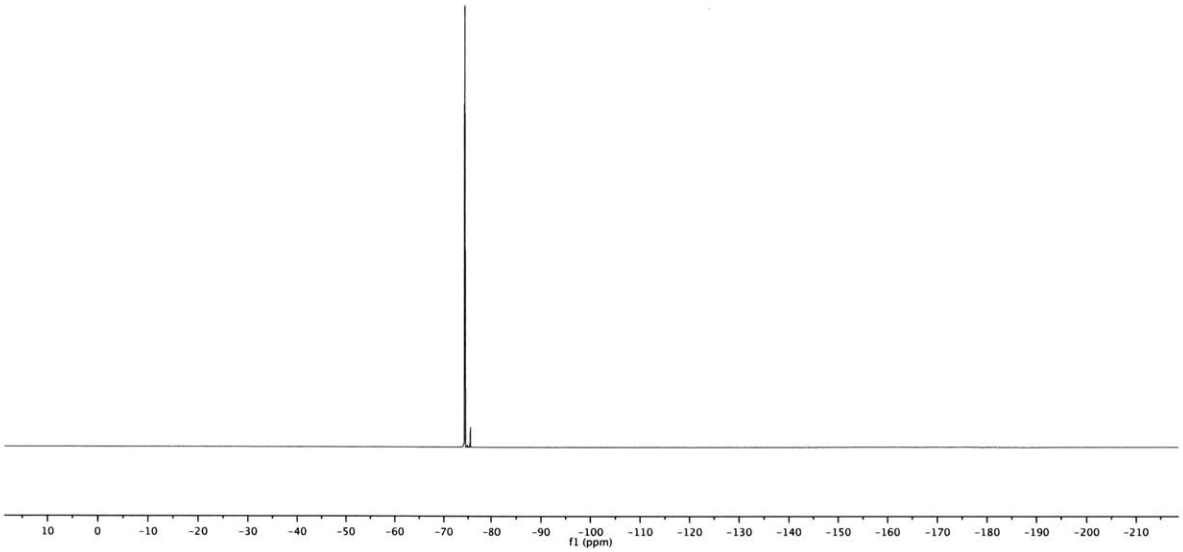

2-(4-(trifluoromethyl)phenyl)cyclopent-1-en-1-yl triflouromethanesulfonate (1m)

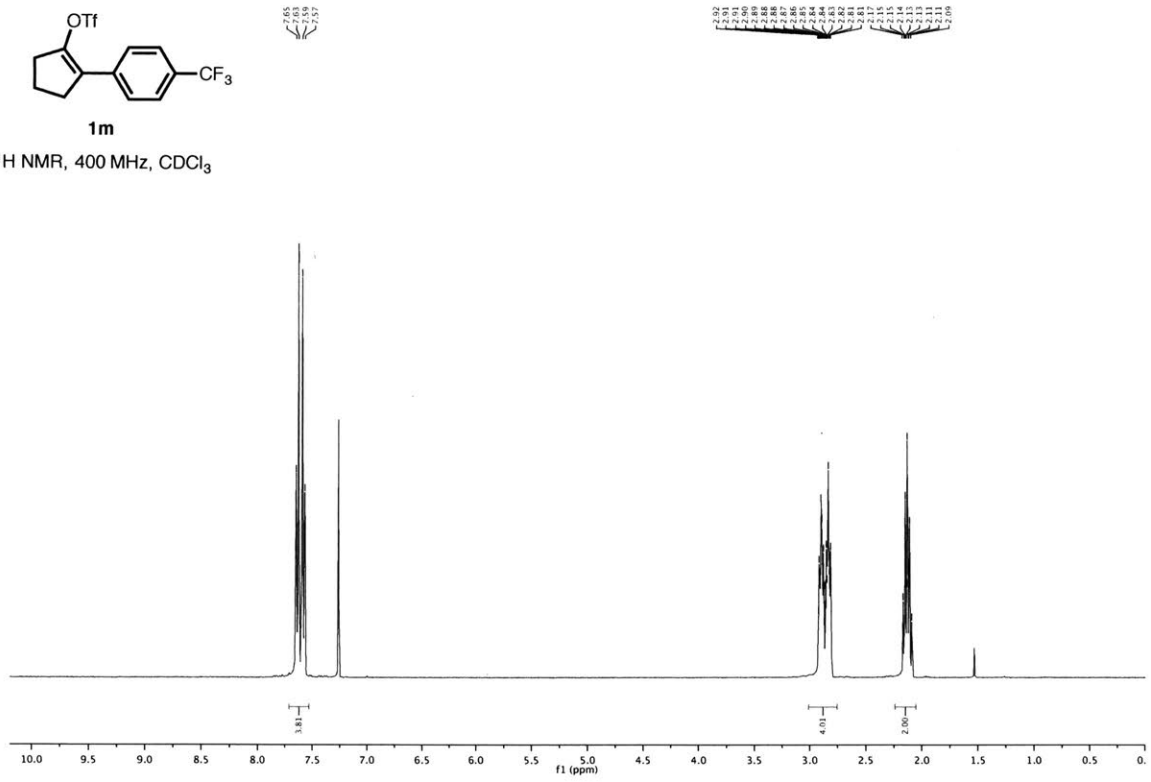

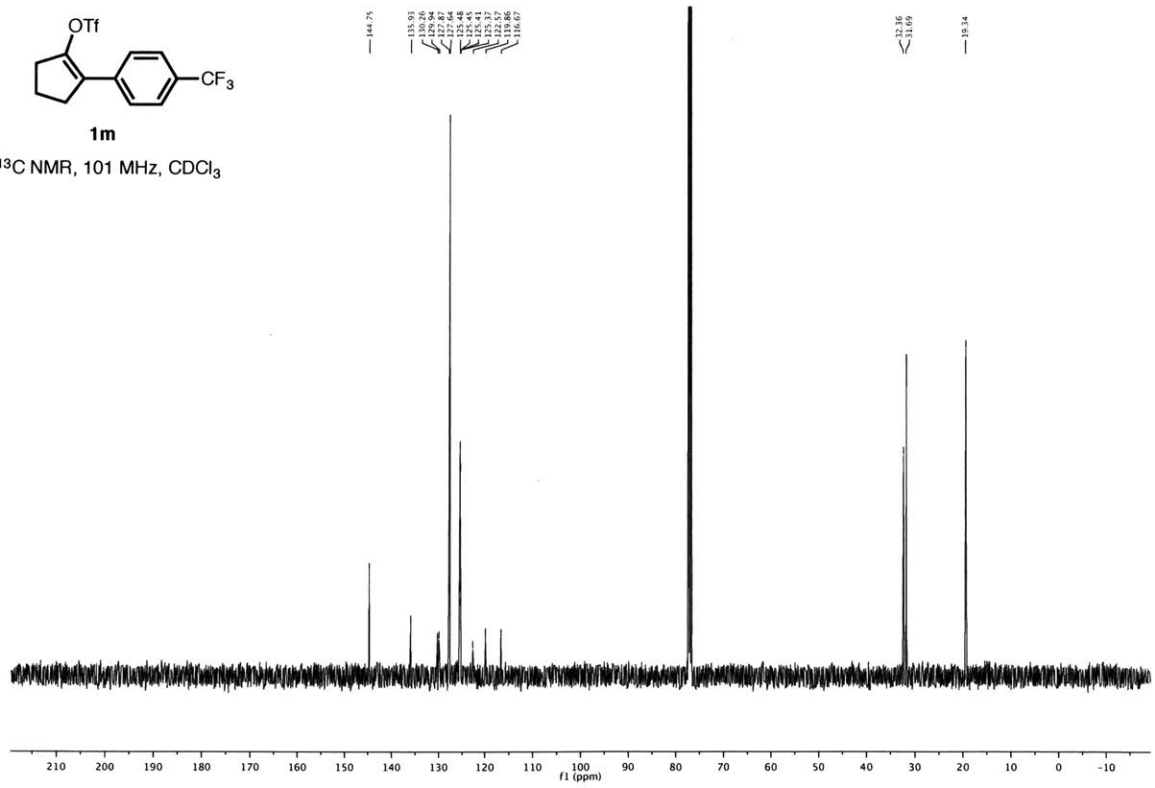

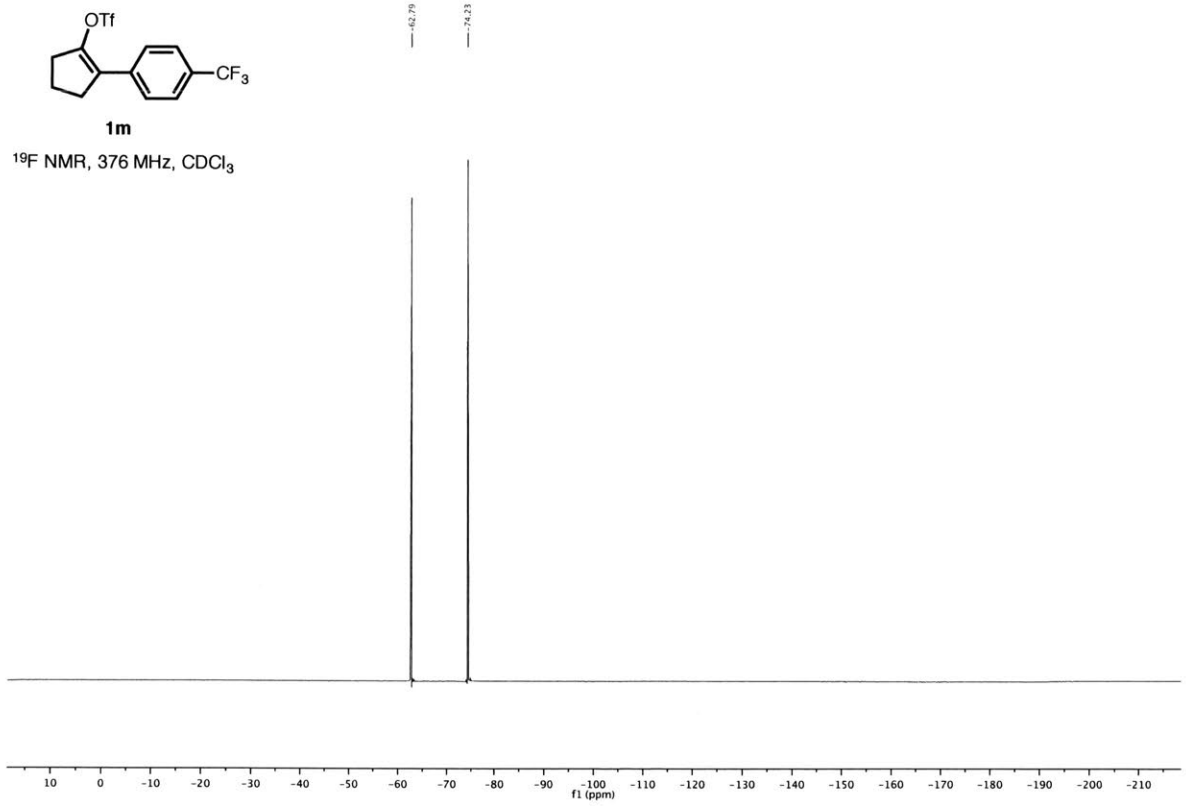
OTf
CF3
1m
19F NMR, 376 MHz, CDCl3
-62.79
-74.23
10 0 -10 -20 -30 -40 -50 -60 -70 -80 -90 -100 -110 -120 -130 -140 -150 -160 -170 -180 -190 -200 -210
f1 (ppm)

2-(4-(diethylcarbamoyl)phenyl)cyclopent-1-en-1-yl triflouromethanesulfonate (1n)

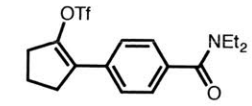

1n

^{1}H NMR, 400 MHz, $CDCl_3$

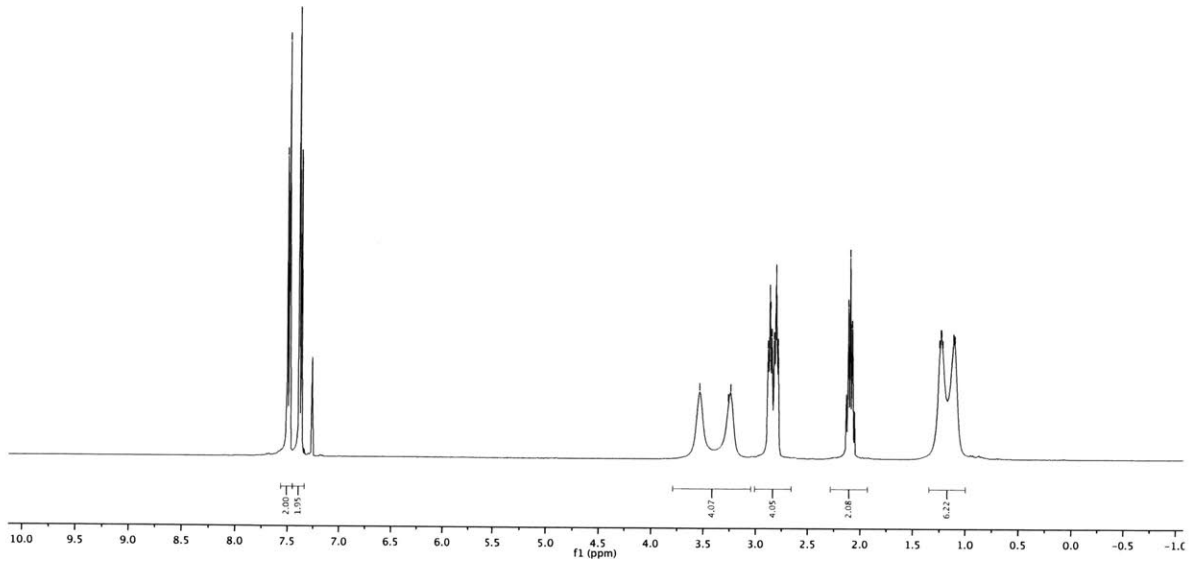

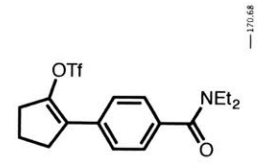

1n

^{13}C NMR, 101 MHz, $CDCl_3$

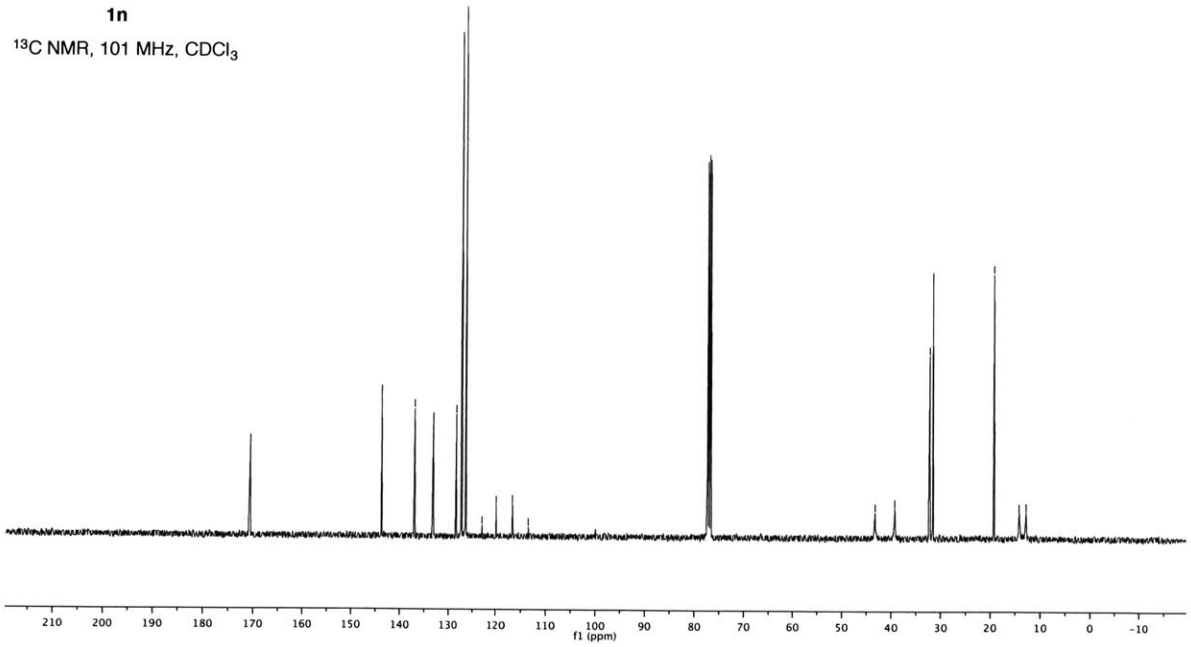

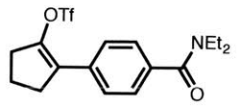

1n

^{19}F NMR, 376 MHz, $CDCl_3$

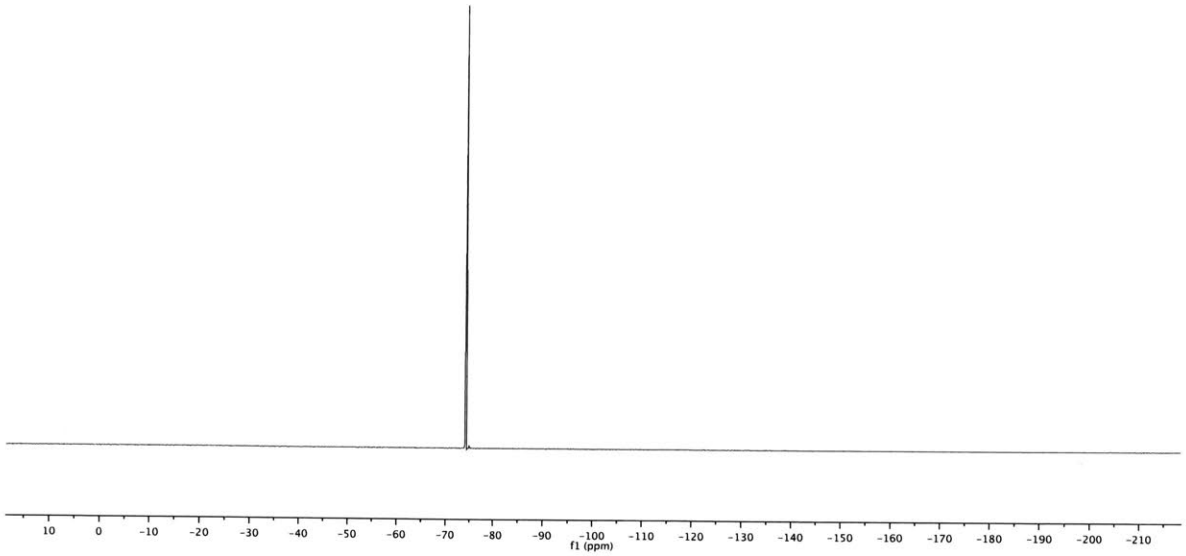

8-(2-methylpyrimidin-5-yl)-6,7-dihydro-5*H*-benzo[7]annulen-9-yl trifluoromethanesulfonate (1p)

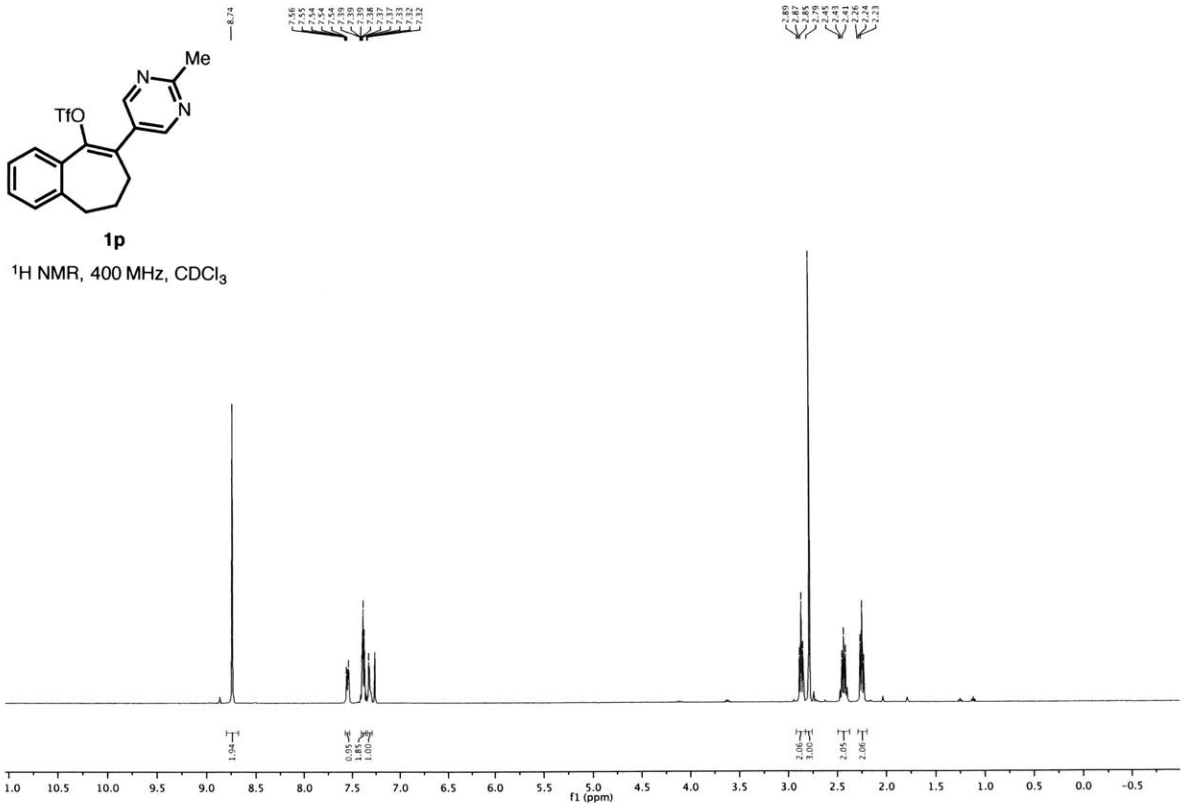

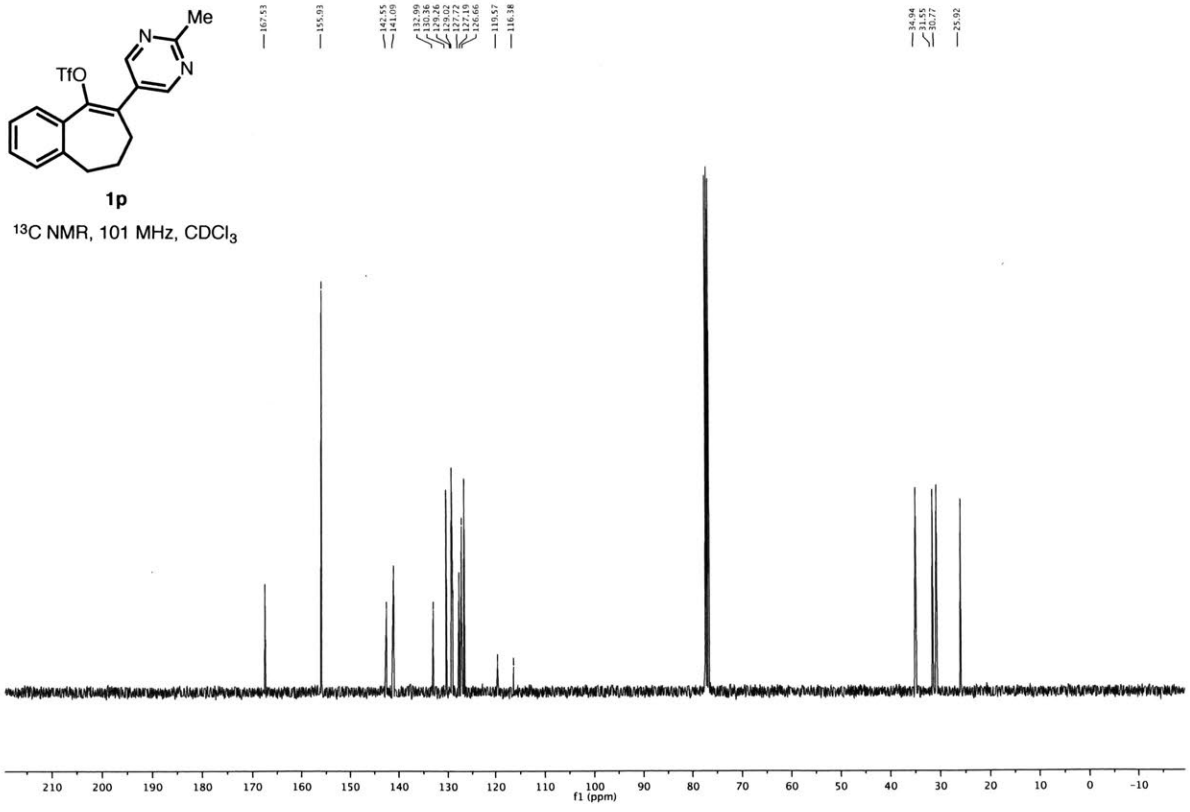

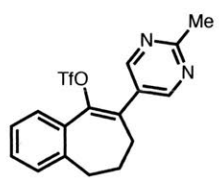

1p

^{19}F NMR, 376 MHz, $CDCl_3$

8-(6-methoxypyridin-3-yl)-6,7-dihydro-5H-benzo[7]annulen-9-yl triflouromethanesulfonate (1q)

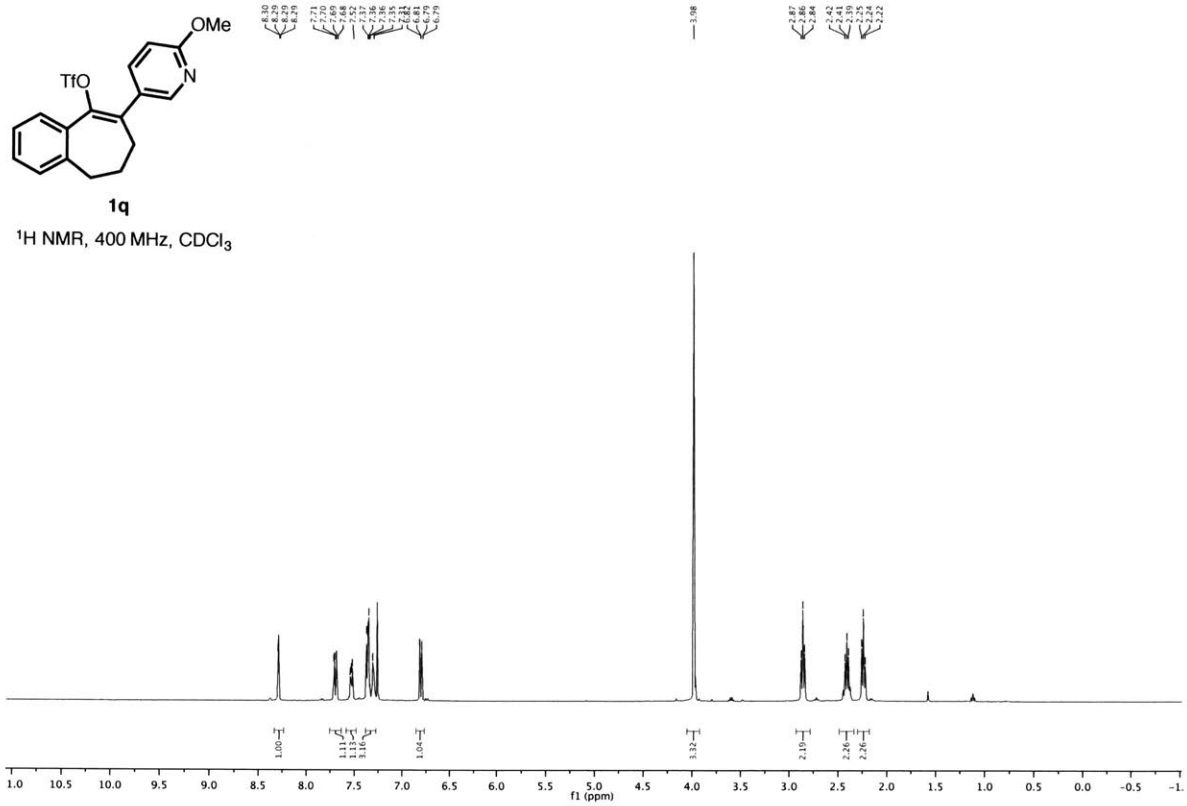

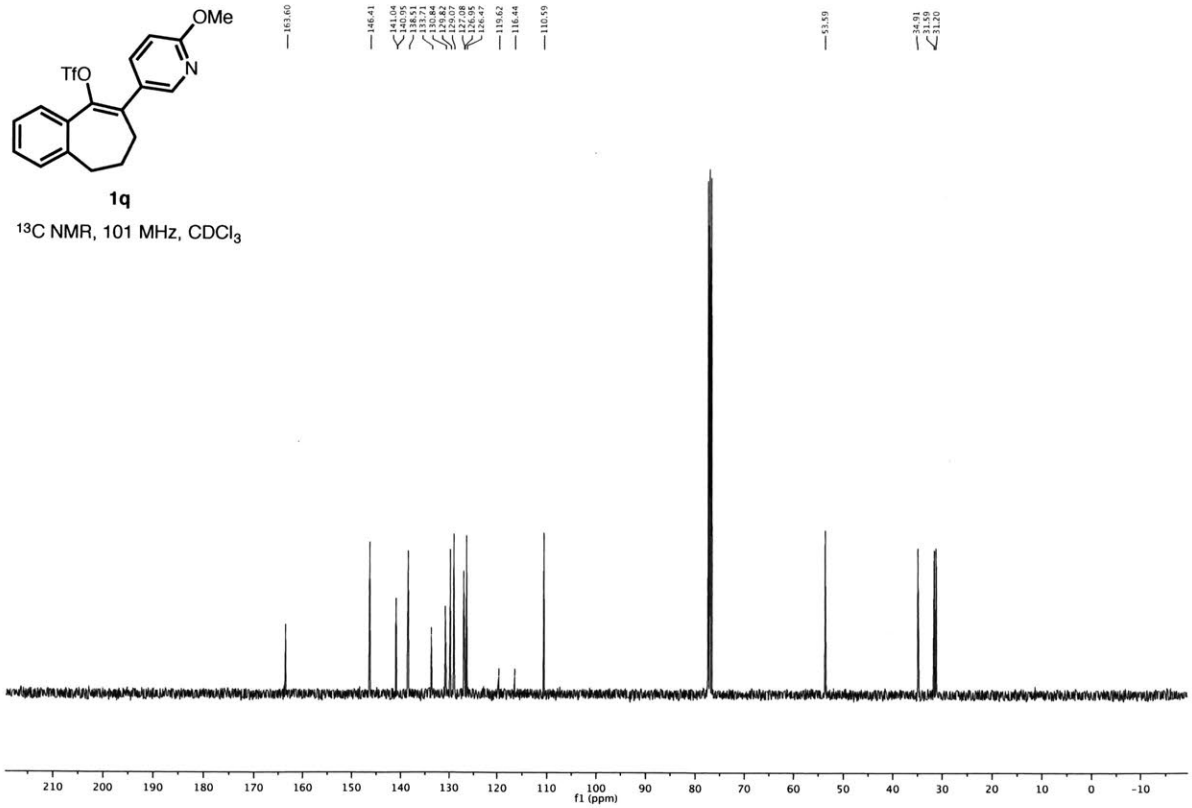

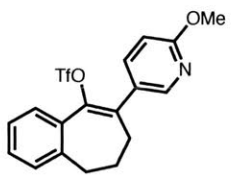

1q

^{19}F NMR, 376 MHz, $CDCl_3$

8-(4-nitrophenyl)-6,7-dihydro-5*H*-benzo[7]annulen-9-yl triflouromethanesulfonate (1r)

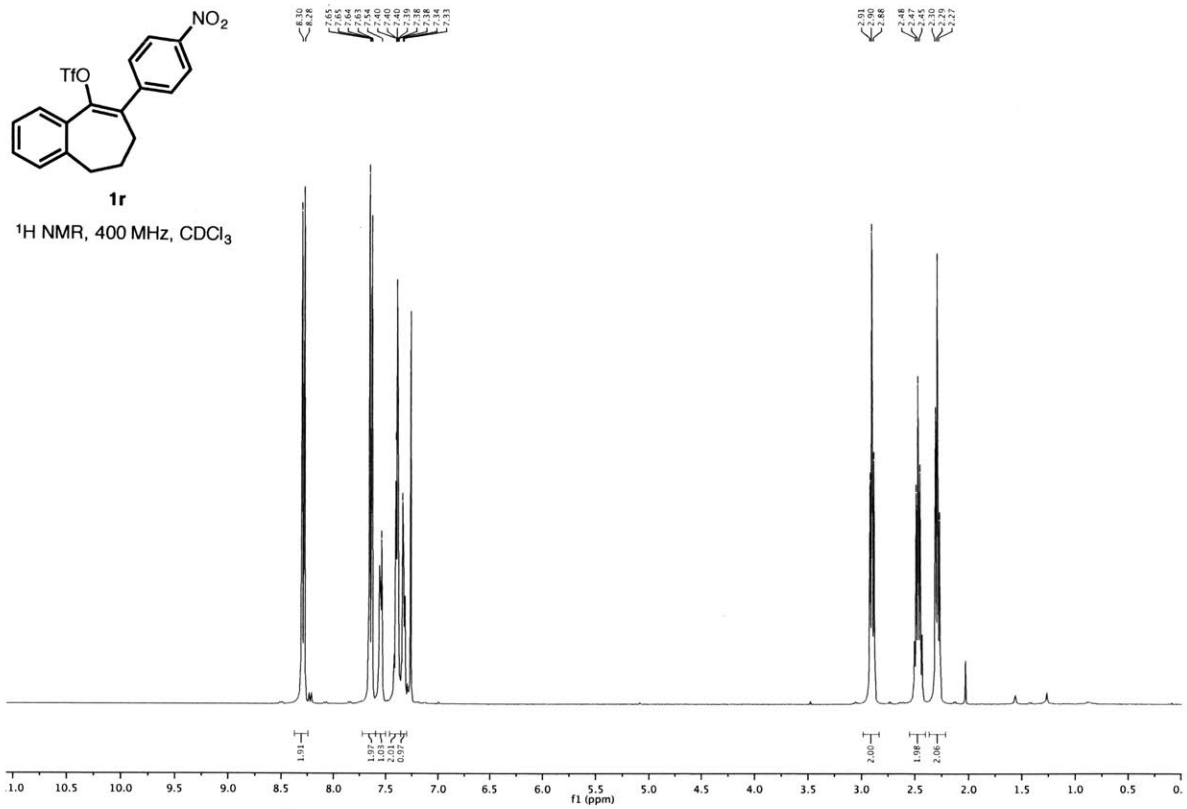

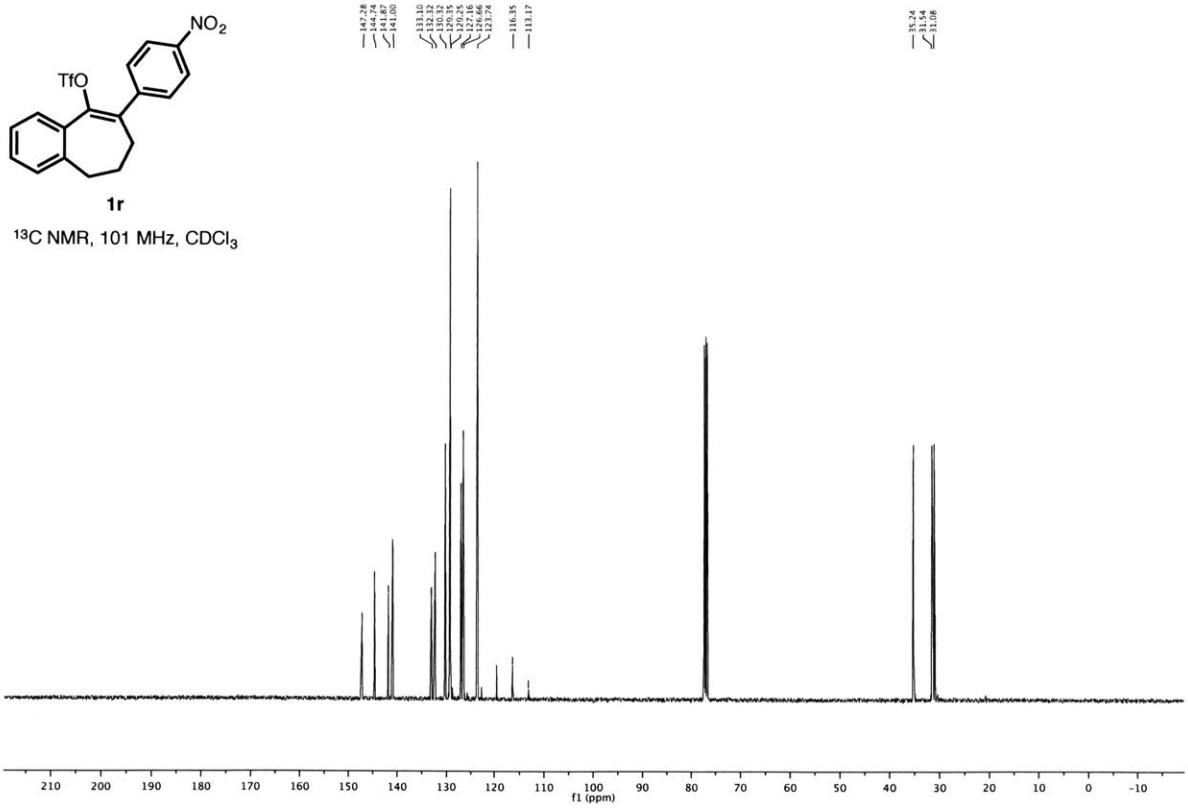

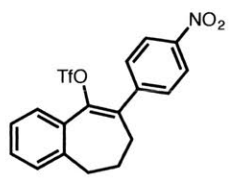

1r

^{19}F NMR, 376 MHz, $CDCl_3$

4-fluoro-1,2,3,6-tetrahydro-1,1'-biphenyl (2a)

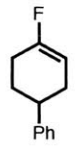

2a

^{1}H NMR, 400 MHz, $CDCl_3$

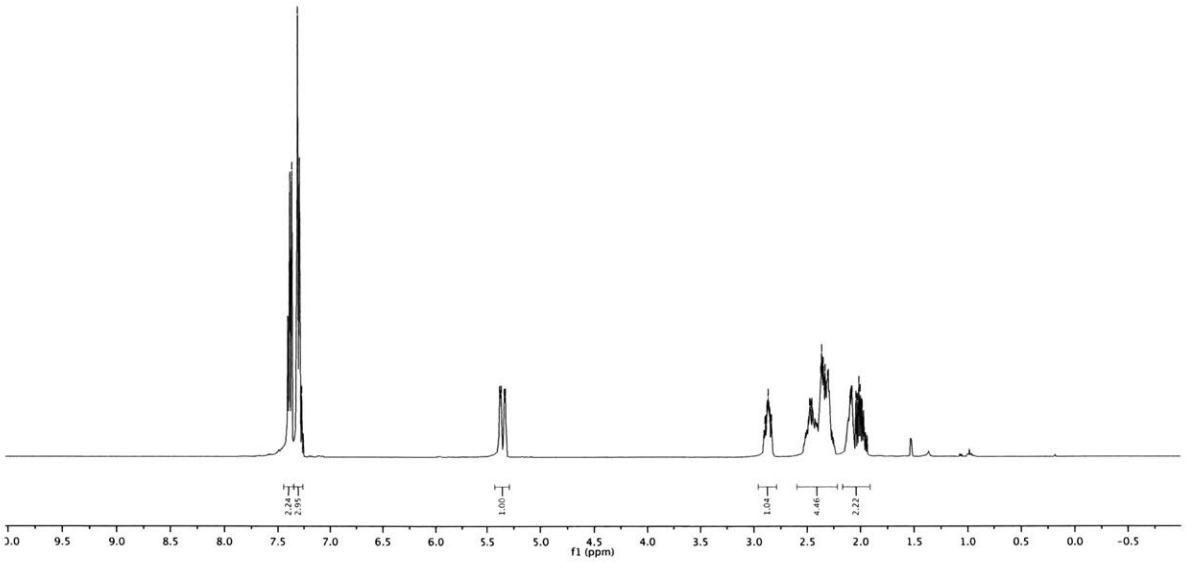

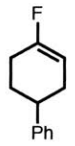

2a

^{13}C NMR, 101 MHz, $CDCl_3$

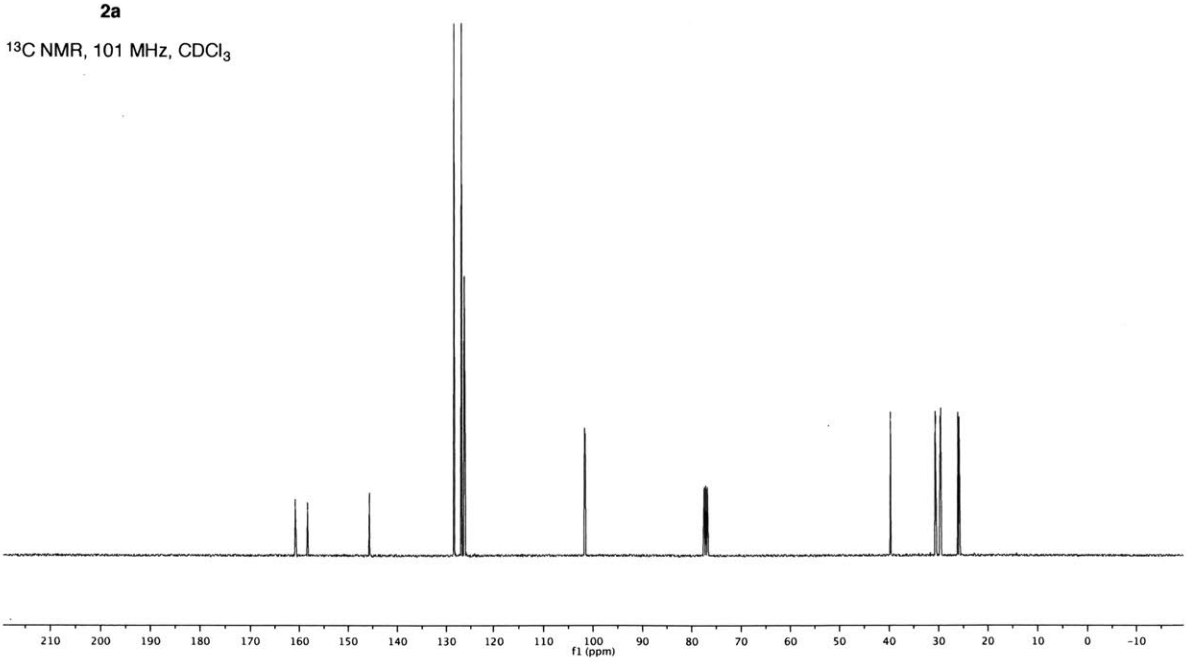

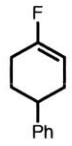

2a

^{19}F NMR, 376 MHz, $CDCl_3$

6-fluoro-2,3,4,5-tetrahydro-1,1'-biphenyl (2b)

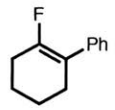

2b

^{1}H NMR, 400 MHz, $CDCl_3$

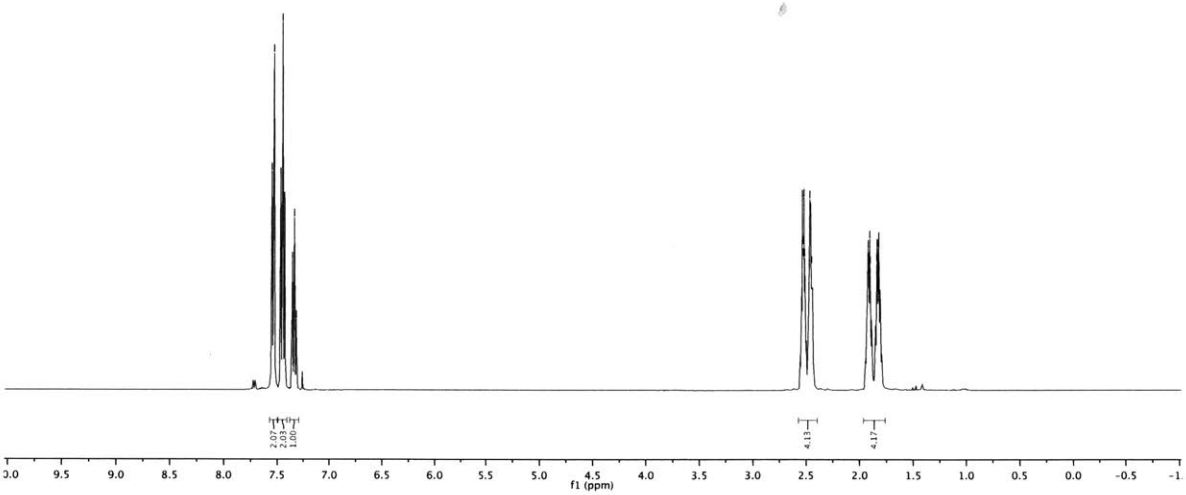

1-fluoro-4-pentylcyclohex-1-ene (2c)

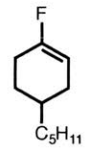

2c

^{1}H NMR, 400 MHz, $CDCl_3$

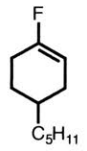

2c

^{13}C NMR, 101 MHz, $CDCl_3$

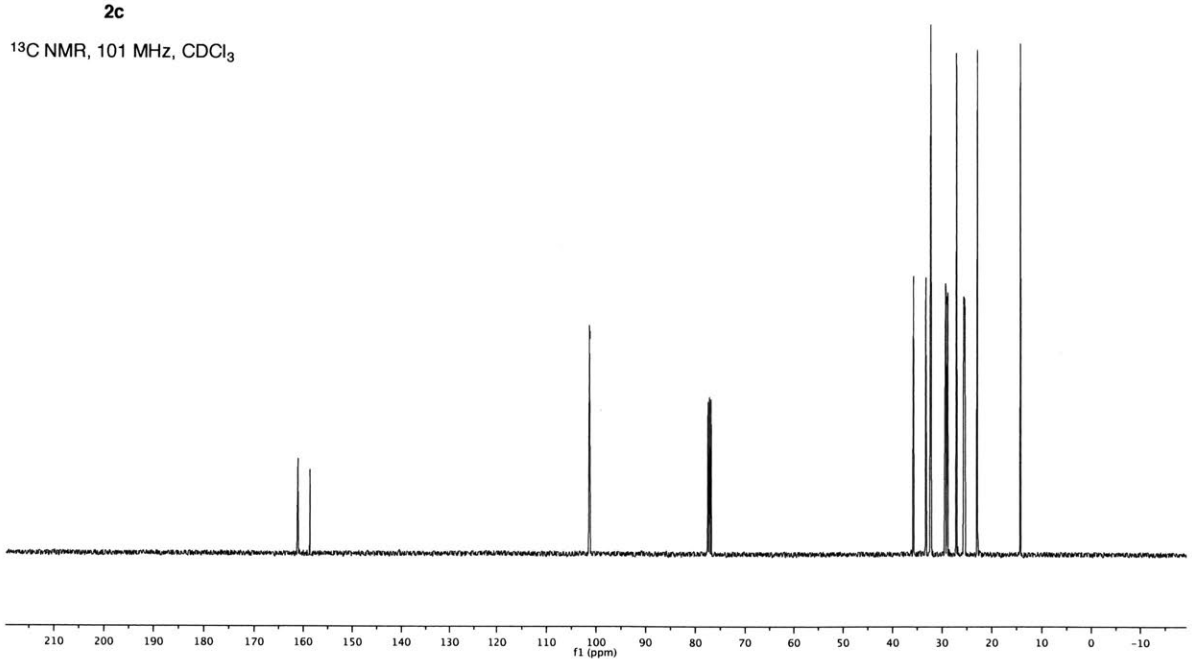

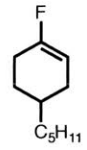

2c

^{19}F NMR, 376 MHz, $CDCl_3$

9-fluoro-3,3-dimethyl-1,5-dioxaspiro[5.5]undec-8-ene (2d)

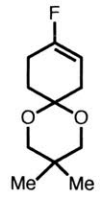

2d

^{1}H NMR, 400 MHz, $CDCl_3$

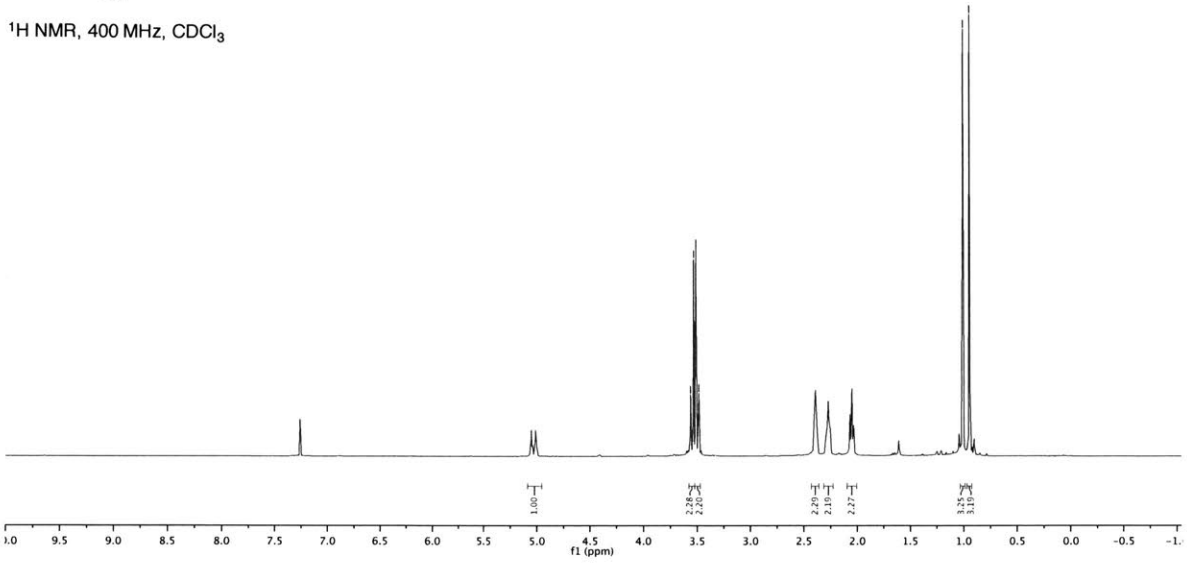

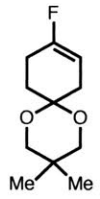

2d

^{13}C NMR, 101 MHz, $CDCl_3$

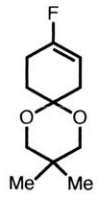

2d

^{19}F NMR, 376 MHz, $CDCl_3$

3-(3-fluorocyclohex-2-en-1-yl)-1-methyl-1*H*-indole (2e)

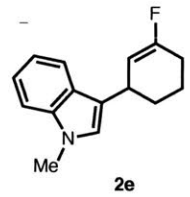

2e

^{1}H NMR, 400 MHz, $CDCl_3$

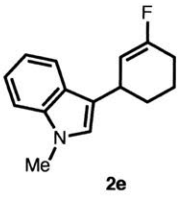

2e

^{13}C NMR, 101 MHz, $CDCl_3$

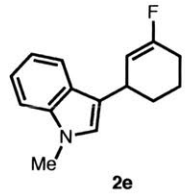

2e

^{19}F NMR, 376 MHz, $CDCl_3$

3-fluoro-6-methoxy-1,2-dihydronaphthalene (2f)

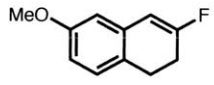

2f

^{1}H NMR, 400 MHz, $CDCl_3$

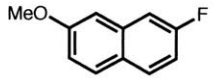

< 5%

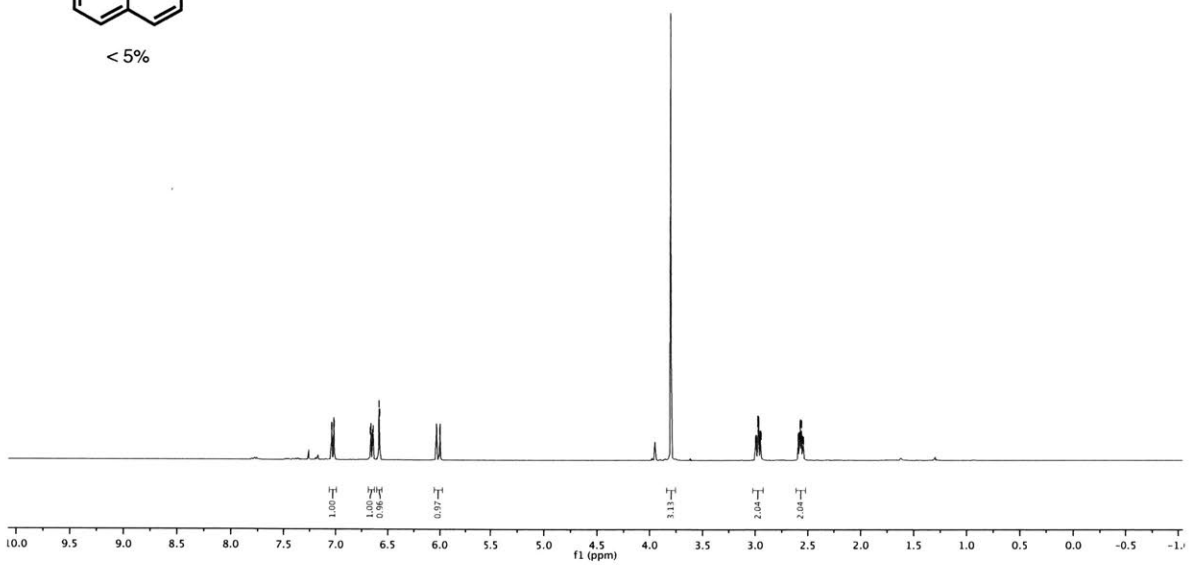

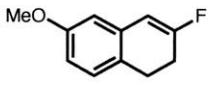

2f

^{13}C NMR, 101 MHz, $CDCl_3$

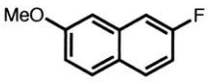

< 5%

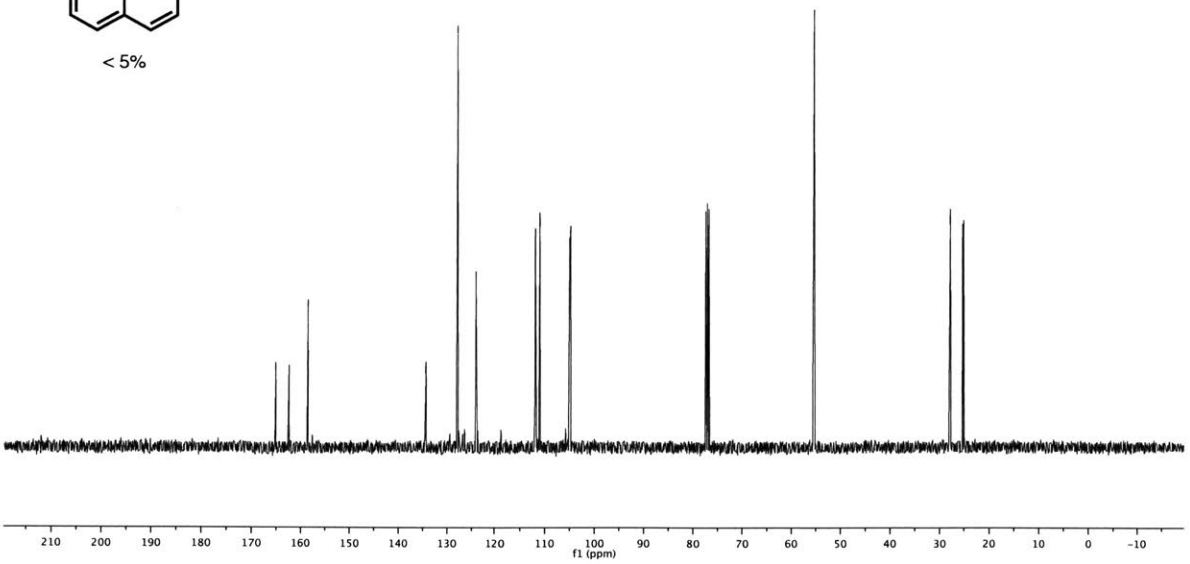

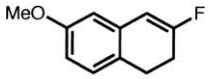

2f

^{19}F NMR, 376 MHz, $CDCl_3$

4-fluoro-5-phenyl-3,6-dihydro-2*H*-pyran (2g)

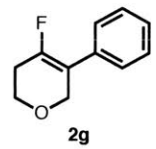

2g

^{1}H NMR, 400 MHz, $CDCl_3$

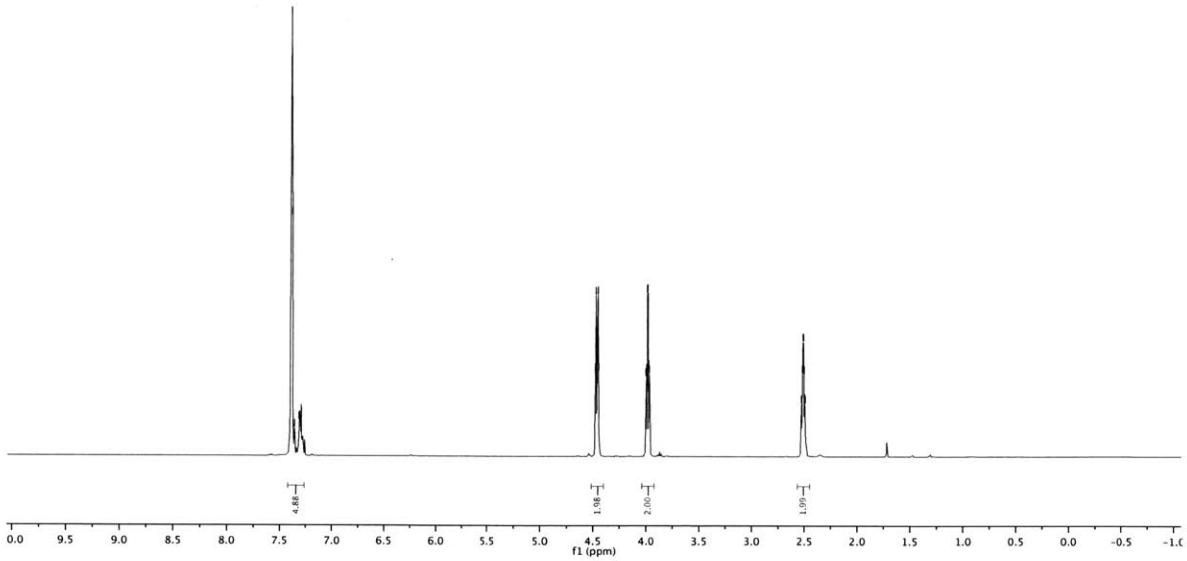

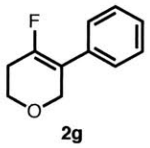

2g

^{13}C NMR, 101 MHz, $CDCl_3$

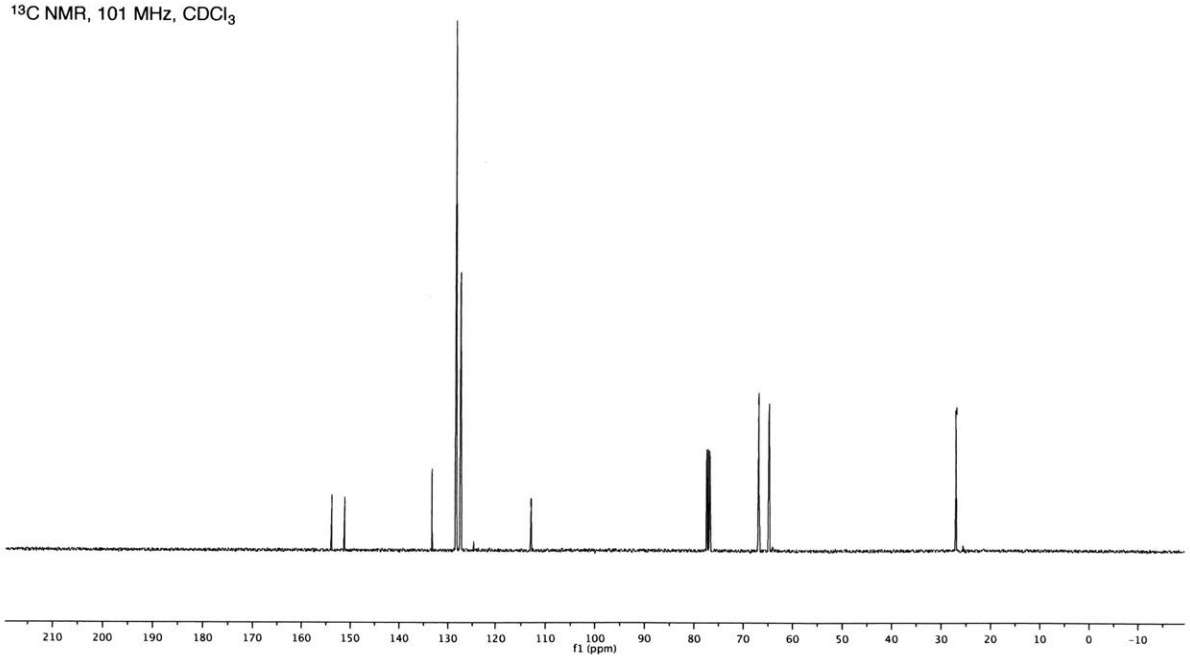

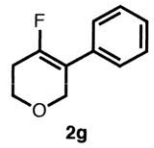

2g

^{19}F NMR, 376 MHz, $CDCl_3$

4-fluoro-5-phenyl-3,6-dihydro-2*H*-pyran (2h)

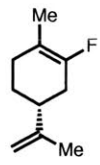

2h

^{1}H NMR, 400 MHz, $CDCl_3$

(8*S*,9*S*,10*R*,13*R*,14*S*)-3-fluoro-10,13-dimethyl-17-((*R*)-6-methylheptan-2-yl)-2,7,8,9,10,11,12,13,14,15,16,17-dodecahydro-1*H*-cyclopenta[*a*]phenanthrene (2i)

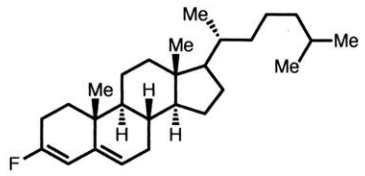

2i

^{1}H NMR, 400 MHz, $CDCl_3$

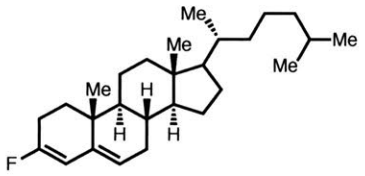

2i

^{13}C NMR, 101 MHz, $CDCl_3$

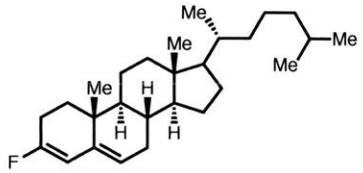

2i

^{19}F NMR, 376 MHz, $CDCl_3$

(4a*S*,5*R*)-7-fluoro-4a,5-dimethyl-3-(propan-2-ylidene)-1,2,3,4,4a,5-hexahydronaphthalene

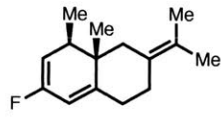

2i

^{1}H NMR, 400 MHz, $CDCl_3$

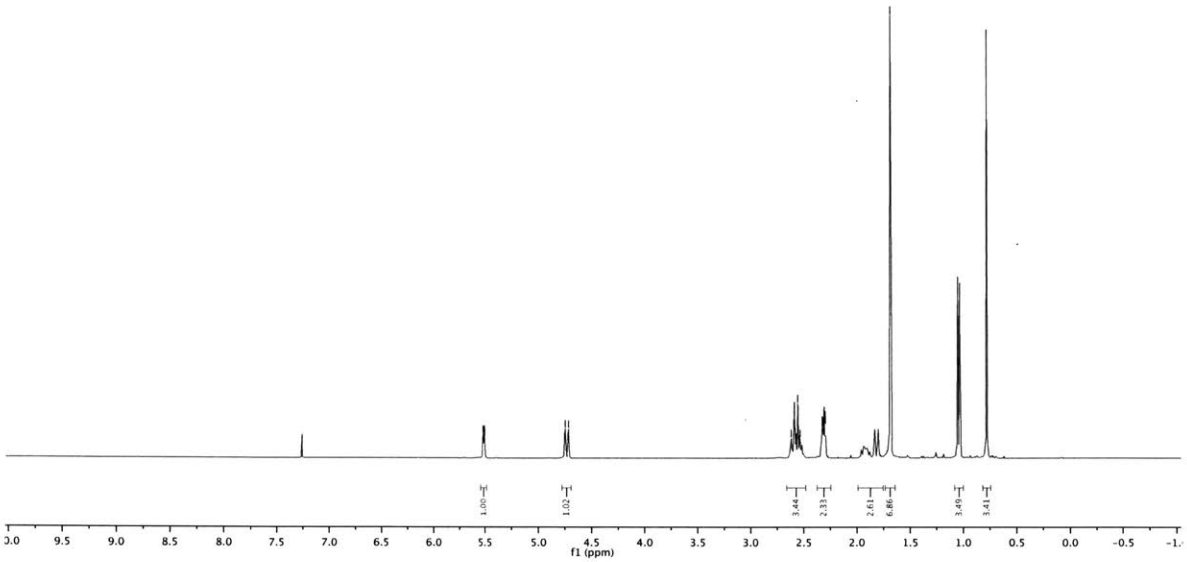

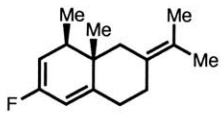

2j

^{13}C NMR, 101 MHz, $CDCl_3$

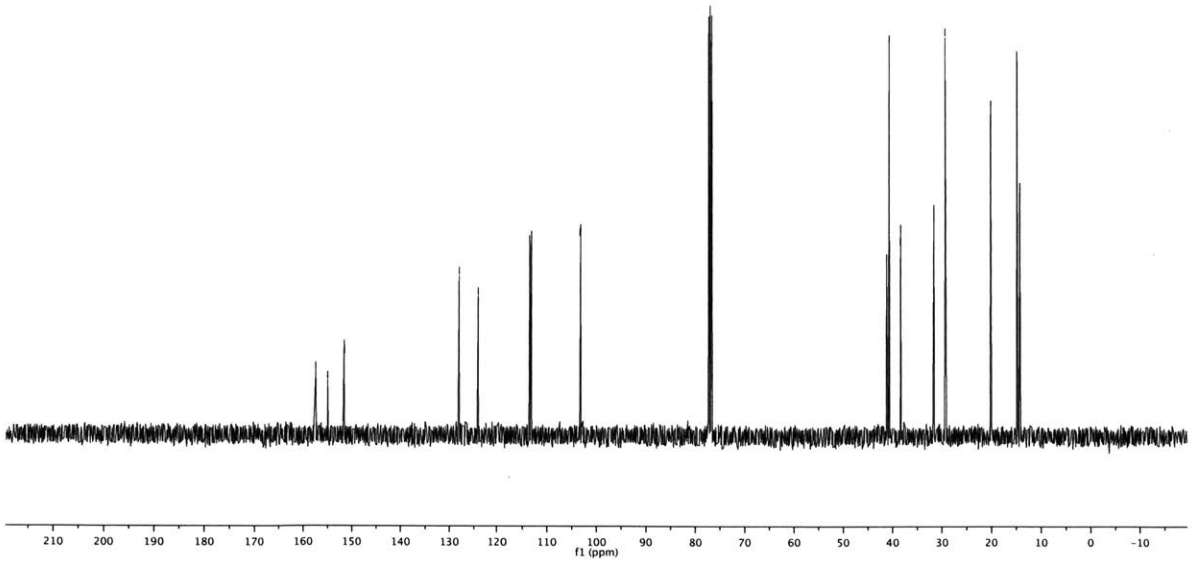

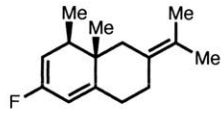

2j

^{19}F NMR, 376 MHz, $CDCl_3$

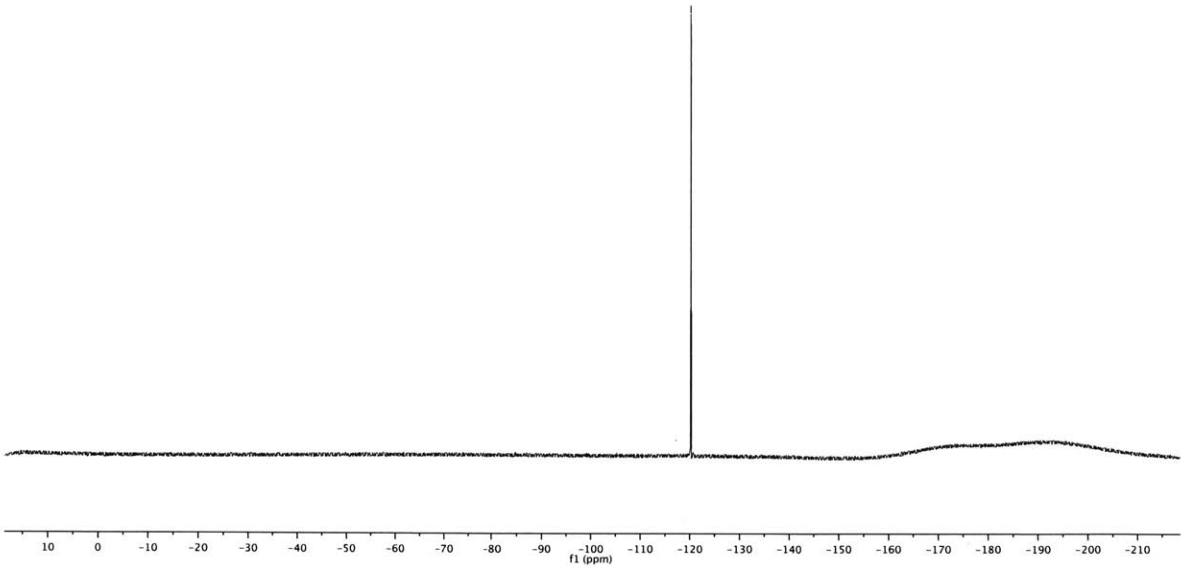

3-(2-fluorocyclopent-1-en-1-yl)benzonitrile (2l)

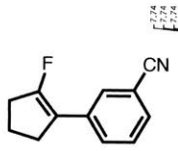

2l

^{1}H NMR, 400 MHz, $CDCl_3$

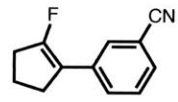

2l

^{13}C NMR, 101 MHz, $CDCl_3$

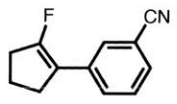

2l

^{19}F NMR, 376 MHz, $CDCl_3$

1-(2-fluorocyclopent-1-en-1-yl)-4-(trifluoromethyl)benzene (2m)

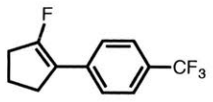

2m

^{1}H NMR, 400 MHz, $CDCl_3$

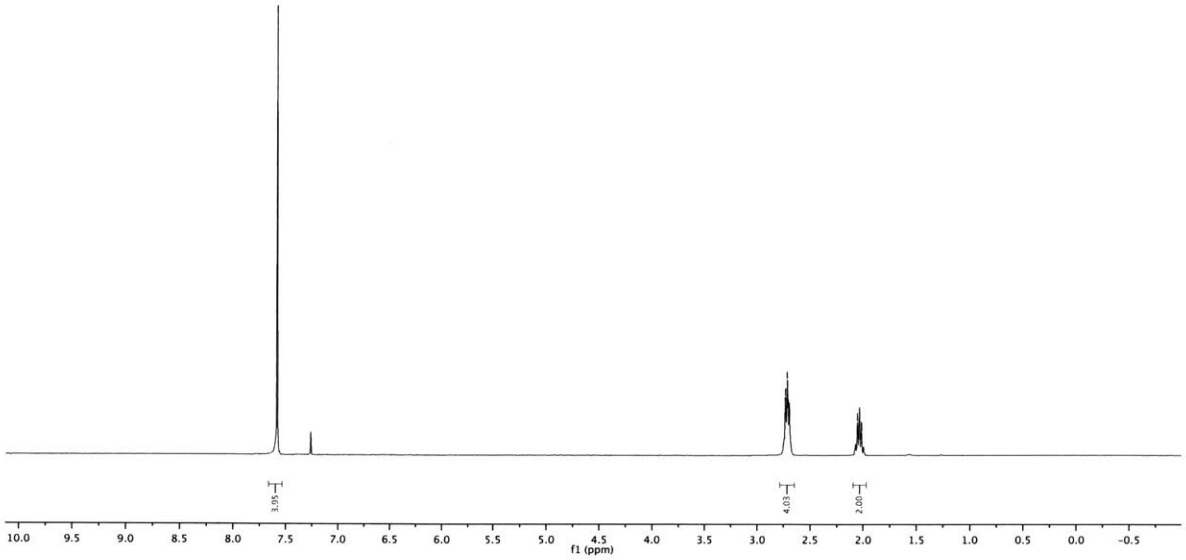

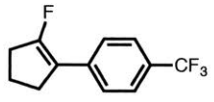

2m

^{13}C NMR, 101 MHz, $CDCl_3$

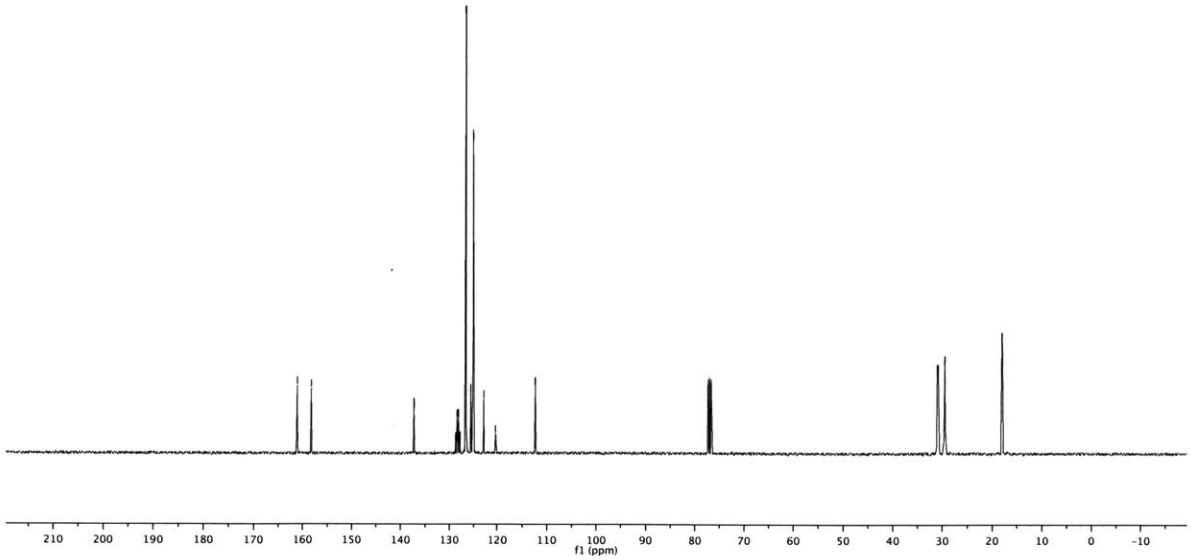

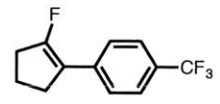

2m

^{19}F NMR, 376 MHz, $CDCl_3$

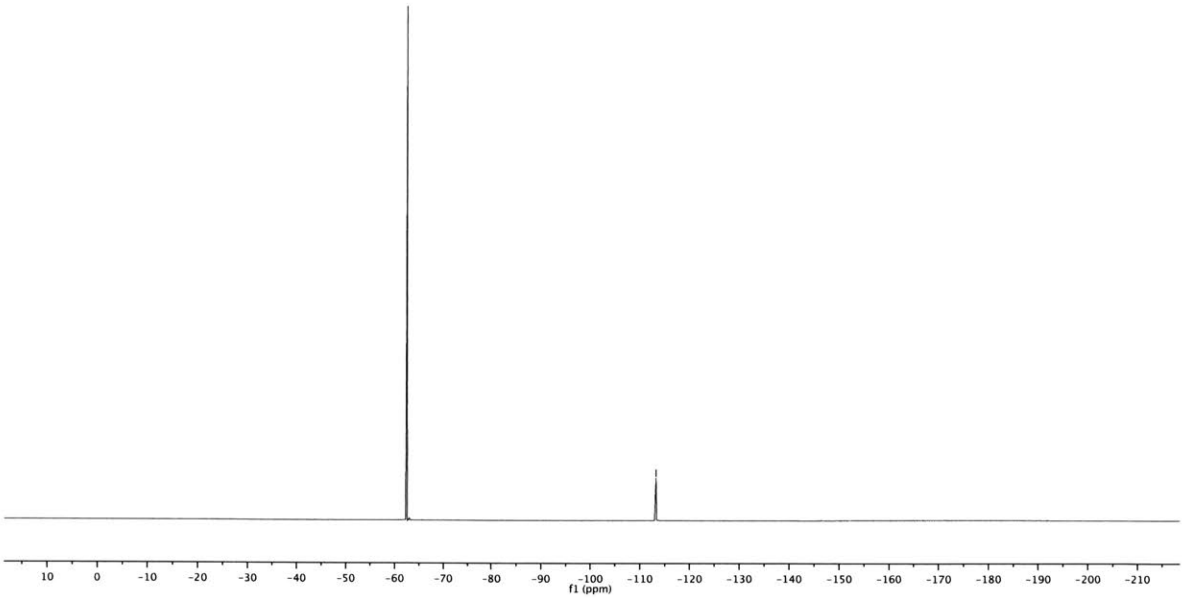

N,*N*-diethyl-4-(2-fluorocyclopent-1-en-1-yl)benzamide (2n)

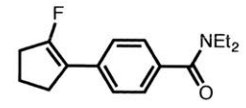

2n

^{1}H NMR, 400 MHz, $CDCl_3$

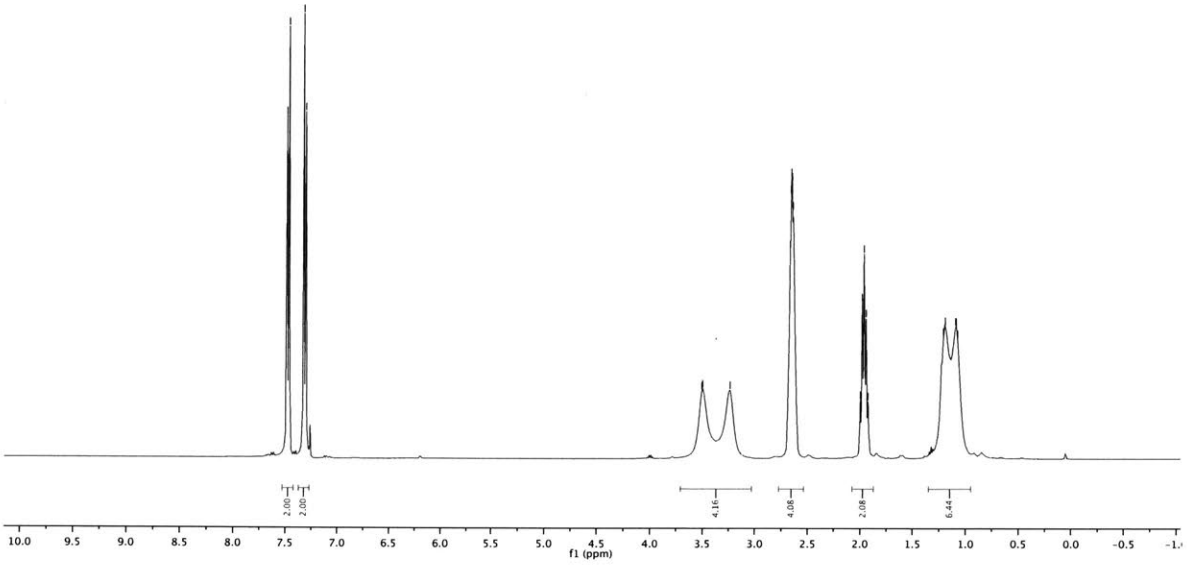

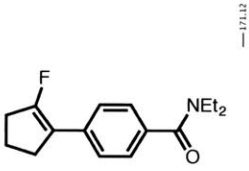

2n

^{13}C NMR, 101 MHz, $CDCl_3$

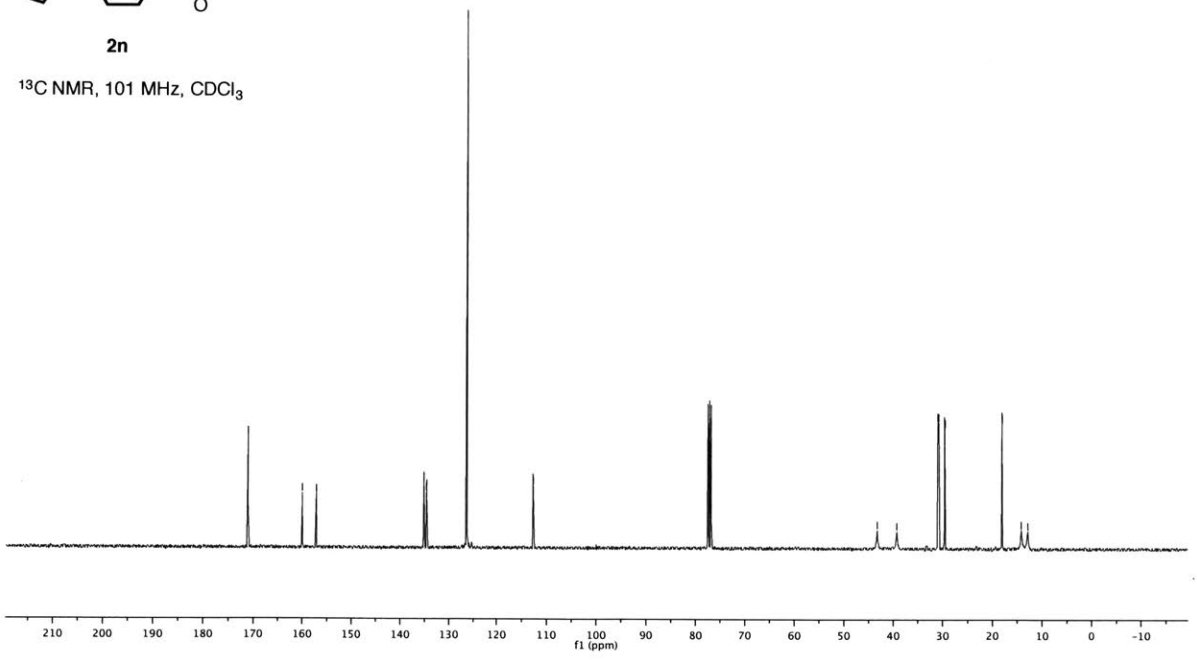

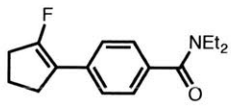

2n

^{19}F NMR, 376 MHz, $CDCl_3$

5-(9-fluoro-6,7-dihydro-5*H*-benzo[7]annulen-8-yl)-2-methylpyrimidine (2p)

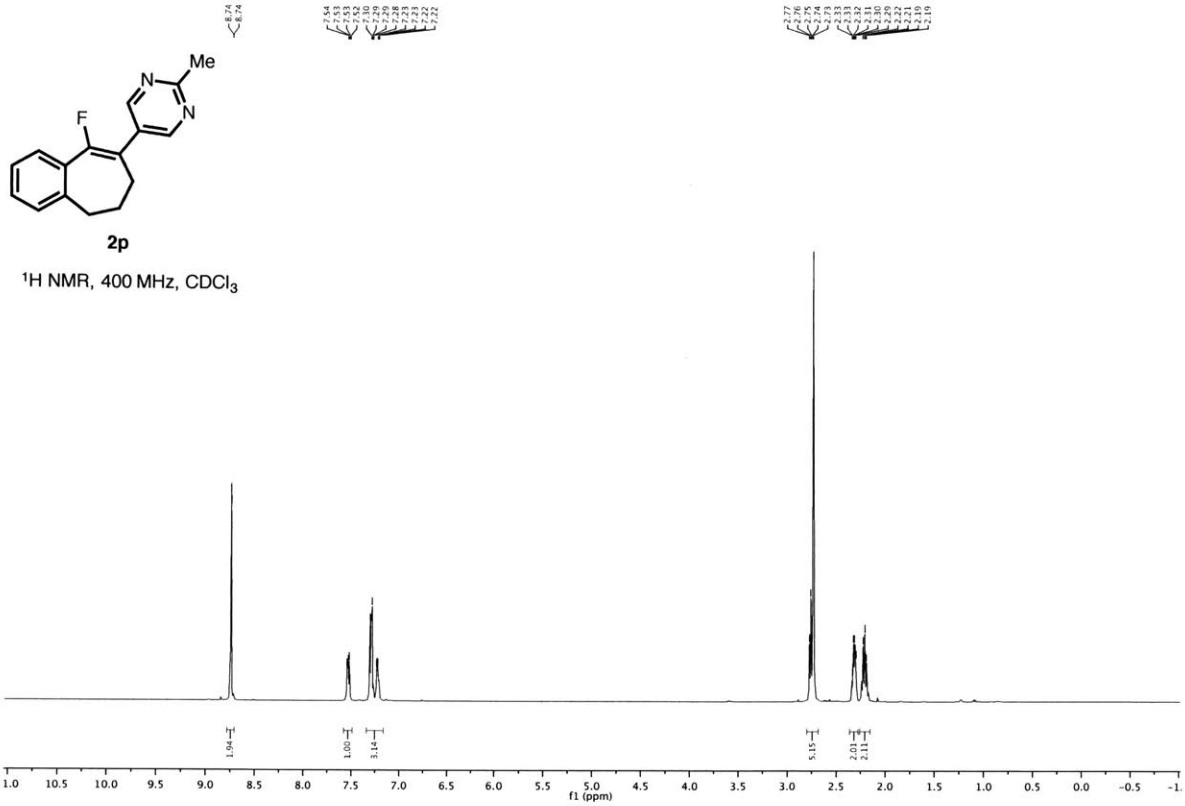

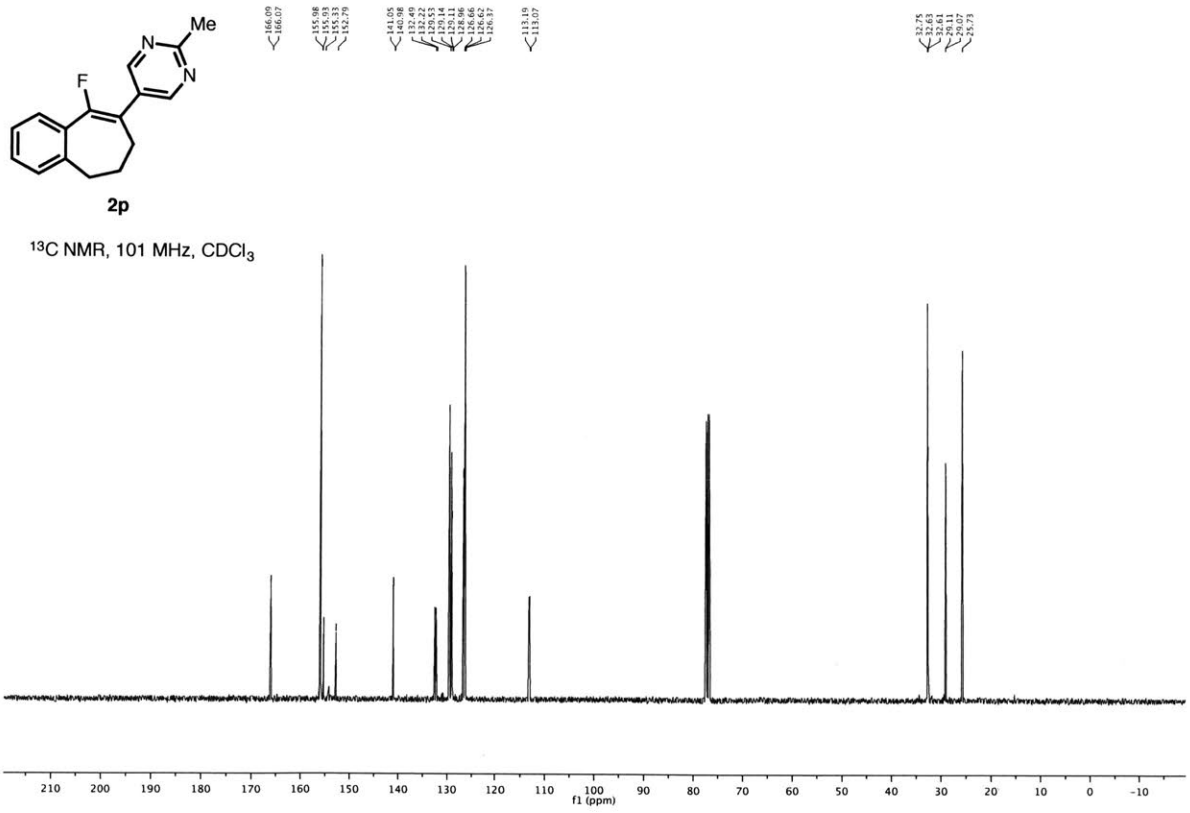

2p

^{19}F NMR, 376 MHz, $CDCl_3$

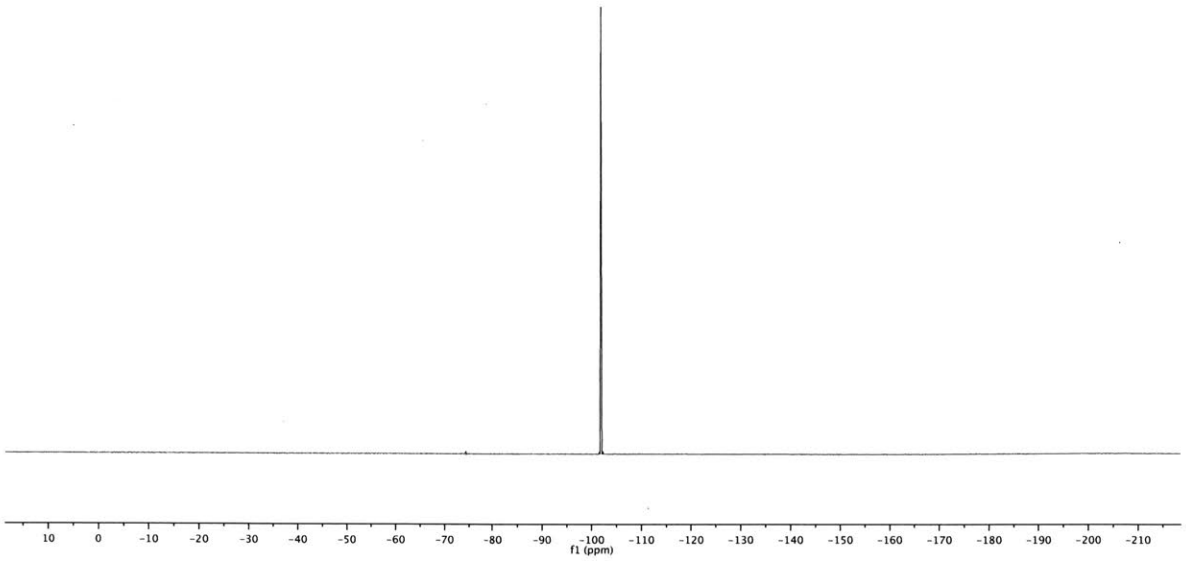

5-(9-fluoro-6,7-dihydro-5*H*-benzo[7]annulen-8-yl)-2-methoxypyridine (2q)

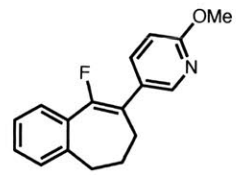

2q

^{1}H NMR, 400 MHz, $CDCl_3$

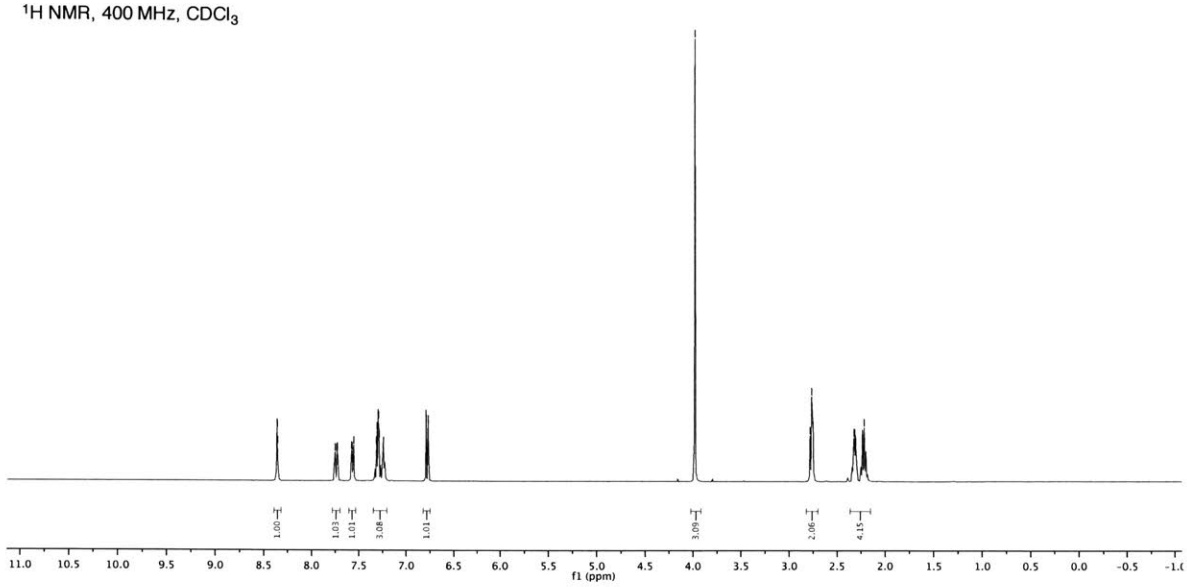

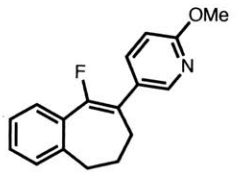

2q

^{13}C NMR, 101 MHz, $CDCl_3$

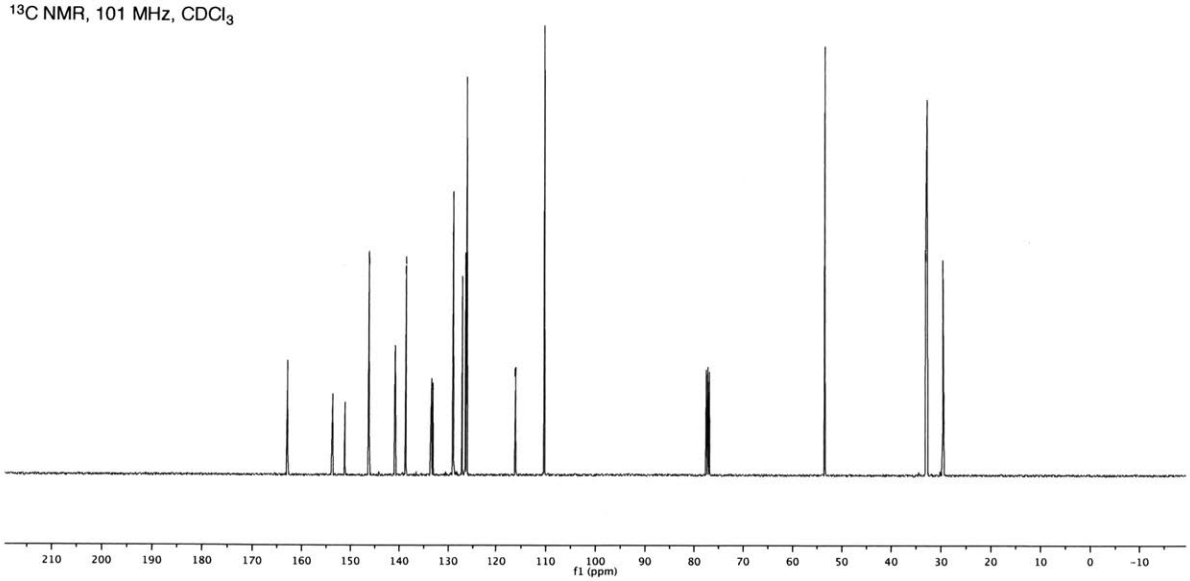

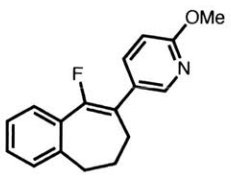

2q

^{19}F NMR, 376 MHz, $CDCl_3$

9-fluoro-8-(4-nitrophenyl)-6,7-dihydro-5*H*-benzo[7]annulene (2r)

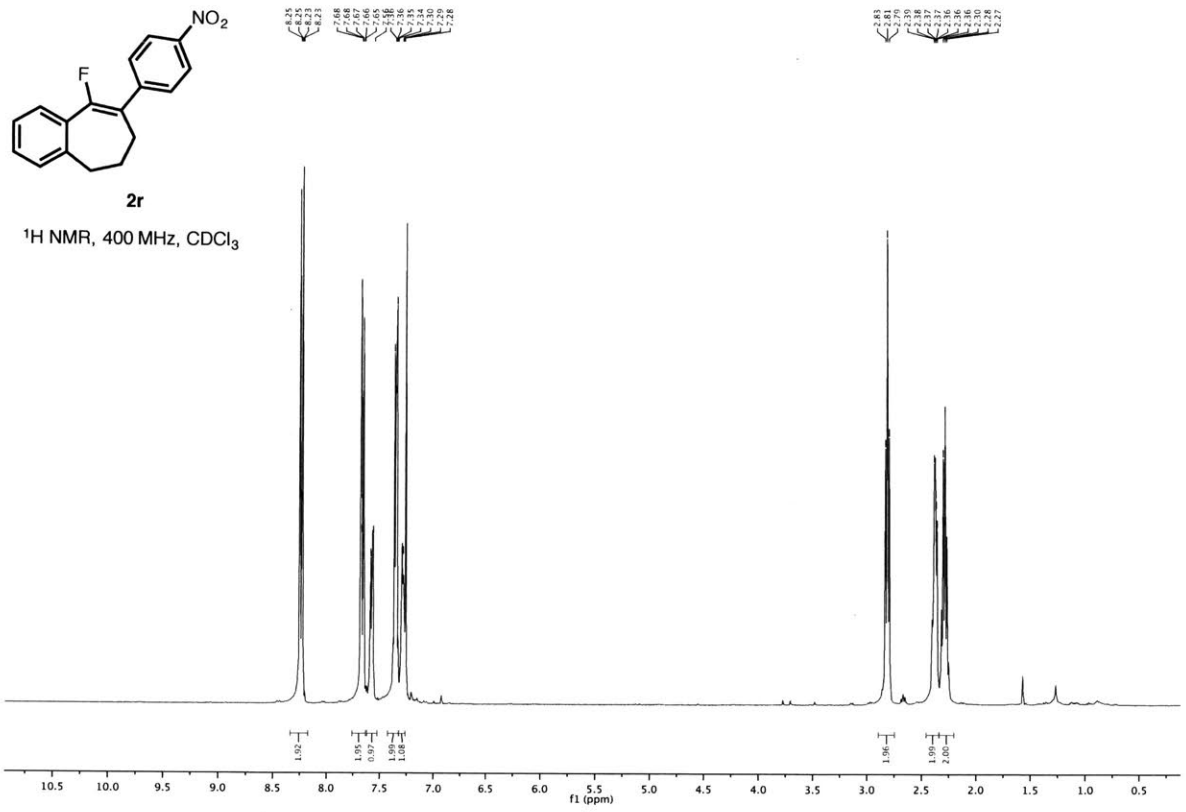

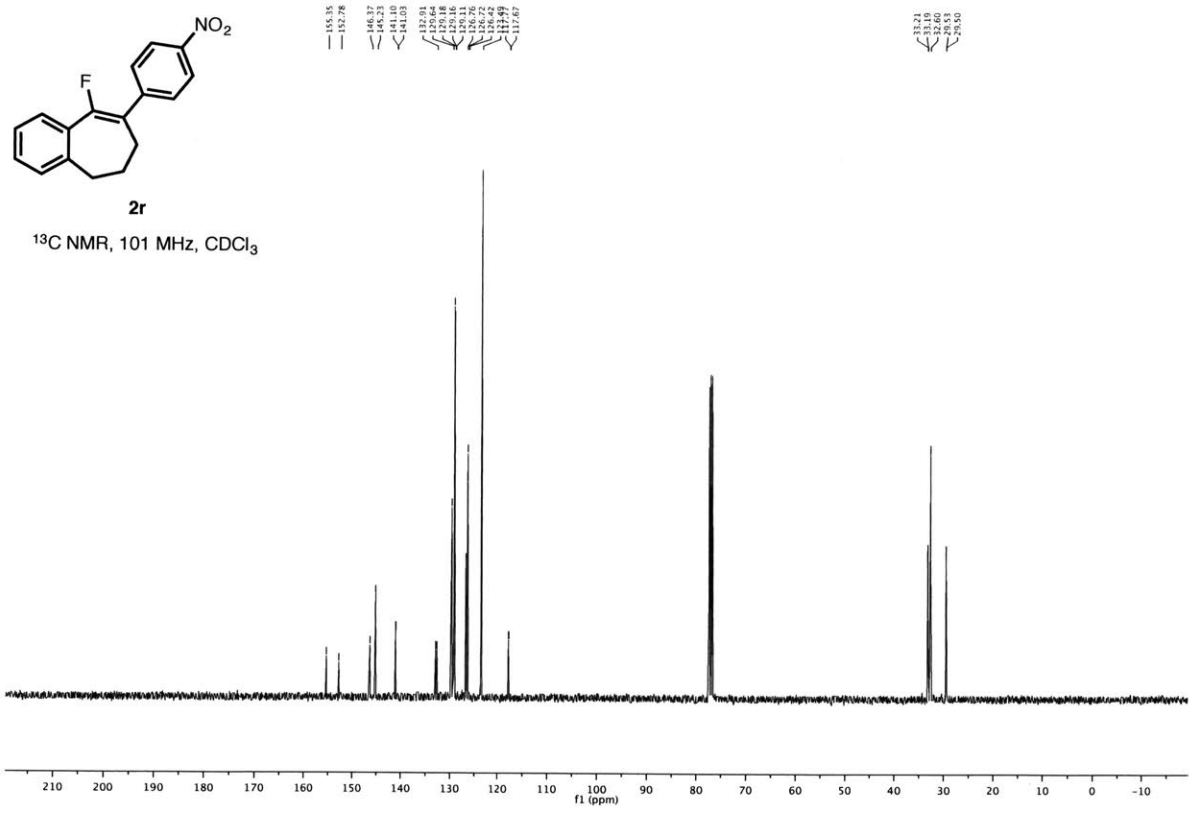

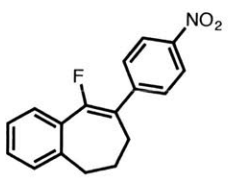

2r

^{19}F NMR, 376 MHz, $CDCl_3$

(2-fluoroethene-1,1-diyl)dibenzene (2t)

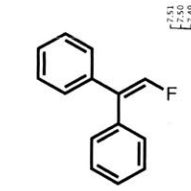

2t

^{1}H NMR, 400 MHz, $CDCl_3$

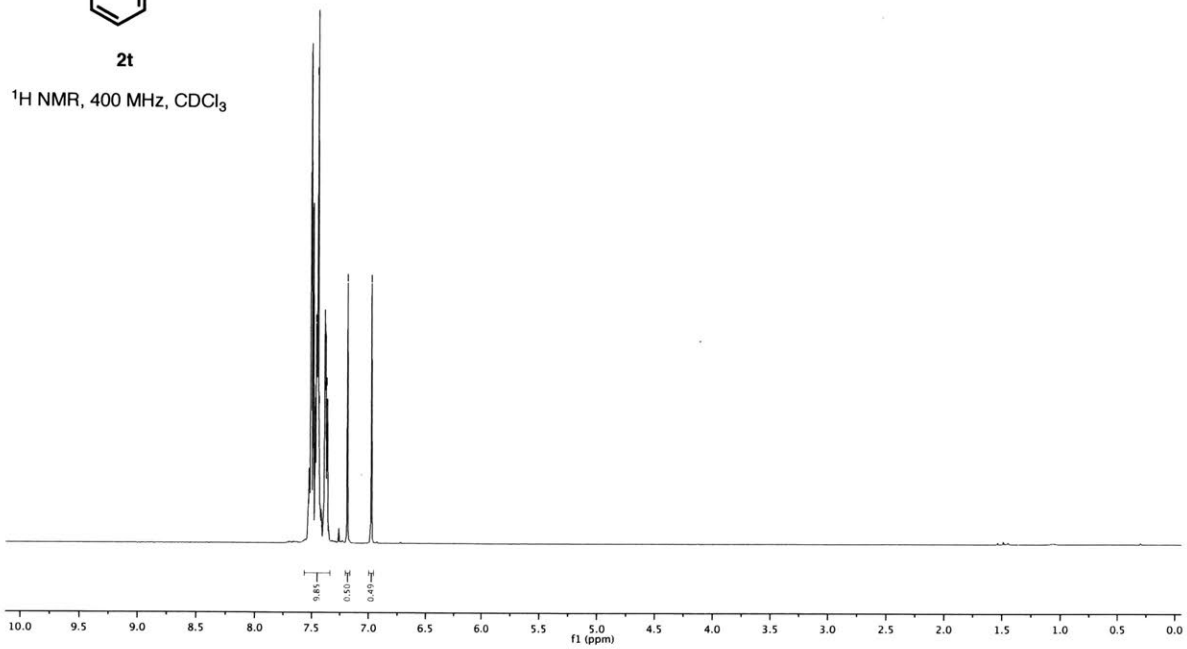

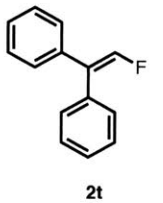

2t

^{13}C NMR, 101 MHz, $CDCl_3$

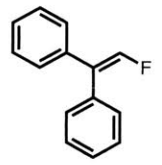

2t

^{19}F NMR, 376 MHz, $CDCl_3$

(2-fluoroprop-1-ene-1,1-diyl)dibenzene (2u)

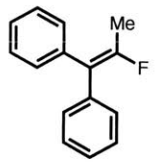

2u

^{1}H NMR, 400 MHz, $CDCl_3$

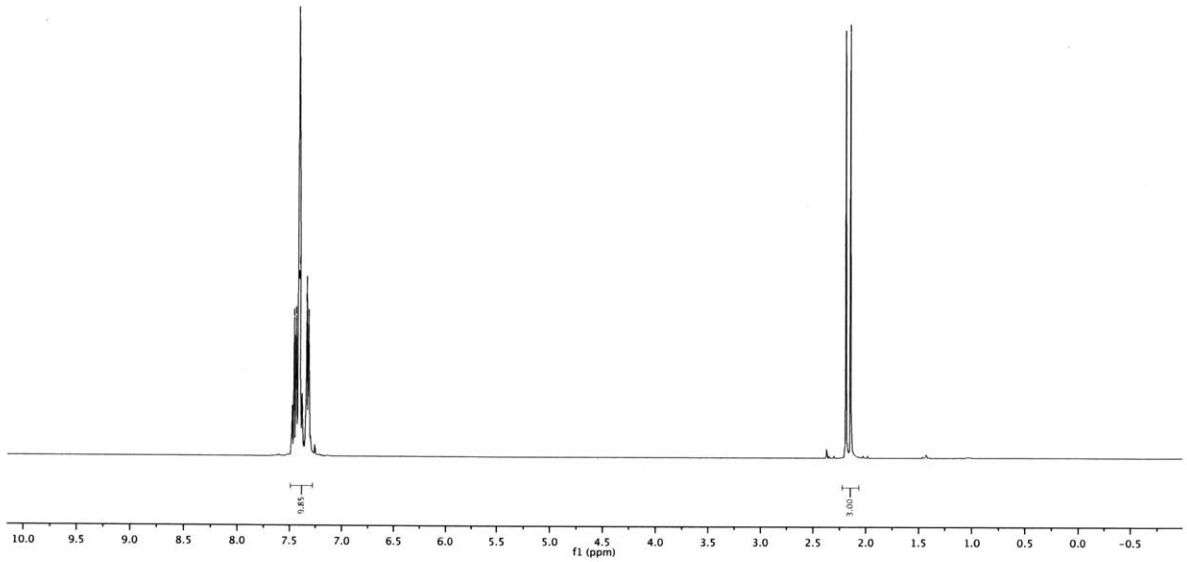

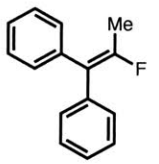

2u

^{13}C NMR, 101 MHz, $CDCl_3$

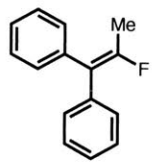

2u

^{19}F NMR, 376 MHz, $CDCl_3$

Chapter 2
Mechanistic Studies on Pd-Catalyzed Fluorination of Cyclic Vinyl Triflates: Evidence for *in situ* Ligand Modification by $TESCF_3$ as an Additive

2.1 Introduction

Organofluorine compounds[1] are ubiquitous among pharmaceuticals[2] and agrochemicals[3] due to their desirable biological properties.[4] Nonetheless, mild and general methods for their preparation are still lacking.[5] Pd^0/Pd^{II}-catalyzed coupling of aryl/vinyl (pseudo)halides with simple metal fluoride salts ("F^-") is an attractive approach, although it is associated with several challenges mainly derived from the high barrier for C–F reductive elimination from Pd(II) complexes.[6] To circumvent these problems, reactions based on reductive elimination from a Pd(IV) species using electrophilic fluorinating agents ("F^+") have been developed.[7]

Our solution to this problem has taken advantage of the unique C–F reductive elimination from LPdArF complexes supported by biaryl monophosphine ligands, thereby permitting the Pd^0/Pd^{II}-catalyzed fluorination of (hetero)aryl (pseudo)halides (bromides, iodides and triflates).[8] Mechanistic studies were performed to elucidate the *in situ* ligand modification process,[9a] and to understand the formation of regioisomeric side products[9b] in these reactions. These mechanistic discoveries prompted the rational design and synthesis of a series of novel bulky biarylphosphine ligands (*t*-BuBrettPhos, AdBrettPhos, HGPhos, and AlPhos), culminating in the discovery of the currently optimal ligand AlPhos. This ligand facilitates the Pd-catalyzed aromatic fluorination via a Pd(0)-Pd(II) cycle, under mild reaction conditions with improved substrate scope and regiochemical control (Scheme 1, a).[8e]

In 2016, motivated by the utility of fluorine-substituted olefins as amide linkage surrogates in medicinal chemistry and chemical biology,[10,11] a Pd-catalyzed fluorination of cyclic vinyl triflates was developed (Scheme 1, b).[12] During this investigation, several experimental observations were made that could not be explained by current mechanistic hypotheses for the aromatic fluorination reaction. First, despite the success of the use of AlPhos as a ligand in aromatic fluorination reactions, poor results were observed in the fluorination of cyclic vinyl triflates. Instead, ligand **L1** with a more rigid structure was found to be optimal in this case. Second, the generation of regioisomers of the vinyl fluoride products was an even bigger problem than for the fluorination of aromatic substrates. Moreover, little influence of the regiochemical outcome could be made by changing the ligand. Of significance was that the addition of $TESCF_3$ to the reaction mixture was found to significantly improve the regiochemical outcome. This dramatic effect was the key to the success of the vinyl fluorination reaction that we reported. Thus, we conducted a combined experimental and computational study to

understand the general mechanism of our Pd-catalyzed vinyl fluorination process and particularly the effect of the $TESCF_3$ additive.

Scheme 1. Pd-catalyzed fluorination of aryl triflates and cyclic vinyl triflates.

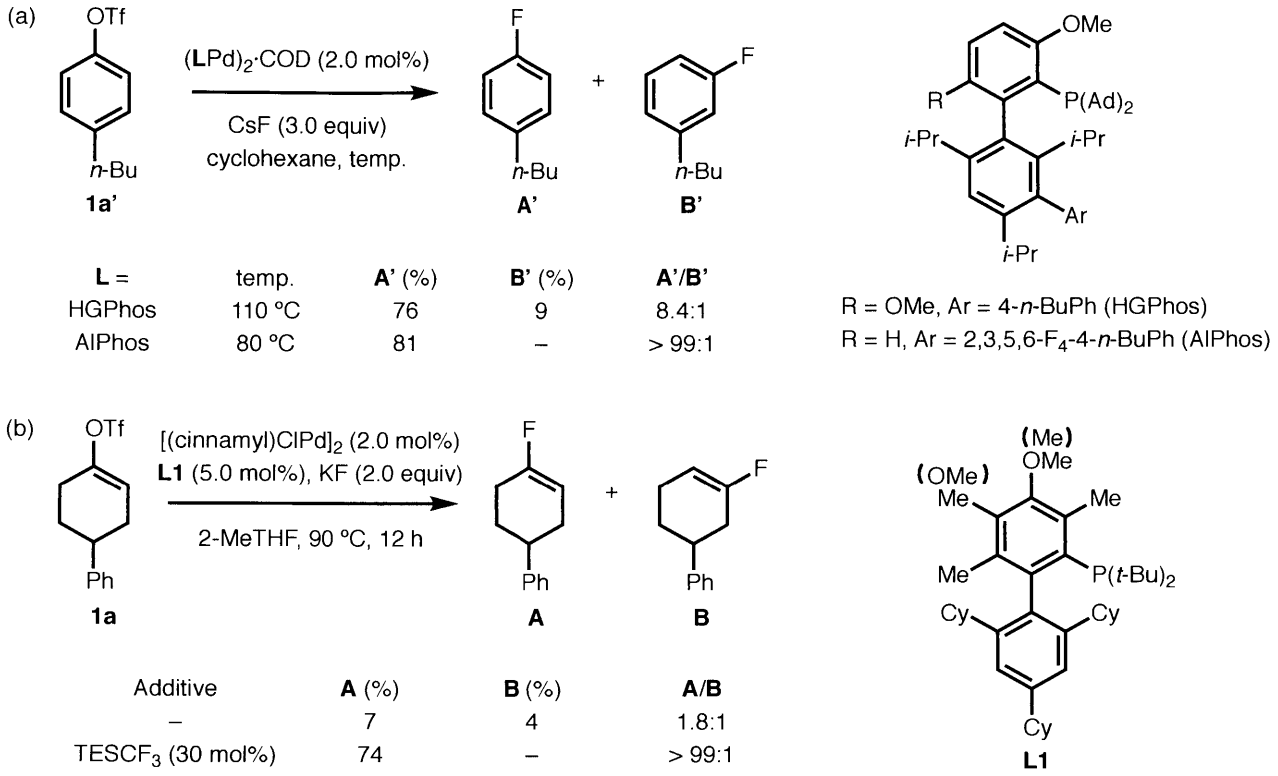

2.2 Results and Discussion

2.2.1 Pd-catalyzed fluorination of cyclic vinyl triflates in the absence of $TESCF_3$ as the additive

Based on the previous studies in our group on the Pd-catalyzed aromatic fluorination reaction,[9] we proposed the mechanism for the fluorination of cyclic vinyl triflates **1a** with ligand **L1** in the absence of $TESCF_3$ as the additive shown in Scheme 2. This catalytic cycle involves the oxidative addition of **1a** to the phosphine-ligated Pd(0) species **1** to form **L1**Pd(vinyl)(OTf) **3** (pathway A), transmetalation with KF to form **L1**Pd(vinyl)F **5** (pathway B), and C–F reductive elimination from **5** (pathway C), to form the fluorinated product **A**. In a separate pathway D, KF or a second molecule of **L1**Pd(vinyl)F **5** could act as a base and deprotonate the vinylic proton of **3** to form **L1**Pd(II)-cyclohexyne intermediate **6A**, generating one molecule of HF in the process. Intermediate **6A** is in fast equilibrium with isomer **6B**. The nonselective reaction of **6A** and **6B** with HF provides regioisomeric **L1**Pd(vinyl)F **5** and **7B** (pathway F), which can both undergo C–F reductive elimination to generate the observed mixture of regioisomeric vinyl fluorides **A**

and **B**. In addition, we anticipated that β-hydride elimination from **5** or **7B** could compete with C–F reductive elimination to generate the **L1**Pd(II)-cyclohexyne intermediates (pathway E).

Scheme 2. Proposed catalytic cycle for Pd(II)-catalyzed fluorination of cyclic vinyl triflates in the absence of $TESCF_3$ as the additive.

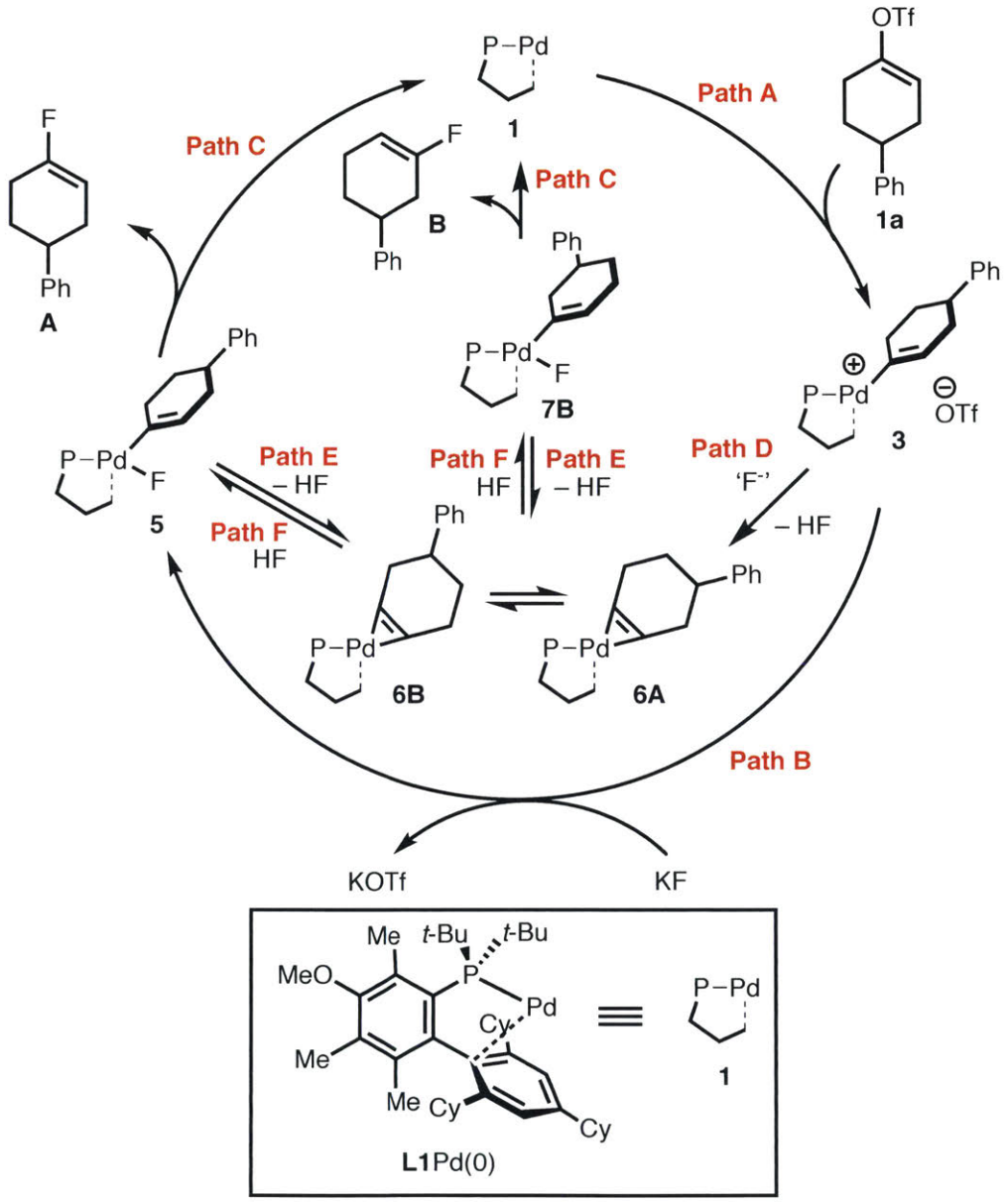

The reaction progress in the absence of $TESCF_3$ was monitored and the fluorination of **1a** was found to be sluggish at 90 °C, providing the fluorinated products in ~11% yield (7% **A**, 4% **B**, 1.8:1 regioselectivity) with ~30% starting material conversion after five hours (Scheme 3). The poor regioselectivity and mass imbalance suggested that an unproductive decomposition pathway might be occuring, which we hypothesized to involve the formation of the **L1**Pd(II)-cyclohexyne intermediates, **6A** and **6B**.

Scheme 3. Reaction kinetic profile under $TESCF_3$-free conditions.

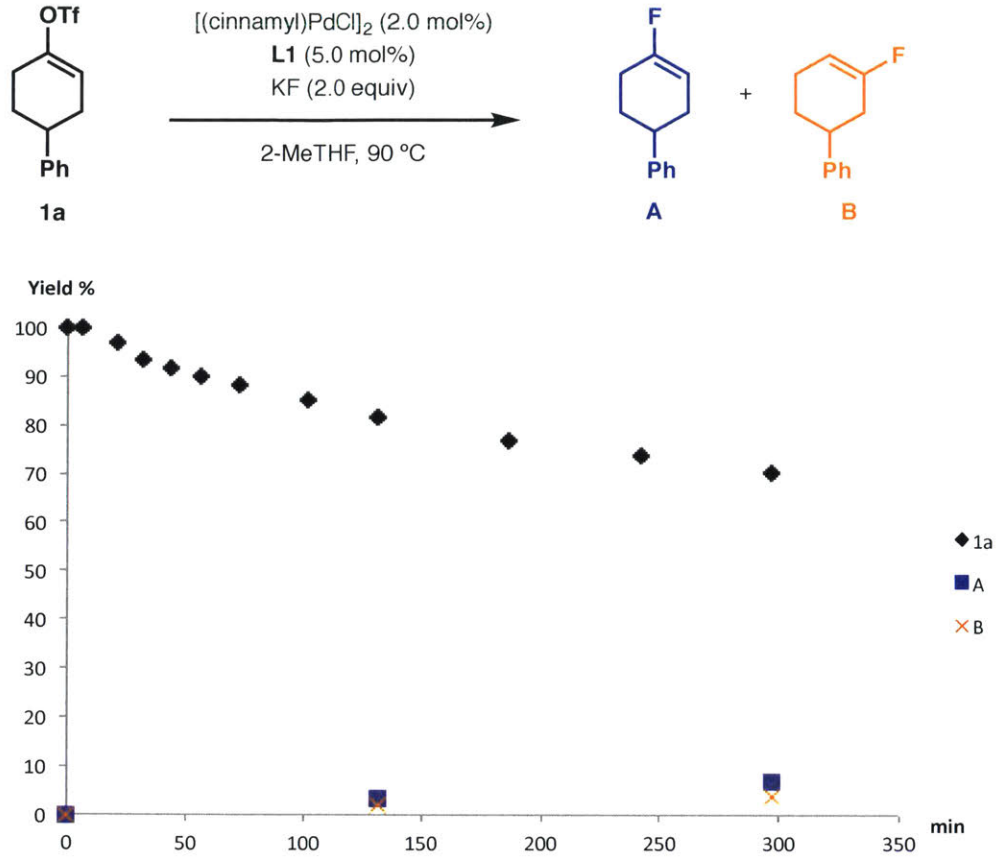

[a]Yields were determined by GC analysis of aliquots taken from the reaction mixture. The reaction was conducted at 1.0 mmol scale.

We speculated that **6A** and **6B**, would be generated with the formation of HF in a reversible process. Thus, as we did for the fluorination of aromatic substrates, we carried out the reaction in the presence of an exchangeable deuterium source. This would presumably form DF *in situ*, which could recombine with **6A** and **6B** to allow deuterium incorporation into the vinyl fluoride products. Indeed, when 1.0 equiv of *t*-BuOD was added to the reaction mixture, in addition to the formation of products **A** and **B**, a significant amount of products, 2-**A**-d_1 and 2-**B**-d_1, was also observed by ^{19}F NMR and confirmed by GC/MS (Scheme 4a). Additionally, a crossover experiment using **A** and 2,6,6-**A**-d_3 provided eight products, representing the isotopologues of **A** and regioisomer **B** (Scheme 4b). These observations of proton and deuterium exchange into the products at 2-position are consistent with the presence of **L1**Pd-cyclohexyne intermediates (**6A** and **6B**).

To further understand the proposed mechanism, especially the generation of **L1**Pd(II)-cyclohexyne intermediates, we performed density function theory (DFT) calculations in

collaboration with the Baik group at KAIST. Seoung-Tae (Baik group) conducted all the calculations discussed in this chapter. Figure 1a shows the reaction energy profile of the oxidative addition and the transmetalation step in the proposed mechanism. **L1**Pd(0) **1** engages **1a** through the initial π-complex **2**, and undergoes the oxidative addition with a barrier of 12.7 kcal/mol (via transition state **2-TS**) to afford **L1**Pd(vinyl)OTf **3**. Further dissociation of triflate and association of fluoride from **3** gives the intermediate *trans*-**L1**Pd(vinyl)F **5**.

Scheme 4. Deuterium labeling experiments under TESCF$_3$-free conditions.[a]

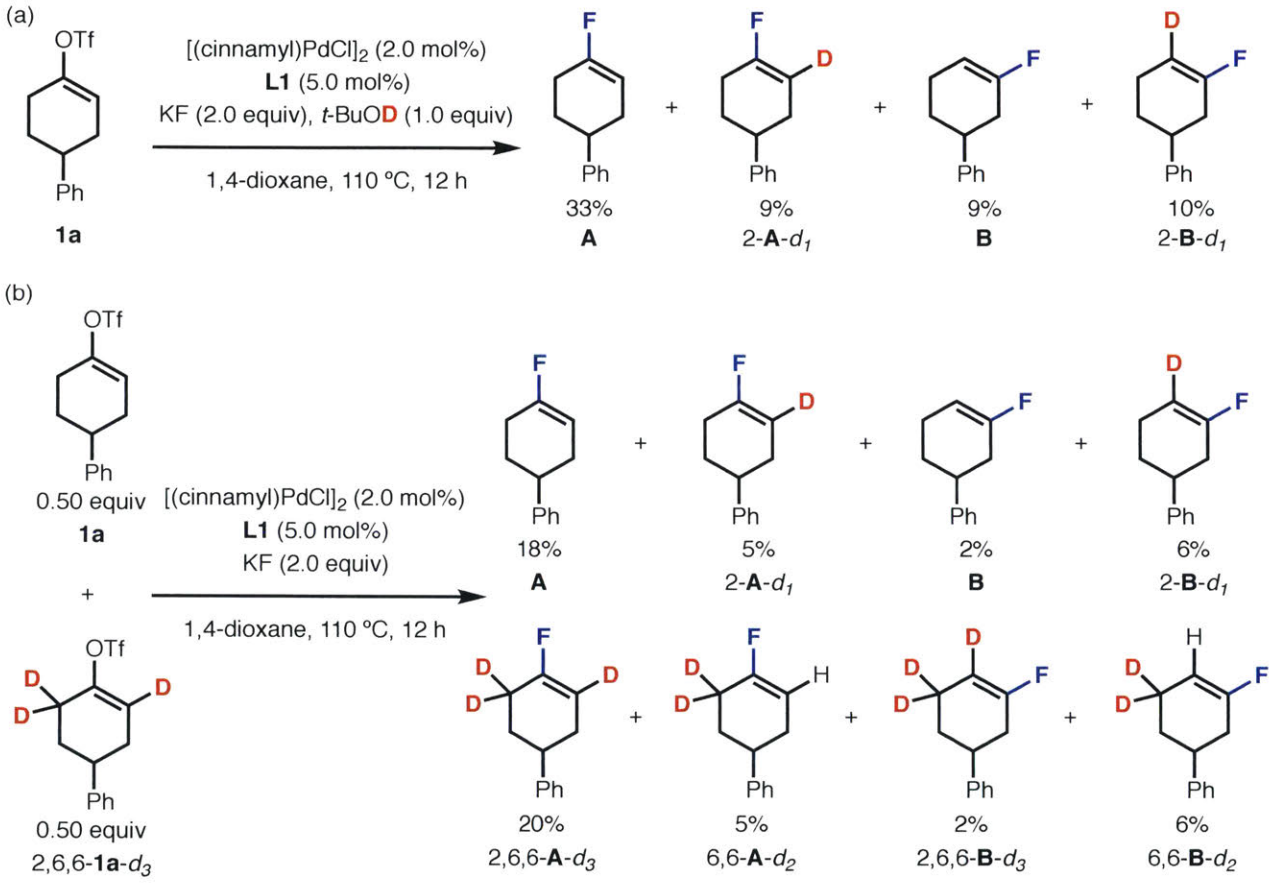

[a]Reactions were run at 0.10 mmol scale and at elevated temperature (110 °C) and dioxane to get better yields for analysis.

We envisioned that the addition of a fluoride anion to intermediate **4** could potentially provide complex **5** or **5A**, where the fluoride is either bound in *trans* or *cis* arrangement to the phosphine ligand (Figure 2). In principle, the *trans*-isomer **5** should be lower in energy due to the trans-effect. Indeed, our DFT calculations indicated that isomer **5** is 2.4 kcal/mol lower in energy than **5A**. The computed bond lengths illustrate the impact of the *trans*-effect. In **5**, the computed Pd–P and Pd–F bond lengths are 2.388 and 2.017 Å, respectively, and the Pd–C(vinyl) bond is

2.024 Å. In **5A**, due to the mismatch in *trans*-directing strengths, the Pd–P, Pd–F, and the Pd–C(vinyl) bonds elongate to 2.481, 2.024, and 2.037 Å, respectively.

a) Initial phase of the energy profile

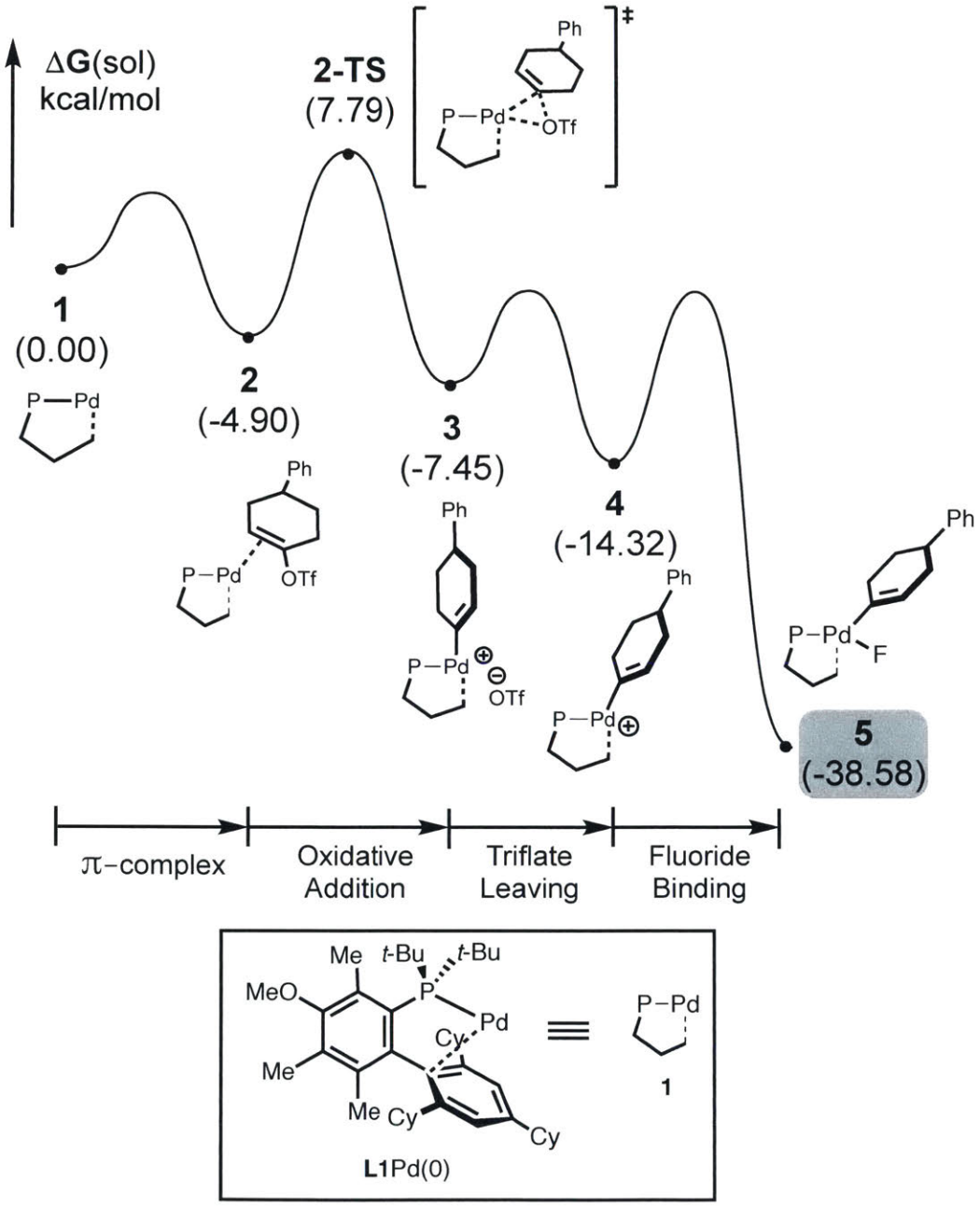

b) Last phase of the energy profile

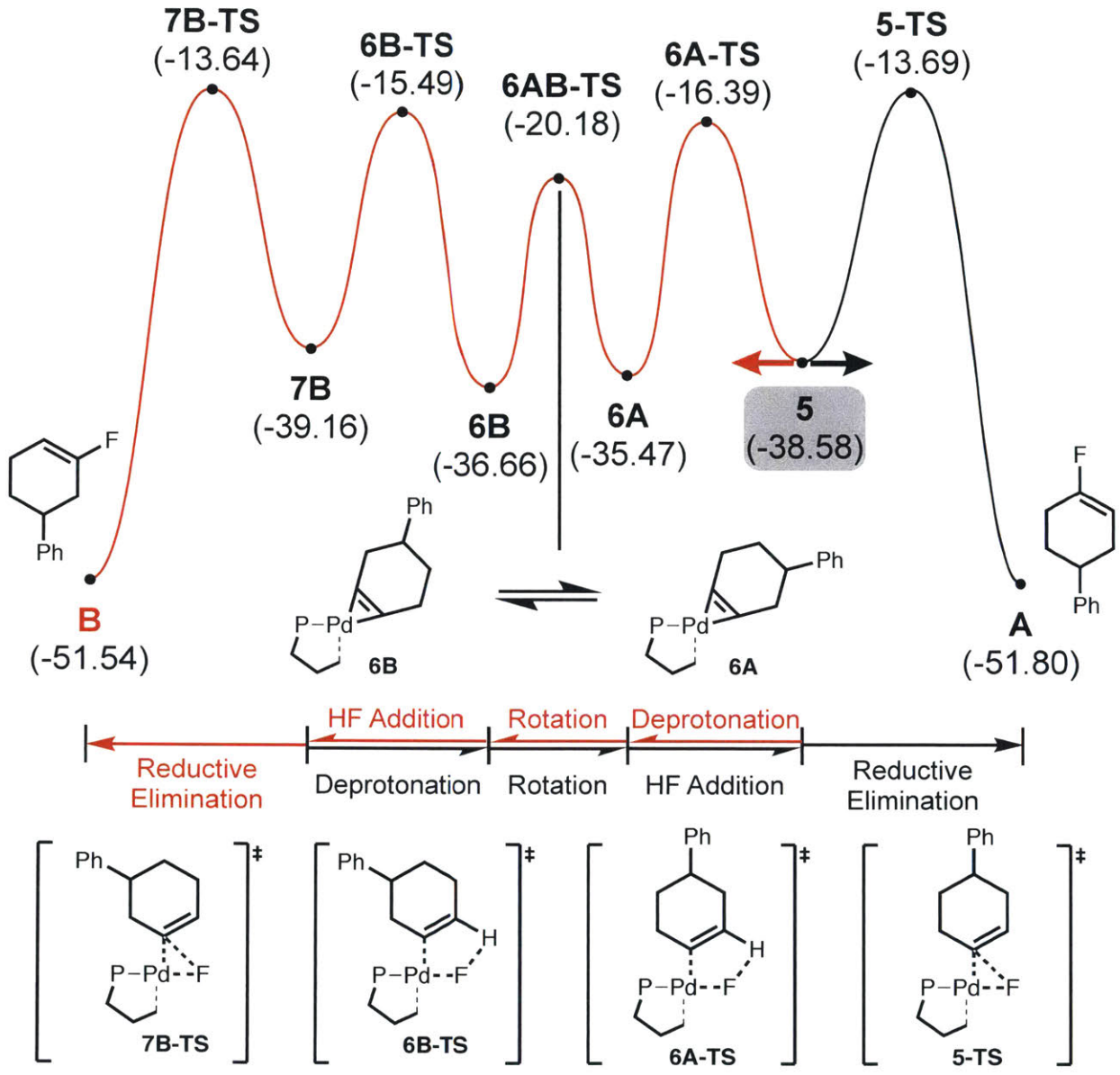

Figure 1. Energy profiles of the proposed mechanism under $TESCF_3$-free conditions.

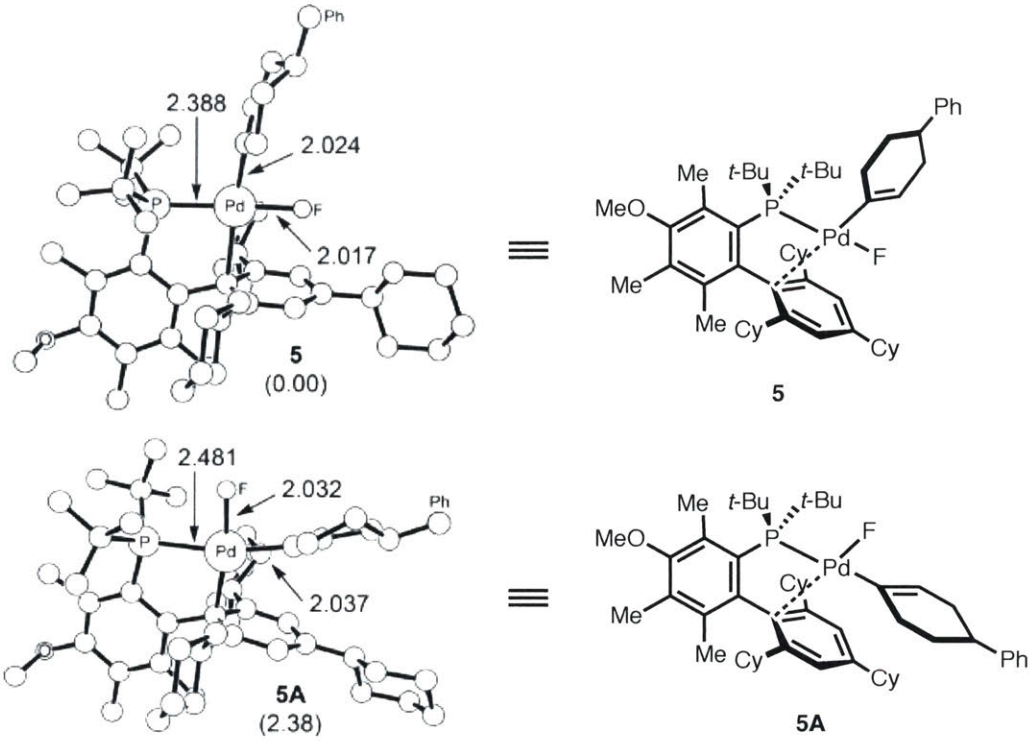

Figure 2. Optimized structure of 5 and 5A with selected bond lengths in Å and relative free energies in kcal/mol. Hydrogen atoms and phenyl group of the substrate are omitted for clarity.

As **5** is the major isomer generated after transmetalation in the fluorination process, we next considered the reactivity of this *trans*-complex. As discussed above, **5** can either provide the fluorinated product **A** via reductive elimination or undergo β-hydride elimination to yield the **L1**Pd(II)-cyclohexyne intermediate (**6A** and **6B**). As illustrated in Figure 1b, DFT calculations indicated that the reductive elimination from **5** is associated with a barrier of 24.9 kcal/mol (via **5-TS**), while the competing β-hydride elimination to form **6A** requires a lower activation energy of 22.2 kcal/mol (via **6A-TS**). The 2.7 kcal/mol energy difference favoring pathway E suggested that the generation of **6A** is much faster than the productive reductive elimination. Once **6A** is formed, it readily rearranges to **6B** through rotation of the cyclohexyne group (via **6AB-TS**) with a barrier of 18.4 kcal/mol, which is achievable under the fluorination conditions. The recombination of **6B** and HF generates **7B** (the *trans*-isomer is generated preferentially in this step due to the *trans*-effect, see Supporting Information for details), which could form the undesired fluorinated product **B** by reductive elimination. The transition state **6B-TS** and **6A-TS**, **7B-TS** and **5-TS** are isoenergetic, indicating that **7B** also favors β-hydride elimination than reductive elimination. Overall, the calculations suggested a Curtin–Hammett situation in the vinyl fluorination process in the absence of $TESCF_3$, whereas **5** and **7B** interconvert rapidly via a

low energy barrier, each proceeding irreversibly to a different product through a higher energy barrier (**A** and **B**, respectively). It is the preference of **5** and **7B** to undergo β-hydride elimination rather than the productive elimination that lowers both the efficiency and selectivity of the fluorination.

To gain experimental evidence for the above hypothesis, we sought to prepare the *trans*-**L1**Pd(vinyl)F **5** and investigate its reactivity stoichiometrically. After several attempts, we found that the synthesis of Pd(II) complexes supported by **L1** to be difficult, presumably due to the large size of **L1**. We therefore employed **L2** as the supporting ligand for our studies with stoichiometric Pd complexes. As previously reported, **L2** was also effective for vinyl fluorination, although the regioselectivity of the process was not as high as when **L1** was employed.[12] We felt that *trans*-**L2**Pd(vinyl)F (**C2**) could be prepared from *trans*-**L2**Pd(vinyl)Br (**C1**) via salt metathesis with AgF (Scheme 5). When **C1** was treated with AgF, little or none of the complex **C2** was observed under any of the reaction conditions we attempted. Instead, fluorinated products **A** and **B** were readily formed, even at room temperature (Scheme 5, see Supporting Information for details). This suggested that the reductive elimination of **C2** is relatively rapid, which is consistent with the computed barrier of ~24 kcal/mol for the reductive elimination. In 2-MeTHF at 90 °C, which is the solvent and temperature used in the catalytic reaction, **A** and **B** were generated in 26% and 25% NMR yields, respectively. The regioselectivity of this stoichiometric process (1.0:1) is consistent with the theoretical regioselectivity (~1:1) based on the computed energies.

Scheme 5. Attempted synthesis of L2Pd(vinyl)F.

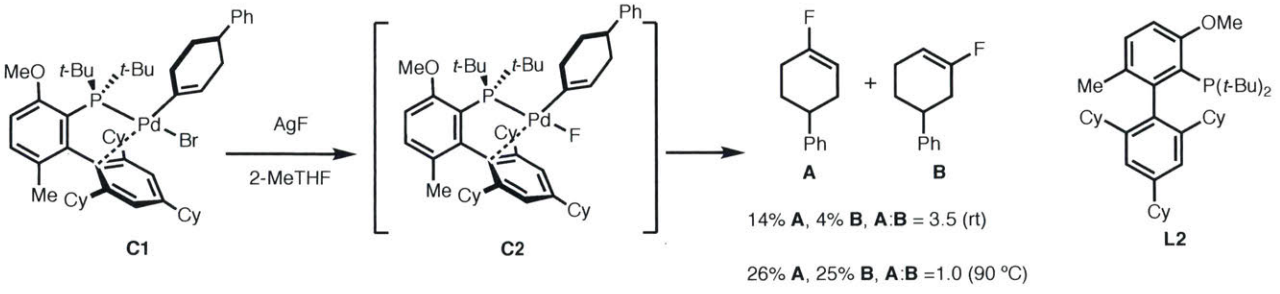

2.2.2 Fluorination of cyclic vinyl triflates with $TESCF_3$ as the additive.

We next looked into the mechanism of the fluorination process employing $TESCF_3$ as an additive. As discussed above, the addition of a substoichiometric amount of $TESCF_3$ has a dramatic impact on the reaction, and the desired vinyl fluoride **A** was formed in good yield (74%) with >99:1 regioselectivity (Scheme 1b).

Scheme 6. Reaction kinetic profile with 30 mol% $TESCF_3$ as an additive.

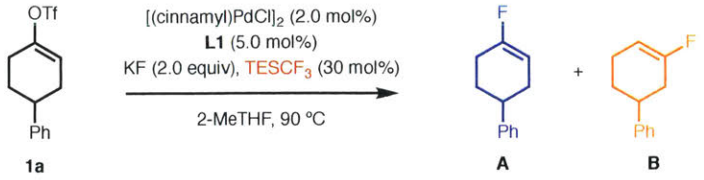

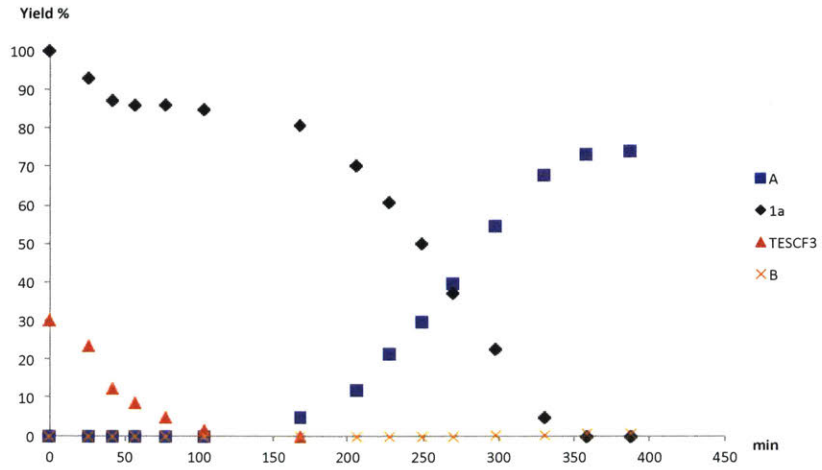

[a]The reaction was run at 1.0 mmol scale. Yields were determined by GC analysis of aliquots taken from the reaction mixture.

Scheme 7. Reaction kinetic profile of adding extra $TESCF_3$ after the inhibition period.

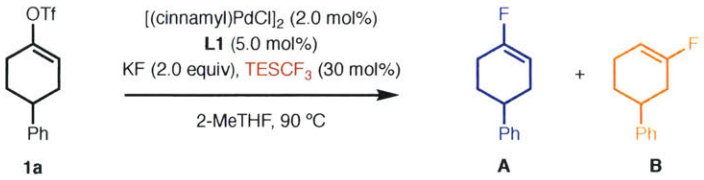

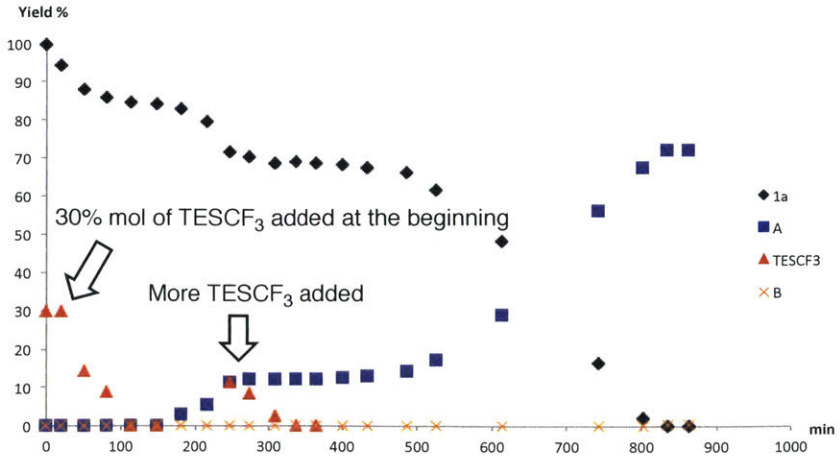

[a]The reaction was run at 1.0 mmol scale. Yields were determined by GC analysis of aliquots taken from the reaction mixture.

The kinetic profile of the fluorination process in the presence of $TESCF_3$ (30%) is shown in Scheme 6. We noticed relatively fast consumption of **1a** at the beginning of the reaction (10%–15%). This loss of starting material was likely related to some process which generates the true active catalyst (*vide infra*). After this, the conversion of **1a** slowed down and $TESCF_3$ was consumed. During this time no vinyl fluoride products were formed. Although an active catalyst had been generated, the fluorination process did not commence until all of the $TESCF_3$ had been consumed. We hypothesized that this is caused by $TESCF_3$ inhibiting the fluorination process. Indeed, longer induction period was observed when more than 30 mol% of $TESCF_3$ was added at the beginning of the reaction. In addition, introduction of more $TESCF_3$ to an ongoing fluorination reaction, which was providing product, completely shut down the reaction (Scheme 7). Only after the $TESCF_3$ had, again, been totally consumed does formation of **A** resume. We reasoned that when the concentration of $TESCF_3$ is much larger than **L1**Pd(vinyl)$^+$ **4** in the reaction solution, fluoride anion reacts preferentially with $TESCF_3$ instead of **4**, therefore preventing the generation of **L1**Pd(vinyl)F and in turn inhibiting the formation of **A**.[13] These observations indicated that although $TESCF_3$ was a crucial additive for improving the regioselectivity of the reaction, the presence of too much $TESCF_3$ postponed the start of the productive fluorination process and lowered the overall efficiency of the reaction. Studies on the influence of the quantity of $TESCF_3$ added to the fluorination reaction mixture illustrated that 30 mol% was the minimal amount to achieve the highest regiochemical ratio of products (Table 1).

Table 1. Influence of the quantity of $TESCF_3$ on the fluorination reaction.

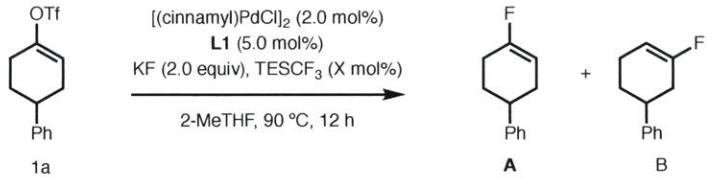

Entry[a]	$TESCF_3$ (mol%)	**A** (%)	**B** (%)	**A**:**B**
1	0	7	4	1.8:1
2	10	66	2	33:1
3	20	70	1	70:1
4	30	74	<0.5	>99:1
5	50	73	<0.5	>99:1
6	100	71	<0.5	>99:1

[a]Reactions were run at 0.10 mmol scale. Yields were determined by ^{19}F NMR analysis of the crude reaction mixture using 1-fluoronaphthalene as an internal standard.

After the induction period, the fluorination reaction proceeded efficiently providing the desired fluorinated product **A** in 74% yield with less than 0.5% of **B** as indicated by ^{19}F NMR (regioselectivity >99:1). The significantly improved regioselectivity as compared to the additive-free conditions (1.8:1) suggested that the **L1**Pd(II)-cyclohexyne intermediates **6A** and **6B** were either not generated or were not part of the product-determining step. Indeed, when the deuterium labeling crossover experiment was carried out as before but with the addition of 30 mol% $TESCF_3$, **A** and 2,6,6-**A**-d_3 were the only fluorination products formed, and no deuterium crossover or regioisomer formation was observed (Scheme 8).

Scheme 8. Deuterium labeling experiment with the addition of 30 mol% $TESCF_3$.[a]

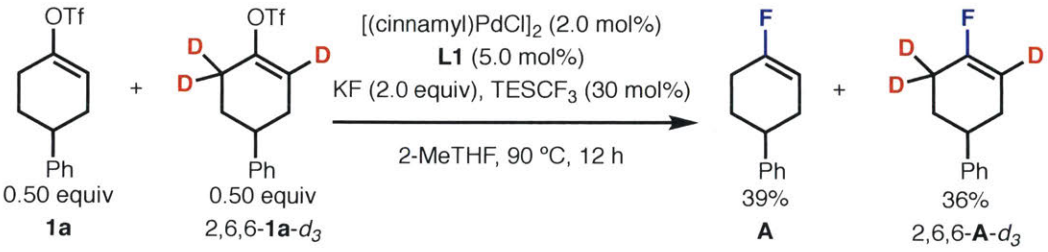

[a]The reaction was run at 0.10 mmol scale and at elevated temperature (110 °C) and dioxane in order to get better yields for analysis.

We therefore started to investigate the potential roles of $TESCF_3$ in the fluorination process. As previously reported, $TMSCF_3$ or $TIPSCF_3$, although less efficient additives than $TESCF_3$, exhibit the same effect of improving the regioselectivity of the vinyl fluorination reaction when used as additives. These trifluoromethylsilanes are widely employed trifluoromethyl anion (CF_3^-) sources[14–16] and, in particular, have been used to deliver CF_3^- in the Pd-catalyzed trifluoromethylation reactions.[17,18] However, even with 1.0 equiv of $TESCF_3$ added in the fluorination reaction, the trifluoromethylated side product was barely detectable. As the generation of such a side product through reductive elimination from a **L1**Pd(vinyl)CF_3 species should occur under our reaction conditions,[18] we reasoned that such an intermediate is not formed in this fluorination process. Our attempts to prepare **L2**Pd(vinyl)CF_3 from either **L2**Pd(vinyl)Br or **L2**Pd(vinyl)OTf all provided <5% of **L2**Pd(vinyl)CF_3, as observed by ^{19}F NMR analysis of the crude reaction mixture (see Supporting Information for details). We surmise that the rigidity of the ligand backbone and the steric hindrance of the two di-*tert*-butyl

groups on the phosphorous of these ligands (**L1** and **L2**) prevents CF_3^- from attacking the Pd(II) center.

We therefore considered alternative roles of CF_3^- in the vinyl fluorination reaction. In 2012, researchers at Amgen observed the generation of complex **D** with a dearomatized ligand in the Pd-catalyzed cross-coupling reactions. Complex D can be independently synthesized by heating *t*-BuXPhos and $Pd_2(dba)_3{\cdot}CHCl_3$ in toluene (Scheme 9)[19]. The key step for its generation is a cyclopropanation reaction, in which a dichlorocarbene (CCl_2:) attacks the bottom ring of the ligand in *t*-BuXPhosPd(0). Inspired by their work, we hypothesized a similar process in the fluorination reaction where a difluorocarbene (CF_2:) or a trifluoromethyl anion (CF_3^-) attacks the bottom ring of **L1** in **L1**Pd(vinyl)$^+$ **4**. DFT calculations were performed to investigate the plausibility of this proposal.

Scheme 9. Generation of Pd complexes with ligand with a dearomatized bottom ring.

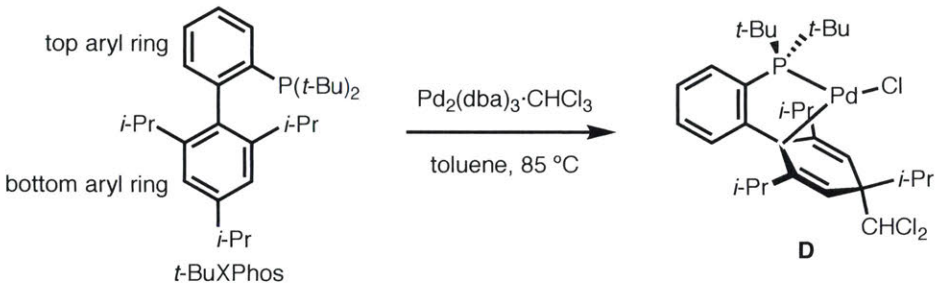

Based on calculations, the reaction of **4** with CF_3^- is more favored than with difluorocarbene (see Supporting Information for details), requiring an activation energy of 16.5 kcal/mol via transition state **4'-TS** to form the dearomatized intermediate **6**. The trifluoromethylation at both the *meta*- and *para*-positions of the bottom ring of **L1** were considered. The reaction at the *meta*-position is kinetically favored, while the *para*-position is thermodynamically favorable (see Supporting Information for details).

After the generation of **6**, we envisioned that it reacts with a fluoride anion to form intermediate **7** or **7'**, where the fluoride is bound either in *cis* or *trans*-disposition to the phosphine ligand. Unlike in the case of **5** and **5A** where the *trans*-isomer **5** is more stable, we found that the *cis*-isomer **7** is energetically preferred by as much as 6.7 kcal/mol over the *trans*-isomer **7'**. A detailed analysis of the structures and relative energies of these two species revealed that the trifluoromethylation of the bottom ring of **L1** places a negative charge on the aryl component and turns the weakly coordinating, neutral, π-basic arene ligand into a stronger,

anionic donor ligand. As a result, it is now energetically much more favorable to place the fluoride *trans* to this donor.

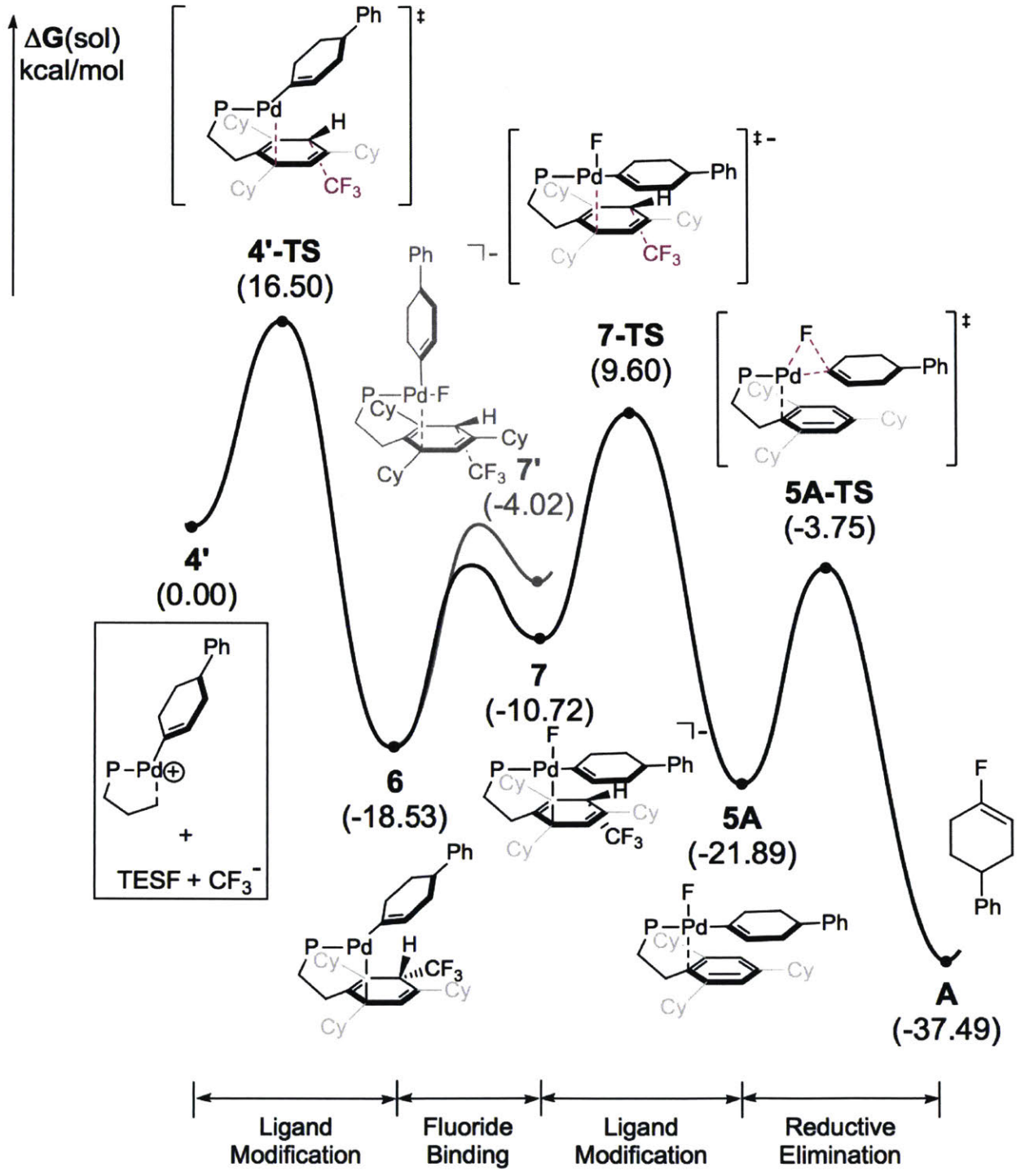

Figure 3. Energy profile of the possible reaction between CF_3^- and 4.

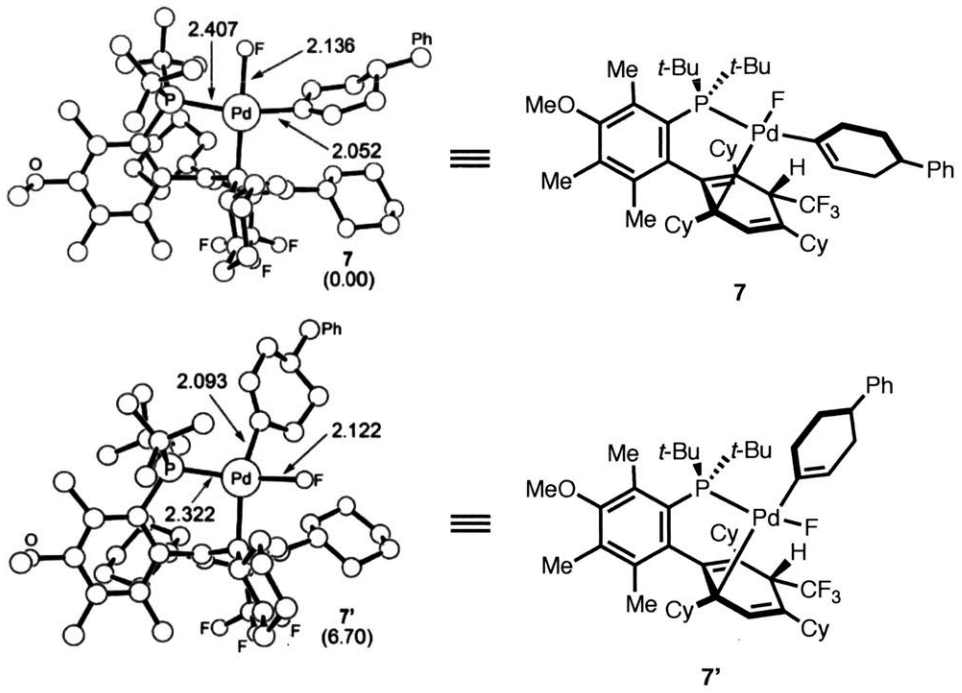

Figure 4. Optimized structure of 7 and 7' with selected bond lengths in Å and relative free energies in kcal/mol. Hydrogen atoms and phenyl group of the substrate are omitted for clarity.

The subsequent elimination of CF_3^- from intermediate **7** provides the corresponding *cis*-isomer **5A**. Interestingly, as we investigated the preferred reaction pathway of **5A** between β-hydride elimination and reductive elimination, we found that **5A** displays opposite reaction preferences than **5** does. It undergoes reductive elimination with a barrier of 18.1 kcal/mol, while the β-hydride elimination from **5A** has a barrier of 25.4 kcal/mol (Scheme 10). Therefore as showed in Figure 3, once formed from **7**, **5A** undergoes facile reductive elimination to provide the fluorinated product **A** with the desired regioselectivity. Overall, Figure 3 illustrates a potential fluorination process catalyzed by CF_3^-, whereas the **L1**Pd(II)-cyclohexyne intermediates that are responsible for the poor regioselectivity, are never formed, consistent with our experimental finding of no deuterium exchange or crossover.

Scheme 10. Reaction preference of intermediates 5 and 5A.

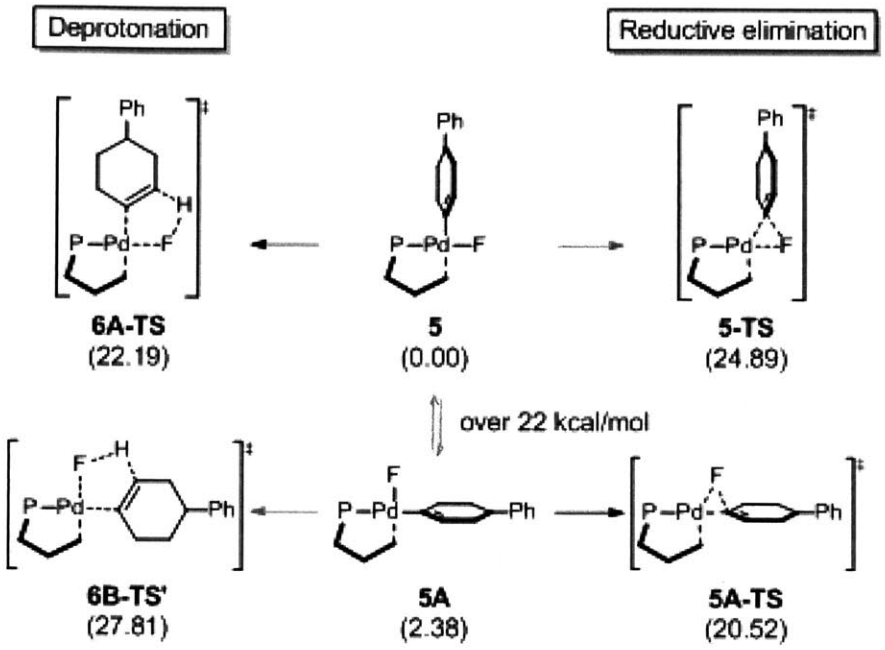

We attempted to obtain experimental evidence for the existence of the key intermediate **6**. We were unable to observe **6** by spectroscopic analysis of the crude reaction mixture. Our attempts to independently prepare an analogous complex supported by **L2** were also unsuccessful. However, when we treated **L2**$PdCl_2$ (**E1**) with $TMSCF_3$ in the presence of CsF, we were able to obtain complex **E2**, in which the bottom ring of **L2** was dearomatized by CF_3^- at the *para*-position (Scheme 11). The synthesis and isolation of **E2** provides support for the hypothesis that CF_3^- is able to attack and dearomatize the bottom ring of the ligand when the Pd(II) center is difficult to access due to steric hindrance and also is consistent with DFT calculations that the *para*-substituted isomer is more stable than the *ortho*-substituted isomer (see Supporting Information for details).

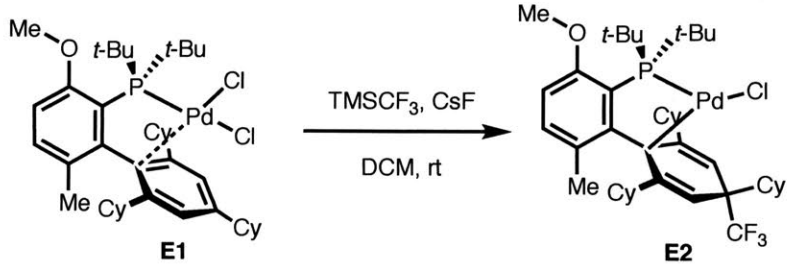

Scheme 11. Synthesis of Pd complexes supported by CF_3^--dearomatized L2.

The experiments described above suggested that complex **6**, if involved in the fluorination process, must be generated in low concentration. We wanted to investigate its

generation by quantifying the fate of CF_3^-. The release of CF_3^- from $TESCF_3$ in the presence of KF is a heterogeneous process and difficult to control. In addition to the main byproduct TESF, a significant amount of $CHCF_3$ and CF_2CF_2 was formed as well. These compounds are volatile and could not easily be accurately quantified. We speculated that a $LPd(Ph)CF_3$ complex could serve as an CF_3^- source for our study. In addition potentially releasing CF_3^-,[20] it mainly undergoes reductive elimination to provide trifluorobenzene, which could be quantified accurately by ^{19}F NMR. We prepared the BrettPhos-supported $Pd(Ph)(CF_3)$ (**F**) complex according to a previously reported protocol.[18] BrettPhos is known to facilitate the Pd-catalyzed trifluoromethylation reaction but is less effective in Pd-catalyzed fluorination reactions.[7] When BrettPhos-supported $Pd(Ph)(CF_3)$ (4 mol%) was used as both the Pd precatalyst and the CF_3^- additive, together with 5 mol% **L1**, the fluorination proceeded successfully giving the fluorinated products in 59% yield and 29:1 regioselectivity (Scheme 12a). This regioselectivity was significantly improved compared to the $TESCF_3$-free conditions (1.8:1). As expected, **F** alone was unable to facilitate the fluorination process (Scheme 12b). We believe that, in the reaction in Scheme 12a, some of **F** first undergoes reductive elimination to generate trifluorobenzene and the BrettPhosPd(0) species. Subsequent ligand exchange with **L1** would form **L1**Pd(0) (**B0**) as the viable catalyst for vinyl fluorination. Meanwhile, the remaining **F** acts a source of CF_3^- in the fluorination process. Analysis of the crude reaction mixture by ^{19}F NMR showed that close to 4% of trifluoromethyl benzene (4 mol% **F** was used) was generated, suggesting that only a trace amount of CF_3^- is released into the reaction mixture. Thus, the active species responsible for the improved regioselectivity in the fluorination reaction (**6**) is generated at extremely low concentrations.

Scheme 12. BrettPhosPd(Ph)CF_3 species used as both the Pd precursor and the CF_3^- additive.[a]

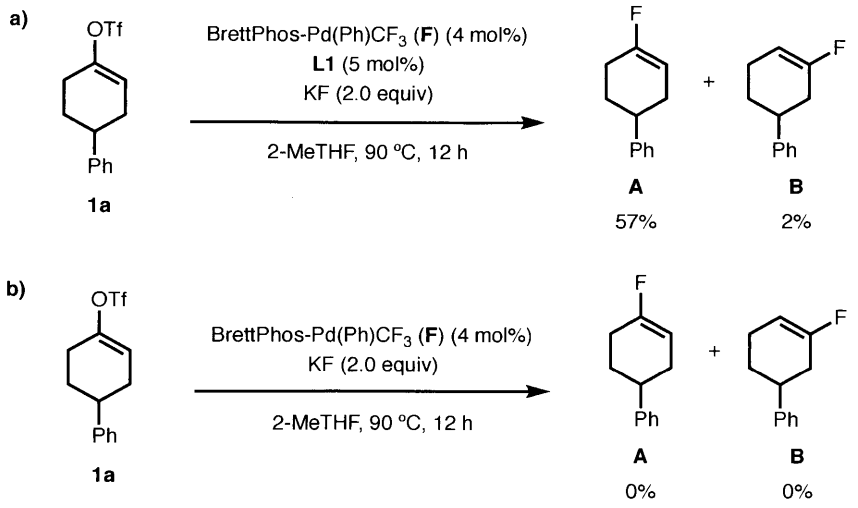

[a]Reactions were run at 0.10 mmol scale.

Based on these studies, we propose a possible mechanism of the fluorination process with $TESCF_3$ as the additive as is summarized in Scheme 13. Upon the generation of **L1**Pd(0) (**1**) from [(cinnamyl)PdCl]$_2$ and **L1**, **1** undergoes oxidative addition with the vinyl triflate **1a** to form **L1**Pd(vinyl)$^+$ (**4**). The CF_3^- in the reaction then reacts with **4** to form the CF_3^--modified intermediate **6**, which further interacts with F^- to provide *cis*-**L1**Pd(vinyl)F (**5A**) and regenerate CF_3^-. **5A** then undergoes reductive elimination to form the fluorinated product with the desired regioselectivity (**A**).

Scheme 13. Proposed fluorination process using $TESCF_3$ as an additive.

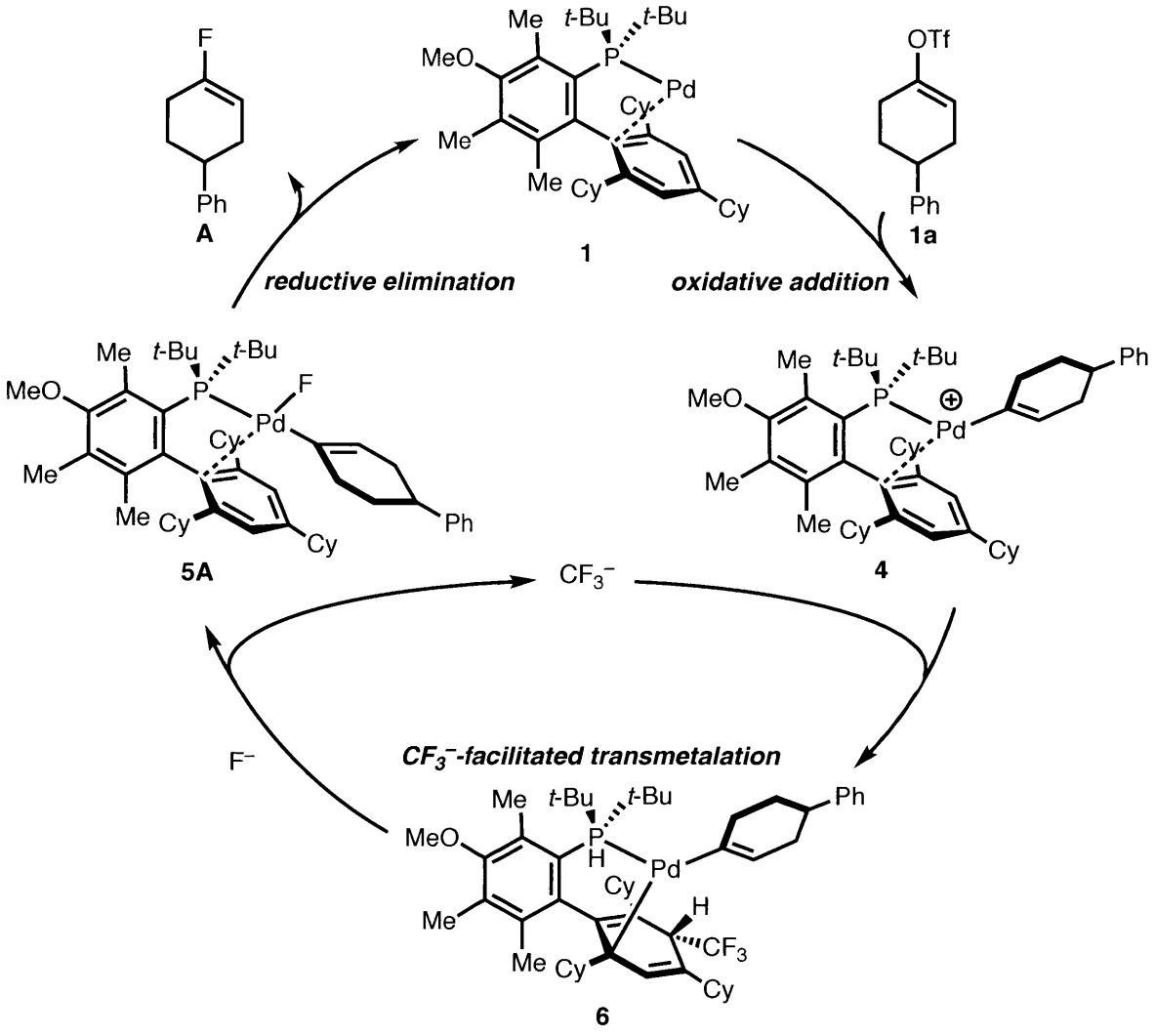

2.3 Conclusion

In conclusion, we developed a detailed mechanistic hypothesis for the Pd(II)-catalyzed fluorination of cyclic vinyl triflates. Based on combined experimental and computational studies, a plausible mechanistic model for the dramatic effect of $TESCF_3$ as an additive was postulated. In the absence of $TESCF_3$, the *trans*-**L1**Pd(vinyl)F **5** is generated predominantly due to the *trans*-effect. **5** preferentially undergoes β-hydride elimination to form the **L1**Pd(II)-cyclohexyne intermediates (**6A** and **6B**), which ultimately produces mixtures of products. In the presence of $TESCF_3$, by temporarily dearomatizing the bottom aryl ring of ligand **L1** with CF_3^-, the rate of formation of these two intermediates, the *trans*-isomer (**7'**) and *cis*-isomer (**7**), is reversed, leading to the generation of *cis*-**L1**Pd(vinyl)F **5A** as the major isomer. **5A** undergoes facile reductive elimination rather than β-hydride elimination to provide the fluorinated product **A** with the desired regioselectivity. While we were unable to obtain direct experimental proof for the mechanistic role of the $TESCF_3$ additive, all of our experimental results are consistent with the proposal.

2.4 Experimental

General Procedures. All reactions were set up and carried out in a nitrogen-filled glovebox using oven-dried glassware and anhydrous degassed solvents unless otherwise noted. Anhydrous, oxygen-free toluene, dichloromethane (CH_2Cl_2), and tetrahydrofuran (THF) were obtained by passage through activated alumina columns under argon pressure before use. Cyclohexane was purchased from Aldrich in Sure-SealTM bottles. CD_2Cl_2 (99.9%) and other deuterium sources (Table S1) were purchased in sealed ampules from Cambridge Isotopes. *t*BuOD (99%) and $CDCl_3$ were purchased from Cambridge Isotopes. Potassium fluoride (99.9%) was purchased from Strem and dried at 200 °C under high vacuum for 24 h. The dried potassium fluoride was then transferred to a nitrogen-filled glovebox where it was thoroughly ground using an oven-dried mortar and pestle. The finely ground potassium fluoride was filtered through a stainless-steel sieve (purchased from Cole Parmer) to obtain potassium fluoride with particle size of <45 μm. The preparations of **L1**, **L2** have been previously described. All other reagents were purchased from commercial sources and used without further purification. All ^{19}F NMR yields stated for fluorination reactions are calculated from ^{19}F NMR (282 MHz) spectra relative to an internal standard of 1-fluoronaphthalene. All compounds were analyzed by ^{1}H, ^{13}C, ^{31}P, and ^{19}F NMR, IR spectroscopy, as well as GC/MS or elemental analysis. Copies of NMR data are

attached at the end of the Supporting Information. ^{1}H and ^{13}C NMR spectra were recorded on Varian XL 300 MHz, Varian Inova 500 MHz or Bruker AMX-400 spectrometer spectrometers and calibrated using residual solvent as internal reference. The following abbreviations were used to explain multiplicities: s = singlet, d = doublet, t = triplet, pt = pseudotriplet, q = quartet, p = pentet, m = multiplet. ^{19}F NMR spectra were recorded on Varian XL 300 MHz, Varian Inova 500 MHz or Bruker AMX-400 spectrometer spectrometers and calibrated to an external standard of $CFCl_3$ (δ 0.0 ppm). $^{31}P\{^{1}H\}$ NMR spectra were recorded on Varian XL 300 MHz, Varian Inova 500 MHz or Bruker AMX-400 spectrometer calibrated to an external standard of *aq.* H_3PO_4 (δ 0.0 ppm). IR spectra were recorded on a Thermo Scientific Nicolet iS5 Fourier Transform IR Spectrometer. Elemental analysis was performed by Atlantic Microlabs Inc., Norcross, GA. High Resolution Mass Spectrometry (HRMS) data were recorded on a Bruker Daltonics APEXIV 4.7 Tesla Fourier Transform ion cyclotron resonance mass spectrometer. Unless specified otherwise, reactions were carried out in oven-dried Fisher Scientific 16 × 125 mm screw-cap tubes (Cat. No. 1495925C) using Thermo Scientific PTFE/silicon F/15-425 10 septa (Cat. No. 03394A). All reactions performed in sealed reaction tubes should be carried out behind a blast shield or a closed hood sash.

2.4.1 General Procedure to Monitor the Kinetics of the fluorination reaction

In a nitrogen-filled glovebox, an oven-dried reaction tube (Fisher 20 × 125 mm tubes – Cat. No. 1495937A) equipped with a stir bar, was charged successively with $[(cinnamyl)PdCl]_2$ (0.010 g, 0.020 mmol, 0.20 mol%), **L1** (0.031 g, 0.050 mmol, 0.50 mol%), KF (0.12 g, 2.0 mmol, 2.0 equiv), **1a** (0.31 g, 1.0 mmol, 1.0 equiv), 1-fluoronaphthalene (internal standard) (150 μL, 1.16 mmol, 1.16 equiv), and 5 mL of 2-MeTHF. $TESCF_3$ was added if necessary. The reaction tube was sealed with a screw cap containing a Teflon septum and removed from the glovebox. The reaction mixture was vigorously stirred at 90 °C. Syringes (1 mL) with a long needle were used to take aliquots from the ongoing reaction. The ~0.01 mL reaction solution taken was diluted with 1 mL EtOAc and subjected to GC analysis. The first aliquot was taken at T = ~15 min and then periodically in ~30 min intervals.

Fluorination in the absence of $TESCF_3$

The general procedure was followed. The normalized quantities of **1a**, **A**, and **B** relative to the internal standard were then plotted (Scheme 3).

Fluorination in the presence of $TESCF_3$

The general procedure was followed with the addition of 55 μL of $TESCF_3$ via syringe at the beginning of the reaction. The normalized quantities of **1a**, **A**, **B**, and **$TESCF_3$** relative to the internal standard were then plotted (Scheme 6)

Fluorination with an extra amount of $TESCF_3$.

The general procedure was followed with the addition of 55 μL of $TESCF_3$ via syringe at the beginning of the reaction. At T = ~ 250 min, an extra amount of TESCF3 (18 μL, 10 mol%) was added via syringe. The normalized quantities of **1a**, **A**, **B**, and **$TESCF_3$** relative to the internal standard were then plotted (Scheme 6)

2.4.2 General Procedure for deuterium labeling experiments

In a nitrogen-filled glovebox, an oven-dried reaction tube (Fisherbrand, 16 x 125 mm, catalog no. 1495925C) equipped with a stir bar, was charged successively with $[(cinnamyl)PdCl]_2$ (0.0010 g, 0.0020 mmol, 0.20 mol%), **L1** (0.0031 g, 0.0050 mmol, 0.50 mol%), KF (0.012 g, 2.0 mmol, 2.0 equiv), **1a**, and 0.5 mL of 1,4-dioxane. *t*-BuOD, 2,6,6-**1a**-d_3, $TESCF_3$ were added if necessary. The reaction tube was sealed with a screw cap containing a Teflon septum and removed from the glovebox. The reaction mixture was vigorously stirred at 110 °C for 12 h. The reaction mixture was then allowed to cool to room temperature, and 1-fluoronaphthalene (15.0 μL, 1.16 eq.) was added. The crude reaction mixture was analyzed directly by ^{19}F NMR (282 MHz) to determine conversion, yield, and regioselectivity, as necessary.

Deuterium labeling experiments using *t*-BuOD under $TESCF_3$-free conditions

The general procedure was followed with the addition of **1a** (0.031 g, 0.10 mmol, 1.0 equiv) and *t*-BuOD (0.0075 g, 0.10 mmol, 1.0 equiv) (Scheme 4a).

Crossover experiments between 1a and 2,6,6-1a-d_3 under $TESCF_3$-free conditions

The general procedure was followed with the addition of **1a** (0.015 g, 0.050 mmol, 0.5 equiv) and 2,6,6-**1a**-d_3 (0.015 g, 0.050 mmol, 0.5 equiv) (Scheme 4b).

Crossover experiment between 1a and 2,6,6-1a-d_3 with the addition of 30 mol% $TESCF_3$

The general procedure was followed with the addition of **1a** (0.015 g, 0.050 mmol, 0.5 equiv), 2,6,6-**1a**-d_3 (0.015 g, 0.050 mmol, 0.5 equiv), and $TESCF_3$ (5.5 μL, 30 mol%) (Scheme 8).

2.4.3 Procedure for the attempted synthesis of 5

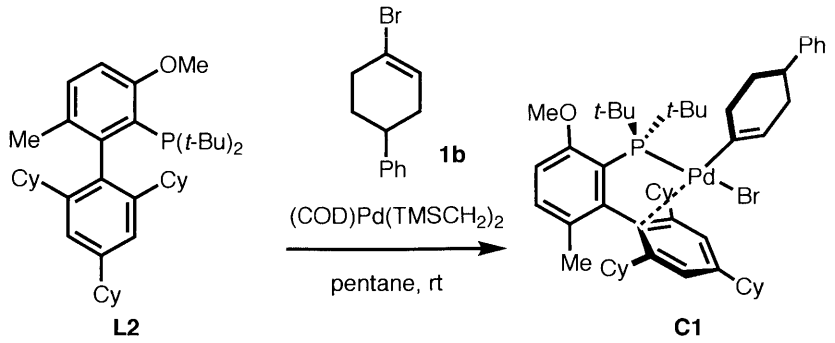

Synthesis of C1

The reaction was set up in a nitrogen-filled glovebox. An oven-dried reaction tube (Fisher 20 x 150 mm tubes – Cat. No. 1495937C) equipped with a stir bar, was charged with **L2** (0.59 g, 1.0 mmol, 1.0 equiv), 4-bromo-1,2,3,6-tetrahydro-1,1'-biphenyl (0.47 g, 2.0 mmol, 2.0 equiv), and pentane (5 mL) to give a colorless solution. To this solution, (COD)Pd($TMSCH_2$)$_2$ (0.39 g, 1.0 mmol, 1.00 equiv) was added, followed by pentane (1 mL) to rinse the sides of the reaction tube. The reaction mixture was stirred at room temperature for 24 h to give a yellow suspension and the heterogeneous mixture was filtered over a fine sintered glass filter. The filter cake was washed with pentane (5 mL) and dried under vacuum to give **L2**Pd(vinyl)Br **C1** as a yellow solid (217 mg, 82% yield).

Attempted synthesis of 5

The reaction was set up in a nitrogen-filled glovebox. An oven-dried reaction tube (Fisher 20 x 150 mm tubes – Cat. No. 1495937C) equipped with a stir bar, was charged with **C1** (0.036 g, 0.039 mmol, 1.00 equiv), AgF (0.025 g, 0.20 mmol, 5.0 equiv), solvent, and additives if necessary were added to give a dark yellow solution. The mixture was protected from light by wrapping the reaction tube in foil and was stirred overnight.

Table S1. Representative experiments for the synthesis of 5

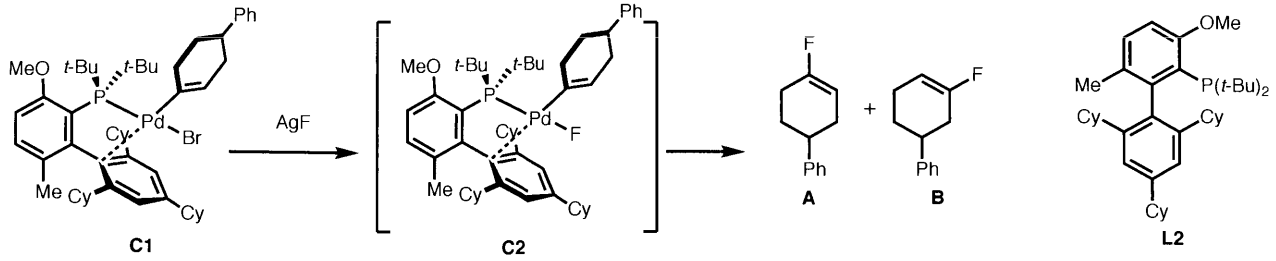

Entry	AgF (equiv)	Solvent	Temp.	Additive	**A** (%)	**B** (%)
1	5.0	CD_2Cl_2	rt	/	52	2
2	5.0	CD_2Cl_2	rt	**1b** (2.0 equiv)	102	17
3	5.0	CD_2Cl_2	rt	**L2** (1.0 equiv), **1b** (2.0 equiv)	85	15
4	5.0	C_6D_6	rt	/	39	trace
5	5.0	CD_2Cl_2	rt	$TMSCF_3$ (5.0 equiv)	trace	trace
6	2.0	CD_2Cl_2	rt	/	43	trace

2.4.4 Procedure for investigating the influence of $TESCF_3$ loadings on the fluorination reaction

In a nitrogen-filled glovebox, an oven-dried reaction tube (Fisherbrand, 16 x 125 mm, catalog no. 1495925C) equipped with a stir bar, was charged successively with $[(cinnamyl)PdCl]_2$ (0.0010 g, 0.0020 mmol, 0.20 mol%), **L1** (0.0031 g, 0.0050 mmol, 0.50 mol%), KF (0.012 g, 2.0 mmol, 2.0 equiv), **1a** (0.031 g, 0.10 mmol, 1.0 equiv), and 0.5 mL of 2-MeTHF. The corresponding amount of $TESCF_3$ was added. The reaction tube was sealed with a screw cap containing a Teflon septum and removed from the glovebox. The reaction mixture was vigorously stirred at 90 °C for 12 h. The reaction was then allowed to cool to room temperature, and 1-fluoronaphthalene (15.0 μL, 1.16 eq.) was added. The crude reaction mixture was analyzed directly by ^{19}F NMR (282 MHz) to determine the yield and regioselectivity.

2.4.5 Procedure for fluorination using BrettPhosPd(Ph)CF_3 as both the Pd and CF_3^- sources

In a nitrogen-filled glovebox, an oven-dried reaction tube (Fisherbrand, 16 x 125 mm, catalog no. 1495925C) equipped with a stir bar, was charged successively with **BrettPhosPd(Ph)CF_3 F** (0.0032 g, 0.0040 mmol, 4 mol%, **F** was prepared according to a previously reported protocol[18]), **L1** (0.0031 g, 0.0050 mmol, 0.50 mol%), KF (0.012 g, 2.0 mmol, 2.0 equiv), **1a** (0.031 g, 0.10 mmol, 1.0 equiv), and 0.5 mL of 2-MeTHF. The reaction tube was sealed with a screw cap

containing a Teflon septum and removed from the glovebox. The reaction mixture was vigorously stirred at 90 °C for 12 h. The reaction was then allowed to cool to room temperature, and 1-fluoronaphthalene (15.0 μL, 1.16 eq.) was added. The crude reaction mixture was analyzed directly by ^{19}F NMR (282 MHz) to determine the yield and regioselectivity.

2.5 References and Notes

(1) O'Hagan, D. *Chem. Soc. Rev.* **2008**, *37*, 308.

(2) (a) Wang, J.; Sánchez-Roselló, M.; Aceña, J. L.; delPozo, C.; Sorochinsky, A. E.; Fustero, S.; Soloshonok, V. A.; Liu, H. *Chem. Rev.* **2014**, *114*, 2432. (b) Zhou, Y.; Wang, J.; Gu, Z.; Wang, S.; Zhu, W.; Aceña, J. L.; Soloshonok, V. A.; Izawa, K.; Liu, H. *Chem. Rev.* **2016,** *116*, 422.

(3) Jeschke, P. *ChemBioChem* **2004**, *5*, 570

(4) (a) Gillis, E. P.; Eastman, K. J.; Hill, M. D.; Donnelly, D. J.; Meanwell, N. A. *J. Med. Chem.* **2015**, *58*, 8315. (b) Hagmann, W. K. *J. Med. Chem.* **2008**, *51*, 4359.

(5) Balz–Schiemann reaction: Balz, G.; Schiemann, G. *Ber. Dtsch. Chem. Ges. B* **1927**, *60*, 1186.; Halex process: Finger, G. C.; Kruse, C. W. *J. Am. Chem. Soc.* **1956**, *78*, 6034.

(6) (a) Grushin, V. V. *Acc. Chem. Res.* **2010**, *43*, 160. (b) Grushin, V. V.; Marshall, W. J. *Organometallics* **2007**, *26*, 4997. (c) Grushin, V. V. *Chem. -Eur. J.* **2002**, *8*, 1006. (d) Yandulov, D. V.; Tran, N. T. *J. Am. Chem. Soc.* **2007**, *129*, 1342.

(7) (a) Wang, X.; Mei, T.-S.; Yu, J.-Q. *J. Am. Chem. Soc.* **2009**, *131*, 7520. (b) Mazzotti, A. R.; Campbell, M. G.; Tang, P.; Murphy, J. M.; Ritter, T. *J. Am. Chem. Soc.* **2013**, *135*, 14012. (c) Hull, K. L.; Anani, W. Q.; Sanford, M. S. *J. Am. Chem. Soc.* **2006**, *128*, 7134. (d) Chan, K. S. L.; Wasa, M.; Wang, X.; Yu, J.-Q. *Angew. Chem., Int. Ed.* **2011**, *50*, 9081. (e) Peŕez-Temprano, M. H.; Racowski, J. M.; Kampf, J. W.; Sanford, M. S. *J. Am. Chem. Soc.* **2014**, *136*, 4097. (f) Ball, N. D.; Sanford, M. S. *J. Am. Chem. Soc.* **2009**, *131*, 3796. (g) Furuya, T.; Benitez, D.; Tkatchouk, E.; Strom, A. E.; Tang, P.; Goddard, W. A.; Ritter, T. *J. Am. Chem. Soc.* **2010**, *132*, 3793. (h) Ding, Q.; Ye, C.; Pu, S.; Cao, B. *Tetrahedron* **2014**, *70*, 409. (i) Lou, S.-J.; Xu, D.-Q.; Xia, A.-B.; Wang, Y.-F.; Liu, Y.-K.; Du, X.-H.; Xu, Z.-Y. *Chem. Commun.* **2013**, *49*, 6218.

(8) (a) Watson, D. A.; Su, M.; Teverovskiy, G.; Zhang, Y.; Garcia-Fortanet, J.; Kinzel, T.; Buchwald, S. L. *Science*, **2009**, *325*, 1661. (b) Sather, A. C.; Buchwald, S. L. *Acc. Chem. Res.* **2016**, *49*, 2146. (c) Lee, H. G.; Milner, P. J.; Buchwald, S. L. *Org. Lett.* **2013**, *15*, 5602. (d) Lee, H. G.; Milner, P. J.; Buchwald, S. L. *J. Am. Chem. Soc.* **2014**, *136*, 3792. (e) Sather, A. C.; Lee, H. G.; De La Rosa, V. Y.; Yang, Y.; Müller, P.; Buchwald, S. L. *J. Am. Chem. Soc.* **2015**, *137*, 13433. (f) Milner, P. J.; Yang, Y.; Buchwald, S. L. *Organometallics* **2015**, *34*, 4775.

(9) (a) Maimone, T. J.; Milner, P. J.; Kinzel, T.; Zhang, Y.; Takase, M. K.; Buchwald, S. L. *J. Am. Chem. Soc.* **2011**, *133*, 18106. (b) Milner, P. J.; Maimone, T. J.; Su, M.; Chen, J.; Müller, P.; Buchwald, S. L. *J. Am. Chem. Soc.* **2012**, *134*, 19922. (c) Milner, P. J.; Kinzel, T.; Zhang, Y.; Buchwald, S. L. *J. Am. Chem. Soc.* **2014**, *136*, 15757.

(10) For reviews, see: (a) Purser, S.; Moore, P. R.; Swallow, S.; Gouverneur, V. *Chem. Soc. Rev.* **2008**, *37*, 320. (b) Neumann, C. N.; Ritter, T. *Angew. Chem. Int. Ed.* **2015**, *54*, 3216; *Angew. Chem.* **2015**, *127*, 3261. (c) Kirk, K. L. *Org. Process Res. Dev.* **2008**, *12*, 305. (d) Müller, K.; Faeh, C.; Diederich, F. *Science* **2007**, *317*, 1881.

(11) (a) Welch, J.; Lin, J. *Tetrahedron* **1996**, *52*, 291. (b) Narumi, T.; Hayashi, R.; Tomita, K.; Kobayashi, K.; Tanahara, N.; Ohno, H.; Naito, T.; Kodama, E.; Matsuoka, M.; Oishi, S.; Fujii, N. *Org. Biomol. Chem.* **2010**, *8*, 616. (c) Lamy, C.; Hofmann, J.; Parrot-Lopez, H.; Goekjian, P. *Tetrahedron Lett.* **2007**, *48*, 6177. (d) Niida, A.; Tomita, K.; Mizumono, M.; Tanigaki, H.; Terada, T.; Oishi, S.; Otaka, A.; Inui, K.-I.; Fuji, N. *Org. Lett.* **2006**, *8*, 613. (e) Niida, A.; Mizumoto, M.; Narumi, T.; Inokuchi, E.; Oishi, S.; Ohno, H.; Otaka, A.; Kitaura, K.; Fujii, N. *J. Org. Chem.* **2006**, *71*, 4118.

(12) Ye, Y.; Takada, T.; Buchwald, S. L. *Angew. Chem., Int. Ed.* **2016**, *55*, 15559.

(13) When the stoichiometric experiment in Scheme 5 was conducted in the presence of $TESCF_3$, no fluorinated products were observed.

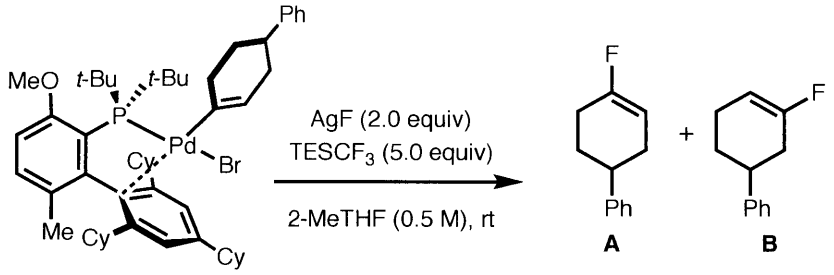

C1 0% total yield

(14) Liu, X.; Xu, C.; Wang, M.; Liu, Q. *Chem. Rev.* **2015**, *115*, 683.

(15) Prakash, G. K. S.; Wang, F.; Zhang, Z.; Haiges, R.; Rahm, M.; Christe, K. O.; Mathew, T.; Olah, G. A. *Angew. Chem. Int. Ed.* **2014**, *53*, 11575.

(16) Lishchynskyi, A.; Miloserdov, F. M.; Martin, E.; Benet-Buchholz, J.; Escudero-Adán, E. C.; Konovalov, A. I.; Grushin, V. V. *Angew. Chem. Int. Ed.* **2015**, *54*, 15289.

(17) Cho, E. J.; Buchwald, S. L. *Org. Lett.* **2011**, *13*, 6552.

(18) Cho, E. J.; Senecal, T. D.; Kinzel, T.; Zhang, Y.; Watson, D. A.; Buchwald, S. L. *Science* **2010**, *328*, 1679.

(19) Allgeier, A. M.; Shaw, B. J.; Hwang, T.-L.; Milne, J. E.; Tedrow, J. S.; Wilde, C. N. *Organometallics* **2012**, *31*, 519.

(20) Using LPd(Ph)CF_3 complex supported by BrettPhos as an example, one possible pathway of CF_3^- generation is illustrated below:[21,22]

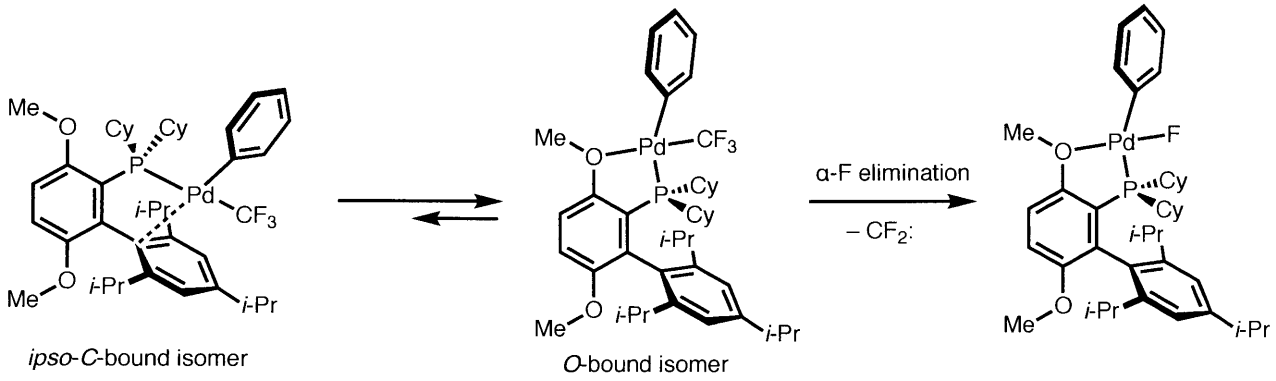

In solution, BrettPhosPd(Ph)CF_3 mainly exists as the *O*-bound isomer. At high temperature, it could potentially undergo α-fluoride elimination to generate difluorocarbene, which transforms to CF_3^- in the presence of KF.

It is also possible that the *O*-bound isomer gives an ion pair from which the CF_3^- is released and replaced by F^- from the KF.

(21) Zhang, S.-L.; Huang, L.; Sun, L.-J. *Dalton Trans.* **2015**, *44*, 4613.

(22) Grushin, V. V.; Marshall, W. J. *J. Am. Chem. Soc.* **2006**, *128*, 4632.

Chapter 3
CuH-Catalyzed Enantioselective Alkylation of Indoles with Ligand-Controlled Regiodivergence

3.1 Introduction

The indole framework is widely recognized as a 'privileged' scaffold in numerous research areas such as pharmaceuticals, fragrances, agrochemicals, pigments, and materials science (Figure 1a).[1] In particular, enantiomerically enriched indole derivatives are ubiquitous in both biologically active natural products and pharmacologically relevant compounds.[2] Therefore, the development of efficient enantioselective synthesis of indoles has been a prominent objective in organic synthesis. Traditionally, the indole is generally used as the nucleophile partner in conjunction with a variety of electrophilic partners, including activated olefins, ketones or imines, allylic alcohol derivatives, and alkynes.[3,4] The preference for bond formation at the C3-, C2- or N1-position in these reactions is usually determined by the intrinsic nucleophilicity of these positions of the indole reactant. For instance, most alkylation reactions largely or entirely take place at C3 due to the higher nucleophilicity at this position.[5] In contrast, reactions that selectively generate enantioenriched N1-alkylated indoles, despite their potential utility, remain rare and underdeveloped (Figure 1b). To date, several strategies have been employed to favor reaction at the N1-position, particularly in the context of the enantioselective N-allylation of indoles. These include: 1) the installation of an electron-withdrawing substituent at C2 or C3;[6] 2) the employment of specialized allylation reagents;[7] and 3) two-step synthesis by asymmetric allylation/oxidation of indolines and asymmetric allylation/Fischer indolization of aryl hydrazines.[8] Despite these advances, the enantioselective synthesis of N1-alkylated indoles is still unknown.[9] Herein we report a CuH-catalyzed enantioselective alkylation of indoles with interesting ligand-controlled regiodivergence using a polarity reversal strategy.

In this method, electrophilic indoles (*N*-benzoyloxyindole derivatives) are employed as starting materials instead of the nucleophilic reagents that are commonly used (Figure 1c). N1-alkylated indoles can be efficiently synthesized with high levels of regio- and enantioselectivity with a DTBM-SEGPHOS-modified CuH catalyst. Meanwhile, chiral C3-alkylated indoles can also be selectively accessed when Ph-BPE is used as the ligand.

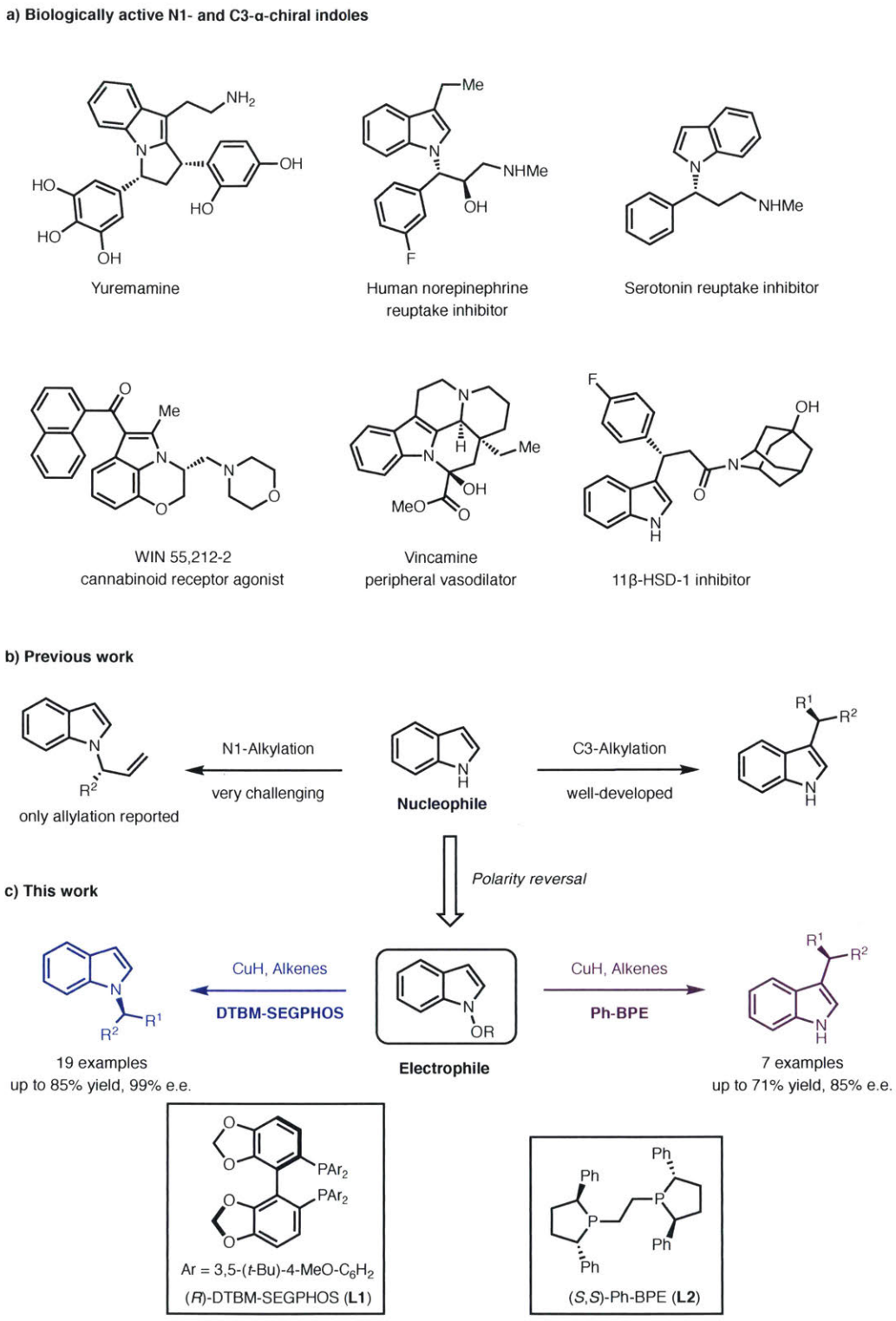

Figure 1. Bioactive indoles, traditional chiral indole synthesis and indole alkylation using an umpolung strategy. a, Representative biologically active N1- and C3-substituted α-chiral indoles. **b**, Regioselectivity in enantioselective alkylation of nucleophilic indoles. **c**, Ligand-controlled regiodivergent alkylation of electrophilic indoles.

3.2 Results and Discussion

3.2.1 Reaction Design

Since the typical C3-selectivity observed in indole alkylation reactions originates from the nucleophilic character of the indole, we envisioned that if the indole could be employed as an electrophile, this intrinsic preference might no longer be dominant. Over the past decade, the study of transformations of electrophilic indole derivatives has emerged as an active area of research,[10] enabling novel bond constructions in indole synthesis that would be difficult to realize by conventional methodology.

During the same period, CuH-catalysis emerged as an efficient method for the enantioselective formation of C–N and C–C bonds.[11,12] In these reactions, enantioenriched alkylcopper intermediates generated from alkenes can act as nucleophiles. We reasoned that these same species could react with an electrophilic indole reagent and provide alkylated indoles, potentially with high enantioselectivity and chemoselectivity.

For our proposed transformation to be viable, the electrophilic indole reagent must satisfy certain criteria. For example, the electrophilic indole must be stable in the presence of the catalytic LCuH, yet reactive enough to productively interact with a short-lived alkylcopper(I) intermediate. Furthermore, the reagent must be effective in delivering a range of indole fragments in order to maximize the synthetic utility of the process. In analogy to our previous hydroamination reactions, we considered *N*-benzoyloxyindole derivatives to be promising reagents for this purpose. Compared with other electrophilic indoles such as indolynes or indoles bearing electron-withdrawing groups, *N*-benzoyloxyindoles with many substitution patterns can be reliably synthesized.[13] Furthermore, the stability of the electrophilic indole reagent could be modulated by tuning the character of the leaving group.

Using a *N*-benzoyloxyindole as the electrophile partner, the mechanism of our proposed reaction is outlined in Figure 2. At the beginning of the reaction, the phosphine-ligated CuH catalyst (LCuH, **I**) is formed *in situ* from the combination of $Cu(OAc)_2$, a phosphine ligand, and silane. Next, olefin insertion into LCuH (**I**) forms alkyl copper(I) species **II**. Interception of **II** by indole electrophile **2** generates chiral indole **3** or **4**, as well as phosphine-ligated copper(I) benzoate ($LCuO_2CAr$, **III**). From here, regeneration of LCuH (**I**) from the reaction of a hydrosilane with **III** closes the catalytic cycle.[14]

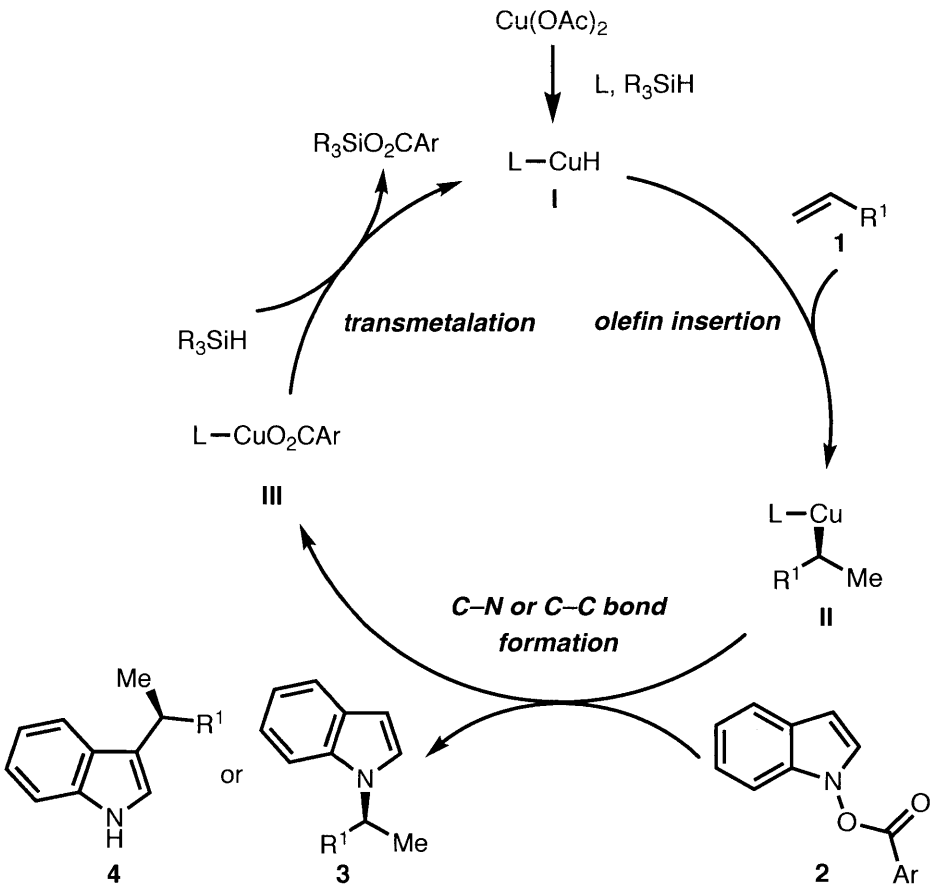

Figure 2. Proposed mechanism for CuH-catalyzed indole alkylation.

3.2.2 Reaction Discovery

Several *N*-benzoyloxyindole derivatives with different *O*-benzoate substituents were synthesized on gram-scale in 30-60% yields (see Supporting Information for details). The feasibility of the alkylation process was first investigated using styrene as the precursor to the benzyl copper nucleophile, copper(II) acetate as the precatalyst, and DTBM-SEGPHOS as the ligand. The N1-alkylated indole was generated with excellent regioselectivity (N1:C3 > 99:1) and with good enantioselectivity (Table 1). Among the indole electrophiles tested, the *N*-(2,4,6-trimethylbenzoyl)indole (**2d**) provided the best yield and the highest enantiometric excess. We hypothesized that the steric hindrance provided by the two *ortho*-methyl groups on the benzoate slows direct reduction of the carbonyl, allowing the reagent to undergo the desired transformation at a higher temperature. Interestingly, the regioselectivity was found to switch from C–N to C–C bond formation when DTBM-SEGPHOS was replaced with Ph-BPE (Table 2,

entries 1 and 2). Catalysts based on DuanPhos provided the alkylated indoles in diminished yields and with no chemoselectivity (Table 2, entry 3). JosiPhos and MeO-BIPHEP showed limited ability to facilitate the reaction (Table 2, entries 4 and 5). With these initial results in hand, these two alkylation processes were further studied with DTBM-SEGPHOS and Ph-BPE as the ligands, respectively.

Table 1. Investigation of *N*-benzoyloxyindole Derivatives as Electrophilic Indole Reagents.

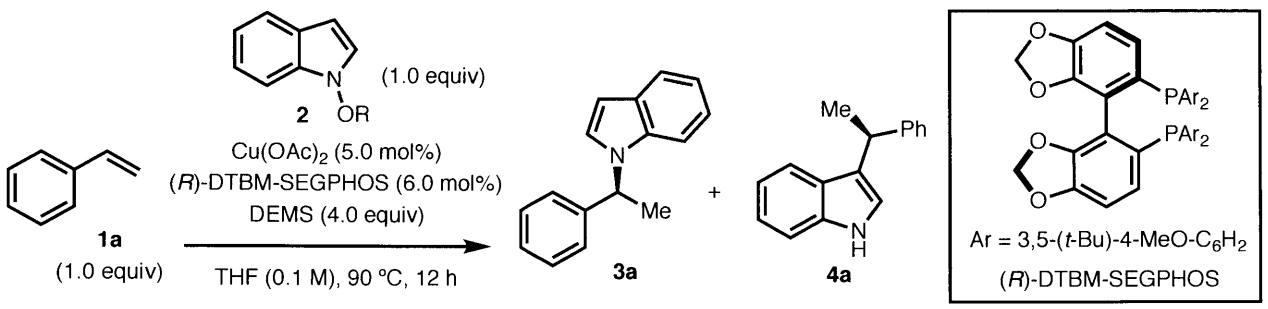

Entry	2	Yield of **3a** (%)[a]	e.e. (%)[b]	r.r. (**3a**:**4a**)
1	**2a**	48	83	> 20:1
2	**2b**	37	78	> 20:1
3	**2c**	5	/	> 20:1
4	**2d**	54	88	> 20:1

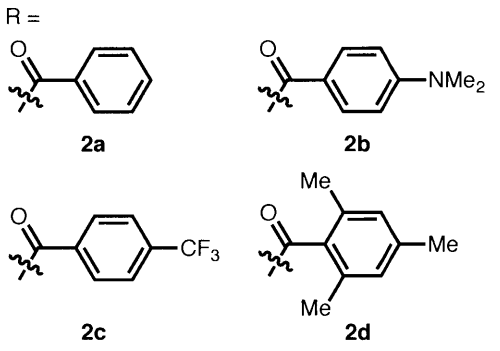

[a]Reactions were conducted on 0.1 mmol scale. Yields were determined by gas chromatography using dodecane as internal standard. [b]The e.e. was determined by SFC analysis using columns with chiral stationary phases.

3.2.3 Optimization of the N1-Alkylation Reaction

After evaluating a variety of reaction parameters, we found that the N1-alkylated chiral indole could be accessed in good yield with excellent regio- and enantioselectivity at 90 °C using $Cu(OAc)_2$ as the copper source, DTBM-SEGPHOS as the ligand, diethoxymethylsilane (DEMS) as the hydride source, and triethylmethanol as an additive (Table 3, entry 1). A higher than usual temperature, compared to most CuH-catalyzed processes, was required to achieve an optimal yield (Table 3, entry 2). Substituting diethoxymethylsilane (DEMS) with dimethoxymethylsilane (DMMS) decreases the observed yield and enantioselectivity (Table 3, entry 3). Since one of the major side reactions in this transformation is the reduction of the indole electrophile **2d** by CuH,

it was necessary to employ a slight excess of this reagent (1.5 equiv) to achieve a better yield (Table 3, entry 4). In addition, the reaction gave a better result at 0.1 M of substrate than at 0.5 M (Table 3, entry 5). Further we found that the inclusion of an alcohol as an additive provided the desired product with improved efficiency (Table 3, entry 6). We believe that the protonation of an off-cycle copper indolyl species[15] with Et_3COH bypasses its slow transmetalation with a hydrosilane and thus facilitates catalyst regeneration.[16]

Table 2. Investigation of Ligand Dependence on the Regioselectivity of the Process.

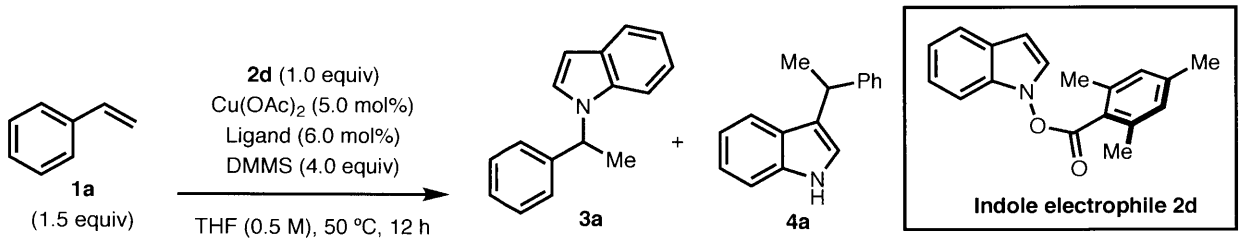

Entry[a]	Ligand	Yield of **3a** (%)	Yield of **4a** (%)	Total yield (%, **3a**+**4a**)	C–N:C–C
1	(*R*)-DTBM-SEGPHOS	36	trace	36	>20:1
2	(*S*,*S*)-Ph-BPE	11	65	76	1:6
3	(1*R*,1'*R*,2*S*,2'*S*)-DuanPhos	10	10	20	1:1
4	JosiPhos SL-J009-1	trace	trace	trace	/
5	(*R*)-MeO-BIPHEP	trace	trace	trace	/

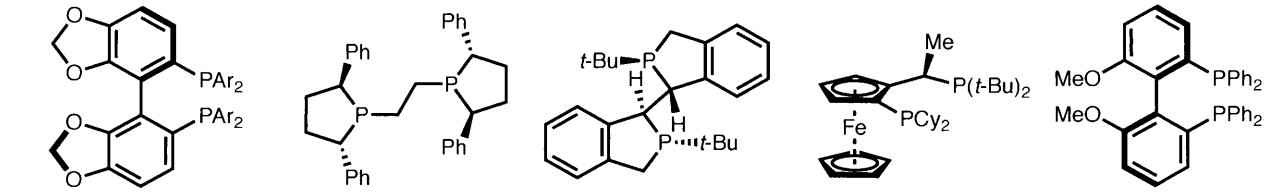

[a]Reactions were conducted on 0.1 mmol scale. Yields were determined by gas chromatography using dodecane as internal standard.

3.2.4 N1-Alkylation Substrate Scope.

Utilizing the optimized reaction conditions described above, a range of styrenes was first investigated as substrates (Table 4). In all cases, we observed that the N1-to-C3 selectivity was >20:1. Styrenes bearing *ortho*- (**3b**, **3n**), *meta*- (**3c**, **3m**, **3r**), and *para*-substituents (**3e**) were

all suitable, yielding the desired N1-alkylated indoles with high efficiency and high levels of enantioselectivity. Electron-withdrawing groups on the aryl ring of the styrenes facilitated the reaction (**3c**), while an electron-donating group (**3d**) slowed down the reaction. Trans-β-substituted styrenes were also successfully transformed using this protocol (**3g**, **3h**). In particular, **3h**, an important serotonin reuptake inhibitor derivative, was efficiently prepared in a reaction that proceeded with excellent levels of regio- and enantioselectivity. A more sterically hindered β,β-substituted styrene was transformed to the desired product (**3i**) in moderate yield as a single diastereomer.

Alkyl-substituted terminal alkenes could also be employed as coupling partners (**3j**) with a nearly complete change in preference toward the anti-Markovnikov product. Monosubstituted C=C double bonds underwent the transformation selectively (**3k**, **3l**, **3o**), with *cis*-disubstituted or trisubstituted olefins remaining intact.

Table 3. Optimization of CuH-Catalyzed Enantioselective N1-Alkylation.

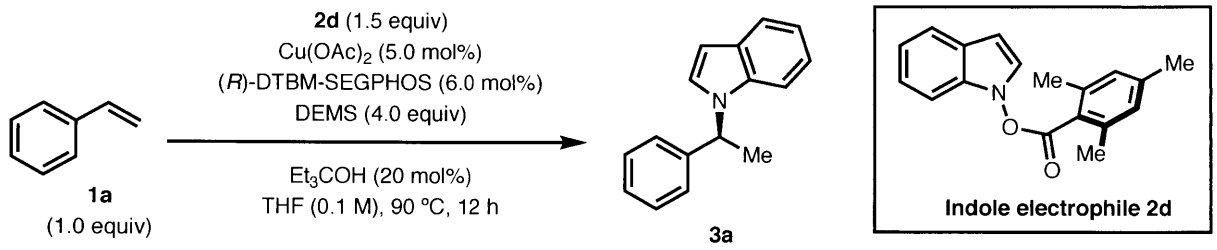

Entry	Change from the "standard conditions"	Yield (%)[a]	e.e. (%)[c]	r.r.[d]
1	none	91 (85)[b]	91	> 20:1
2	70 °C	75	93	> 20:1
3	DMMS instead of DEMS	69	22	> 20:1
4	1.0 instead of 1.5 equiv of **2d**	86	89	> 20:1
5	0.5 M instead of 0.1 M	71	93	13:1
6	no Et_3COH	68	92	> 20:1

[a]Reactions were conducted on 0.1 mmol scale. Yields were determined by gas chromatography using dodecane as internal standard. [b]Isolated yield on a 0.5 mmol scale. [c]The e.e. was determined by SFC analysis using columns with chiral stationary phases. [d]The regioselectivity (r.r.) was determined by GC analysis of the crude reaction mixture.

Table 4. Substrate Scope of CuH-Catalyzed Enantioselective N1-Alkylation.

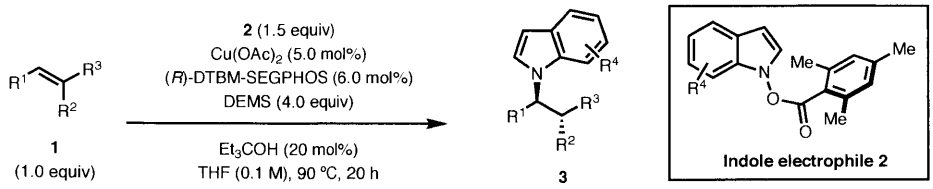

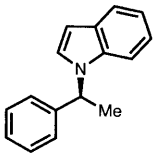

3a
85% yield, 91% e.e.
r.r. > 20:1

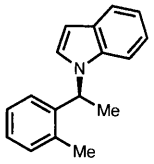

3b
81% yield, 87% e.e.
r.r. > 20:1

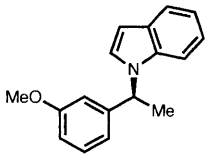

3c
71% yield, 93% e.e.
r.r. > 20:1

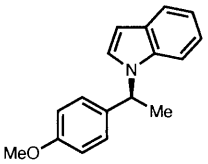

3d
10% yield
r.r. > 20:1

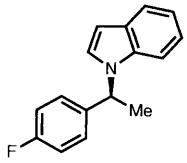

3e
81% yield, 92% e.e.
r.r. > 20:1

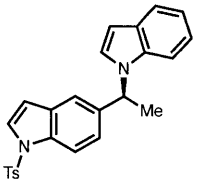

3f
63% yield, 93% e.e.
r.r. > 20:1

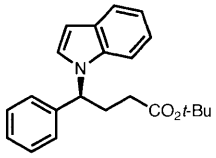

3g
78% yield, 96% e.e.
r.r. > 20:1

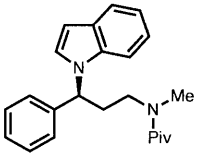

3h
69% yield, > 99% e.e.
r.r. > 20:1

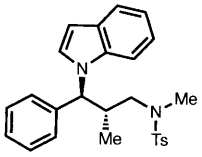

3i[a]
41% yield, > 99% e.e.
d.r. > 20:1, r.r. > 20:1

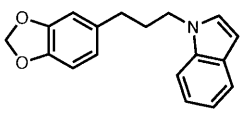

3j[a]
61% yield
r.r. > 20:1

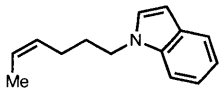

3k[a]
73% yield
r.r. > 20:1

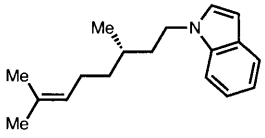

3l[a]
71% yield
r.r. > 20:1

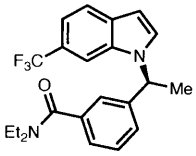

3m
56% yield, 82% e.e.
r.r. > 20:1

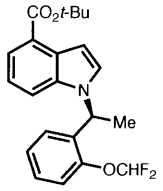

3n
61% yield, 92% e.e.
r.r. > 20:1

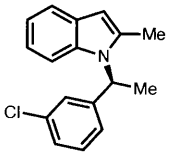

3r
81% yield, 93% e.e.
r.r. > 20:1

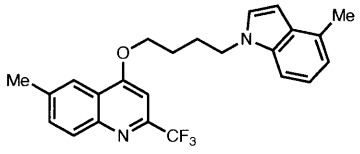

3p[a]
76% yield, r.r > 20:1

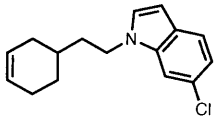

3o[a]
63% yield, r.r > 20:1

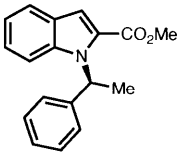

3q[b]
43% yield, 0% e.e.
r.r. > 20:1

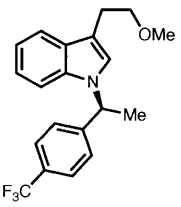

3s[c]
16% yield, 21% e.e
r.r. > 20:1

Condition: **1** (0.50 mmol), **2** (0.75 mmol), Et_3COH (0.10 mmol), $Cu(OAc)_2$ (5.0 mol%), (*R*)-DTBM-SEGPHOS (6.0 mol%), DEMS (4.0 equiv), THF (0.1 M), 90 °C, 20 h. The e.e. was determined by SFC analysis using columns with chiral stationary phases. [a]Condition: **1** (0.75 mmol), **2** (0.50 mmol), KF (0.10 mmol), $Cu(OAc)_2$ (5.0 mol%), (*R*)-DTBM-SEGPHOS (6.0 mol%), DEMS (4.0 equiv), THF (0.1 M), 70 °C, 20 h. [b]Using 1,4-dioxane instead of THF. [c]Condition: **1** (0.50 mmol), **2** (1.5 mmol), Et_3COH (0.10 mmol), $Cu(OAc)_2$ (5.0 mol%), (*R*)-DTBM-SEGPHOS (6.0 mol%), DEMS (4.0 equiv), 1,4-dioxane (0.1 M), 90 °C, 20 h.

In terms of the scope of indole electrophiles, a variety of functional groups were accommodated at different positions on the benzene ring of the indole, including a 6-trifluoromethyl (**3m**), a 4-*tert*-butyl ester (**3n**), and a 6-chloro (**3o**) substituent. Alkyl groups at the 2- and 4-position of the indole electrophile were tolerated and the corresponding products were synthesized in good yields with excellent enantioselectivities (**3r**, **3p**). An indole electrophile with a 2-carbomethoxy substituent exhibited low reactivity under the standard reaction conditions (10% conversion). However, using excess styrene and dioxane as solvent, the desired product was obtained in moderate yield (**3q**) albeit in racemic form. Indole electrophiles bearing substituents at the 3-position were generally poor substrates in this N1-alkylation reaction. The desired product was generated in low yield with diminished stereoselectivity.[17]

3.2.5 C3-Alkylation Reaction Optimization

Using Ph-BPE as the ligand, the desired C3-alkylated indole **4a** was formed in high yield and with good enantioselectivity. The regioselectivity of this reaction is greater than 5:1 (C3:N1, Table 5, entry 1). Compared with N1-alkylation employing DTBM-SEGPHOS, this C3-alkylation proceeds at lower temperature (Table 5, entry 2). The reaction with 1.0 mol% catalyst loading gave comparable yield and better enantioselectivity than with 5.0 mol% (Table 5, entry 3). DMMS was employed instead of DEMS to achieve a better yield (Table 5, entry 4). The use of an excess amount of alkene (2.0 equiv) in this reaction was crucial to achieve an acceptable yield, although a corresponding diminishment of the enantioselectivity was observed (Table 5, entry 5). The addition of an alcohol additive again improved both yield and the enantioselectivity (Table 5, entry 7).

3.2.6 C3-Alkylation Substrate Scope.

With the optimized reaction conditions in hand, a number of C3-alkylated indoles were prepared in moderate to good yields and with useful levels of enantiomeric excess (Table 6). 4-Trifluoromethyl styrene was found to be an efficient substrate in this transformation, providing the desired indole product (**4b**) in moderate yield with a high level of regioselectivity. The lower enantioselectivity observed compared to **4a** might due to fast racemization of the electron-deficient alkylcopper species.[18] In contrast, 1-tosyl-5-vinylindole, a relatively electron-rich alkene, underwent the transformation with lower regioselectivity but better enantioselectivity (**4c**). A *trans*-β-substituted styrene was also effectively transformed by this protocol (**4d**). To further demonstrate the synthetic utility of this method, chiral C3-alkylated chiral indoles derived from estrone and loratadine, a common antihistamine, were prepared with good regio- and enantioselectivities (**4e**, **4f**). In addition to styrenes, a terminal alkyl-substituted olefin was used as the coupling partner, generating the corresponding product in a moderate yield and with excellent regioselectivity (**4g**, >99:1).

Table 5. Optimization of CuH-catalyzed Enantioselective C3-Alkylation.

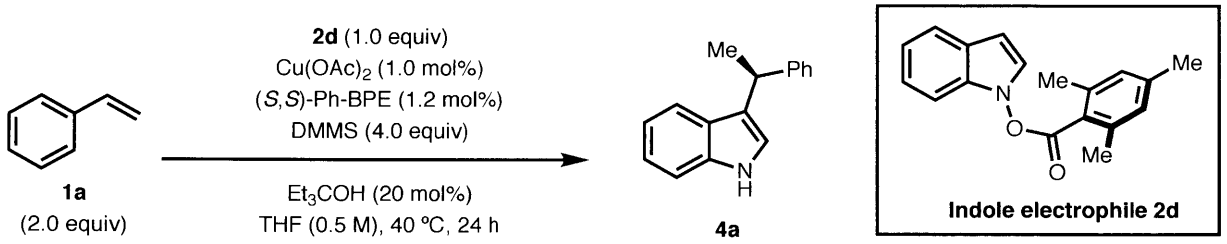

Entry	Change from the "standard conditions"	Yield (%)[a]	e.e. (%)[c]	r.r.[d]
1	none	79 (71)[b]	79	5.3:1
2	90 °C	59	67	2.1:1
3	5 mol% instead of 1 mol% $Cu(OAc)_2$	78	72	6.0:1
4	DEMS instead of DMMS	22	94	2.3:1
5	1.0 instead of 2.0 equiv of **1a**	37	83	4.9:1
6	0.1 M instead of 0.5 M	55	73	3.7:1
7	no Et_3COH	67	73	5.6:1

[a]Reactions were conducted on 0.1 mmol scale. Yields were determined by gas chromatography using dodecane as internal standard. [b]Isolated yield on a 0.5 mmol scale. [c]The e.e. was

determined by SFC analysis using columns with chiral stationary phases. [d]The regioselectivity (r.r.) was determined by GC analysis of the crude reaction mixture.

Table 6. Substrate Scope of CuH-Catalyzed Enantioselective C3-Alkylation.

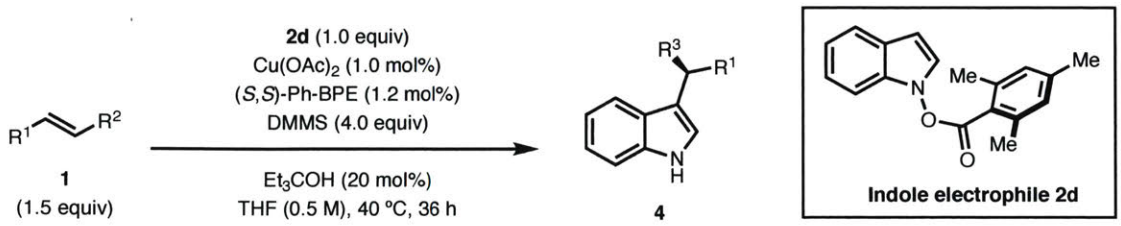

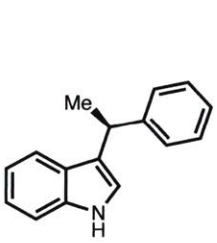

4a
71% yield, 76% e.e.
r.r. = 5:1

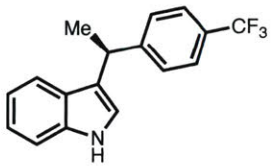

4b
61% yield, 50% e.e.
r.r. = 53:1

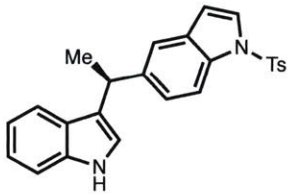

4c
55% yield, 85% e.e.
r.r. = 3:1

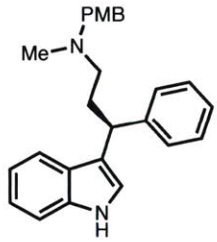

4d
61% yield, 69% e.e.
r.r. = 4:1

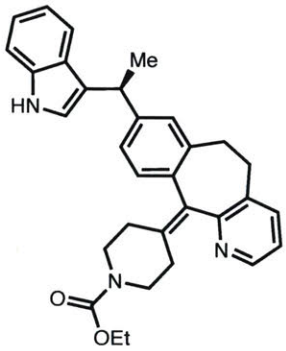

4f
41% yield, XX% e.e.
r.r = 5:1

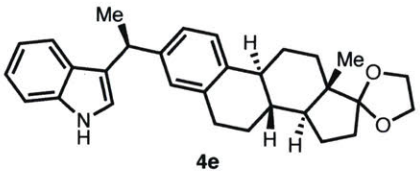

4e
62% yield, 84% e.e.
r.r. = 5:1

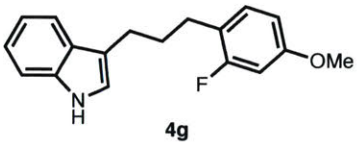

4g
32% yield
r.r. > 99:1

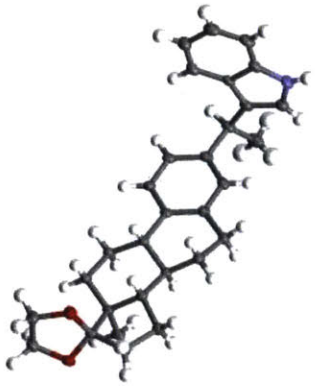

Crystal structure of **4e**

Condition: **1** (1.0 mmol), **2d** (0.50 mmol), Et_3COH (0.10 mmol), $Cu(OAc)_2$ (1.0 mol%), (*S*,*S*)-Ph-BPE (1.2 mol%), DMMS (4.0 equiv), THF (0.5 M), 40 °C, 24 h. The e.e. was determined by SFC analysis using columns with chiral stationary phases. The regioselectivity (r.r.) was determined by GC analysis of the crude reaction mixture.

3.2.7 Mechanistic Discussion

In order to analyze the origin of the ligand-controlled regiodivergence, density functional theory (DFT) calculations were performed in collaboration with the Baik group at KAIST, to elucidate the mechanism of this alkylation process. We focused on the reaction between the alkylcopper intermediate **II** and the indole electrophile, which determines the regioisomer of product that is formed. Based on previous mechanistic studies on CuH chemistry[14] and experimental observations,[19] two pathways were proposed (Figure 3).

In pathway 1 (blue), the copper center of **II** undergoes oxidative insertion into the N1–O bond of the indole electrophile **2d** via transition state **II-TS'** to generate intermediate $\mathbf{III_N}$. Next, the oxidative addition complex $\mathbf{III_N}$ produces the N1-alkylated product **3a** by reduction elimination via transition state $\mathbf{III_N}$**-TS**. Alternatively, in Pathway 2 (purple), the oxidative addition takes place at the C3-position of the indole electrophile **2d** via **II-TS** to generate $\mathbf{III_C}$. Subsequent reductive elimination from $\mathbf{III_C}$ (via $\mathbf{III_C}$**-TS**) followed by rearomatization through tautomerization forms the C3-alkylated product **4a**. Notably, intermediate $\mathbf{III_N}$ and $\mathbf{III_C}$ could potentially interconvert via intermediate **IV**. However, computational studies suggest that these 1,3-migration processes can be neglected since the competing reductive elimination processes are much faster (see below, as well as the full energy profile in the Supporting Information). Therefore, if irreversible, the oxidative addition process should determine the overall regioselectivity of the reaction.

DFT calculations were then conducted on the oxidative addition step using different ligands (Figure 4). Instead of DTBM-SEGPHOS, SEGPHOS, which experimentally gives the same regioselectivity as DTBM-SEGPHOS (>20:1 N1:C3), was used for the calculation to reduce the complexity of the systems and facilitate computational analysis.

When SEGPHOS was employed as the supporting ligand, the alkylcopper complex **II** prefers the N1-oxidative addition with **2d** over the alternative C3-oxidative addition. The N1-oxidative addition is associated with a barrier of 23.4 kcal/mol ($\mathbf{II_S}$**-TS'**), while the C3-oxidative addition transition state $\mathbf{II_S}$**-TS** is 2.8 kcal/mol higher in energy. This computed energy difference agrees with the experimental observations that the N1-alkylated indoles are formed with excellent (>20:1) regioselectivities. In contrast, in the case of the Ph-BPE system, oxidative additions at N1- and C3-positions have barrier of 19.8 kcal/mol ($\mathbf{II_P}$**-TS'**) and 18.8 kcal/mol ($\mathbf{II_P}$**-TS**), respectively. This moderate preference for the C3-alkylated regioisomer is consistent with the experimental results (~ 5:1 C3:N1).

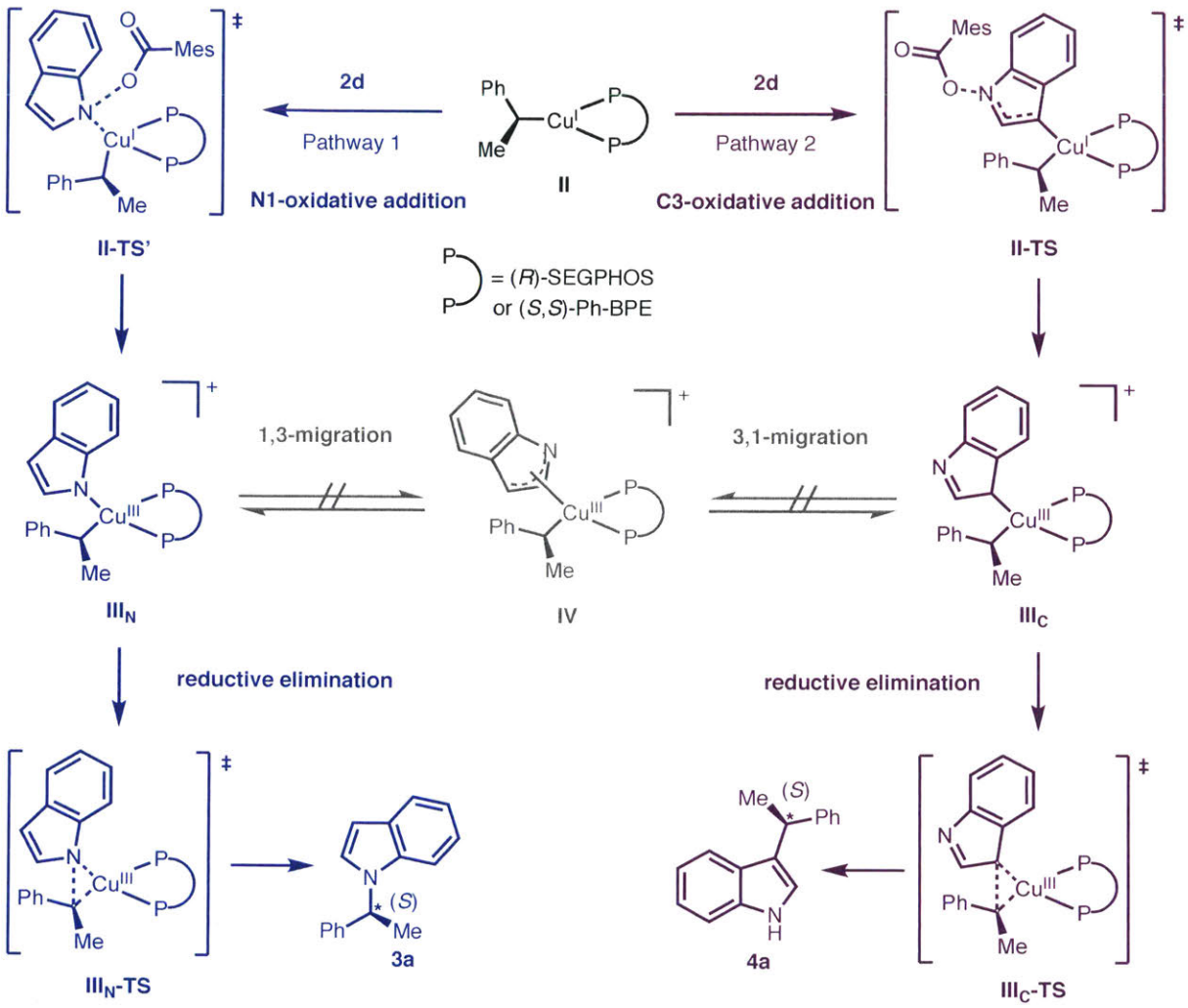

Figure 3. Proposed regioselectivity-determining reaction pathway.

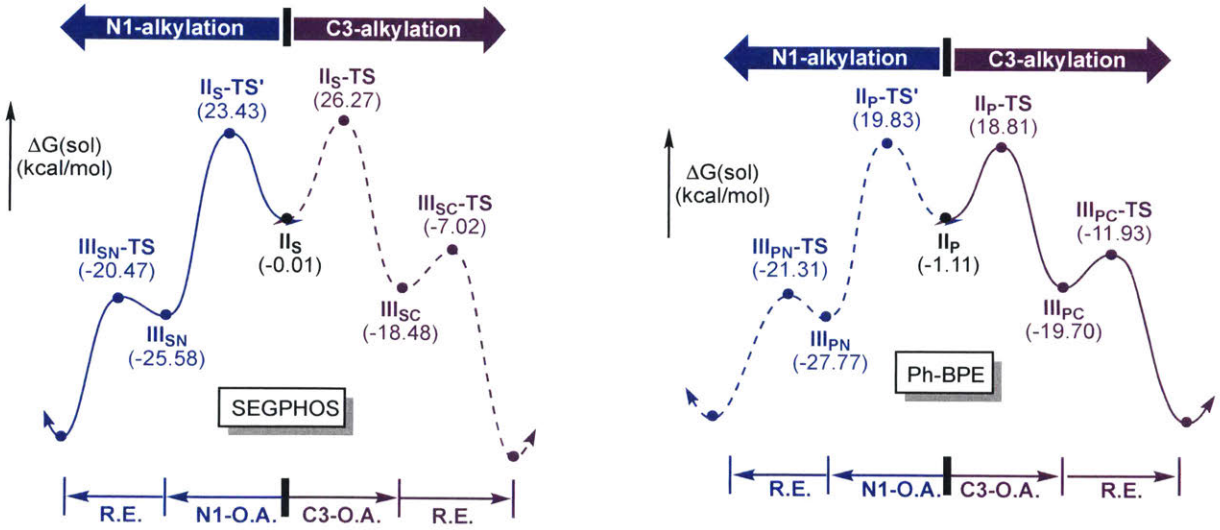

Figure 4. Energy profiles of oxidative addition steps with 2d and alkylcopper complex II.

(Subscript S and P indicates SEGPHOS and Ph-BPE as the supporting ligand, respectively)

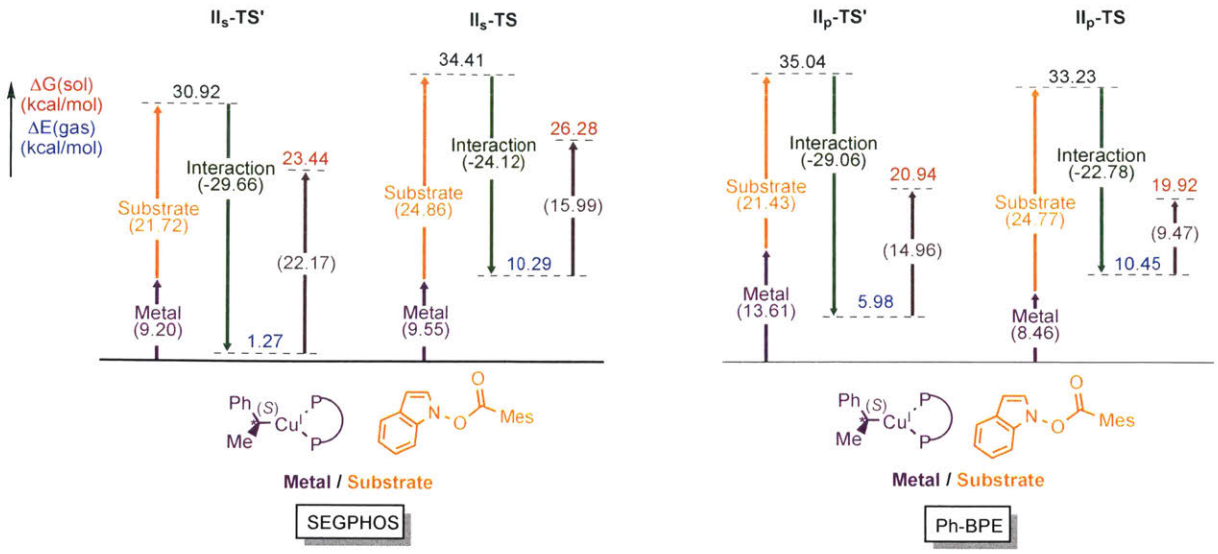

Figure 5. Energy decomposition analysis of transition states II-TS' and II-TS supported by SEGPHOS and Ph-BPE. (Subscripts S and P indicate SEGPHOS and Ph-BPE as the supporting ligand, respectively)

To elucidate the fundamental origin of these barrier difference, we carried out energy decomposition analysis of the two transition states, **II-TS'** and **II-TS**. As illustrated in Figure 5, the transition state structure was partitioned into a substrate fragment and a metal fragment. The energies labeled "substrate" and "metal" represent the distortion energy during transformation of the isolated fragments from the ground state geometry into the transition state geometry. The interaction energy is the energy of association between these two fragments in the transition state. The sum of these three energy components results in the electronic energy barrier of the transition state (ΔE_{gas}). Additionally, entropy and solvation corrections were added, resulting in a predicted free energy barrier (ΔG_{sol}).

In the case of SEGPHOS, the distortion energies of the metal fragment in the N1- and C3-oxidative addition steps are almost the same. The substrate distortion has a 3.1 kcal/mol energy difference favoring the N1-oxidative addition. In addition, the interaction energy is more favorable in the N1-oxidative addition by 5.5 kcal/mol. In total, this leads to a relatively large energy difference (9 kcal/mol) in the electronic energy barrier favoring N1-oxidative addition. The free energy correction attenuates this preference since the solvation penalty for N1-oxidative addition is more substantial; however, the final free energy barrier of the N1-oxidative addition is still 2.8 kcal/mol lower than the C3-oxidative addition.

In the case of Ph-BPE, the distortion of substrate fragment and interaction energy in the N1- or C3-oxidative addition transition states show the same trends as the SEGPHOS system. In

contrast, the distortion energy of metal fragment is markedly different. When Ph-BPE is used as the ligand, N1-oxidative addition distorts the alkylcopper species more than C3-oxidative addition, resulting in 5.2 kcal/mol difference in distortion energy. As a result, the electronic energy difference between the two oxidative addition pathways is 4.5 kcal/mol, which is significantly smaller than the difference in the case of SEGPHOS (9 kcal/mol). This smaller electronic energy difference is overwhelmed by the 5.5 kcal/mol difference in free energy correction, ultimately resulting in a reversal of preference toward oxidative addition at the C3-position. Analysis of the transition state structure shows that while the Cu–P bond in the SEGPHOS system elongates by ~0.05 Å during the oxidative addition, the same bond in the Ph-BPE system is lengthened by ~0.12 Å (see the Supporting Information for details). The more severe structural distortion of the alkylcopper species supported by Ph-BPE is a major contributor to the preference for generating C3-alkylated products.

3.3 Conclusion

In summary, we have developed an enantioselective CuH-catalyzed process to access either N1- and C3-alkylated indoles, depending on the choice of ligand. In contrast to conventional indole functionalization in which indoles are used as nucleophiles, *N*-benzoyloxyindole derivatives are employed as electrophiles in this method. DFT calculations were performed in order to understand the origin of the ligand-controlled regiodivergence. The extent to which the Cu–P bonds of the alkylcopper intermediate distort is suggested to affect the site of oxidative addition, which in turn determines the regioselectivity of the reaction. We anticipate that this general umpolung strategy may not be limited to indole electrophiles, but could be further extended to the catalytic functionalization of other important heterocyclic compounds.

3.4 Experimental

General Reagent Information: All reactions were performed under a nitrogen atmosphere using the indicated method in the general procedures. Tetrahydrofuran (THF) was purchased from J.T. Baker in CYCLE-TAINER® solvent delivery kegs and purified by passage under argon pressure through two packed columns of neutral alumina and copper(II) oxide. Anhydrous 1,4-dioxane was purchased from Aldrich Chemical Company in a Sure-Seal™ bottle and used as received. Copper(II) acetate was purchased from Strem and was used as received. 1,2-Bis((2*S*,5*S*)2,5-diphenylphospholano)ethane, 1,2- Bis((2*R*,5*R*)2,5-diphenylphospholano)ethane (Ph-BPE) ligands were purchased from Namena Corp. and stored in a nitrogen-filled glove box. DTBM-SEGPHOS was purchased from Takasago International Co. and used as received. Diethoxymethylsilane was purchased from TCI America. Dimethoxy(methyl)silane (DMMS) was purchased from Tokyo Chemical Industry Co. (TCI). Both silanes were stored in a nitrogen-filled glove box at –20 °C for long term storage. (***Caution**: Dimethoxy(methyl)silane (DMMS, CAS#16881-77-9) is listed by several vendors (TCI, Alfa Aesar) SDS or MSDS as a H318, a category 1 Causes Serious Eye Damage Other vendors (Sigma-Aldrich, Gelest) list DMMS as a H319, a category II Eye Irritant. DMMS should be handled in a well- ventilated fumehood using proper precaution as outlined for the handling of hazardous materials in prudent practices in the laboratory. At the end of the reaction either ammonium fluoride in methanol, aqueous sodium hydroxide (1 M) or aqueous hydrochloric acid (1 M) should be carefully added to the reaction mixture. This should be allowed to stir for at least 30 min or the time indicated in the detailed reaction procedure*). All other solvents and commercial reagents were used as received from Sigma Aldrich, Alfa Aesar, Acros Organics, TCI and Combi-Blocks, unless otherwise noted. Flash column chromatography was performed using 40-63 μm silica gel (SiliaFlash® F60 from Silicycle), or with the aid of a Biotage Isolera Automated Flash Chromatography System using prepacked SNAP silica cartridges (10-100 g). Organic solutions were concentrated *in vacuo* using a Buchi rotary evaporator.

General Analytical Information: All new compounds were characterized by NMR spectroscopy, IR spectroscopy, elemental analysis or high resolution mass spectrometry, optical rotation and melting point analysis (if solids). ^{1}H, ^{13}C and ^{19}F NMR spectra were recorded in $CDCl_3$ on a Bruker AMX-400 spectrometer. Chemical shifts for ^{1}H NMR are reported as follows: chemical shift in reference to residual $CHCl_3$ at 7.26 ppm (δ ppm), multiplicity (s =

singlet, br s = broad singlet, d = doublet, t = triplet, q = quartet, sex = sextet, sep = septet, ddd = doublet of double of doublets, td = triplet of doublets, m = multiplet), coupling constant (Hz), and integration. Chemical shifts for ^{13}C NMR are reported in terms of chemical shift in reference to the $CDCl_3$ solvent signal (77.16 ppm). Chemical shifts for ^{19}F-NMR are reported in terms of chemical shift in reference to an external standard (α,α,α-trifluorotoluene set to δ -63.7 ppm). IR spectra were recorded on a Thermo Scientific Nicolet iS5 spectrometer (iD5 ATR, diamond) and are reported in terms of frequency of absorption (cm^{-1}). Melting points were measured on a Mel-Temp capillary melting point apparatus. Optical rotations were measured using a Jasco P-1010 digital polarimeter. Elemental analyses were performed by Atlantic Microlabs Inc., Norcross, GA. ESI- and DART-MS spectrometric data were recorded on a Bruker Daltonics APEXIV 4.7 Tesla Fourier transform ion cyclotron resonance mass spectrometer (FT-ICR-MS). Enantiomeric excesses (ee's) were mostly determined by chiral SFC analysis using a Waters Acquity UPC2 instrument; specific columns and analytical methods are provided in the experimental details for individual compounds; the wavelengths of light used for chiral analyses are provided with the associated chromatograms. The enantiomeric excesss of certain compounds were determined by High pressure liquid chromatography (HPLC) performing on Agilent 1200 Series chromatographs using chiral columns (25 cm). Thin-layer chromatography (TLC) was performed on silica gel 60Å F_{254} plates (SiliaPlate from Silicycle) and visualized with UV light or potassium permanganate stain. Preparatory thin-layer chromatography (Prep-TLC) was performed on silica gel GF with UV 254 (20 x 20 cm, 1000 microns, catalog # TLG-R10011B-341 from Silicycle) and visualized with UV light. Isolated yields reported reflect the average values from two independent runs.

3.4.1 CuH-Catalyzed Enantioselective N1-Alkylation

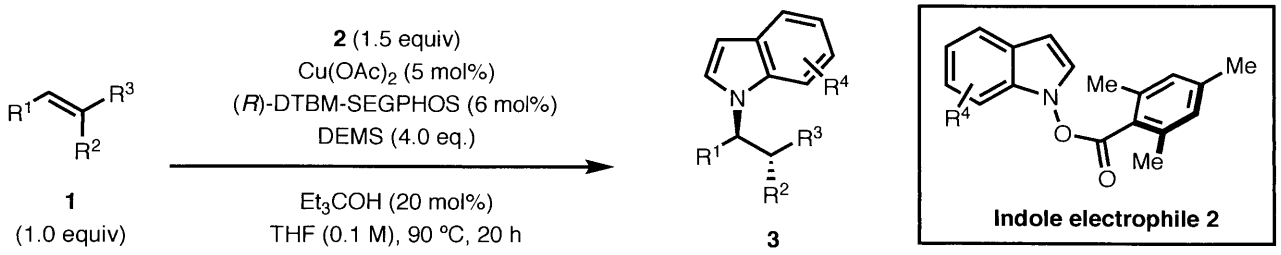

General Procedure A:

Preparation of CuH solution: In a nitrogen-filled glovebox, an oven-dried screw-top reaction tube (Fisherbrand, 13 x 100 mm, catalog no. 14-959035C) equipped with a magnetic stir bar was charged with $Cu(OAc)_2$ (4.5 mg, 0.025 mmol, 5 mol %) and (*R*)-DTBM-SEGPHOS (35.4 mg,

0.030 mmol, 6 mol %). Anhydrous THF (0.5 mL) was added via a syringe and the reaction solution was stirred at room temperature (rt) for 15 min. $HSiMe(OEt)_2$ (0.32 mL, 2.0 mmol, 4.0 equiv) was added sequentially via syringe and the resulting mixture was stirred at rt to afford a pale yellow to orange solution of CuH (about 15 min).

N1-Alkylation: In a nitrogen-filled glovebox, a second oven-dried screw-top reaction tube (Fisherbrand, 16 x 125 mm, catalog no. 1495925C) equipped with a stir bar was charged with indole electrophile **2d** (0.21 g, 0.75 mmol, 1.5 equiv). Anhydrous THF (4.2 mL), styrene (0.50 mmol, 1.0 equiv), and 3-ethyl-3-pentanol (14 μl, 0.10 mmol, 0.20 equiv) were added, followed by addition of the CuH solution from the first reaction tube to the stirred reaction mixture at rt via syringe. The reaction tube was sealed with a Teflon-lined screw cap and removed from the glovebox, placed in a 90 °C oil bath and stirred for 20 h. After cooling to rt, the reaction cap was removed and 50 μl dodecane was added as an internal standard. An aliquot of the solution was taken into a GC vial and diluted by EtOAc. GC analysis was used for determination of the conversion, yield and regioselectivity. Sat. NH_4F in MeOH (5 mL) was slowly added to the reaction tube to quench the reaction as part of the workup (Caution: gas evolution observed). The mixture was stirred uncapped for 30 min, transferred to a 20 mL scintillation vial, the reaction tube was rinsed with EtOAc (2 mL × 3), and concentrated *in vacuo* with the aid of a rotary evaporator. The resulting residue was redissolved in EtOAc, filtered through a shot pad of Celite and washed with additional EtOAc (about 100 mL). The collected EtOAc solution was concentrated *in vacuo* using a rotary evaporator, and the crude material was purified by silica gel column chromatography.

General Procedure B:

Preparation of CuH solution: see General Procedure A.

N1-Alkylation: In a nitrogen-filled glovebox, a second oven-dried screw-top reaction tube (Fisherbrand, 16 x 125 mm, catalog no. 1495925C) equipped with a stir bar was charged with indole electrophile **2d** (0.14 g, 0.50 mmol, 1.0 equiv). Anhydrous THF (4.2 mL), styrene (0.75 mmol, 1.5 equiv) and KF (0.0058 g, 0.10 mmol, 0.20 equiv) were added, followed by addition of the CuH solution from the first reaction tube to the stirred reaction mixture at rt via syringe. The reaction tube was then removed from the glovebox, placed in a 70 °C oil bath and stirred for 20 h. After cooling to rt, the reaction cap was removed and 50 μL dodecane was added as an internal standard. An aliquot of the solution was taken into a GC vial and diluted by EtOAc. GC analysis was used for determination of the conversion, yield and regioselectivity. Sat. NH_4F in MeOH (5 mL) was slowly added to the reaction tube to quench the reaction as part of the workup

(Caution: gas evolution observed). The mixture was stirred uncapped for 30 min, transferred to a 20 mL scintillation vial, the reaction tube was rinsed with EtOAc (2 mL × 3), and concentrated *in vacuo* using a rotary evaporator. The resulting residue was redissolved in EtOAc, filtered through a shot pad of Celite and washed with additional EtOAc (about 100 mL). The collected EtOAc solution was concentrated *in vacuo* with the aid of a rotary evaporator, and the crude material was purified by silica gel column chromatography.

Characterization Data for N1-Alkylated Chiral Indoles

(*S*)-1-(1-phenylethyl)-1*H*-indole (3a)

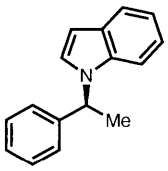

The general procedure A was followed using styrene (0.052 g, 0.50 mmol, 1.0 equiv). The crude material was purified by flash column chromatography (Hexanes ~ Hexanes : EtOAc = 15 : 1) to provide the title compound as a white solid in 85% yield (Run 1: 98 mg, 89%, 91% ee; Run 2: 90 mg, 81%, 91% ee). m.p. 63-67 °C. ^{1}H NMR (400 MHz, $CDCl_3$) δ 7.70–7.66 (m, 1H), 7.35–7.24 (m, 5H), 7.19–7.10 (m, 4H), 6.61 (dd, *J* = 3.2 Hz, *J* = 0.8, 1H), 5.70 (q, *J* = 7.1 Hz, 1H), 1.95 (d, *J* = 7.1 Hz, 3H) ppm. ^{13}C NMR (101 MHz, $CDCl_3$) δ 142.7, 136.1, 128.8, 128.7, 127.5, 125.9, 124.9, 121.5, 120.9, 119.6, 110.1, 101.5, 54.8, 21.8 ppm. IR (thin film) 3028, 1458, 1311, 1300, 1228, 1014, 737, 697 cm^{-1}. EA Calcd. for $C_{16}H_{15}N$: C, 86.84; H, 6.83. Found: C, 86.83; H, 6.98. $[\alpha]_D^{22}$ = -85.0. **SFC** analysis: ODH (5:95 MeOH: scCO2 to 15:85 MeOH: scCO2 linear gradient over 20 min, 2.50 mL/min), 6.66 min (major), 7.15 min (minor), 91% ee. The absolute stereochemistry was assigned as (*S*) by analogy.

(*S*)-1-(1-(*o*-tolyl)ethyl)-1*H*-indole (3b)

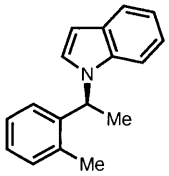

The general procedure A was followed using 1-methyl-2-vinylbenzene (0.059 g, 0.50 mmol, 1.0 equiv). The crude material was purified by flash column chromatography (Hexanes ~ Hexanes : EtOAc = 15 : 1) to provide the title compound as a white solid in 81% yield (Run 1: 99 mg, 84%, 87% ee; Run 2: 92 mg, 78%, 87% ee). m.p. 38-42 °C. ^{1}H NMR (400 MHz, $CDCl_3$) δ 7.72–7.68 (m, 1H), 7.30–7.12 (m, 8H), 6.57 (dd, *J* = 3.2 Hz, *J* = 0.8 Hz, 1H), 5.85 (q, *J* = 6.9 Hz, 1H), 2.33–2.29 (s, 3H), 1.91 (d, *J* = 7.0 Hz, 3H) ppm. ^{13}C NMR (101 MHz, $CDCl_3$) δ 140.1, 140.0, 135.7, 130.8, 128.9, 127.7, 126.6, 125.4, 125.1, 121.5, 121.0, 119.6, 109.7, 101.3, 51.8, 20.5, 19.1 ppm. EA Calcd. for $C_{17}H_{17}N$: C, 86.77; H, 7.28. Found: C, 86.81; H, 7.33. $[\alpha]_D^{22}$ = -72.3. **SFC** analysis: ODH

(1:99 MeOH over 40 min, 2.50 mL/min), 21.95 min (minor), 22.68 min (major), 88% ee. The absolute stereochemistry was assigned as (*S*) by analogy.

(*S*)-1-(1-(3-methoxyphenyl)ethyl)-1*H*-indole (3c)

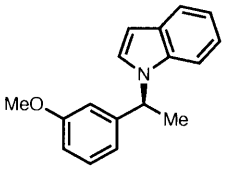

The general procedure A was followed using 1-methoxy-3-vinylbenzene (0.067 g, 0.50 mmol, 1.0 equiv). The crude material was purified by flash column chromatography (Hexanes ~ Hexanes : EtOAc = 10 : 1) to provide the title compound as a colorless oil in 71% yield (Run 1: 83 mg, 66%, 93% ee; Run 2: 96 mg, 76%, 93% ee). ^{1}H NMR (400 MHz, $CDCl_3$) δ 7.74–7.70 (m, 1H), 7.36 (d, *J* = 3.3 Hz, 1H), 7.34–7.30 (m, 1H), 7.29–7.24 (m, 1H), 7.23–7.14 (m, 2H), 6.68–6.74 (m, 3H), 6.64 (dd, *J* = 3.3 Hz, *J* = 0.8 Hz, 1H), 5.70 (q, *J* = 7.1 Hz, 1H), 3.79–3.76 (s, 3H), 1.96 (d, *J* = 7.1 Hz, 3H) ppm. ^{13}C NMR (101 MHz, $CDCl_3$) δ 160.0, 144.5, 136.2, 129.8, 128.9, 124.9, 121.5, 121.0, 119.6, 118.4, 112.4, 112.2, 110.1, 101.6, 55.2, 54.8, 21.8 ppm. IR (thin film) 2978, 2834, 1458, 1309, 1284, 1223, 1042, 738, 717, 696 cm^{-1}. EA Calcd. for $C_{17}H_{17}NO$: C, 81.24; H, 6.82. Found: C, 81.22; H, 6.85. $[\alpha]_D^{23}$ = -52.3. **SFC** analysis: ODH (5:95 MeOH: scCO2 to 15:85 MeOH: scCO2 linear gradient over 20 min, 2.50 mL/min), 9.33 min (major), 10.29 min (minor), 93% ee. The absolute stereochemistry was assigned as (*S*) by analogy.

(*S*)-1-(1-(4-fluorophenyl)ethyl)-1*H*-indole (3e)

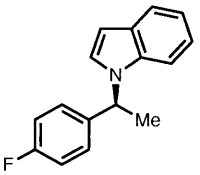

The general procedure A was followed using 1-fluoro-4-vinylbenzene (0.061 g, 0.50 mmol, 1.0 equiv). The crude material was purified by flash column chromatography (Hexanes ~ Hexanes : EtOAc = 15 : 1) to provide the title compound as a white solid in 81% yield (Run 1: 93 mg, 78%, 91% ee; Run 2: 99 mg, 83%, 91% ee). m.p. 78-81 °C. ^{1}H NMR (400 MHz, $CDCl_3$) δ 7.76–7.69 (m, 1H), 7.33 (d, *J* = 3.3 Hz, 1H), 7.30–7.26 (m, 1H), 7.24–7.12 (m, 4H), 7.06–7.00 (m, 2H), 6.65 (dd, *J* = 3.3 Hz, *J* = 0.8 Hz, 1H), 5.71 (q, *J* = 7.1 Hz, 1H), 1.96 (d, *J* = 7.1 Hz, 3H) ppm. ^{13}C NMR (101 MHz, $CDCl_3$) δ (d, *J* = 247.5 Hz), 138.5 (d, *J* = 3.0 Hz), 136.0, 128.9, 127.6 (d, *J* = 8.1 Hz), 124.7, 121.6, 121.0, 119.7, 115.6 (d, *J* = 21.2 Hz), 110.0, 101.8, 54.2, 21.8 ppm. ^{19}F NMR (376 MHz, $CDCl_3$) δ -115.1 ppm. IR (thin film) 3049, 2979, 1508, 1459, 1310, 1299, 1226, 1158, 1013, 833, 763, 738 cm^{-1}. EA Calcd. for $C_{16}H_{14}FN$: C, 80.31; H, 5.90. Found: C, 80.35; H, 6.04. $[\alpha]_D^{22}$ = -80.6. **SFC** analysis: ODH (5:95 MeOH: scCO2 to 15:85 MeOH: scCO2 linear gradient over 20 min, 2.50 mL/min), 6.66 min (major), 7.15 min (minor), 91% ee. The absolute stereochemistry was assigned as (*S*) by analogy.

(*S*)-5-(1-(1*H*-indol-1-yl)ethyl)-1-tosyl-1*H*-indole (3f)

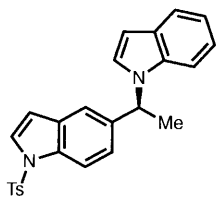

The general procedure A was followed using 1-tosyl-5-vinyl-1*H*-indole (0.149 g, 0.50 mmol, 1.0 equiv). The crude material was purified by flash column chromatography (Hexanes ~ Hexanes : EtOAc = 4 : 1) to provide the title compound as a white solid in 52% yield (Run 1: 101 mg, 49%, 95% ee; Run 2: 114 mg, 55%, 95% ee). m.p. 142-158 °C. ^{1}H NMR (400 MHz, $CDCl_3$) δ 7.89 (d, J = 8.6 Hz, 1H), 7.79–7.71 (m, 2H), 7.67–7.62 (m, 1H), 7.54 (d, J = 3.7 Hz, 1H), 7.33–7.05 (m, 8H), 6.58 (d, J = 3.1 Hz, 1H), 6.55 (d, J = 3.7 Hz, 1H), 5.74 (q, J = 7.1 Hz, 1H), 2.36–2.31 (s, 3H), 1.93 (d, J = 7.1 Hz, 3H) ppm. ^{13}C NMR (101 MHz, $CDCl_3$) δ 145.0, 138.0, 136.0, 135.3, 134.0, 130.9, 129.9, 128.8, 126.9, 126.8, 124.8, 122.8, 121.4, 120.9, 119.6, 118.5, 113.7, 110.0, 108.9, 101.5, 54.8, 22.1, 21.6 ppm. $[\alpha]_D^{22}$ = -103.1. **SFC** analysis: ADH (5:95 MeOH (0.1% DEA): scCO2 to 30:70 MeOH (0.1% DEA): scCO2 linear gradient over 25 min, 2.50 mL/min), 15.96 (major), 16.49 min (minor), 95% ee. The absolute stereochemistry was assigned as (*S*) by analogy.

***tert*-butyl (*S*)-4-(1*H*-indol-1-yl)-4-phenylbutanoate (3g)**

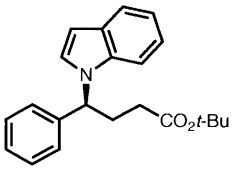

The general procedure A was followed using *tert*-butyl (*E*)-4-phenylbut-3-enoate (0.109 g, 0.50 mmol, 1.0 equiv). The crude material was purified by flash column chromatography (Hexanes ~ Hexanes : EtOAc = 10 : 1) to provide the title compound as a white solid in 78% yield (Run 1: 124 mg, 74%, 96% ee; Run 2: 138 mg, 82%, 96% ee). m.p. 66-69 °C. ^{1}H NMR (400 MHz, $CDCl_3$) δ 7.71 (d, J = 7.7 Hz, 1H), 7.42–7.34 (m, 9H), 6.66 (d, J = 3.2 Hz, 1H), 5.66 (t, J = 7.9 Hz, 1H), 2.74–2.60 (m, 2H), 2.34–2.22 (m, 2H), 1.55–1.45 (s, 9H) ppm. ^{13}C NMR (101 MHz, $CDCl_3$) δ 172.2, 141.1, 136.6, 128.8, 128.7, 127.7, 126.5, 124.9, 121.7, 121.0, 119.7, 109.9, 102.3, 80.7, 58.6, 32.2, 30.3, 28.2 ppm. IR (thin film) 2976, 1722, 1458, 1366, 1307, 1244, 1223, 1147, 847, 738, 698 cm^{-1}. EA Calcd. for $C_{22}H_{25}NO_2$: C, 78.77; H, 7.51. Found: C, 78.56; H, 7.35. $[\alpha]_D^{22}$ = -65.8. **SFC** analysis: ODH (5:95 MeOH: scCO2 to 15:85 MeOH: scCO2 linear gradient over 20 min, 2.50 mL/min), 7.17 min (major), 8.40 min (minor), 96% ee. The absolute stereochemistry was assigned as (*S*) by analogy.

(*S*)-*N*-(3-(1*H*-indol-1-yl)-3-phenylpropyl)-*N*-methylpivalamide (3h)

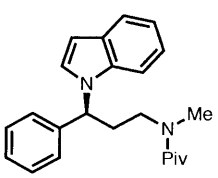

The general procedure A was followed using *N*-cinnamyl-*N*-methylpivalamide (0.116 g, 0.50 mmol, 1.0 equiv). The crude material was purified by flash

column chromatography (Hexanes ~ Hexanes : EtOAc = 3:1) to provide the title compound as a colorless oil in 69% yield (Run 1: 115 mg, 66%, 96% ee; Run 2: 125 mg, 72%, 96% ee). ^{1}H NMR (400 MHz, $CDCl_3$) δ 7.69 (d, *J* = 7.6 Hz, 1H), 7.47 (d, *J* = 3.3 Hz, 1H), 7.38–7.11 (m, 8H), 6.66 (d, *J* = 3.3 Hz, 1H), 5.56 (t, *J* = 7.7 Hz, 1H), 3.49–3.27 (m, 2H), 3.07–3.01 (s, 3H), 2.68–2.56 (m, 2H), 1.33–1.23 (s, 9H) ppm. ^{13}C NMR (101 MHz, $CDCl_3$) δ 177.5, 141.1, 136.3, 128.8, 127.7, 126.3, 124.9, 121.7, 121.0, 119.7, 109.8, 102.3, 57.8, 48.8, 38.7, 37.2, 32.8, 28.2 ppm. IR (thin film) 2956, 1616, 1478, 1458, 1404, 1363, 1304, 1208, 1103, 909, 762, 698 cm^{-1}. EA Calcd. for $C_{22}H_{25}NO_2$: C, 78.77; H, 7.51. Found: C, 78.56; H, 7.35. $[\alpha]_D^{22}$ = -60.2. **SFC** analysis: ODH (5:95 MeOH: scCO2 to 15:85 MeOH: scCO2 linear gradient over 20 min, 2.50 mL/min), 14.86 min (major), 16.75 min (minor), 96% ee. The absolute stereochemistry was assigned as (*S*) by analogy.

_N_-((2_S_,3_S_)-3-(1_H_-indol-1-yl)-2-methyl-3-phenylpropyl)-_N_,4-dimethylbenzenesulfonamide (3i)

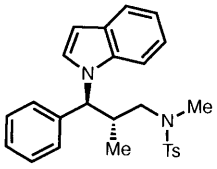

The general procedure B was followed using (*E*)-*N*,4-dimethyl-*N*-(2-methyl-3-phenylallyl)benzenesulfonamide (0.237 g, 0.75 mmol, 1.5 equiv). The crude material was purified by flash column chromatography (Hexanes ~ Hexanes : EtOAc = 5:1) to provide the title compound as a foam solid in 41% yield (Run 1: 78 mg, 36%, 99% ee; Run 2: 99 mg, 46%, 99% ee). ^{1}H NMR (400 MHz, $CDCl_3$) δ 7.51 (d, *J* = 7.9 Hz, 1H), 7.44–7.37 (m, 3H), 7.33–6.95 (m, 10H), 6.50 (d, *J* = 3.2 Hz, 1H), 4.98 (d, *J* = 10.5 Hz, 1H), 3.00–2.86 (m, 1H), 2.78–2.60 (m, 2H), 2.62–2.57 (s, 3H), 2.28–2.30 (s, 3H), 0.99 (d, *J* = 6.5 Hz, 3H) ppm. ^{13}C NMR (101 MHz, $CDCl_3$) δ 143.4, 139.3, 136.4, 133.7, 129.7, 128.8, 128.5, 127.9, 127.4, 127.3, 124.2, 121.8, 120.9, 119.6, 109.6, 102.7, 63.5, 54.6, 37.2, 37.0, 21.5, 16.2 ppm. IR (thin film) 2969, 2924, 1458, 1337, 1304, 1159, 1089, 973, 741, 700, 655 cm^{-1}. $[\alpha]_D^{23}$ = -72.6. **SFC** analysis: ADH (5:95 MeOH: scCO2 to 20:80 MeOH: scCO2 linear gradient over 15 min, 2.50 mL/min), 11.89 min (major), 12.70 min (minor), 99% ee. The absolute stereochemistry was assigned as (*S*) by analogy.

1-(3-(benzo[*d*][1,3]dioxol-5-yl)propyl)-1*H*-indole (3j)

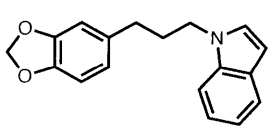

The general procedure B was followed using Safrole (0.122 g, 0.75 mmol, 1.5 equiv). The crude material was purified by flash column chromatography (Hexanes ~ Hexanes : EtOAc = 10:1) to provide the title compound as an colorless oil in 61% yield (Run 1: 78 mg, 56%; Run 2: 92 mg, 66%). ^{1}H NMR

(400 MHz, $CDCl_3$) δ 7.69 (d, J = 7.9 Hz, 1H), 7.34 (d, J = 8.2 Hz, 1H), 7.25 (td, J = 8.1 Hz, J = 1.0 Hz, 1H), 7.19–7.10 (m, 2H), 6.78 (d, J = 7.9 Hz, 1H), 6.70 (d, J = 1.6 Hz, 1H), 6.64 (dd, J = 7.9 Hz, J = 1.7 Hz, 1H), 6.55 (dd, J = 3.2 Hz, J = 0.8 Hz, 1H), 5.96 (s, 2H), 4.15 (d, J = 7.0 Hz, 2H), 2.59 (dd, J = 8.4 Hz, J = 6.8 Hz, 2H), 2.17 (p, J = 7.3 Hz, 2H) ppm. ^{13}C NMR (101 MHz, $CDCl_3$) δ 147.8, 145.9, 136.0, 134.8, 128.7, 127.77, 121.4, 121.2, 121.0, 119.3, 109.4, 108.8, 108.3, 101.1, 100.9, 45.6, 32.7, 31.8 ppm. IR (thin film) 2925, 1501, 1487, 1441, 1243, 1036, 926, 808, 738, 719 cm^{-1}. EA Calcd. for $C_{18}H_{17}NO_2$: C, 77.40; H, 6.13. Found: C, 77.10; H, 6.18.

(*Z*)-1-(hex-4-en-1-yl)-1*H*-indole (3k)

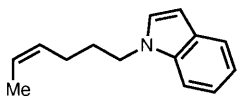

The general procedure B was followed using (*Z*)-hexa-1,4-diene (0.062 g, 0.75 mmol, 1.5 equiv). The crude material was purified by flash column chromatography (Hexanes ~ Hexanes : EtOAc = 10:1) to provide the title compound as a colorless oil in 73% yield (Run 1: 70 mg, 70%; Run 2: 76 mg, 76%). ^1H NMR (400 MHz, $CDCl_3$) δ 7.72 (d, J = 7.8 Hz, 1H), 7.42 (dd, J = 8.3 Hz, J = 1.0 Hz, 1H), 7.29 (td, J = 7.7 Hz, J = 1.2 Hz, 1H), 7.19 (td, J = 7.5 Hz, J = 1.0 Hz, 1H), 7.16 (d, J = 3.1 Hz, 1H), 6.57 (dd, J = 3.2 Hz, J = 0.9 Hz, 1H), 5.67–5.66 (m, 1H), 5.52–5.42 (m, 1H), 4.18 (t, J = 7.1 Hz, 2H), 2.14 (q, J = 7.2 Hz, 2H), 1.98 (p, J = 7.2 Hz, 2H), 1.66 (d, J = 6.7 Hz, 3H) ppm. ^{13}C NMR (101 MHz, $CDCl_3$) δ 136.0, 129.1, 128.7, 127.9, 125.3, 121.4, 121.0, 119.3, 109.5, 101.0, 45.8, 30.0, 24.2, 13.0 ppm.

(*S*)-1-(3,7-dimethyloct-6-en-1-yl)-1*H*-indole (3l)

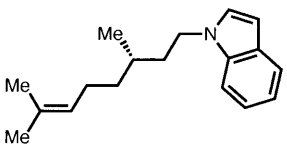

The general procedure B was followed using (*S*)-3,7-dimethylocta-1,6-diene (0.104 g, 0.75 mmol, 1.5 equiv). The crude material was purified by flash column chromatography (Hexanes ~ Hexanes : EtOAc = 10:1) to provide the title compound as a colorless oil in 71% yield (Run 1: 86 mg, 67%; Run 2: 97 mg, 76%). ^1H NMR (400 MHz, $CDCl_3$) δ 7.68 (d, J = 7.9 Hz, 1H), 7.39 (d, J = 8.2 Hz, 1H), 7.25 (t, J = 7.6 Hz, 1H), 7.18–7.11 (m, 2H), 6.54 (d, J = 2.9 Hz, 1H), 5.13 (t, J = 7.1 Hz, 1H), 4.26–4.10 (m, 2H), 2.14–1.86 (m, 3H), 1.73 (s, 3H), 1.71 (m, 1H), 1.64 (m, 3H), 1.60–1.40 (m, 2H), 1.34–1.22 (m, 1H), 1.03 (d, J = 6.6 Hz, 3H) ppm. ^{13}C NMR (101 MHz, $CDCl_3$) δ 135.9, 131.5, 128.6, 127.6, 124.5, 121.3, 121.0, 119.2, 109.4, 101.0, 44.5, 37.2, 36.9, 30.2, 25.8, 25.4,.19.5, 17.7 ppm. IR (thin film) 2958, 2915, 1512, 1464, 1376, 1334, 1315, 1194, 1085, 1012, 762, 736 cm^{-1}. EA Calcd. for $C_{18}H_{25}N$: C, 84.65; H, 9.87. Found: C, 84.68; H, 9.84.

(*S*)-*N*,*N*-diethyl-3-(1-(6-(trifluoromethyl)-1*H*-indol-1-yl)ethyl)benzamide (3m)

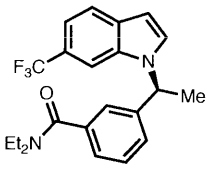

The general procedure A was followed using *N*,*N*-diethyl-3-vinylbenzamide (0.102 g, 0.50 mmol, 1.0 equiv), and indole electrophile **2e** (0.26 g, 0.75 mmol, 1.5 equiv). The crude material was purified by flash column chromatography (Hexanes ~ Hexanes : EtOAc = 1:1) to provide the title compound as a colorless oil in 56% yield (Run 1: 99 mg, 51%, 81% ee; Run 2: 117 mg, 60%, 81% ee). ^{1}H NMR (400 MHz, $CDCl_3$) δ 7.72 (d, *J* = 8.3 Hz, 1H), 7.46 (d, *J* = 3.3 Hz, 1H), 7.43 (s, 1H), 7.40–7.25 (m, 3H), 7.19 (d, *J* = 7.7 Hz, 1H), 7.03 (s, 1H), 6.65 (d, *J* = 3.3 Hz, 1H), 5.71 (q, *J* = 7.1 Hz, 1H), 3.65–3.35 (m, 2H), 3.15–2.95 (m, 2H), 1.94 (d, *J* = 7.0 Hz, 3H), 1.3–1.1 (m, 3H), 0.9–0.7 (m, 3H) ppm. ^{13}C NMR (101 MHz, $CDCl_3$) δ 170.8, 142.5, 137.8, 134.8, 131.3, 129.2, 127.7, (q, *J* = 31 Hz), 125.2 (q, *J* = 272.9 Hz), 126.6, 125.8, 123.4, 121.4, 116.3 (q, *J* = 3.4 Hz), 107.5 (q, *J* = 4.5 Hz), 102.1, 55.2, 43.2, 39.3, 21.6, 13.7, 12.8 ppm. ^{19}F NMR (376 MHz, $CDCl_3$) δ -60.5 ppm. IR (thin film) 2978, 2937, 1623, 1338, 1273, 1157, 1111, 1056, 911, 816, 726, 667 cm^{-1}. EA Calcd. for $C_{22}H_{25}NO_2$: C, 78.77; H, 7.51. Found: C, 78.56; H, 7.35. $[\alpha]_D^{22}$ = -63.7. **SFC** analysis: ODH (5:95 MeOH: scCO2 to 15:85 MeOH: scCO2 linear gradient over 20 min, 2.50 mL/min), 8.15 min (major), 8.72 min (minor), 81% ee. The absolute stereochemistry was assigned as (*S*) by analogy.

***tert*-butyl (*S*)-1-(1-(2-(difluoromethoxy)phenyl)ethyl)-1*H*-indole-4-carboxylate (3n)**

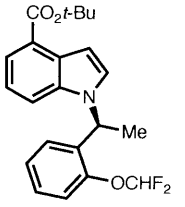

The general procedure A was followed using 1-(difluoromethoxy)-2-vinylbenzene (0.085 g, 0.50 mmol, 1.0 equiv), and indole electrophile **2f** (0.28 g, 0.75 mmol, 1.5 equiv). The crude material was purified by flash column chromatography (Hexanes ~ Hexanes : EtOAc = 5:1) to provide the title compound as a colorless oil in 61% yield (Run 1: 112 mg, 58%, 92% ee; Run 2: 124 mg, 64%, 92% ee). ^{1}H NMR (400 MHz, $CDCl_3$) δ 7.85 (d, *J* = 7.5 Hz, 1H), 7.53 (d, *J* = 3.3 Hz, 1H), 7.38 (d, *J* = 8.2 Hz, 1H), 7.26–7.10 (m, 4H), 7.03 (t, *J* = 7.5 Hz, 1H), 6.82 (dd, *J* = 7.8 Hz, *J* = 1,7 Hz, 1H), 6.57 (t, *J* = 73.7 Hz, 1H), 6.05 (q, *J* = 7.0 Hz, 1H), 1.92 (d, *J* = 7.0 Hz, 3H), 1,68 (s, 9H) ppm. ^{13}C NMR (101 MHz, $CDCl_3$) δ 166.8, 148.0, 136.8, 134.2, 129.0, 128.2, 126.7, 126.5, 126.0, 123.6, 123.3, 120.8, 118.5, 116.2 (t, *J* = 260.3 Hz), 114.3, 102.9, 80.7, 49.4, 28.5, 20.7 ppm. ^{19}F NMR (376 MHz, $CDCl_3$) δ -79.7 (dd, *J* = 169.2 Hz, *J* = 73.6 Hz), -80.2 (dd, *J* = 169.2 Hz, *J* = 73.6 Hz) ppm. IR (thin film) 2979, 1698, 1366, 1291, 1271, 1254, 1166, 1120, 1037, 750.0, 728.2 cm^{-1}. EA Calcd. for $C_{22}H_{25}NO_2$: C, 78.77; H, 7.51. Found: C, 78.56; H, 7.35. $[\alpha]_D^{22}$ = +53.9. **SFC** analysis: ODH (5:95 MeOH: scCO2 to 10:90 MeOH: scCO2 linear gradient over

12 min, 2.50 mL/min), 5.38 min (major), 5.65 min (minor), 92% ee. The absolute stereochemistry was assigned as (*S*) by analogy.

(*S*)-1-(1-(3-chlorophenyl)ethyl)-2-methyl-1*H*-indole (3r)

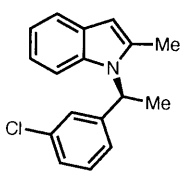

The general procedure A was followed using 1-chloro-3-vinylbenzene (0.069 g, 0.50 mmol, 1.0 equiv), and indole electrophile **2g** (0.22 g, 0.75 mmol, 1.5 equiv). The crude material was purified by flash column chromatography (Hexanes ~ Hexanes : EtOAc = 10:1) to provide the title compound as a yellow oil in 81% yield (Run 1: 105 mg, 78%, 93% ee; Run 2: 113 mg, 84%, 93% ee). ^{1}H NMR (400 MHz, $CDCl_3$) δ 7.58 (d, *J* = 7.6 Hz, 1H), 7.35–7.20 (m, 3H), 7.15–7.00 (m, 4H), 6.35 (s, 1H), 5.74 (q, *J* = 7.2 Hz, 1H), 2.40 (s, 3H), 1.96 (d, *J* = 7.2 Hz, 3H) ppm. ^{13}C NMR (101 MHz, $CDCl_3$) δ 143.8, 136.5, 135.9, 134.7, 129.9, 128.7, 127.4, 126.5, 124.7, 120.5, 119.9, 119.4, 110.8, 101.5, 52.1, 18.6, 14.0 ppm. IR (thin film) 2980, 1596, 1458, 1398, 1308, 782, 748, 720 cm^{-1}. $[\alpha]_D^{22}$ = -42.6. **SFC** analysis: ODH (5:95 MeOH: scCO2 to 15:85 MeOH: scCO2 linear gradient over 20 min, 2.50 mL/min), 7.89 min (minor), 8.81 min (major), 93% ee. The absolute stereochemistry was assigned as (*S*) by analogy.

6-methyl-4-(4-(4-methyl-1*H*-indol-1-yl)butoxy)-2-(trifluoromethyl)quinolone (3p)

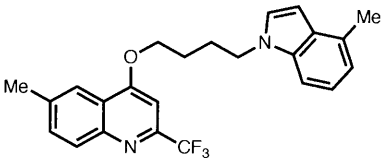

The general procedure B was followed using 6-methyl-4-(4-(4-methyl-1*H*-indol-1-yl)butoxy)-2-(trifluoromethyl)quinoline (0.211 g, 0.75 mmol, 1.5 equiv), and indole electrophile **2h** (0.15 g, 1.0 mmol, 1.0 equiv). The crude material was purified by flash column chromatography (Hexanes ~ Hexanes : EtOAc = 5:1) to provide the title compound as a white solid in 76% yield (Run 1: 151 mg, 73%; Run 2: 163 mg, 79%). m.p. 120-122 °C. ^{1}H NMR (400 MHz, $CDCl_3$) δ 8.18 (d, *J* = 8.6 Hz, 1H), 8.08 (s, 1H), 7.75 (dd, *J* = 8.7 Hz, *J* = 2.0 Hz, 1H), 7.45–7.25 (m, 3H), 7.12–7.05 (m, 2H), 6.70 (d, *J* = 3.0 Hz, 1H), 4.42 (t, *J* = 6.8 Hz, 2H), 4.31 (t, *J* = 6.2 Hz, 2H), 2.72 (s, 3H), 2.71 (s, 3H), 2.38 (m, 2H), 2.26 (m, 2H) ppm. ^{13}C NMR (101 MHz, $CDCl_3$) δ 162.3, 148.1 (q, *J* = 34.0 Hz), 146.7, 137.8, 135.6, 133.1, 130.6, 129.4 128.6, 127.0, 121.8, 121.7 (q, *J* = 275.2 Hz), 121.6, 120.6, 119.7, 106.9, 100.0, 99.9, 96.6 (q, *J* = 2.3 Hz), 68.3, 46.1, 26.8, 26.4, 21.9, 18.7 ppm. ^{19}F NMR (376 MHz, $CDCl_3$) δ -67.6 ppm. IR (thin film) 2932, 1576, 1368, 1280, 1254, 1180, 1132, 1110, 1093, 745, 715 cm^{-1}.

6-chloro-1-(2-(cyclohex-3-en-1-yl)ethyl)-1*H*-indole (3o)

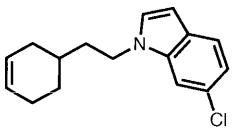

The general procedure B was followed using 4-vinylcyclohex-1-ene (0.081 g, 0.75 mmol, 1.5 equiv), and indole electrophile **2i** (0.16 g, 1.0 mmol, 1.0 equiv). The crude material was purified by flash column chromatography (Hexanes ~ Hexanes : EtOAc = 10:1) to provide the title compound as a colorless oil in 63% yield (Run 1: 79 mg, 61%; Run 2: 84 mg, 65%). ^{1}H NMR (400 MHz, $CDCl_3$) δ 7.53 (d, J = 8.4 Hz, 1H), 7.33 (s, 1H), 7.14–7.00 (m, 2H), 6.46 (d, J = 3.0 Hz, 1H), 5.75–5.60 (m, 2H), 4.13 (t, J = 7.5 Hz, 2H), 2.25–2.00 (m, 3H), 1.90–1.70 (m, 4H), 1.67–1.55 (m, 1H), 1.40–1.25 (m, 1H) ppm. ^{13}C NMR (101 MHz, $CDCl_3$) δ 136.3, 128.4, 127.4, 127.1, 127.1, 125.9, 121.8, 119.9, 109.3, 101.3, 44.3, 36.6, 31.6, 31.1, 28.6, 24.9 ppm. IR (thin film) 3021, 2914, 2836, 1506, 1464, 1434, 1319, 901, 802, 716, 654 cm^{-1}. EA Calcd. for $C_{16}H_{18}ClN$: C, 73.98; H, 6.98. Found: C, 73.90; H, 6.93.

methyl (*S*)-1-(1-phenylethyl)-1*H*-indole-2-carboxylate (3q)

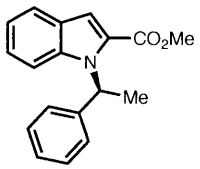

The general procedure A was followed using styrene (0.104 g, 1.0 mmol, 2.0 equiv), and indole electrophile **2j** (0.17 g, 1.0 mmol, 1.0 equiv). Dioxane was used as the solvent instead of THF. The crude material was purified by flash column chromatography (Hexanes ~ Hexanes : EtOAc = 10:1) to provide the title compound as a colorless oil in 43% yield (Run 1: 56 mg, 40%, 0% ee; Run 2: 64 mg, 46%, 0% ee). ^{1}H NMR (400 MHz, $CDCl_3$) δ 7.60–7.54 (m, 1H), 7.30 (s, 1H), 7.24–7.10 (m, 5H), 7.02–6.92 (m, 3H), 6.92–6.86 (m, 1H), 3.81 (s, 3H), 1.87 (d, J = 7.1 Hz, 3H) ppm. ^{13}C NMR (101 MHz, $CDCl_3$) δ 162.9, 141.5, 138.0, 128.5, 127.7, 127.0, 126.9, 126.4, 124.5, 122.8, 120.4, 113.6, 111.6, 53.1, 51.8, 18.2 ppm. **SFC** analysis: ODH (5:95 MeOH: scCO2 to 15:85 MeOH: scCO2 linear gradient over 20 min, 2.50 mL/min), 5.66 min (major), 6.50 min (minor), 0% ee. The absolute stereochemistry was assigned as (*S*) by analogy.

(*S*)-3-(2-methoxyethyl)-1-(1-(4-(trifluoromethyl)phenyl)ethyl)-1*H*-indole (3s)

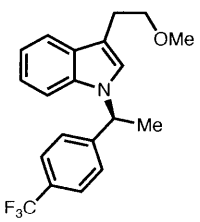

The general procedure A was followed using 1-(trifluoromethyl)-4-vinylbenzene (0.086 g, 0.50 mmol, 1.0 equiv), and indole electrophile **2k** (0.506 g, 1.5 mmol, 3.0 equiv). Dioxane was used as the solvent instead of THF. The crude material was purified by flash column chromatography (Hexanes ~ Hexanes : EtOAc = 10:1) to provide the title compound as a colorless oil in 16% yield (Run 1: 28 mg, 16%, 17% ee). ^{1}H NMR (400 MHz, $CDCl_3$) δ 7.66–7.61 (m, 1H), 7.53 (d, J = 8.1 Hz, 2H), 7.22–7.08 (m, 6H), 5.67 (q, J = 7.1 Hz, 1H), 3.71 (t, J = 7.2 Hz, 2H), 3.42 (s, 3H), 3.09 (t, J = 7.2

Hz, 2H), 1.93 (d, J = 7.1 Hz, 3H) ppm. ^{13}C NMR (101 MHz, $CDCl_3$) δ 147.0, 136.3, 129.7 (q, J = 32.4 Hz), 128.4, 126.2, 125.7 (q, J = 3.7 Hz), 124.0 (q, J = 272.0 Hz), 122.5, 121.8, 119.3, 119.2, 112.5, 109.9, 73.1, 58.7, 54.4, 25.8, 21.7 ppm. ^{19}F NMR (376 MHz, $CDCl_3$) δ -62.5 ppm. IR (thin film) 2922, 1619, 1460, 1322, 1163, 1111, 1069, 1014, 840, 737, 617 cm^{-1}. **SFC** analysis: ODH (5:95 MeOH: scCO2 to 10:90 MeOH: scCO2 linear gradient over 12 min, 2.50 mL/min), 4.80 min (major), 5.94 min (minor), 17% ee. The absolute stereochemistry was assigned as (*S*) by analogy.

3.4.2 CuH-Catalyzed Enantioselective C3-Alkylation

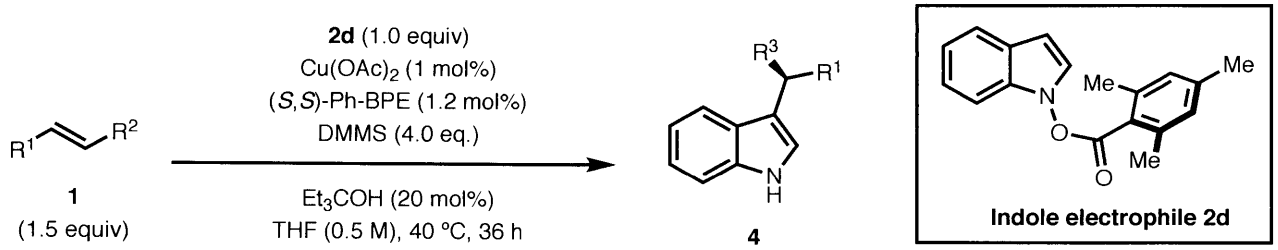

General Procedure C:

Preparation of CuH solution: In a nitrogen-filled glovebox, an oven-dried screw-top reaction tube (Fisherbrand, 13 x 100 mm, catalog no. 14-959035C) equipped with a magnetic stir bar was charged with $Cu(OAc)_2$ (0.9 mg, 0.005 mmol, 1 mol %) and (*S,S*)-Ph-BPE (3.1 mg, 0.006 mmol, 1.2 mol %). Anhydrous THF (0.5 mL) was added via a syringe and the reaction solution was stirred at room temperature (rt) for 15 min. $HSiMe(OMe)_2$ (0.25 mL, 2.0 mmol, 4.0 equiv) [*Note: see warning about this substance at the beginning of the experimental section*] was added sequentially via a syringe and the resulting mixture was stirred at rt to afford a pale yellow to orange solution of CuH (about 15 min).

C3-Alkylation: In a nitrogen-filled glovebox, a second oven-dried screw-top reaction tube (Fisherbrand, 16 x 125 mm, catalog no. 1495925C) equipped with a stir bar was charged with indole electrophile **2d** (0.14 g, 0.50 mmol, 1.0 equiv). Anhydrous THF (0.25 mL), styrene (1.0 mmol, 2.0 equiv), and 3-ethyl-3-pentanol (14 μl, 0.10 mmol, 0.20 equiv) were added, followed by addition of the CuH solution from the first reaction tube to the stirred reaction mixture at rt via syringe. The reaction tube was sealed with a Teflon-lined screw cap and removed from the glovebox, placed in a 40 °C oil bath and stirred for 20 h. After cooling to rt, the reaction cap was removed and 50 μL dodecane was added as an internal standard. An aliquot of the solution was taken into a GC vial and diluted by EtOAc. GC analysis was used for determination of the conversion, yield and regioselectivity. Sat. NH_4F in MeOH (5 mL) was slowly added to the

reaction tube to quench the reaction as part of the workup (Caution: gas evolution observed). The mixture was stirred uncapped for 30 min, transferred to a 20 mL scintillation vial, the reaction tube was rinsed with EtOAc (2 mL × 3), and concentrated *in vacuo* using a rotary evaporator. The resulting residue was redissolved in EtOAc, filtered through a shot pad of Celite and washed with additional EtOAc (about 100 mL). The collected EtOAc solution was concentrated *in vacuo* using a rotary evaporator, and the crude material was purified by silica gel column chromatography.

Characterization Data for C3-Alkylated Chiral Indoles

(*S*)-3-(1-phenylethyl)-1*H*-indole (4a)

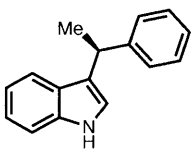

The general procedure C was followed using styrene (0.104 g, 1.0 mmol, 2.0 equiv). The crude material was purified by flash column chromatography (Hexanes ~ Hexanes : EtOAc = 5:1) to provide the title compound as a white solid in 71% yield (Run 1: 74 mg, 67%, 76% ee; Run 2: 83 mg, 75%, 76% ee) with 6:1 regioselectivity (C3:N1). m.p. 98-101 °C. ^{1}H NMR (400 MHz, $CDCl_3$) δ 7.75 (s, 1H), 7.35–6.85 (m, 10H), 4.28 (q, *J* = 7.2 Hz, 1H), 1.61 (d, *J* = 7.2 Hz, 3H) ppm. ^{13}C NMR (101 MHz, $CDCl_3$) δ 146.8, 136.6, 128.3, 127.5, 126.9, 125.9, 122.0, 121.5, 121.1, 119.7, 119.2, 111.0, 34.0, 22.4 ppm. $[\alpha]_D^{22}$ = -6.8. **SFC** analysis: ADH (5:95 MeOH: scCO2 to 20:80 MeOH: scCO2 linear gradient over 15 min, 2.50 mL/min), 8.04 min (minor), 8.93 min (major), 76% ee. The absolute stereochemistry was assigned as (*S*) by analogy.

(*S*)-3-(1-(4-(trifluoromethyl)phenyl)ethyl)-1*H*-indole (4b)

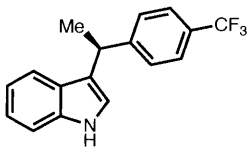

The general procedure C was followed using 1-(trifluoromethyl)-4-vinylbenzene (0.172 g, 1.0 mmol, 2.0 equiv). The crude material was purified by flash column chromatography (Hexanes ~ Hexanes : EtOAc = 5:1) to provide the title compound as a white solid in 61% yield (Run 1: 84 mg, 58%, 65% ee; Run 2: 93 mg, 64%, 65% ee) with 53:1 regioselectivity (C3:N1). m.p. 92-96 °C. ^{1}H NMR (400 MHz, $CDCl_3$) δ 8.01 (s, 1H), 7.58 (d, *J* = 8.1 Hz, 2H), 7.45 (d, *J* = 8.1 Hz, 2H), 7.39 (t, *J* = 8.6 Hz, 2H), 7.24 (t, *J* = 7.6 Hz, 1H), 7.14–7.05 (m, 2H), 4.49 (q, *J* = 7.2 Hz, 1H), 1.78 (d, *J* = 7.2 Hz, 3H) ppm. ^{13}C NMR (101 MHz, $CDCl_3$) δ 151.0, 136.7, 128.3 (q, *J* = 32.2 Hz), 127.8, 126.7, 125.3 (q, *J* = 3.8 Hz), 124.4 (q, *J* = 271.8 Hz), 122.3, 121.2, 120.4, 119.5, 119.4, 111.2, 36.9, 22.2 ppm. ^{19}F NMR (376 MHz, $CDCl_3$) δ -62.1 ppm. IR (thin film) 3412, 2968, 1456, 1321, 1161, 1108, 1067, 1015, 841, 767, 740 cm^{-1}. $[\alpha]_D^{22}$ = -5.4. **SFC** analysis: ADH (5:95 MeOH:

scCO2 to 20:80 MeOH: scCO2 linear gradient over 15 min, 2.50 mL/min), 5.53 min (minor), 5.94 min (major), 65% ee. The absolute stereochemistry was assigned as (*S*) by analogy.

(*S*)-5-(1-(1*H*-indol-3-yl)ethyl)-1-tosyl-1*H*-indole (4c)

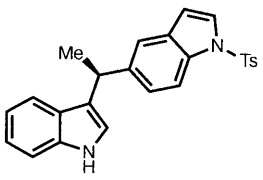

The general procedure C was followed using 1-tosyl-5-vinyl-1*H*-indole (0.297 g, 1.0 mmol, 2.0 equiv). The crude material was purified by flash column chromatography (Hexanes ~ Hexanes : EtOAc = 3:1) to provide the title compound as a foam solid in 55% yield (Run 1: 106 mg, 51%, 85% ee; Run 2: 122 mg, 59%, 85% ee) with 3:1 regioselectivity (C3:N1). ^{1}H NMR (400 MHz, $CDCl_3$) δ 7.81 (s, 1H), 7.76 (d, *J* = 8.6 Hz, 1H), 7.60 (d, *J* = 8.0 Hz, 2H), 7.38 (d, *J* = 3.7 Hz, 1H), 7.30 (s, 1H), 7.20 (d, *J* = 8.0 Hz, 1H), 7.15 (d, *J* = 8.3 Hz, 2H), 7.05–6.95 (m, 3H), 6.85–6.78 (m, 2H), 6.40 (d, *J* = 3.6 Hz, 1H), 4.30 (q, *J* = 7.2 Hz, 1H), 2.12 (s, 3H), 1.56 (d, *J* = 7.1 Hz, 3H) ppm. ^{13}C NMR (101 MHz, $CDCl_3$) δ 144.9, 142.3, 136.7, 135.4, 133.4, 131.0, 129.9, 126.9, 126.8, 126.3, 124.7, 122.0, 121.5, 121.3, 119.8, 119.7, 119.2, 113.3, 111.2, 109.2, 36.9, 22.9, 21.6 ppm. IR (thin film) 3422, 2962, 1456, 1367, 1188, 1170, 1142, 1123, 1092, 812, 703, 676 cm^{-1}. $[\alpha]_D^{22}$ = -12.8. **HPLC** analysis (ADH, 20% IPA in hexanes, 1.0 mL/min, 254 nm) indicated 85% ee: t_R (major) = 18.7 min, t_R (minor) = 25.1 min. The absolute stereochemistry was assigned as (*S*) by analogy.

(*S*)-3-(1*H*-indol-3-yl)-*N*-(4-methoxybenzyl)-*N*-methyl-3-phenylpropan-1-amine (4d)

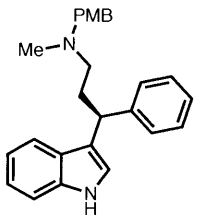

The general procedure C was followed using (*E*)-*N*-(4-methoxybenzyl)-*N*-methyl-3-phenylprop-2-en-1-amine (0.267 g, 1.0 mmol, 2.0 equiv). The crude material was purified by flash column chromatography (Hexanes ~ Hexanes : EtOAc = 1:1) to provide the title compound as a colorless oil in 61% yield (Run 1: 113 mg, 59%, 67% ee; Run 2: 121 mg, 63%, 67% ee) with 4:1 regioselectivity (C3:N1). ^{1}H NMR (400 MHz, $CDCl_3$) δ 8.00 (s, 1H), 7.45 (d, *J* = 8.0 Hz, 1H), 7.37–7.10 (m, 11H), 6.81 (d, *J* = 8.6 Hz, 2H), 4.30 (t, *J* = 7.0 Hz, 1H), 3.80 (s, 3H), 3.44 (s, 2H), 2.60–2.20 (m, 4H), 2.19 (s, 3H) ppm. ^{13}C NMR (101 MHz, $CDCl_3$) δ 158.6, 145.2, 136.5, 130.3, 128.3, 127.9, 127.0, 126.0, 122.0, 121.0, 119.5, 119.2, 113.6, 111.0, 61.5, 55.5, 55.3, 41.9, 40.5, 33.7 ppm. IR (thin film) 3417, 2934, 2834, 2793, 1510, 1455, 1243, 1032, 740, 700 cm^{-1}. $[\alpha]_D^{23}$ = +14.2. **SFC** analysis: ADH (5:95 MeOH (0.1% DEA): scCO2 to 30:70 MeOH (0.1% DEA):

scCO2 linear gradient over 25 min, 2.50 mL/min), 11.82 min (minor), 12.38 min (major), 67% ee. The absolute stereochemistry was assigned as (*S*) by analogy.

3-((*S*)-1-((8*R*,9*S*,13*S*,14*S*)-13-methyl-6,7,8,9,11,12,13,14,15,16-decahydrospiro[cyclopenta[*a*]phenanthrene-17,2'-[1,3]dioxolan]-2-yl)ethyl)-1*H*-indole (4e)

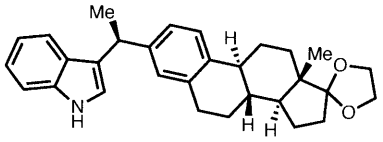

The general procedure C was followed using (8*R*,9*S*,13*S*,14*S*)-13-methyl-2-vinyl-6,7,8,9,11,12,13,14,15,16-decahydrospiro[cyclopenta[*a*]phenanthrene-17,2'-[1,3]dioxolane] (0.325 g, 1.0 mmol, 2.0 equiv). The crude material was purified by flash column chromatography (Hexanes ~ Hexanes : EtOAc = 3:1) to provide the title compound as a white solid in 62% yield (Run 1: 126 mg, 57%, 84% ee; Run 2: 139 mg, 63%, 84% ee) with 5:1 regioselectivity (C3:N1). m.p. 169-173 °C. ^{1}H NMR (400 MHz, $CDCl_3$) δ 7.95 (s, 1H), 7.48 (d, *J* = 7.6 Hz, 1H), 7.34 (d, *J* = 8.2 Hz, 1H), 7.24–6.98 (m, 6H), 4.34 (q, *J* = 7.1 Hz, 1H), 4.05–3.85 (m, 4H), 2.93–2.75 (m, 2H), 2.40–2.20 (m, 2H), 2.12–2.00 (m, 1H), 1.95–1.75 (m, 4H), 1.71 (d, *J* = 7.2 Hz, 3H), 1.70–1.25 (m, 6H), 0.90 (s, 3H) ppm. ^{13}C NMR (101 MHz, $CDCl_3$) δ 143.9, 137.9, 136.6, 136.5, 127.8, 127.0, 125.2, 124.8, 121.9, 121.8, 121.0, 119.8, 119.5, 119.1, 111.0, 65.3, 64.6, 49.6, 46.2, 44.0, 38.9, 36.4, 34.3, 30.8, 29.7, 27.1, 25.9, 22.5, 22.4, 14.4 ppm. IR (thin film) 3414, 2933, 2870, 1456, 1158, 1102, 1043, 1011, 906, 728, 647 cm^{-1}. $[\alpha]_D^{22}$ = -4.4. **HPLC** analysis (ADH, 10% IPA in hexanes, 1.0 mL/min, 254 nm) indicated 84% ee: t_R (major) = 11.1 min, t_R (minor) = 9.5 min. The absolute stereochemistry was assigned as (*S*) by analogy.

Ethyl (*S*)-4-(8-(1-(1*H*-indol-3-yl)ethyl)-5,6-dihydro-11*H*-benzo[5,6]cyclohepta[1,2-*b*]pyridin-11-ylidene)piperidine-1-carboxylate (4f)

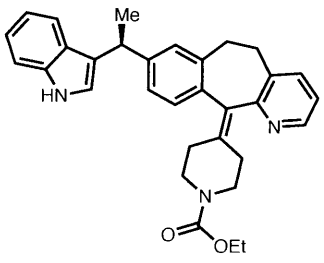

The general procedure C was followed using ethyl 4-(8-vinyl-5,6-dihydro-11*H*-benzo[5,6]cyclohepta[1,2-*b*]pyridin-11-ylidene)piperidine-1-carboxylate (0.375 g, 1.0 mmol, 2.0 equiv). The crude material was purified by flash column chromatography (Dichloromethane ~ Dichloromethane : MeOH = 30:1) to provide the title compound as a white solid in 41% yield (Run 1: 88 mg, 36%; Run 2: 113 mg, 46%) with 5:1 regioselectivity (C3:N1). ^{1}H NMR (400 MHz, $CDCl_3$) δ 8.39 (m, 1H), 8.09 (m, 1H), 7.48–7.38 (m, 2H), 7.34 (dd, *J* = 8.1 Hz, *J* = 2.7 Hz, 1H), 7.19–6.97 (m, 7H), 4.31 (q, *J* = 7.2 Hz, 1H), 4.13 (q, *J* = 7.1 Hz, 2H), 3.90–3.70 (m, 2H), 3.45–3.25 (m, 2H), 3.20–3.05 (m, 2H), 2.90–2.70 (m, 2H), 2.55–2.20 (m, 4H), 1,67 (d, *J* = 7.1 Hz, 3H), 1.24 (t, *J* = 7.1 Hz, 3H) ppm. ^{13}C NMR (101

MHz, $CDCl_3$) δ 158.0, 155.6, 146.3, 146.0, 137.3, 137.2, 136.6, 136.3, 135.3, 134.0, 129.4, 129.3, 128.4, 128.1, 126.9, 125.1, 124.9, 122.1, 121.8, 121.3, 121.2, 121.2, 121.0, 119.6, 119.0, 111.1, 61.3, 45.0, 44.9, 36.6, 32.1, 31.7, 31.7, 30.7, 30.6, 22.5, 22.4, 14.7 ppm. The absolute stereochemistry was assigned as (*S*) by analogy.

3-(3-(2-fluoro-4-methoxyphenyl)propyl)-1*H*-indole (4g)

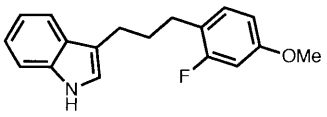

The general procedure C was followed using 1-allyl-2-fluoro-4-methoxybenzene (0.166 g, 1.0 mmol, 2.0 equiv). The crude material was purified by flash column chromatography (Hexanes ~ Hexanes : EtOAc = 5:1) to provide the title compound as a white solid in 32% yield (Run 1: 43 mg, 30%; Run 2: 48 mg, 34%) with > 20:1 regioselectivity (C3:N1). m.p. 86-89 °C. ^{1}H NMR (400 MHz, $CDCl_3$) δ 7.90 (s, 1H), 7.60 (d, *J* = 8.2 Hz, 1H), 7.36 (dt, *J* = 8.1 Hz, *J* = 0.9 Hz, 1H), 7.22–7.16 (m, 1H), 7.14–7.06 (m, 2H), 7.02–6.98 (m, 1H), 6.67–6.57 (m, 2H), 3.78 (s, 3H), 2.80 (t, *J* = 7.6 Hz, 2H), 2.69 (t, *J* = 7.6 Hz, 2H), 2.02 (p, *J* = 7.6 Hz, 2H) ppm. ^{13}C NMR (101 MHz, $CDCl_3$) δ 161.6 (d, *J* = 244.3 Hz), 159.0 (d, *J* = 10.9 Hz), 136.4, 130.8 (d, *J* = 7.3 Hz), 127.6, 121.9, 121.1, 119.1, 119.0, 116.5, 111.0, 109.5 (d, *J* = 3.0 Hz), 101.6, 101.4, 55.5, 30.6, 28.2 (d, *J* = 1.4 Hz), 24.7 ppm. ^{19}F NMR (376 MHz, $CDCl_3$) δ -116.6 ppm. IR (thin film) 3415, 2930, 2859, 2357, 1625, 1506, 1456, 1283, 1141, 1096, 741, 668 cm^{-1}.

3.4.3 Preparation of Indole Electrophile Reagents

Method A (reduction conditions):

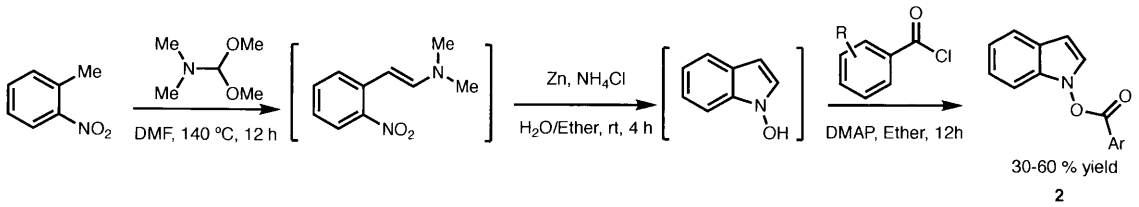

General Procedure:

Hydroxyindole (ether solution) synthesis: A 300 mL round bottom flask equipped with a magnetic stir bar, was charged with 2-nitrotoluene (4.72 mL, 40.0 mmol, 1.0 equiv) and *N*,*N*-dimethylformamide dimethyl acetal (14.3 g, 120 mmol, 3.0 equiv). *N*,*N*-dimethylformamide (DMF, 90 mL) was added and the solution was heated to 140 °C for 12 h with stirring. After cooling to room temperature, the solvent was evaporated under reduced pressure with the aid of a rotary evaporator. The red colored residue (crude enamine) was then dissolved in diethyl ether (240 ml), followed by the addition of zinc powder (52.3 g, 800 mmol, 20.0 equiv), and a solution

of NH_4Cl (7.63 g, 144 mmol, 3.6 equiv) in H_2O (50 ml). The mixture was vigorously stirred for about 4 h at room temperature until the color of the solution turned yellow from red (Caution: hydrogen gas evolution was observed at the beginning of the reaction). The mixture was then filtered through a fritted funnel. The filtrate was collected and the organic phase was separated from the aqueous phase with a separation funnel. The organic layer (crude 1-hydroxyindole in diethyl ether) was dried over anhydrous Na_2SO_4 and filtered.

Indole electrophile synthesis from hydroxyindoles: Under argon, to the resulting dried ether solution from above, was added 4-(dimethylamino)pyridine (5.86 g, 48.0 mmol, 1.2 equiv) followed by the addition of the corresponding benzoyl chloride (44.0 mmol, 1.1 equiv). The reaction mixture was then stirred under argon overnight at room temperature. Upon completion, the mixture was diluted with diethyl ether and quenched with a saturated aqueous $NaHCO_3$ solution. The aqueous phase was extracted with ether and the combined organic phases was dried over Na_2SO_4, filtered and concentrated under reduced pressure using a rotary evaporator. The crude material was purified by flash column chromatography to provide the corresponding indole electrophile reagents.

Method B (oxidation conditions):[20]

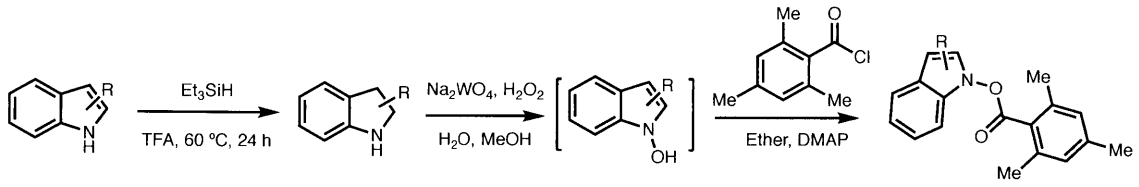

General Procedure:

Indoline synthesis: Triethylsilane (4.65 g, 40.0 mmol, 2.0 equiv) was added to a solution of the indole derivative (20.0 mmol, 1.0 equiv) in trifluoroacetic acid (TFA, 60 mL) and the mixture was stirred at 60 °C for 24 h. After cooling to rt, TFA was removed by distillation under reduced pressure. The crude residue was neutralized with saturated $NaHCO_3$ aqueous solution (100 mL) under ice cooling and extracted with dichloromethane (DCM, 50 mL × 3). The combined organic layers were washed with brine, dried over Na_2SO_4, filtered and concentrated under reduced pressure with the aid of a rotary evaporator. The crude material was purified by flash column chromatography to provide the corresponding indoline derivative.

Hydroxyindole (ether solution) synthesis: A solution of sodium tungstate dihydrate (0.66 g, 2.0 mmol, 0.2 equiv) in water (10 mL) was added to a solution of the indoline derivative (10 mmol, 1.0 equiv) in MeOH (50 mL) and the mixture was cooled to 0 °C with ice bath. Hydrogen peroxide aqueous solution (30%, 10 equiv) was added to the resultant solution slowly at 0 °C with stirring (10 min). Upon the completion of addition, the ice bath was removed and the

reaction mixture was stirred for another 10 min before quenched with water (200 mL) and extracted with diethyl ether (100 mL × 3). The aqueous solution was treated with sat. sodium sulfite solution (Na_2SO_3, 50 equiv) to quench the excess hydrogen peroxide. The combined organic layers were concentrated under reduced pressure with the aid of a rotary evaporator until all the MeOH was removed. The residue was redissolved in diethyl ether (100 mL), washed with brine, and dried over Na_2SO_4.

Indole electrophile synthesis from hydroxyindoles: see Method A.

Characterization Data for Indole Electrophiles

1*H*-indol-1-yl benzoate (2a)

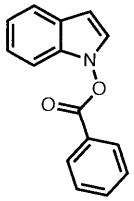

Method A was followed using 1-methyl-2-nitrobenzene (5.49 g, 40.0 mmol, 1.0 equiv) and benzoyl chloride (6.19 g, 44 mmol, 1.1 equiv). The crude material was first purified by a silica gel column (Hexanes ~ Hexanes : EtOAc = 10:1), and subsequently a Aluminum oxide (activated, basic, Brockmann I) column (Hexanes ~ Hexanes : EtOAc = 10:1) to provide the title compound as a white solid in 51% yield (4.84 g). (The extra basic alumina column was performed to get rid of benzoic anhydride which was difficult to separate from **2a** on silica gel). ^{1}H NMR (400 MHz, $CDCl_3$) δ 8.27 (dd, J = 8.3 Hz, J = 1.4 Hz, 2H), 7.80–7.72 (m, 1H), 7.68 (d, J = 7.9 Hz, 1H), 7.61 (t, J = 7.8 Hz, 2H), 7.36–7.17 (m, 4H), 6.60 (d, J = 3.2 Hz, 1H) ppm. ^{13}C NMR (101 MHz, $CDCl_3$) δ 164.7, 134.7, 134.3, 130.3, 129.0, 126.4, 125.5, 124.8, 123.1, 121.4, 120.9, 108.5, 100.4 ppm. EA Calcd. for $C_{15}H_{11}NO_2$: C, 75.94; H, 4.67. Found: C, 76.12; H, 4.86.

1*H*-indol-1-yl 4-(dimethylamino)benzoate (2b)

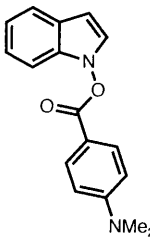

Method A was followed using 1-methyl-2-nitrobenzene (5.49 g, 40.0 mmol, 1.0 equiv) and 4-(dimethylamino)benzoyl chloride (8.08 g, 44 mmol, 1.1 equiv). The crude material was purified by flash column chromatography (Hexanes ~ Hexanes : EtOAc = 5:1) to provide the title compound as a white solid in 36% yield (4.04 g). ^{1}H NMR (400 MHz, $CDCl_3$) δ 8.08 (d, J = 9.1 Hz, 2H), 7.63 (dt, J = 7.8 Hz, J = 1.0 Hz, 1H), 7.31–7.19 (m, 3H), 7.17–7.10 (m, 1H), 6.73 (d, J = 9.1 Hz, 2H), 6.53 (dd, J = 3.5 Hz, J = 0.9 Hz, 1H), 3.11 (s, 6H) ppm. ^{13}C NMR (101 MHz, $CDCl_3$) δ 164.9, 154.2, 134.2, 132.2, 125.6, 124.6, 122.8, 121.2, 120.4, 112.0, 110.9, 108.5, 99.5, 40.1 ppm. EA Calcd. for $C_{17}H_{16}N_2O_2$: C, 72.84; H, 5.75. Found: C, 72.89; H, 5.88.

1*H*-indol-1-yl 4-(trifluoromethyl)benzoate (2c)

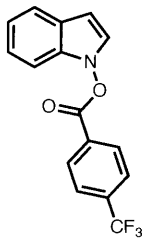

Method A was followed using 1-methyl-2-nitrobenzene (5.49 g, 40.0 mmol, 1.0 equiv) and 4-(trifluoromethyl)benzoyl chloride (9.18 g, 44 mmol, 1.1 equiv). The crude material was purified by flash column chromatography (Hexanes ~ Hexanes : EtOAc = 10:1) to provide the title compound as a white solid in 45% yield (5.49 g). ^{1}H NMR (400 MHz, $CDCl_3$) δ 8.28 (d, J = 3.5 Hz, 2H), 7.77 (d, J = 8.3 Hz, 2H), 7.57 (d, J = 7.8 Hz, 1H), 7.25–7.15 (m, 3H), 7.14–7.07 (m, 1H), 6.50 (d, J = 8.1 Hz, 1H), ppm. ^{13}C NMR (101 MHz, $CDCl_3$) δ 163.6, 136.0 (q, J = 32.9 Hz), 134.5, 130.7, 126.4 (q, J = 3.6 Hz), 125.6, 124.9, 124.7, 123.3 (q, J = 273.0 Hz), 123.4, 121.5, 121.2, 108.5, 101.0 ppm. ^{19}F NMR (376 MHz, $CDCl_3$) δ -63.3 ppm. EA Calcd. for $C_{16}H_{10}F_3NO_2$: C, 62.96; H, 3.30. Found: C, 63.12; H, 3.48.

1*H*-indol-1-yl 2,4,6-trimethylbenzoate (2d)

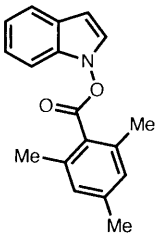

Method A was followed using 1-methyl-2-nitrobenzene (5.49 g, 40.0 mmol, 1.0 equiv) and 2,4,6-trimethylbenzoyl chloride (8.04 g, 44 mmol, 1.1 equiv). The crude material was first purified by a silica gel column (Hexanes ~ Hexanes : EtOAc = 10:1), and subsequently a Aluminum oxide (activated, basic, Brockmann I) column (Hexanes ~ Hexanes : EtOAc = 10:1) to provide the title compound as a white solid in 41% yield (4.58 g). (The extra basic alumina column was performed to get rid of 2,4,6-trimethylbenzoic anhydride which was difficult to separate from **2d** on silica gel). ^{1}H NMR (400 MHz, $CDCl_3$) δ 7.69 (dt, J = 7.9 Hz, J = 1.0 Hz, 1H), 7.38 (dd, J = 8.1 Hz, J = 1.1 Hz, 1H), 7.35–7.30 (m, 1H), 7.29 (d, J = 3.5 Hz, 1H), 7.21 (ddd, J = 8.1 Hz, J = 7.0 Hz, J = 1.2 Hz, 1H), 7.01 (s, 2H), 6.60 (dd, J = 3.5 Hz, J = 0.9 Hz, 1H), 2.56 (s, 6H), 2.38 (s, 3H) ppm. ^{13}C NMR (101 MHz, $CDCl_3$) δ 168.0, 141.3, 136.4, 134.3, 128.9, 126.4, 125.3, 124.9, 123.2, 121.4, 120.9, 108.7, 100.4, 21.3, 20.3 ppm. IR (thin film) 1780, 1610, 1445, 1222, 1155, 1028, 982, 946, 734, 699 cm^{-1}. EA Calcd. for $C_{18}H_{17}NO_2$: C, 77.40; H, 6.13. Found: C, 77.49; H, 6.06.

6-(trifluoromethyl)-1*H*-indol-1-yl 2,4,6-trimethylbenzoate (2e)

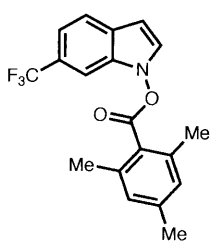

Method A was followed using 1-methyl-2-nitro-4-(trifluoromethyl)benzene (2.05 g, 10.0 mmol, 1.0 equiv) and 2,4,6-trimethylbenzoyl chloride (2.01 g, 11 mmol, 1.1 equiv). The crude material was purified by flash column

chromatography (Hexanes ~ Hexanes : EtOAc = 10:1) to provide the title compound as a white solid in 38% yield (1.32 g). ^{1}H NMR (400 MHz, $CDCl_3$) δ 7.74 (d, J = 8.3 Hz, 1H), 7.66 (s, 1H), 7.43–7.37 (m, 2H), 7.00 (s, 2H), 6.63 (dd, J = 3.5 Hz, J = 0.9 Hz, 1H), 2.53 (s, 6H), 2.36 (s, 3H) ppm. ^{13}C NMR (101 MHz, $CDCl_3$) δ 124.8 (d, J = 271.6 Hz) 167.7, 141.6, 136.6, 132.8, 129.0, 127.5, 126.9, 125.7, 125.4 (d, J = 32.2 Hz), 125.4 (d, J = 32.2 Hz), 121.9, 117.4 (q, J = 3.6 Hz), 106.1 (q, J = 4.4 Hz), 100.2, 21.3, 20.3 ppm. ^{19}F NMR (376 MHz, $CDCl_3$) δ -61.1 ppm. IR (thin film) 1786, 1611, 1449, 1228, 1280, 1224, 1154, 1114, 1053, 979 cm^{-1}.

2-methyl-1*H*-indol-1-yl 2,4,6-trimethylbenzoate (2g)

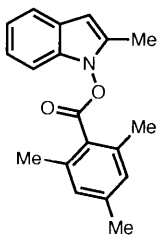

Method B was followed using 2-methylindoline (1.33 g, 10.0 mmol, 1.0 equiv) and 2,4,6-trimethylbenzoyl chloride (2.01 g, 11 mmol, 1.1 equiv). The crude material was first purified by a silica gel column (Hexanes ~ Hexanes : EtOAc = 10:1), and subsequently a Aluminum oxide (activated, basic, Brockmann I) column (Hexanes ~ Hexanes : EtOAc = 10:1) to provide the title compound as a white solid in 28% yield (0.821 g). (The extra basic alumina column was performed to get rid of 2,4,6-trimethylbenzoic anhydride which was difficult to separate from **2g** on silica gel). ^{1}H NMR (400 MHz, $CDCl_3$) δ 7.56 (d, J = 7.8 Hz, 1H), 7.31 (d, J = 8.0 Hz, 1H), 7.22 (t, J = 7.8 Hz, 1H), 7.15 (t, J = 7.5 Hz, 1H), 7.01 (s, 2H), 6.31 (s, 1H), 2.61 (s, 6H), 2.49 (s, 3H), 2.40 (s, 3H) ppm. ^{13}C NMR (101 MHz, $CDCl_3$) δ 168.0, 141.3, 136.7, 135.2, 134.7, 129.1, 126.4, 124.9, 122.0, 120.8, 120.3, 108.3, 98.4, 21.3, 20.8, 12.1 ppm. IR (thin film) 2921, 1777, 1611, 1449, 1220, 1155, 785, 738 cm^{-1}. EA Calcd. for $C_{19}H_{19}NO_2$: C, 77.79; H, 6.53. Found: C, 77.94; H, 6.38.

4-methyl-1*H*-indol-1-yl 2,4,6-trimethylbenzoate (2h)

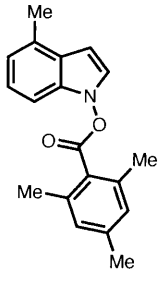

Method A was followed using 1,2-dimethyl-3-nitrobenzene (1.51 g, 10.0 mmol, 1.0 equiv) and 2,4,6-trimethylbenzoyl chloride (2.01 g, 11 mmol, 1.1 equiv). The crude material was first purified by a silica gel column (Hexanes ~ Hexanes : EtOAc = 10:1), and subsequently a Aluminum oxide (activated, basic, Brockmann I) column (Hexanes ~ Hexanes : EtOAc = 10:1) to provide the title compound as a white solid in 43% yield (1.23 g). (The extra basic alumina column was performed to get rid of 2,4,6-trimethylbenzoic anhydride which was difficult to separate from **2h** on silica gel). ^{1}H NMR (400 MHz, $CDCl_3$) δ 7.28 (d, J = 2.1 Hz, 1H), 7.23–7.19 (m, 2H), 7.05–6.95 (m, 3H), 6.61 (d, J = 3.5 Hz, 1H), 2.60 (s, 3H), 2.56 (s, 6H), 2.38 (s, 3H) ppm. ^{13}C NMR (101 MHz, $CDCl_3$) δ 168.0, 141.2, 136.4, 133.84, 130.8, 128.9, 126.4, 124.5, 124.4, 123.3, 121.0, 106.2,

98.7, 21.3, 20.3, 18.3 ppm. EA Calcd. for $C_{19}H_{19}NO_2$: C, 77.79; H, 6.53. Found: C, 78.01; H, 6.76.

6-chloro-1*H*-indol-1-yl 2,4,6-trimethylbenzoate (2i)

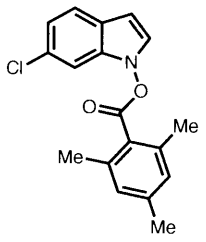

Method A was followed using 4-chloro-1-methyl-2-nitrobenzene (1.72 g, 10.0 mmol, 1.0 equiv) and 2,4,6-trimethylbenzoyl chloride (2.01 g, 11 mmol, 1.1 equiv). The crude material was first purified by a silica gel column (Hexanes ~ Hexanes : EtOAc = 10:1), and subsequently a Aluminum oxide (activated, basic, Brockmann I) column (Hexanes ~ Hexanes : EtOAc = 10:1) to provide the title compound as a white solid in 36% yield (1.13 g). (The extra basic alumina column was performed to get rid of 2,4,6-trimethylbenzoic anhydride which was difficult to separate from **2i** on silica gel). ^{1}H NMR (400 MHz, $CDCl_3$) δ 7.57 (d, J = 8.4 Hz, 1H), 7.33 (s, 1H), 7.26 (d, J = 3.5 Hz, 1H), 7.17 (dd, J = 8.4 Hz, J = 1.8 Hz, 1H), 7.01 (s, 2H), 6.57 (dd, J = 3.5 Hz, J = 0.9 Hz, 1H), 2.55 (s, 6H), 2.38 (s, 3H) ppm. ^{13}C NMR (101 MHz, $CDCl_3$) δ 167.7, 141.5, 136.6, 134.3, 129.3, 129.0, 125.9, 125.8, 123.3, 122.3, 121.6, 108.7, 100.3, 21.3, 20.4 ppm.

3-(2-methoxyethyl)-1*H*-indol-1-yl 2,4,6-trimethylbenzoate (2k)

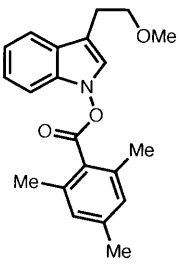

Method B was followed using 3-(2-methoxyethyl)indoline (1.77 g, 10.0 mmol, 1.0 equiv) and 2,4,6-trimethylbenzoyl chloride (2.01 g, 11 mmol, 1.1 equiv). The crude material was purified by flash column chromatography (Hexanes ~ Hexanes : EtOAc = 6:1) to provide the title compound as a white solid in 25% yield (0.844 g). ^{1}H NMR (400 MHz, $CDCl_3$) δ 7.65 (d, J = 7.8 Hz, 1H), 7.36–7.27 (m, 2H), 7.21 (ddd, J = 8.0 Hz, J = 6.8 Hz, J = 1.3 Hz, 1H), 7.15 (s, 1H), 6.99 (s, 2H), 3.74 (t, J = 7.1 Hz, 2H), 3.43 (s, 3H), 3.08 (t, J = 7.1 Hz, 2H), 2.54 (s, 6H), 2.36 (s, 3H) ppm. ^{13}C NMR (101 MHz, $CDCl_3$) δ 168.0, 141.1, 136.4, 135.6, 128.9, 126.7, 125.2, 123.8, 123.4, 120.7, 119.4, 112.2, 109.2, 72.5, 58.7, 25.6, 21.3, 20.3 ppm.

3.4.4 Preparation of Alkene Substrates

All the alkenes used in the paper are listed below. **1a**, **1b**, **1c**, **1d**, **1e**, **1j**, **1k**, **1l**, **1o**, **1q**, and **1r** were purchased from Alfa Aeser, Combi-Blocks or Sigma-Aldrich, and were used as received. **1f**[21], **1g**[22], **1m**[23], **1n**[24], **1p**[25], **1t**[26], **1u**[27] are known compounds and were prepared by previously reported procedures.

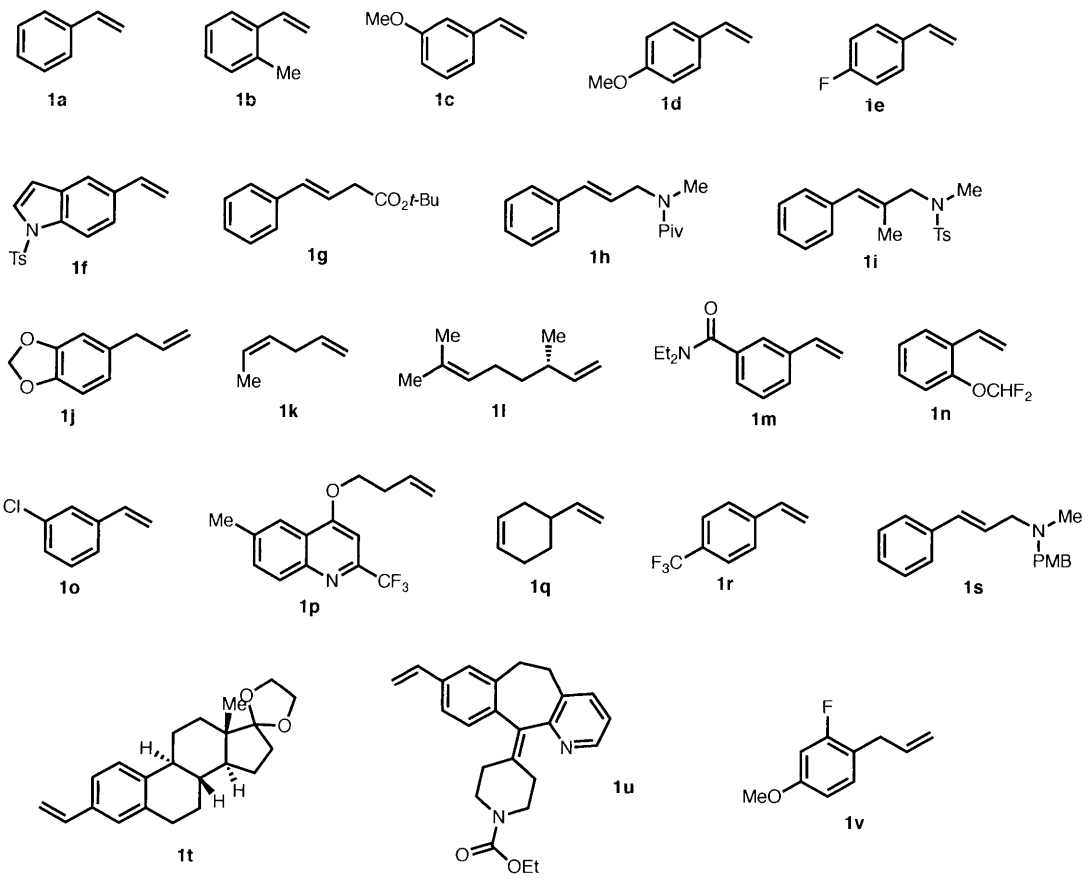

Synthesis of **1h**, **1s**, **1i**, **1v**.

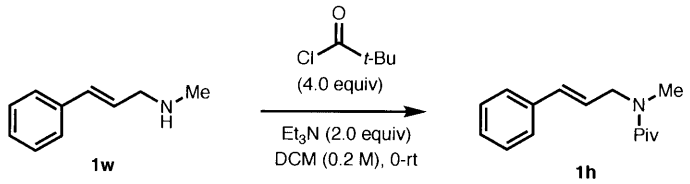

N-cinnamyl-*N*-methylpivalamide (1h)

In a 200 mL round bottom flask with a magnetic stir bar was charged with (*E*)-*N*-methyl-3-phenylprop-2-en-1-amine[i] (1.47 g, 10.0 mmol, 1.0 equiv), dichloromethane (DCM, 50 mL), and triethylamine (2.02 g, 20.0 mmol, 2.0 equiv). The reaction flask was cooled to 0 °C in an ice/water bath. Then pivaloyl chloride (4.82 g, 40 mmol, 4.0 equiv) was added slowly via syringe. The ice bath was then removed and the reaction mixture was allowed to warm to rt and further stirred overnight. The reaction mixture was diluted with DCM (50 mL) and quenched with saturated aqueous $NaHCO_3$ solution (100 mL). The aqueous phase was extracted with DCM (20 mL × 3) and the combined organic phases was dried over Na_2SO_4, filtered and concentrated under reduced pressure using a rotary evaporator. The crude material was purified by flash column chromatography (Hexanes ~ Hexanes : EtOAc = 1:1) to provide **1h** as liquid in 86% yield (1.99 g). ^{1}H NMR (400 MHz, $CDCl_3$) δ 7.43–7.32 (m, 4H), 7.29–7.24 (m, 1H), 6.51 (d, *J* =

15.9 Hz, 1H), 6.18 (dt, J = 15.9 Hz, J = 6.1 Hz, 1H), 4.20 (d, J = 5.4 Hz, 2H), 3.07 (s, 3H), 1.35 (s, 9H) ppm. ^{13}C NMR (101 MHz, $CDCl_3$) δ 177.5, 136.6, 132.5, 128.6, 127.7, 126.4, 125.0, 52.1, 38.9, 35.9, 28.4 ppm.

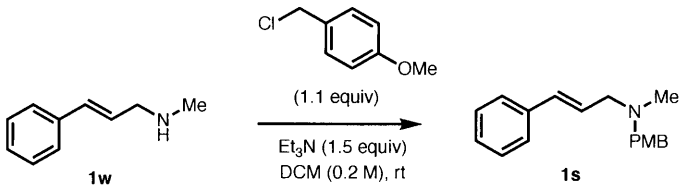

(*E*)-*N*-(4-methoxybenzyl)-*N*-methyl-3-phenylprop-2-en-1-amine (1s)

In a 200 mL round bottom flask with a magnetic stir bar was charged with (*E*)-*N*-methyl-3-phenylprop-2-en-1-amine (1.47 g, 10.0 mmol, 1.0 equiv), dichloromethane (DCM, 50 mL), and triethylamine (1.52 g, 15.0 mmol, 1.5 equiv). 1-(chloromethyl)-4-methoxybenzene (1.72 g, 40 mmol, 4.0 equiv) was added slowly via syringe and the reaction mixture was stirred overnight. The reaction mixture was diluted with DCM (50 mL) and quenched with saturated aqueous $NaHCO_3$ solution (100 mL). The aqueous phase was extracted with DCM (20 mL × 3) and the combined organic phases was tried over Na_2SO_4, filtered and concentrated under reduced pressure using a rotary evaporator. The crude material was purified by flash column chromatography (DCM ~ DCM : MeOH = 10:1) to provide **1s** as liquid in 88% yield (2.35 g). ^{1}H NMR (400 MHz, $CDCl_3$) δ 7.47–7.20 (m, 7H), 6.90 (d, J = 8.1 Hz, 2H), 6.56 (d, J = 15.8 Hz, 1H), 6.34 (dt, J = 15.7 Hz, J = 6.6 Hz, 1H), 3.83 (s, 3H), 3.52 (s, 2H), 3.21 (d, J = 6.6 Hz, 2H), 2.26 (s, 3H) ppm. ^{13}C NMR (101 MHz, $CDCl_3$) δ 158.7, 137.2, 132.5, 131.0, 130.3, 128.5, 127.7, 127.4, 126.3, 113.6, 61.2, 59.7, 55.3, 42.1. ppm. EA Calcd. for $C_{18}H_{21}NO$: C, 80.86; H, 7.92. Found: C, 80.64; H, 8.11.

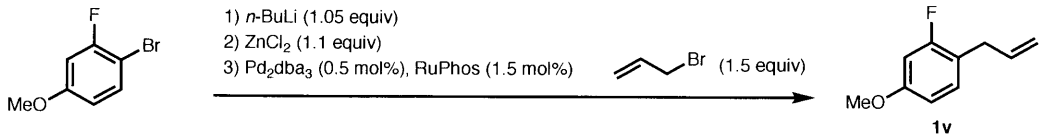

1-allyl-2-fluoro-4-methoxybenzene (1v)

In a 300 mL round bottom flask with a magnetic stir bar was charged with 1-bromo-2-fluoro-4-methoxybenzene (10.3 g, 50.0 mmol, 1.0 equiv) and anhydrous tetrahydrofuran (THF, 60 mL) under argon. The reaction mixture was cooled to -78 °C with a dry ice/acetone bath followed by the slow addition of *n*-BuLi (2.5 M in THF, 1.05 equiv). The reaction was allowed to stirred at -78 °C for 45 min before the addition of $ZnCl_2$ (7.50 g, 55.0 mmol, 1.1 equiv) under argon. The reaction was stirred at -78 °C for 1 h and is allowed to warm to room temperature by removing

the cooling bath. 3-bromoprop-1-ene (9.07 g, 75.0 mmol, 1.5 equiv), and a 10 mL THF solution of Pd_2dba_3 (0.23 g, 0.25 mmol, 1% mol) and RuPhos (0.35 g, 0.75 mmol, 1.5% mmol) were added via syringe. The round bottom flask was equipped with a reflux condenser and the reaction was heated at 60 °C for 1 h. After completion, the reaction mixture was cooled to room temperature and diluted with EtOAc (50 mL). The organic phase was sequentially washed with 1M HCl aqueous solution (50 mL × 2) and brine (50 mL). The combined organic phases was tried over Na_2SO_4, filtered and concentrated under reduced pressure using a rotary evaporator. The crude material was purified by flash column chromatography (Hexanes ~ Hexanes : DCM = 10:1) to provide **1v** as liquid in 47% yield (2.35 g). ^{1}H NMR (400 MHz, $CDCl_3$) δ 7.08 (t, J = 8.5 Hz, 1H), 6.67–6.57 (m, 2H), 5.94 (ddt, J = 15.7 Hz, J = 11.1 Hz, J = 6.5 Hz, 1H), 5.07 (d, J = 1.5 Hz, 1H), 5.04 (dd, J = 6.9 Hz, J = 1.7 Hz, 1H), 3.78 (s, 3H), 3.34 (dd, J = 6.5 Hz, J = 1.6 Hz, 2H) ppm. ^{13}C NMR (101 MHz, $CDCl_3$) δ 161.3 (d, J = 244.9 Hz), 159.3 (d, J = 11.0 Hz), 136.32, 130.8 (d, J = 6.7 Hz), 118.7 (d, J = 16.8 Hz), 115.7, 109.6 (d, J = 3.0 Hz), 101.5 (d, J = 26.2 Hz), 55.5, 32.4 (d, J = 2.8 Hz) ppm. ^{19}F NMR (376 MHz, $CDCl_3$) δ -116.5 ppm.

3.5 References and Notes

(1) Sravanthi, T. V. & Manju, S. L. *Eur. J. Pharm. Sci.* **2016**, *91*, 1.

(2) Mahaney, P. E.; Vu, A. T.; McComas, C. C.; Zhang, P.; Nogle, L. M.; Watts, W. L.; Sarkahian, A.; Leventhal, L.; Sullivan, N. R.; Uveges, A. J.; Trybulski, E. J. *Bioorg. Med. Chem.* **2006**, *14*, 8455.

(3) For reviews, see: (a) Chen, J. B.; Jia, Y. X. *Org. Biomol. Chem.* **2017**, *15*, 3550; Bandini, M. (b) Eichholzer, A. *Angew. Chem. Int. Ed.* **2009**, *48*, 9608.

(4) Cruz, F. A.; Zhu, Y.; Tercenio, Q. D.; Shen, Z.; Dong, V. M. *J. Am. Chem. Soc.* **2017**, *139*, 10641.

(5) (a) Lakhdar, S.; Westermaier, M.; Terrier, F.; Goumont, R.; Boubaker, T.; Ofial, A. R.; Mayr, H. *J. Org. Chem.* **2006**, *71*, 9088. (b) Otero, N.; Mandado, M.; Mosquera, R. A. *J. Phys. Chem. A* **2007**, *111*, 5557.

(6) (a) Stanley, L. M.; Hartwig, J. F. *Angew. Chem. Int. Ed.* **2009**, *48*, 7841. (b) Trost, B. M.; Krische, M. J.; Berl, V.; Grenzer, E. M. *Org. Lett.* **2002**, *4*, 2005. (c) Trost, B. M.; Osipov, M.; Dong, G. *J. Am. Chem. Soc.* **2010**, *132*, 15800.

(7) Cui, H-L.; Feng, X.; Peng, J.; Lei, J.; Jiang, K.; Chen, Y-C. *Angew. Chem. Int. Ed.* **2009**, *48*, 5737.

(8) (a) Liu, W.; Zhang, X.; Dai, L.; You, S. *Angew. Chem. Int. Ed.* **2009**, *51*, 5183. (b) Xu, K.; Gilles, T.; Breit, B. *Nat. Commun.* **2015**, *6*, 7616.

(9) (a) Sevov, C. S.; Zhou, J.; Hartwig, J. F. *J. Am. Chem. Soc.* **2014**, *136*, 3200. (b) Bandini, M.; Eichholzer, A.; Tragni, M.; Umani-Ronchi A. *Angew. Chem. Int. Ed.* **2008**, *47*, 3238.

(10) Bandini, M. *Org. Biomol. Chem.* **2013**, *11*, 5206.

(11) For leading reference on CuH-catalyzed C–N bond formation, see: Miki, Y.; Hirano, K.; Satoh, T.; Miura, M. *Angew. Chem. Int. Ed.* **2013**, *52*, 10830. (b) Zhu, S.; Niljianskul, N.; Buchwald, S. L. *J. Am. Chem. Soc.* **2013**, *135*, 15746. (c) Pirnot, M.; Wang, Y.-M.; Buchwald, S. L. *Angew. Chem. Int. Ed.* **2016**, *55*, 48.

(12) For leading reference on CuH-catalyzed C–C bond formation, see: (a) Wang, Y.-M.; Bruno, N. C.; Placeres, Á. L.; Zhu, S.; Buchwald, S. L. *J. Am. Chem. Soc.* **2015**, *137*, 10524. (b) Wang, Y.-M.; Buchwald, S. L. *J. Am. Chem. Soc.* **2016**, *138*, 5024.

(13) (a) Somei, M. *Heterocycles* **1990**, *50*, 1157. (b) Sundberg, R. J. *J. Org. Chem.* **1965**, *30*, 3604. (c) Nagayoshi, T.; Saeki, S.; Hamana, M. *Heterocycles* **1977**, *6*, 1666. (d) Somei, M.; Shoda, T. *Heterocycles* **1981**, *16*, 1523. (e) Kawasaki, T.; Tabata, M.; Nakagawa, K.; Kobayashi,

K.; Kodama, A.; Kobayashi, T.; Hasegawa, M.; Tanii, K.; Somei, M. *Heterocycles* **2015**, *90*, 1038.

(14) (a) Bandar, J. S.; Pirnot, M. T.; Buchwald, S. L. *J. Am. Chem. Soc.* **2015**, *137*, 14812. (b) Xi, Y.; Hartwig, J. F. *J. Am. Chem. Soc.* **2017**, *139*, 12758.

(15) The reduction of the electrophilic indole reagent by CuH generates indole and CuO_2CMes. The indole undergoes silylation under the reaction conditions through a copper indolyl intermediate.

(16) For the use of an alcohol (*t*-BuOH) in CuH-catalyzed reactions: (a) Chen, J.-X.; Daeuble, J. F.; Stryker, J. M. *Tetrahedron* 2000, 56, 2789. (b) Hughes, G.; Kimura, M.; Buchwald, S. L. *J. Am. Chem. Soc.* **2003**, *125*, 11253. (c) Lipshutz, B. H.; Servesko, J. M.; Taft, B. R. *J. Am. Chem. Soc.* **2004**, *126*, 8352. (d) Rainka, M. P.; Aye, Y.; Buchwald, S. L. *Proc. Natl. Acad. Sci. U. S. A.* **2004**, *101*, 5821. (e)Ascic, E.; Buchwald, S. L. *J. Am. Chem. Soc.* **2015**, *137*, 4666. (f) Yang, Y.; Perry, I. B.; Buchwald, S. L. *J. Am. Chem. Soc.* **2016**, *138*, 9787.

(17) In the case of 3-substituted indole electrophiles, we mainly observed the product of direct reduction of the electrophile to the corresponding indole. Computational studies indicate that this process begins with oxidative insertion of LCuH into the N–O bond of the indole electrophile, rather than hydrocupration of the 2,3-double bond.

(18) Huang, Y.; del Pozo, J.; Torker, S.; Hoveyda, A. H. *J. Am. Chem. Soc.* **2018**, *140*, 2643.

(19) The absolute configurations of the products were assigned to be (S) in both C–N and C–C formation reactions (see supporting information for details). By comparison with previous reactions involving irreversible, stereoselective hydrocupration of styrenes by DTBM-SEGPHOS- and Ph-BPE-ligated copper hydride species, we conclude that the configuration of the benzylic stereogenic center is most likely retained during the subsequent reaction with the electrophilic indole reagent.

(20) For using Na_2WO_4/H_2O_2 for oxidation, see: (a) Somei, M.; Kawasaki, T.; Shimizu, K.; Fukui, Y.; Ohta, T. *Chem. Pharm. Bull.* **1991**, *39*, 1905. (b) Yamada, K.; Tanaka, Y.; Somei, M. *Heterocycles* **2009**, *79*, 635. For using *m*-CPBA for oxidation, see: Tomakinian, T.; Kouklovsky, C.; Vincent, G. *Synlett* **2015**, *26*, 1269. For using dimethyldioxirane (DMDO) for oxidation, see: Hafensteiner, B. D.; Escribano, M.; Petricci, E.; Baran, P. S. *Bioorg. Med. Chem. Lett.* **2009**, *19*, 3808.

(21) Molander, G. A.; Brown, A. R. *J. Org. Chem.* **2006**, *71*, 9681.

(22) Bartoli, G.; Bosco, M.; Carlone, A.; Dalpozzo, R.; Marcantoni, E.; Melchiorre, P.; Sambri, L. *Synthesis* **2007**, *22*, 3489.

(23) Wang, Y.-M.; Buchwald, S. L. *J. Am. Chem. Soc.* **2016**, *138*, 5024.

(24) Zhou, Y.; Engl, O. D.; Bandar, J. S.; Chant, E. D.; Buchwald, S. L. *Angew. Chem. Int. Ed.* **2018**, DOI:10.1002/anie.201802797.

(25) Friis, S. D.; Pirnot, M. T.; Dupuis, L. N.; Buchwald, S. L. *Angew. Chem. Int. Ed.* **2017**, *56*, 7242.

(26) Maltais, R.; Ayan, D.; Poirier, D. *ACS Med. Chem. Lett.* **2011**, *2*, 678.

(27) Niu, D.; Buchwald, S. L. *J. Am. Chem. Soc.* **2015**, *137*, 9716.

Copies of NMR Spectra

(*S*)-1-(1-phenylethyl)-1*H*-indole (3a)

^{1}H NMR, 400 MHz, $CDCl_3$

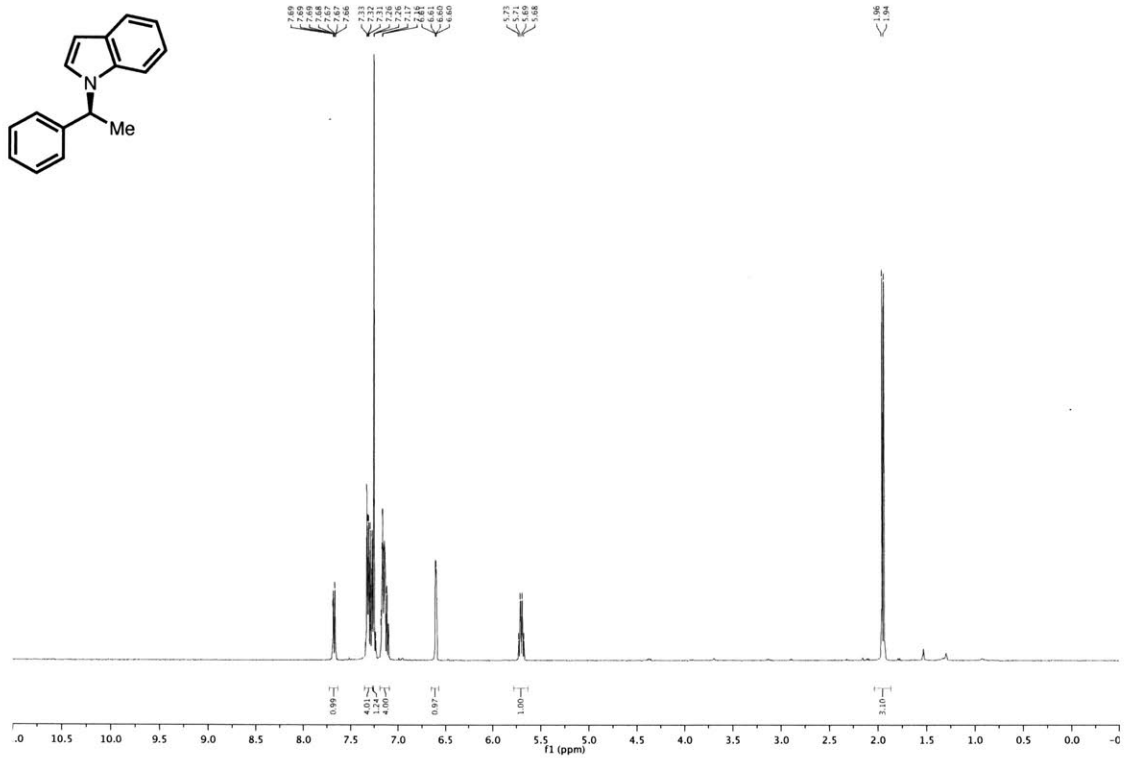

^{13}C NMR, 101 MHz, $CDCl_3$

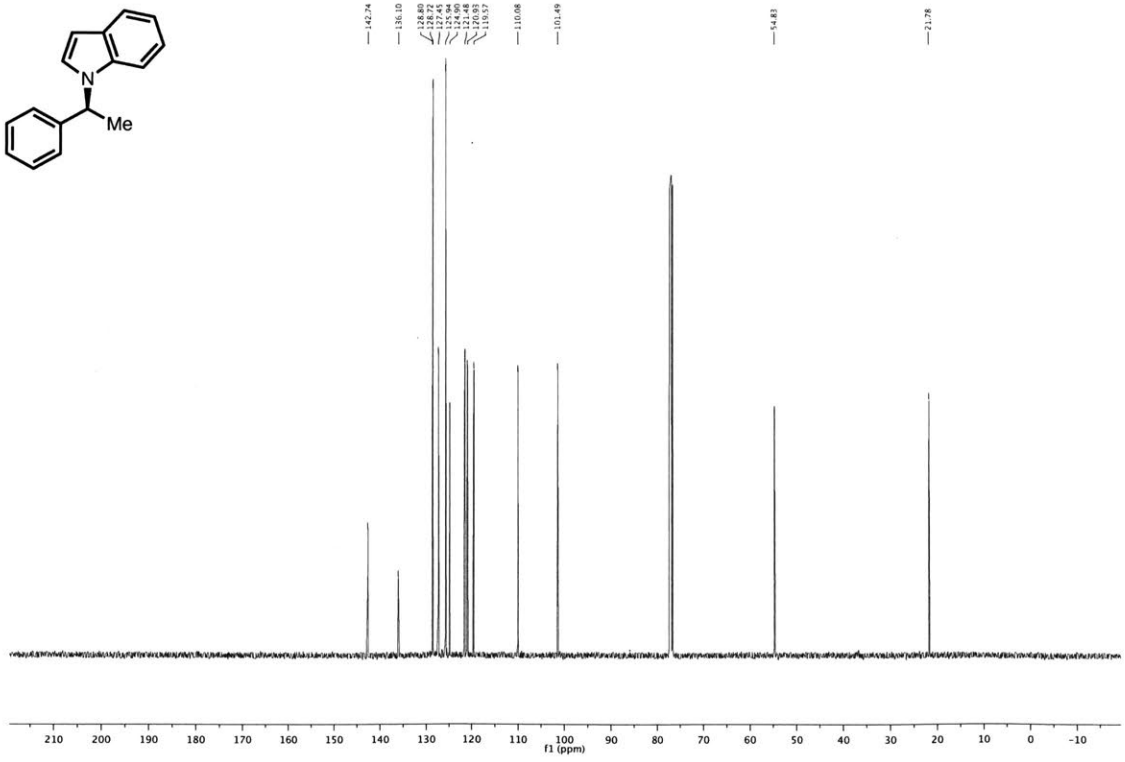

(*S*)-1-(1-(*o*-tolyl)ethyl)-1*H*-indole (3b)

^{1}H NMR, 400 MHz, $CDCl_3$

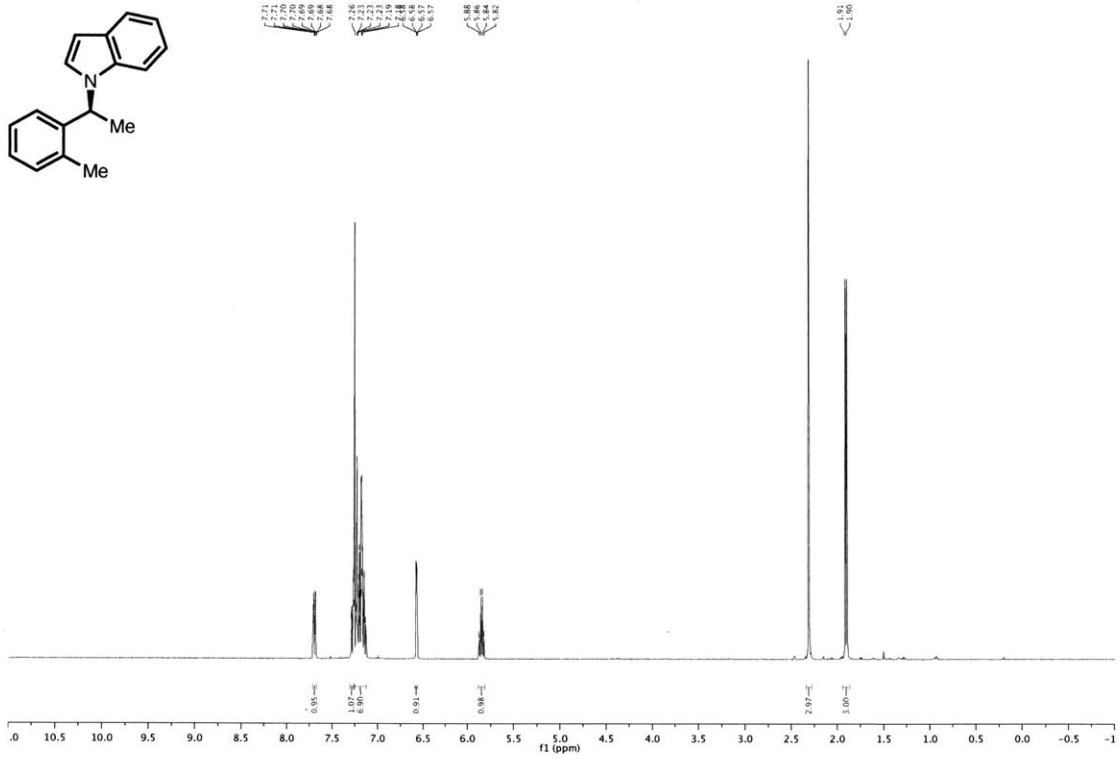

^{13}C NMR, 101 MHz, $CDCl_3$

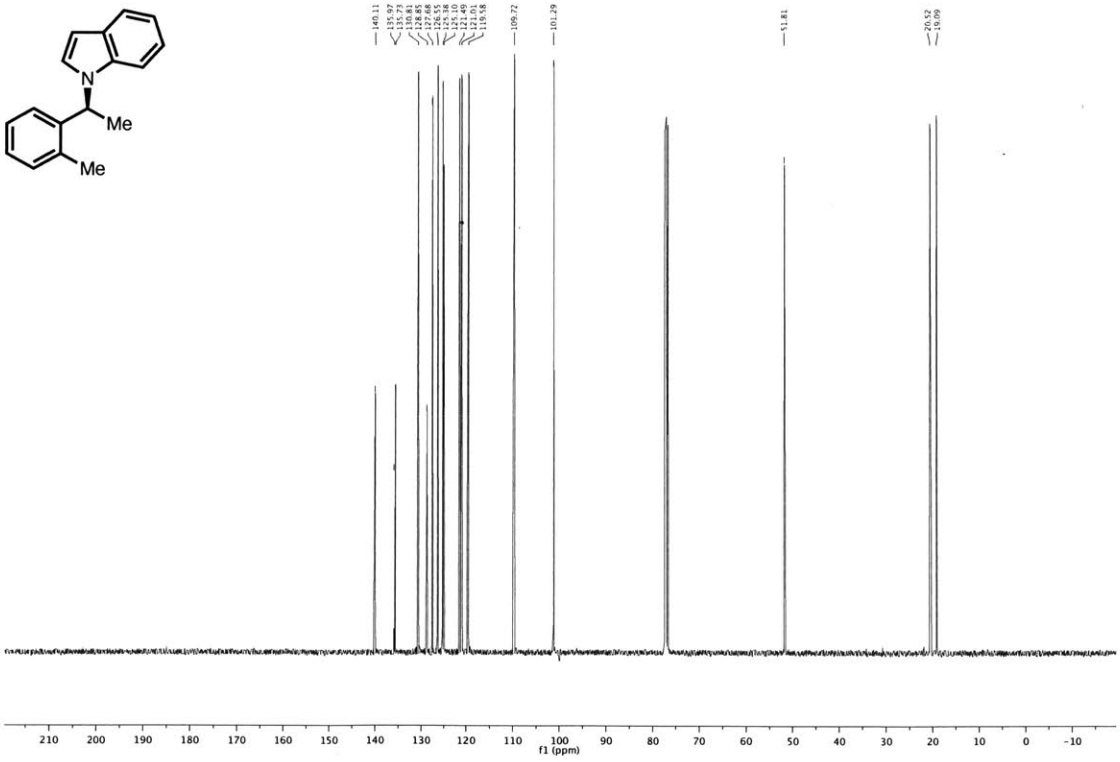

(*S*)-1-(1-(3-methoxyphenyl)ethyl)-1*H*-indole (3c)

^{1}H NMR, 400 MHz, $CDCl_3$

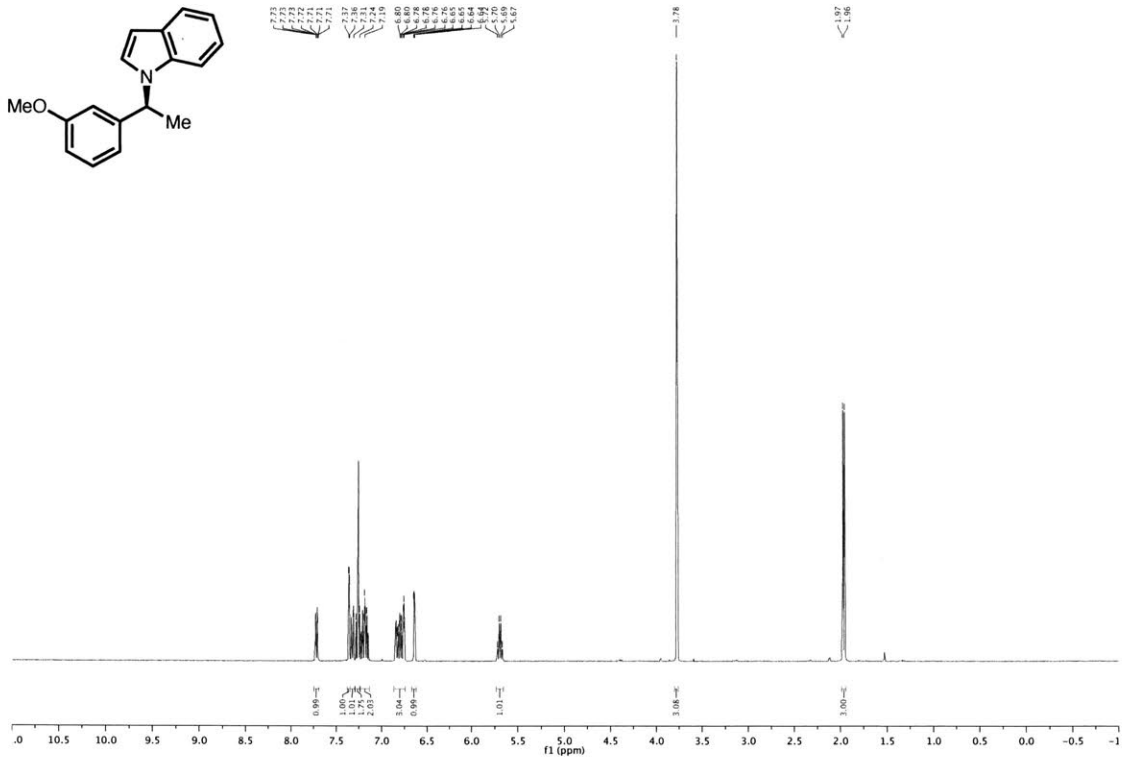

^{13}C NMR, 101 MHz, $CDCl_3$

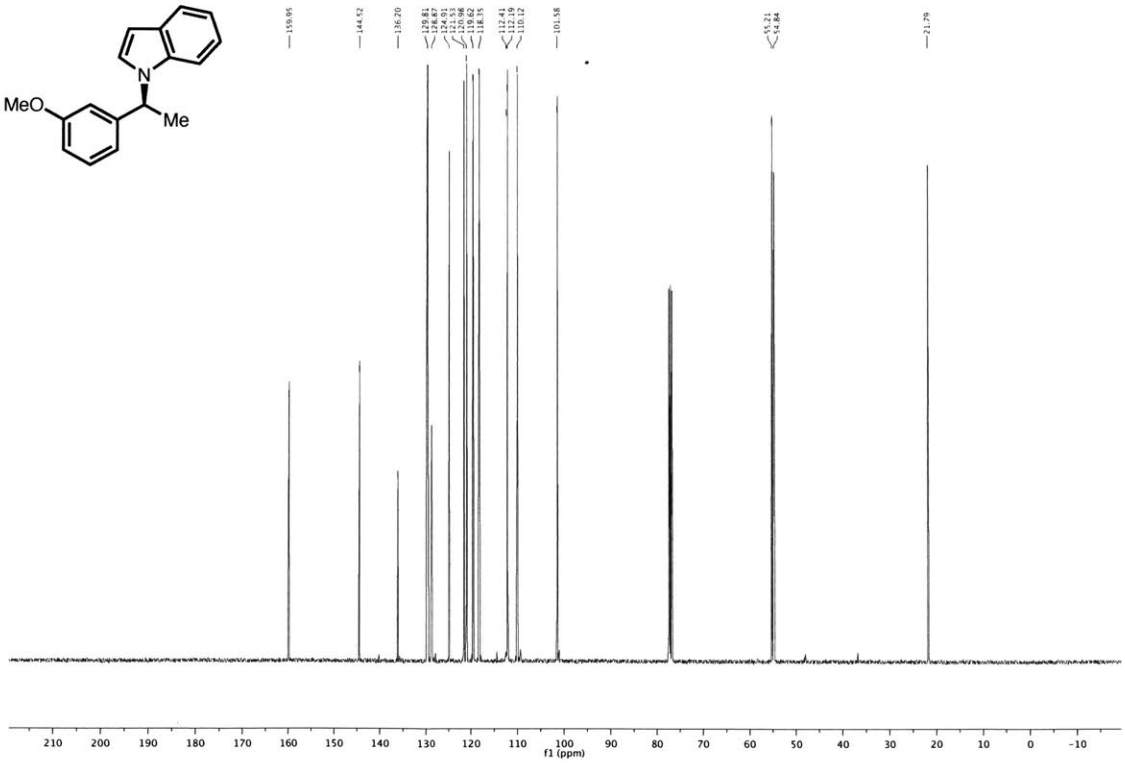

(*S*)-1-(1-(4-fluorophenyl)ethyl)-1*H*-indole (3e)

^{1}H NMR, 400 MHz, $CDCl_3$

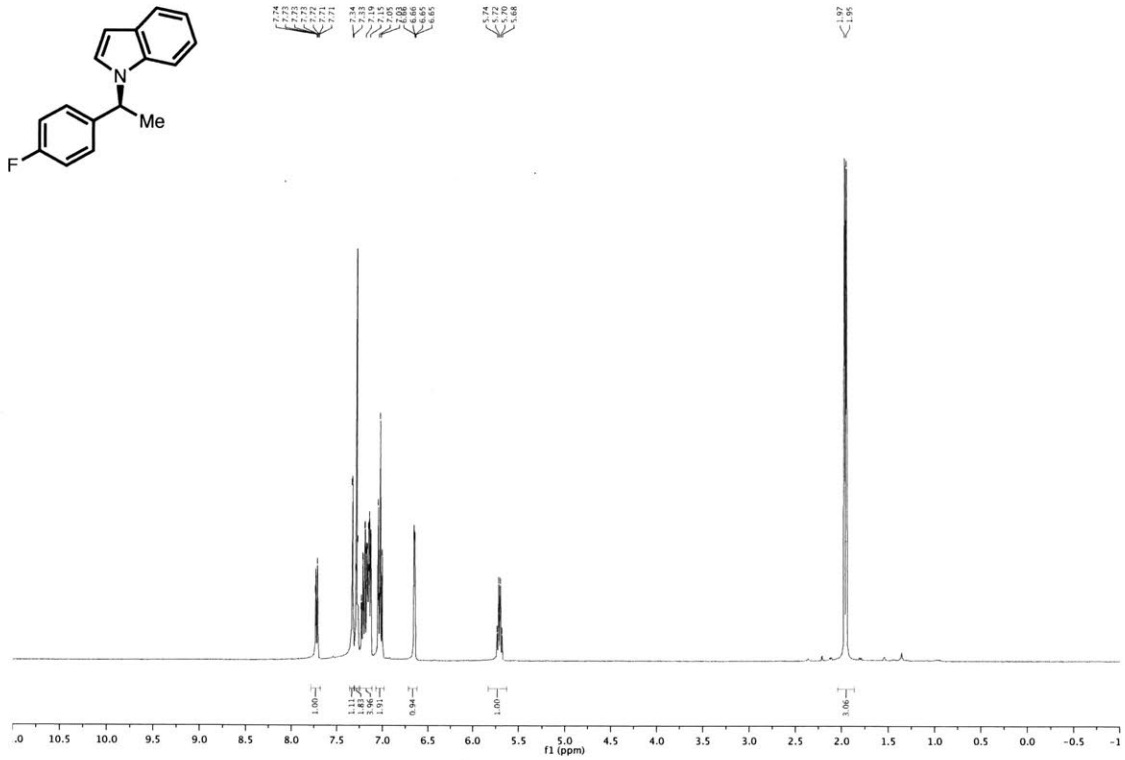

^{13}C NMR, 101 MHz, $CDCl_3$

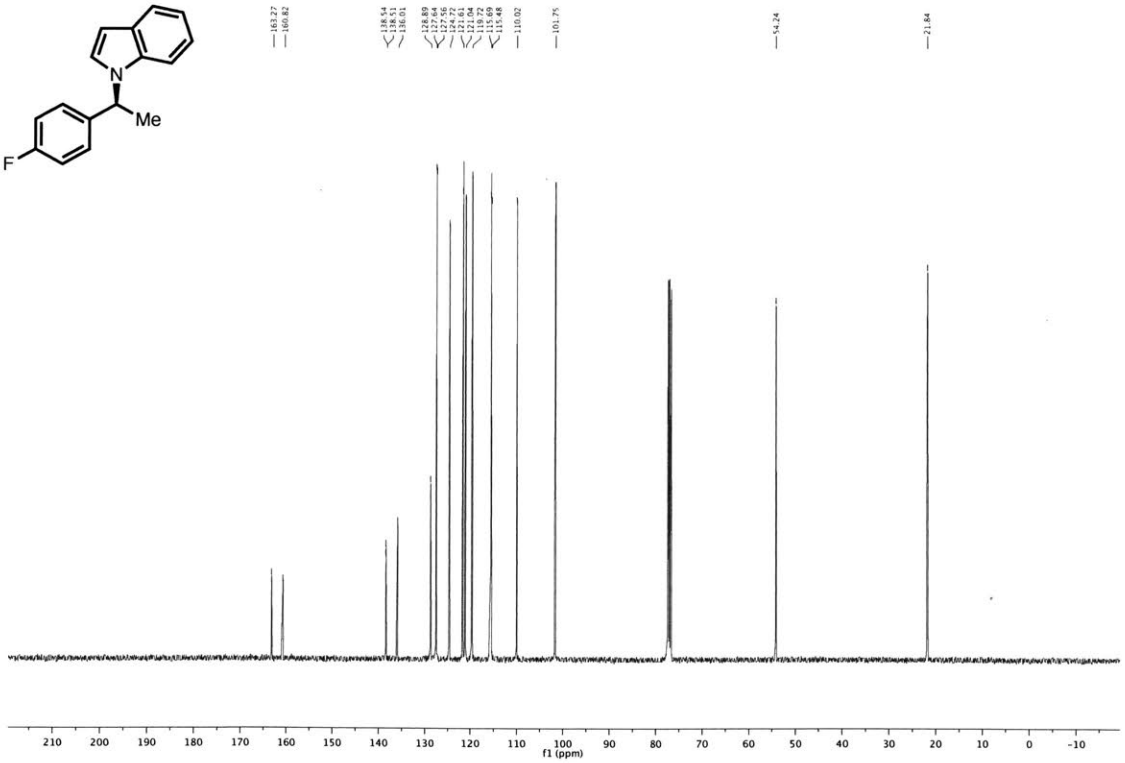

^{19}F NMR, 376 MHz, $CDCl_3$

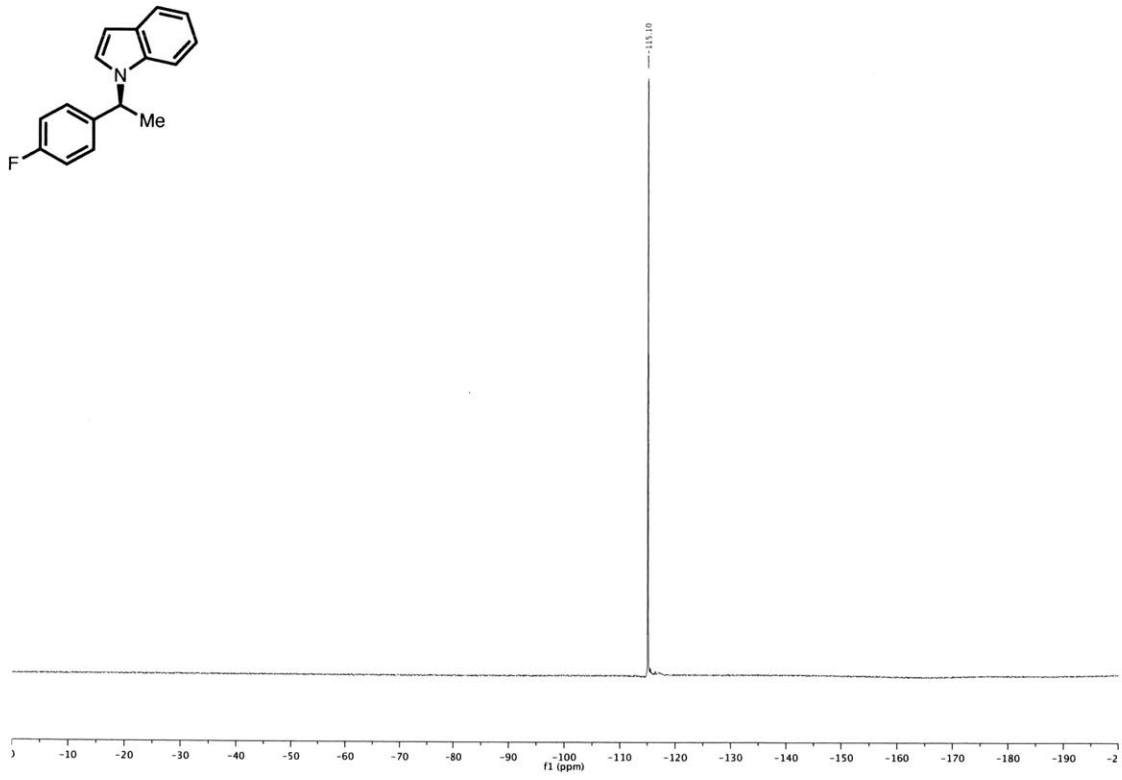

(*S*)-5-(1-(1*H*-indol-1-yl)ethyl)-1-tosyl-1*H*-indole (3f)

^{1}H NMR, 400 MHz, $CDCl_3$

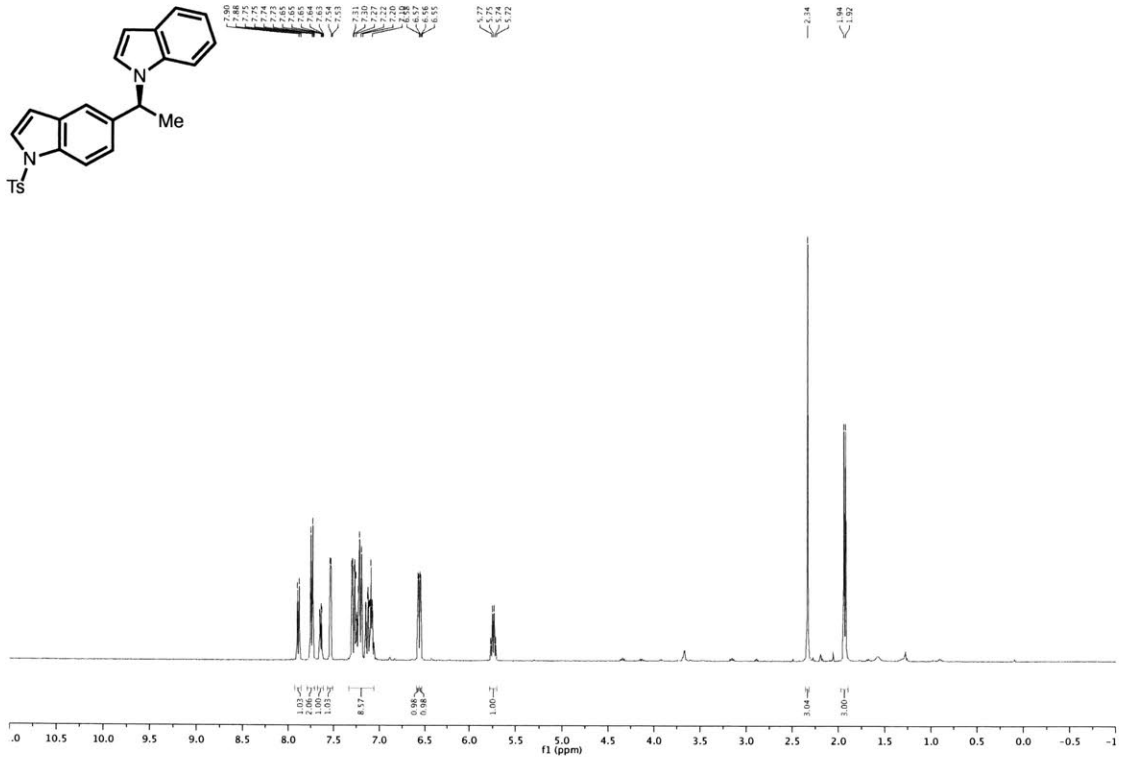

^{13}C NMR, 101 MHz, $CDCl_3$

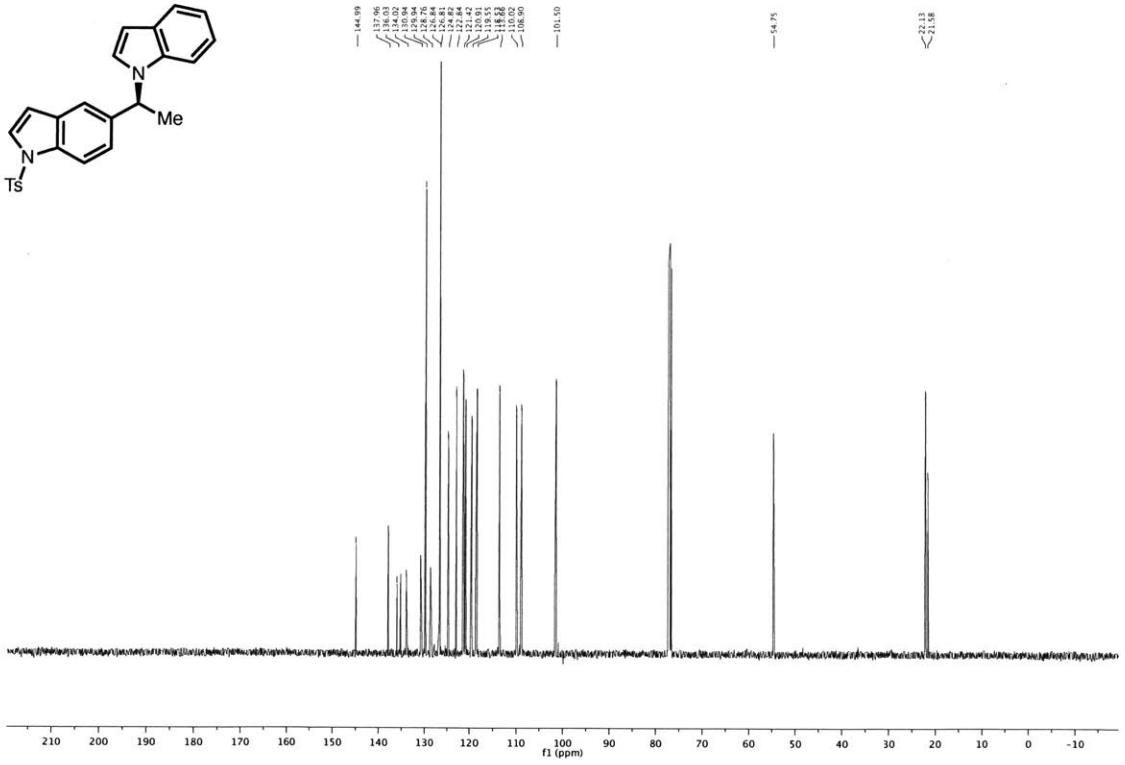

tert-butyl (*S*)-4-(1*H*-indol-1-yl)-4-phenylbutanoate (3g)

^{1}H NMR, 400 MHz, $CDCl_3$

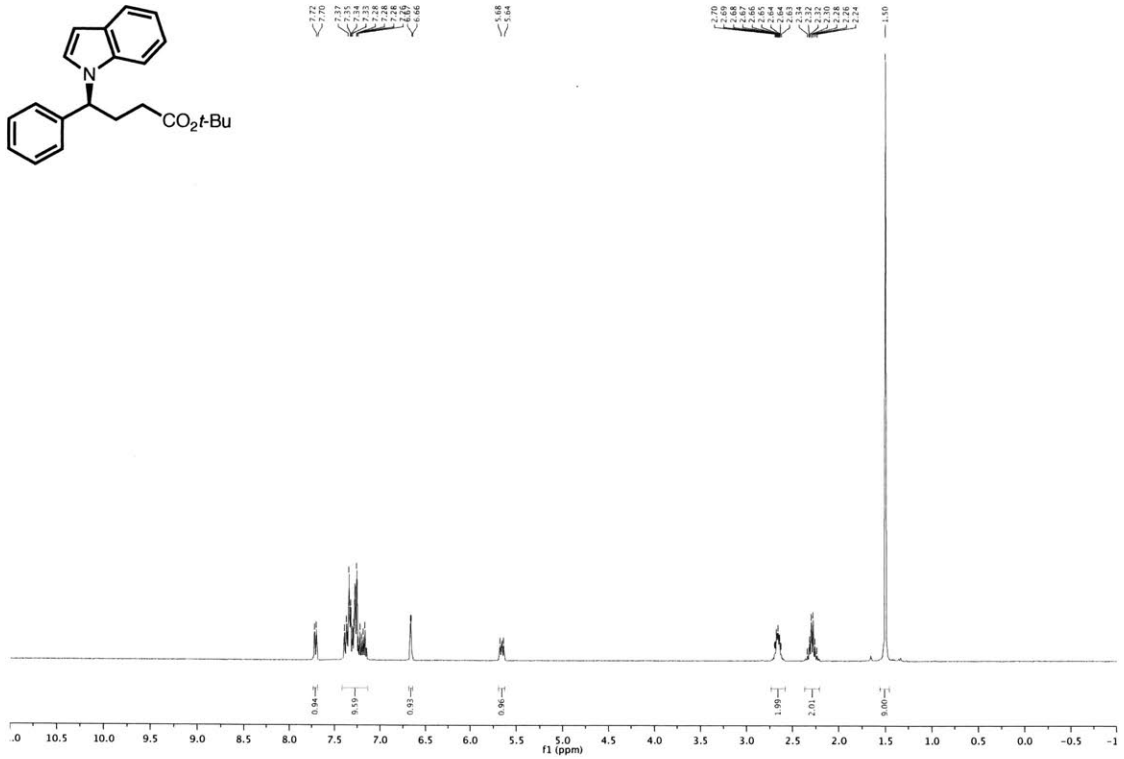

^{13}C NMR, 101 MHz, $CDCl_3$

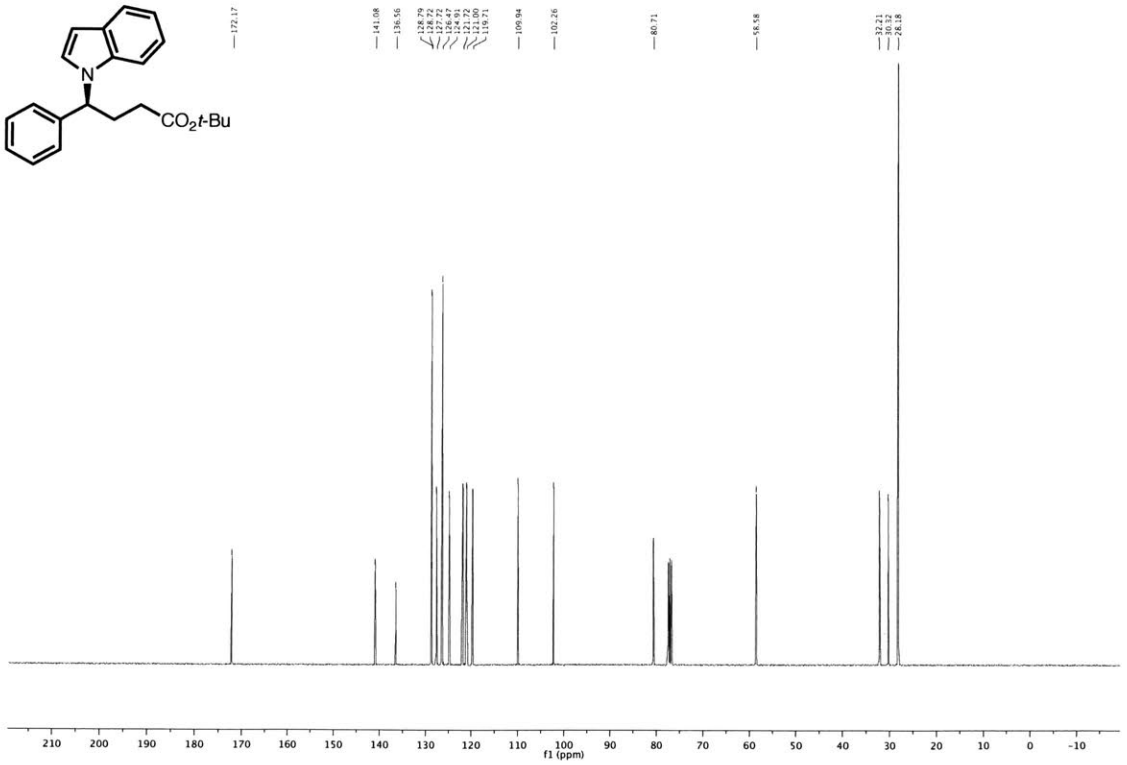

(*S*)-*N*-(3-(1*H*-indol-1-yl)-3-phenylpropyl)-*N*-methylpivalamide (3h)

^{1}H NMR, 400 MHz, $CDCl_3$

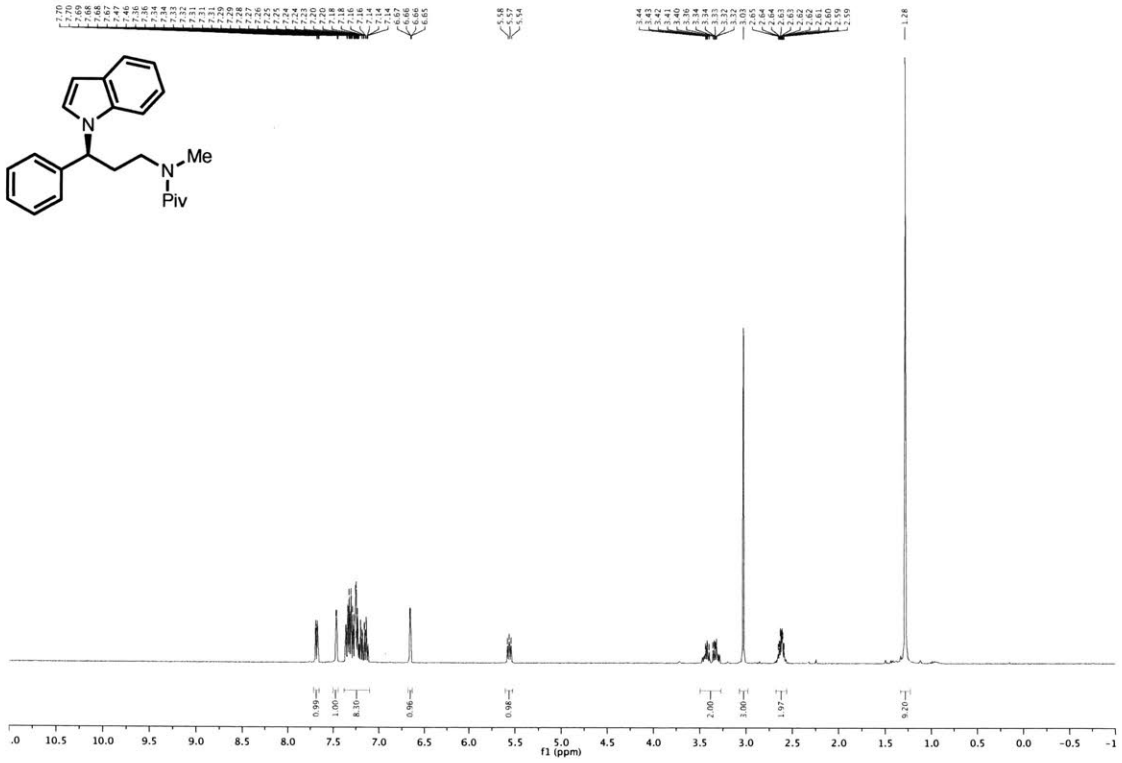

^{13}C NMR, 101 MHz, $CDCl_3$

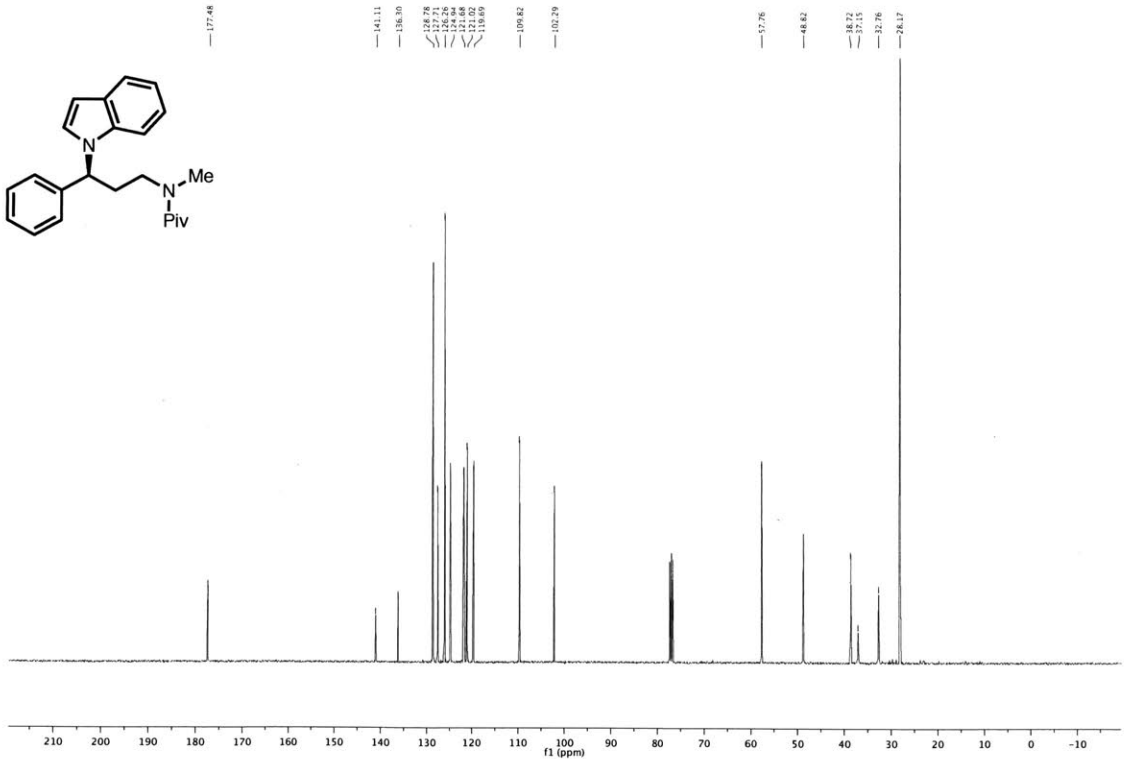

***N*-((2*S*,3*S*)-3-(1*H*-indol-1-yl)-2-methyl-3-phenylpropyl)-*N*,4-dimethylbenzenesulfonamide (3i)**

^{1}H NMR, 400 MHz, $CDCl_3$

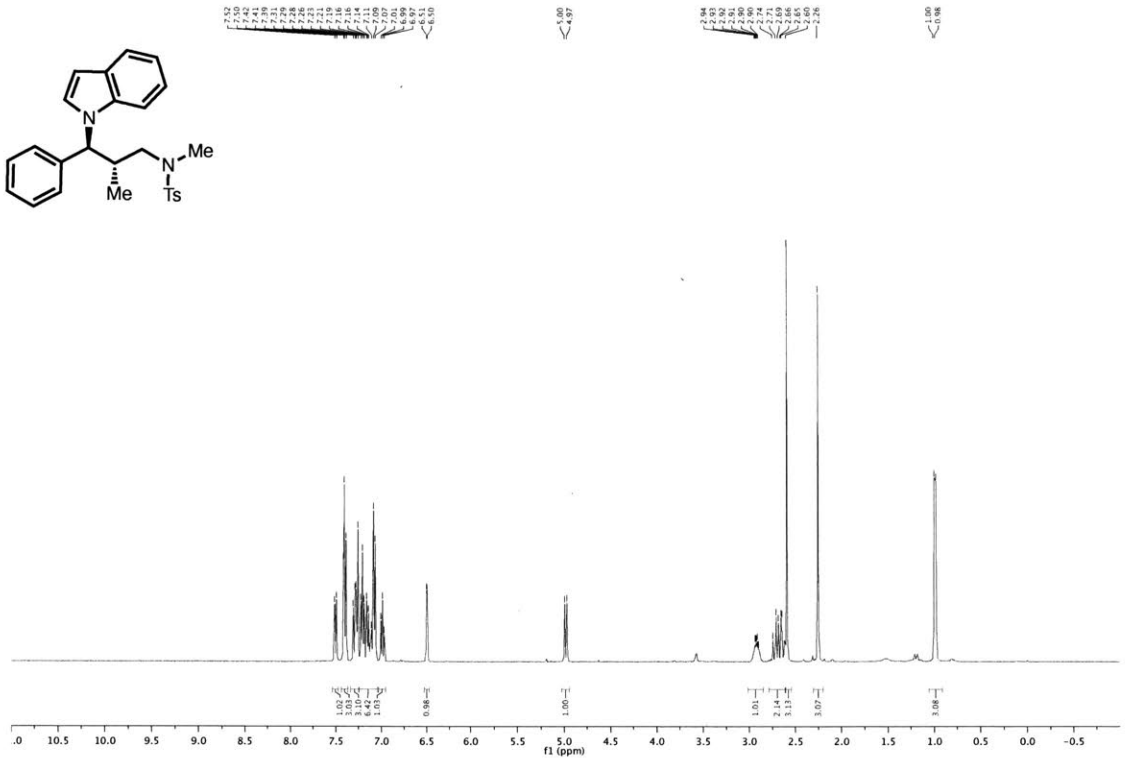

^{13}C NMR, 101 MHz, $CDCl_3$

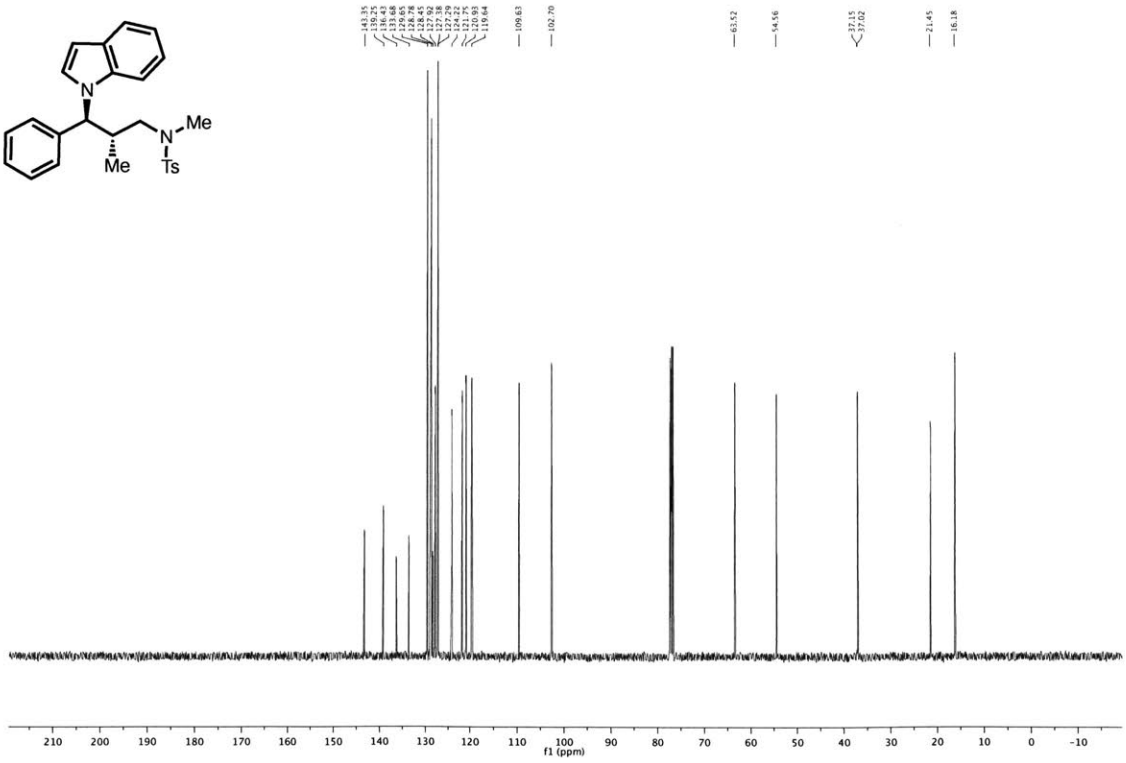

1-(3-(benzo[*d*][1,3]dioxol-5-yl)propyl)-1*H*-indole (3j)

^{1}H NMR, 400 MHz, $CDCl_3$

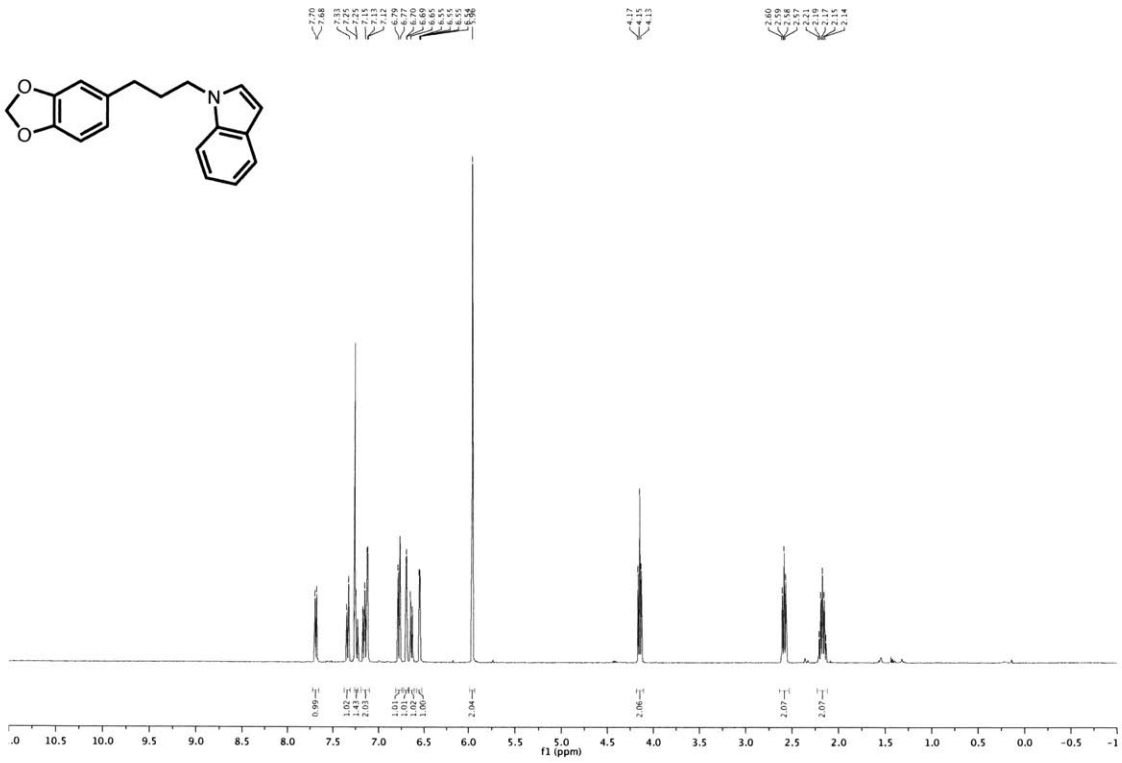

^{13}C NMR, 101 MHz, $CDCl_3$

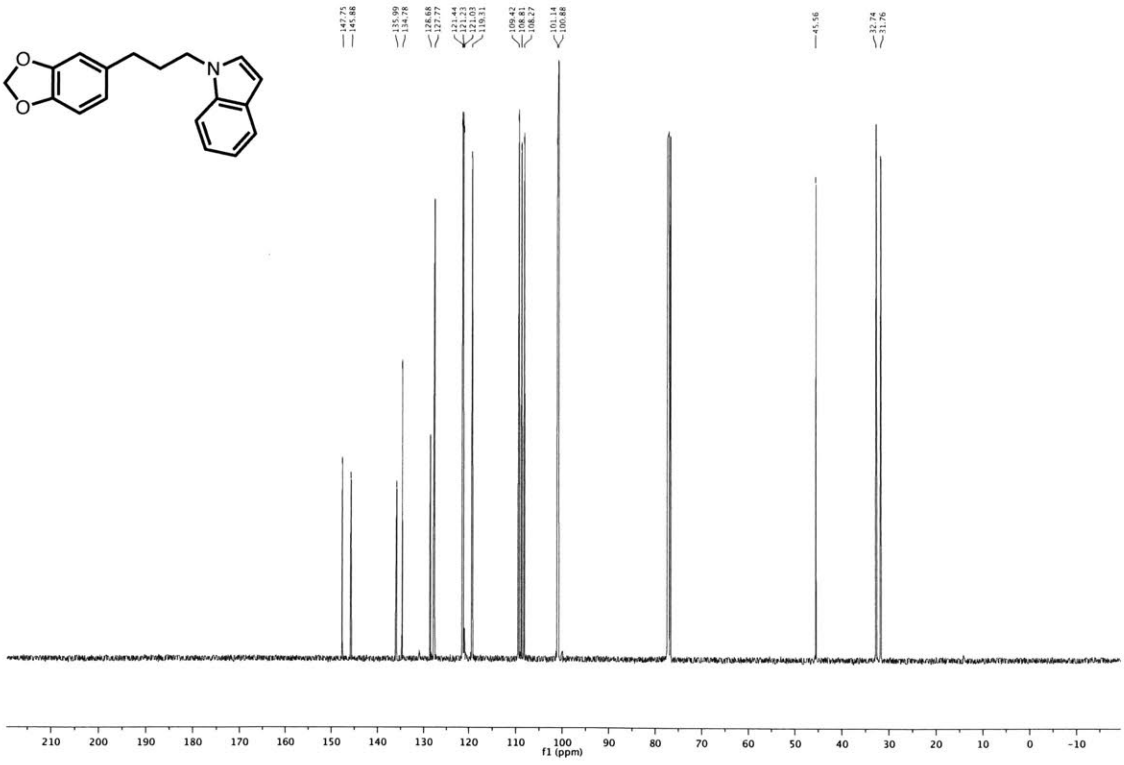

(*Z*)-1-(hex-4-en-1-yl)-1*H*-indole (3k)

^{1}H NMR, 400 MHz, $CDCl_3$

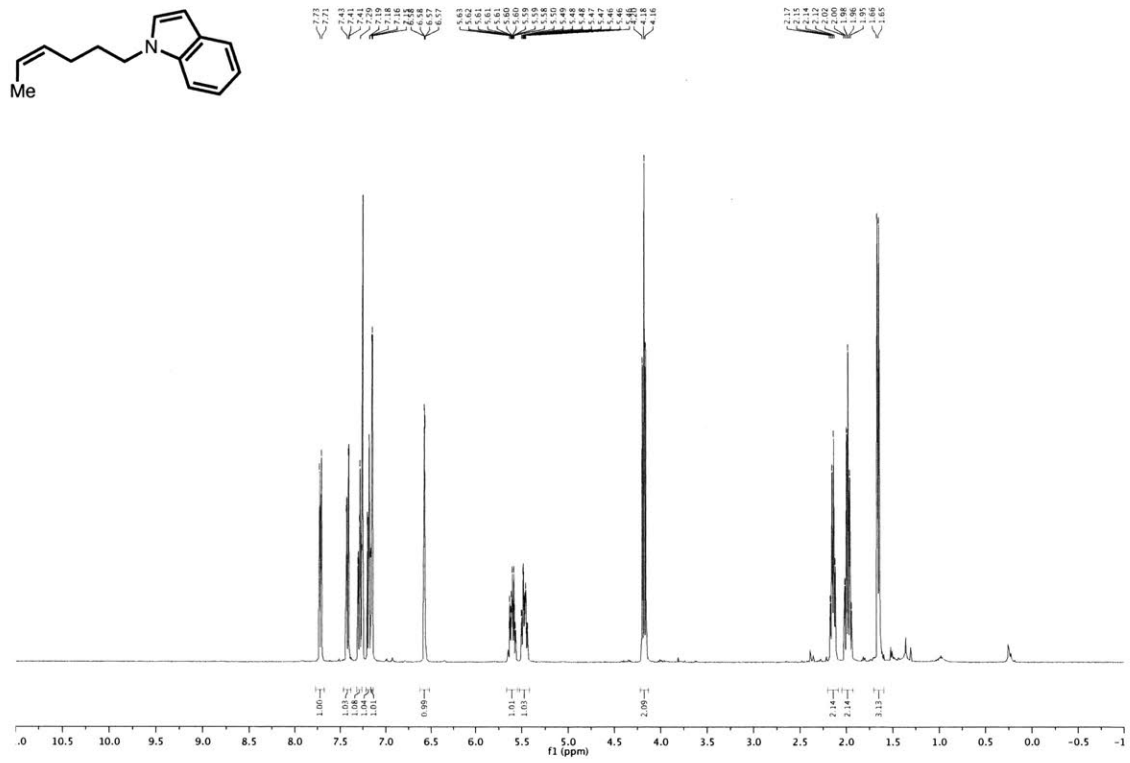

^{13}C NMR, 101 MHz, $CDCl_3$

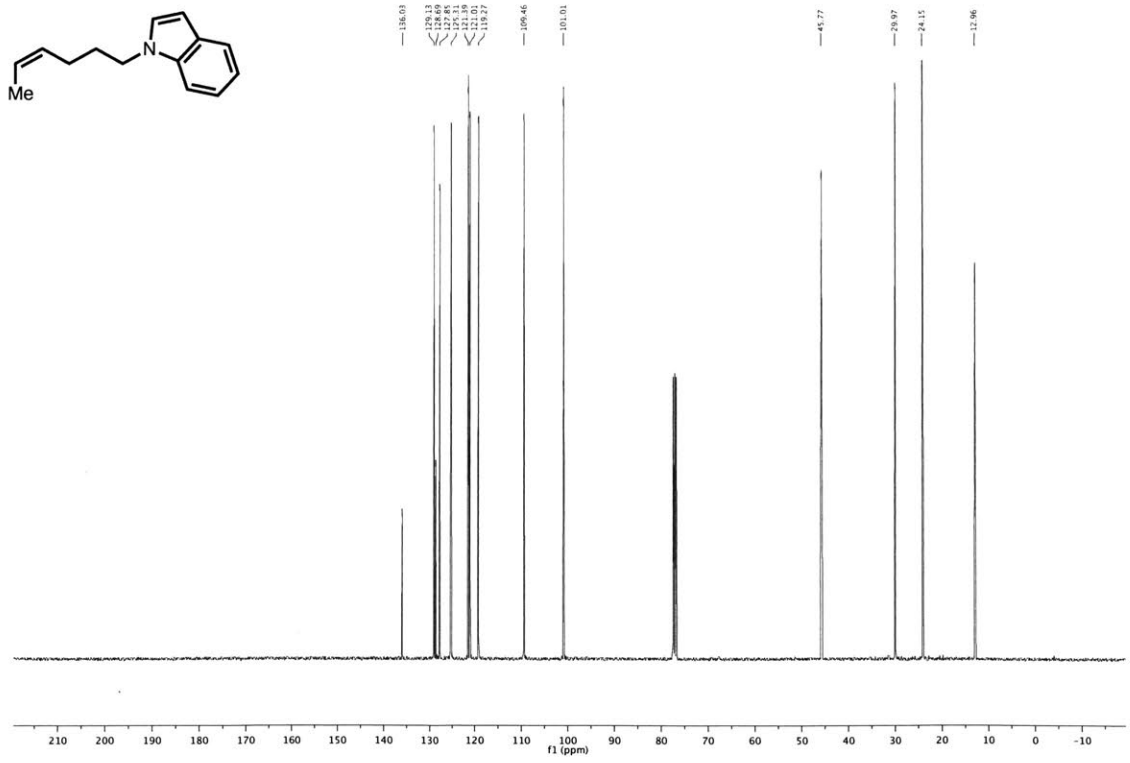

(*S*)-1-(3,7-dimethyloct-6-en-1-yl)-1*H*-indole (3i)

^{1}H NMR, 400 MHz, $CDCl_3$

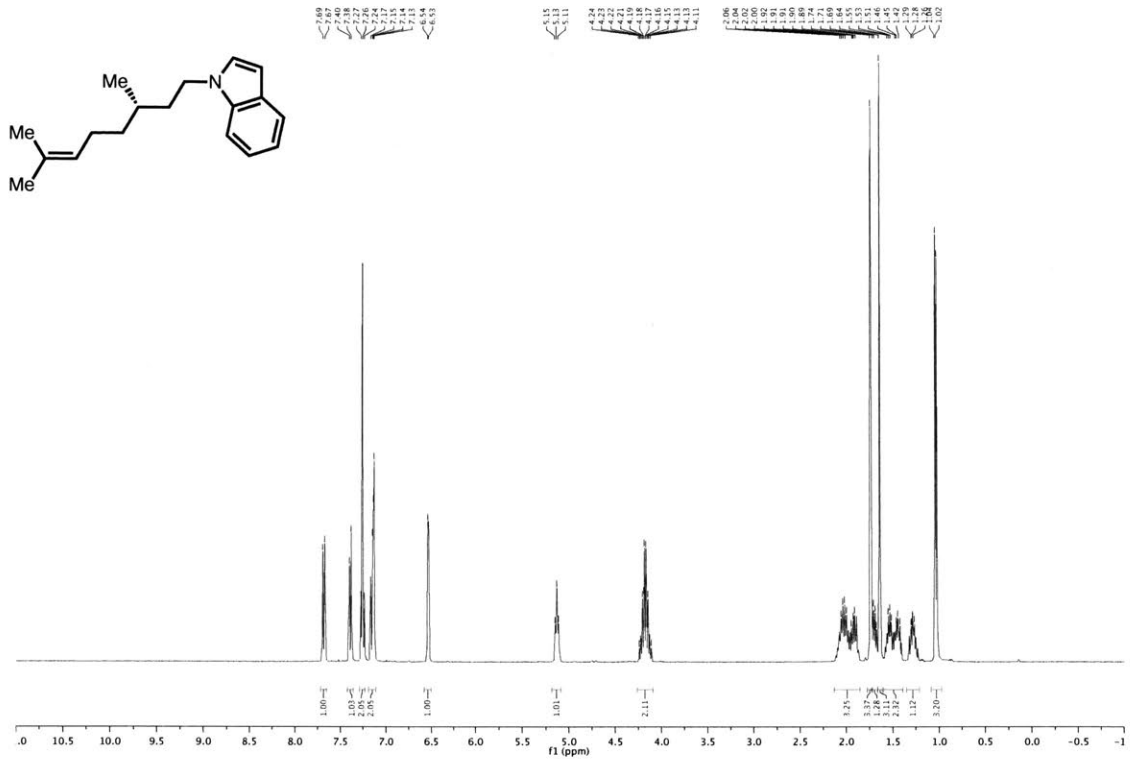

^{13}C NMR, 101 MHz, $CDCl_3$

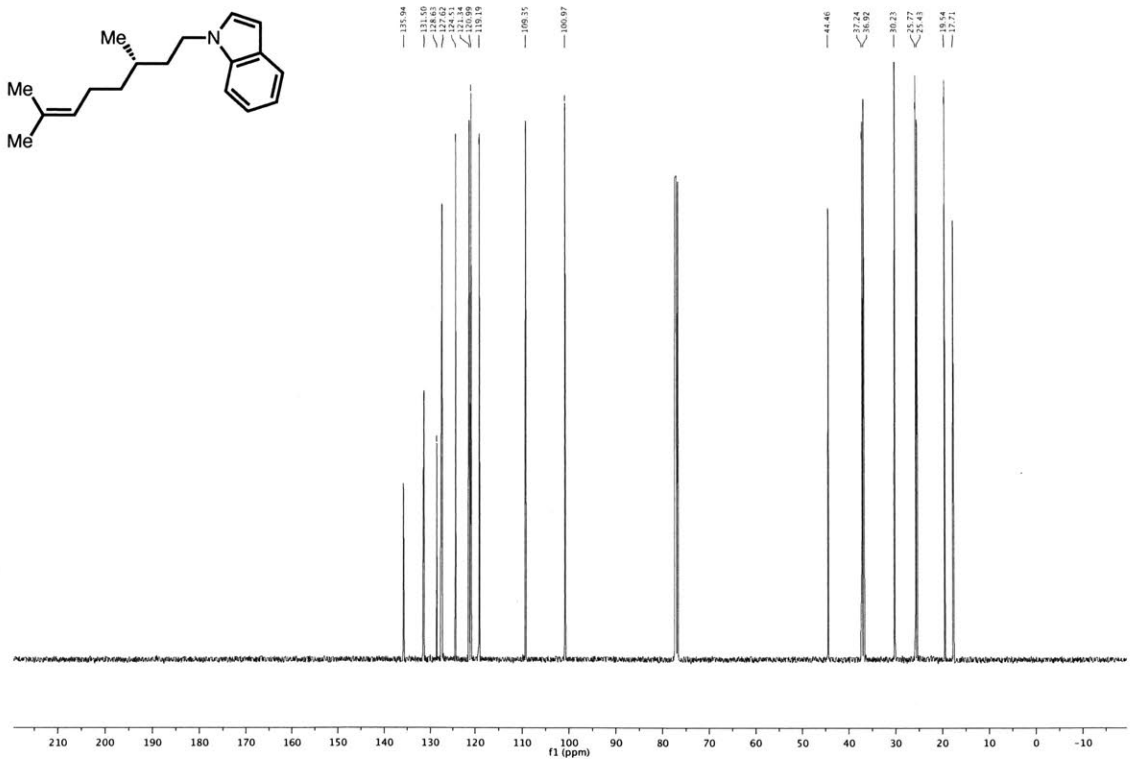

(*S*)-*N*,*N*-diethyl-3-(1-(6-(trifluoromethyl)-1*H*-indol-1-yl)ethyl)benzamide (3m)

^{1}H NMR, 400 MHz, $CDCl_3$

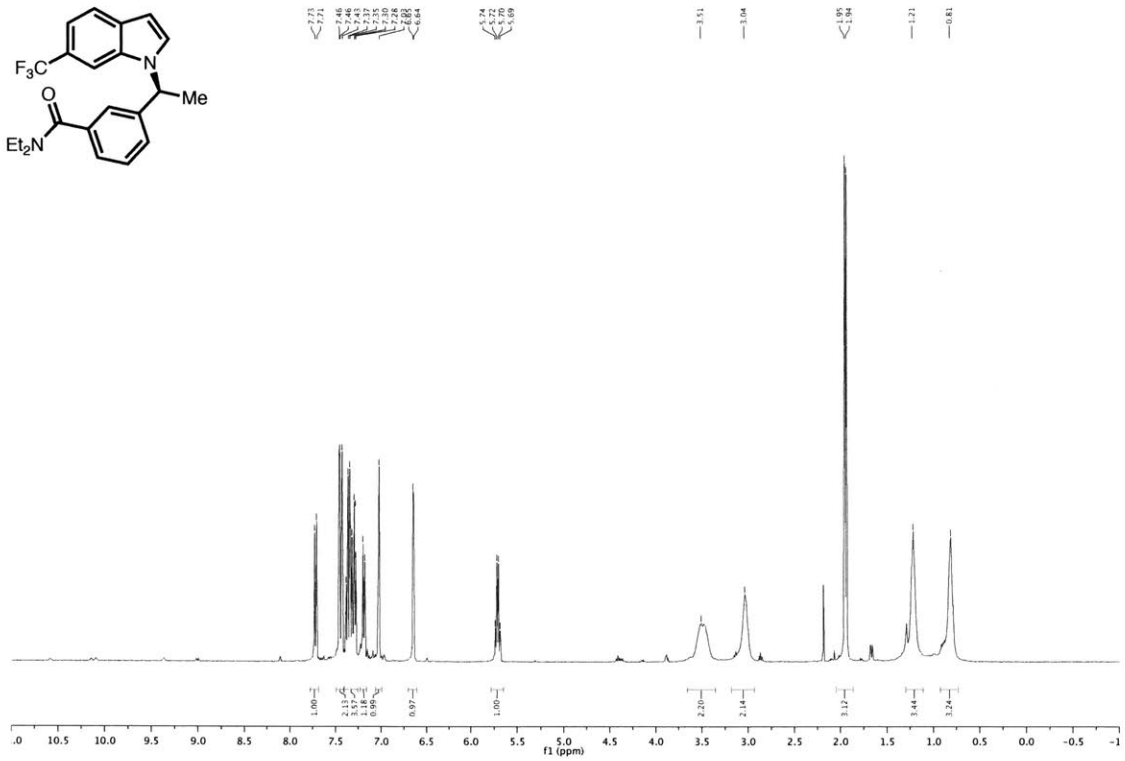

^{13}C NMR, 101 MHz, $CDCl_3$

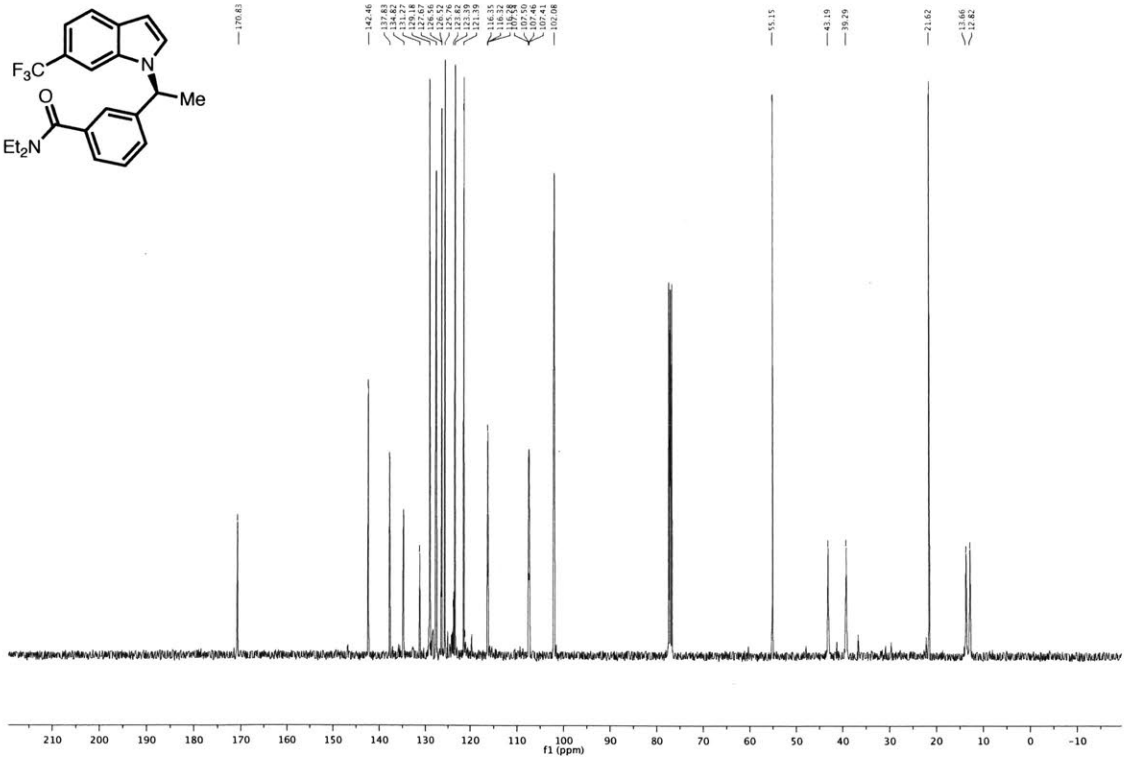

^{19}F NMR, 376 MHz, $CDCl_3$

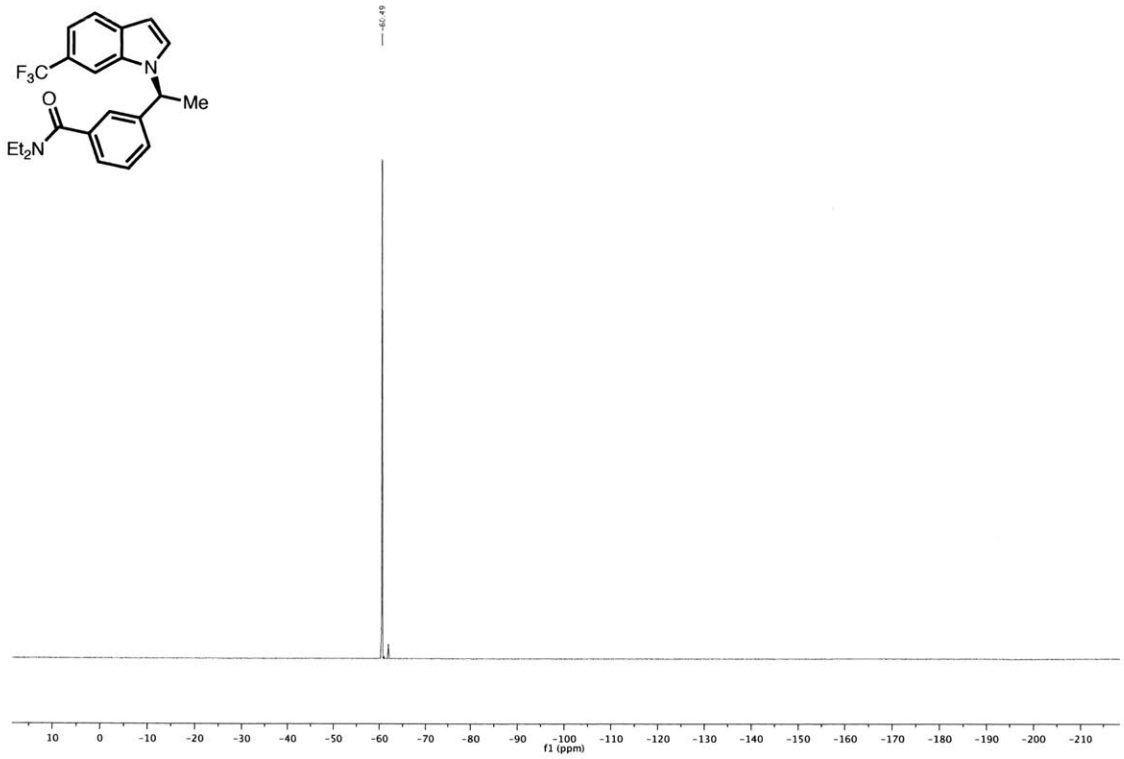

tert-butyl (_S_)-1-(1-(2-(difluoromethoxy)phenyl)ethyl)-1_H_-indole-4-carboxylate (3n)

^{1}H NMR, 400 MHz, $CDCl_3$

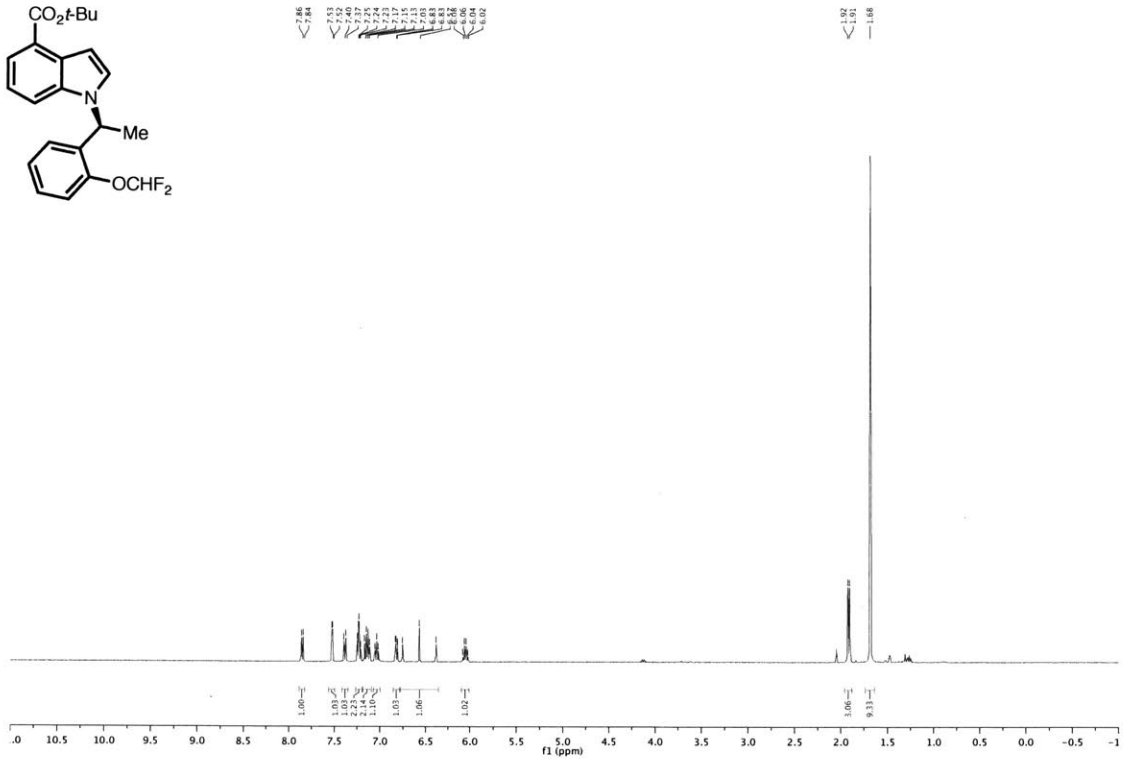

^{13}C NMR, 101 MHz, $CDCl_3$

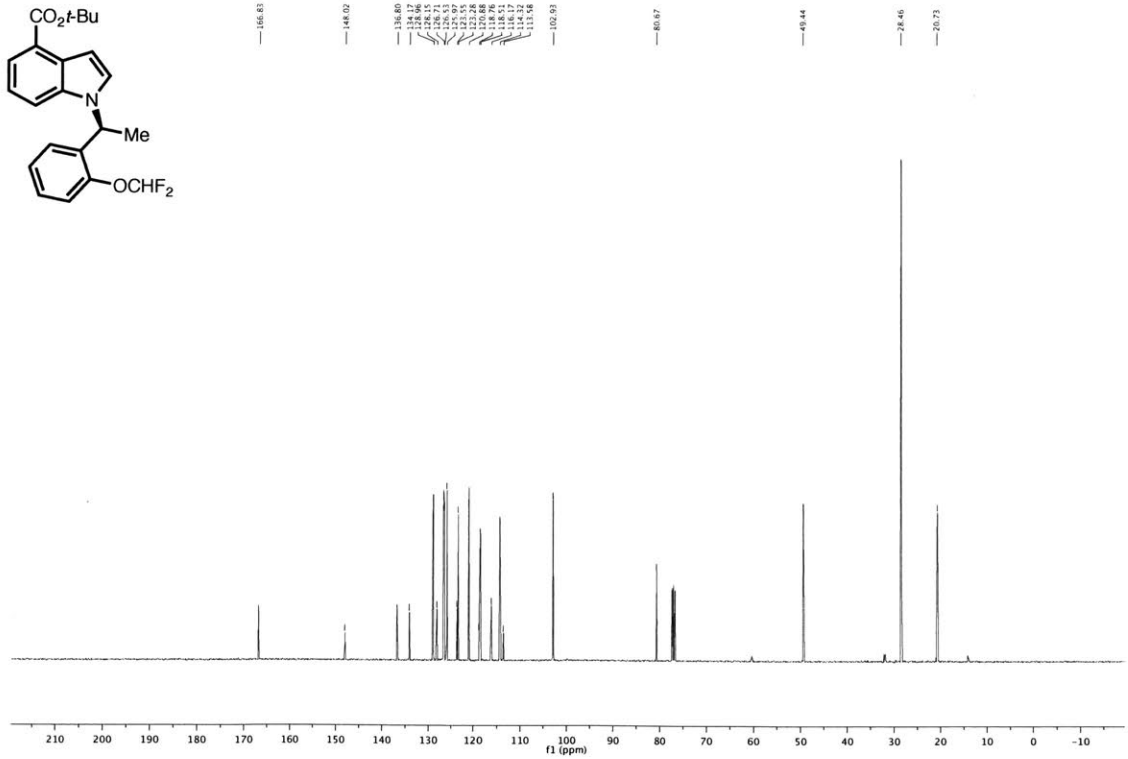

^{19}F NMR, 376 MHz, $CDCl_3$

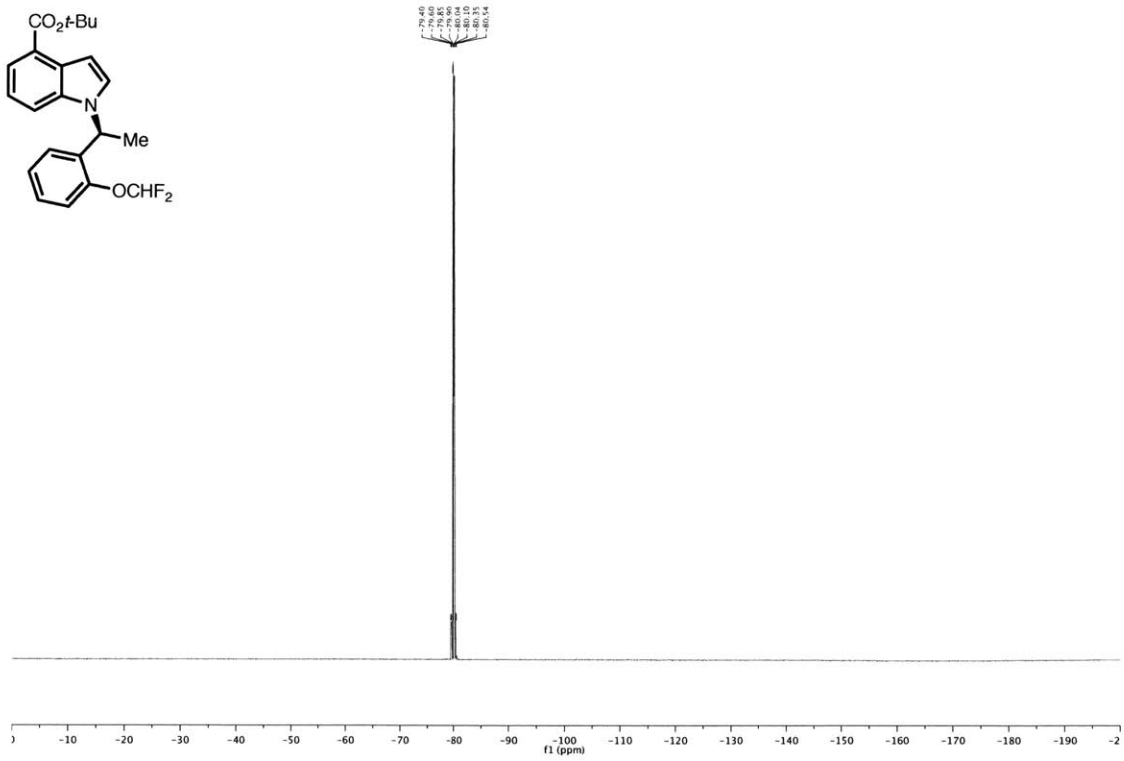

(*S*)-1-(1-(3-chlorophenyl)ethyl)-2-methyl-1*H*-indole (3r)

^{1}H NMR, 400 MHz, $CDCl_3$

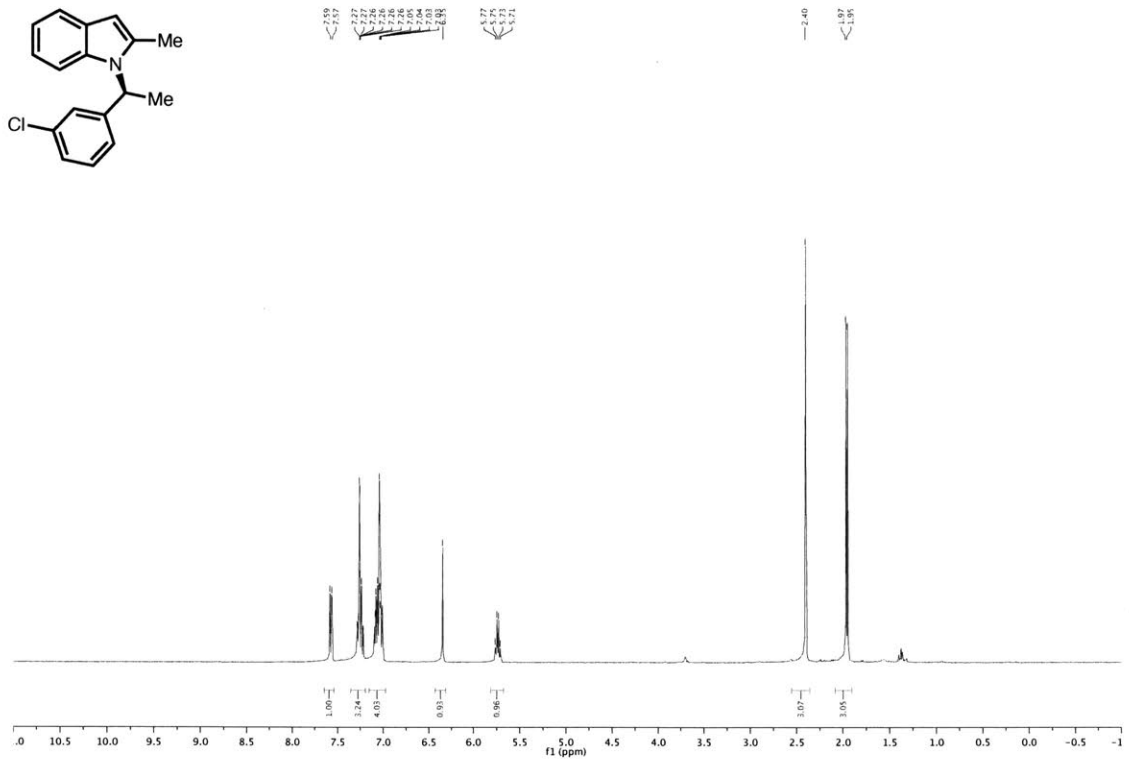

^{13}C NMR, 101 MHz, $CDCl_3$

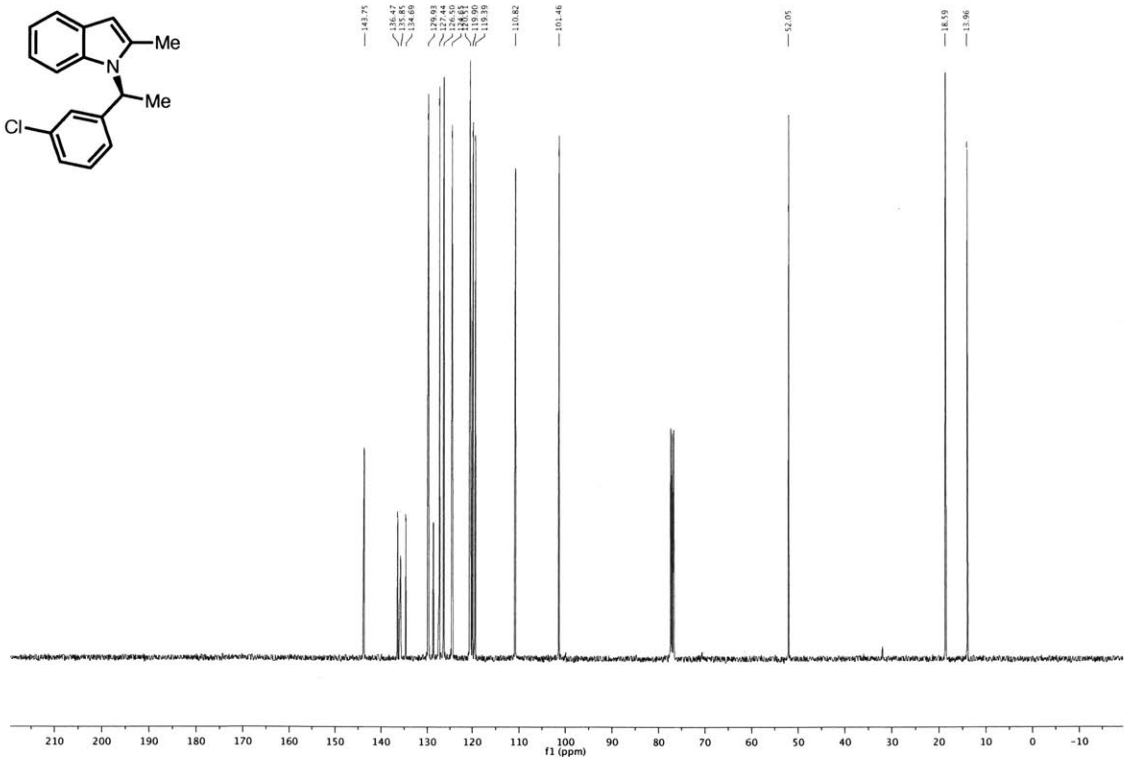

6-methyl-4-(4-(4-methyl-1*H*-indol-1-yl)butoxy)-2-(trifluoromethyl)quinolone (3p)

^{1}H NMR, 400 MHz, $CDCl_3$

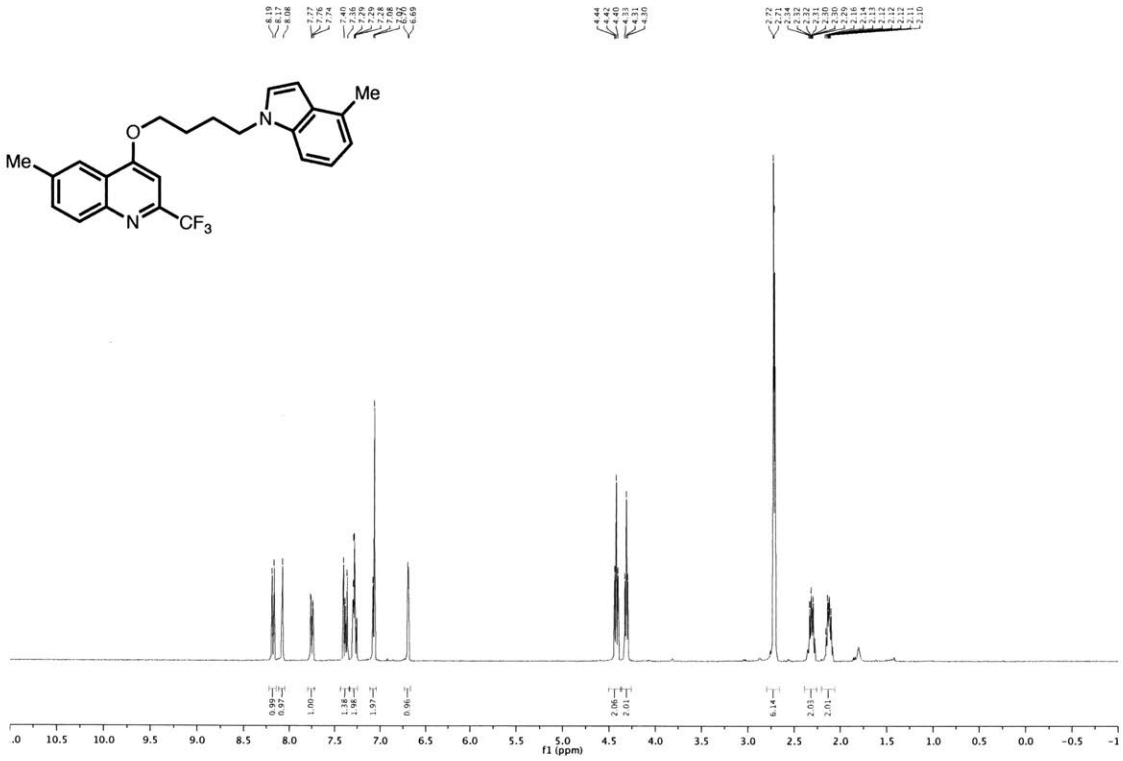

^{13}C NMR, 101 MHz, $CDCl_3$

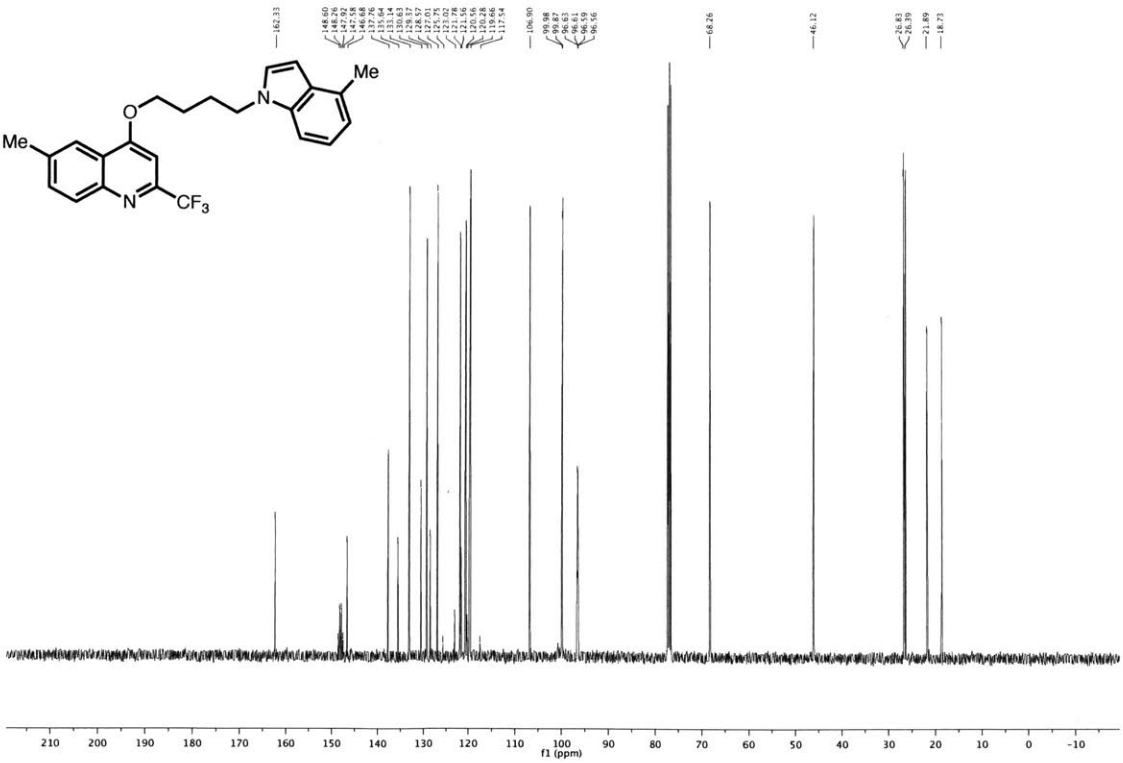

^{19}F NMR, 376 MHz, $CDCl_3$

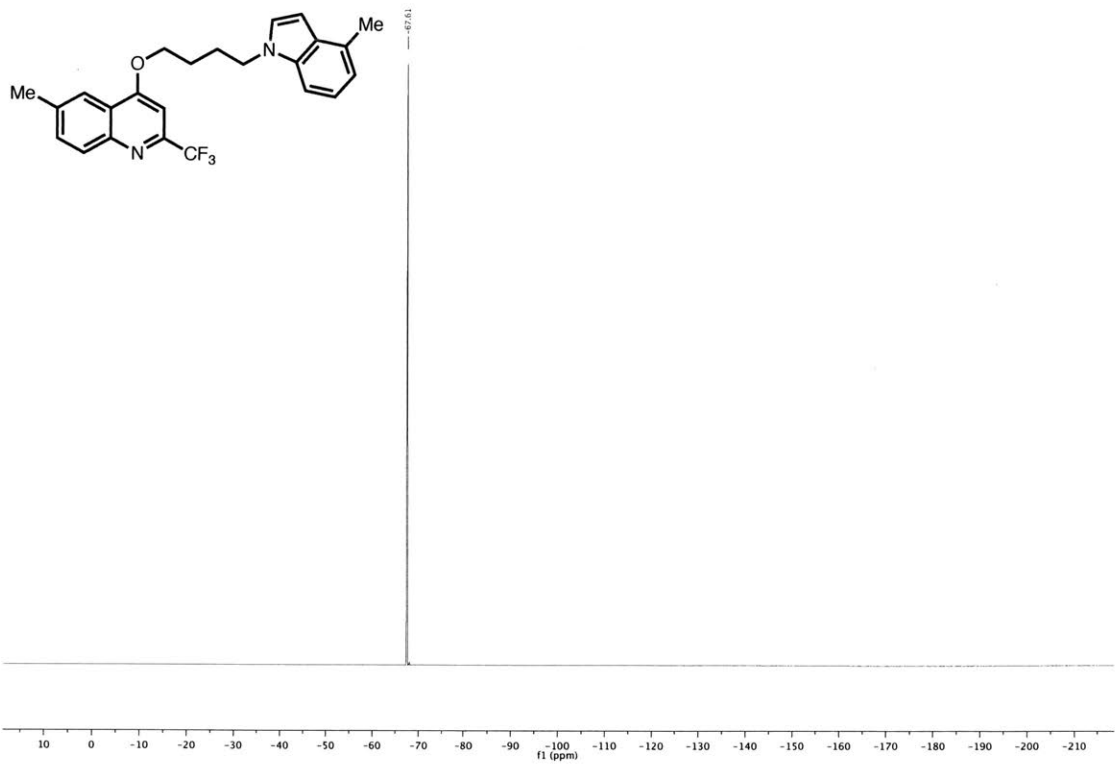

6-chloro-1-(2-(cyclohex-3-en-1-yl)ethyl)-1*H*-indole (3o)

^{1}H NMR, 400 MHz, $CDCl_3$

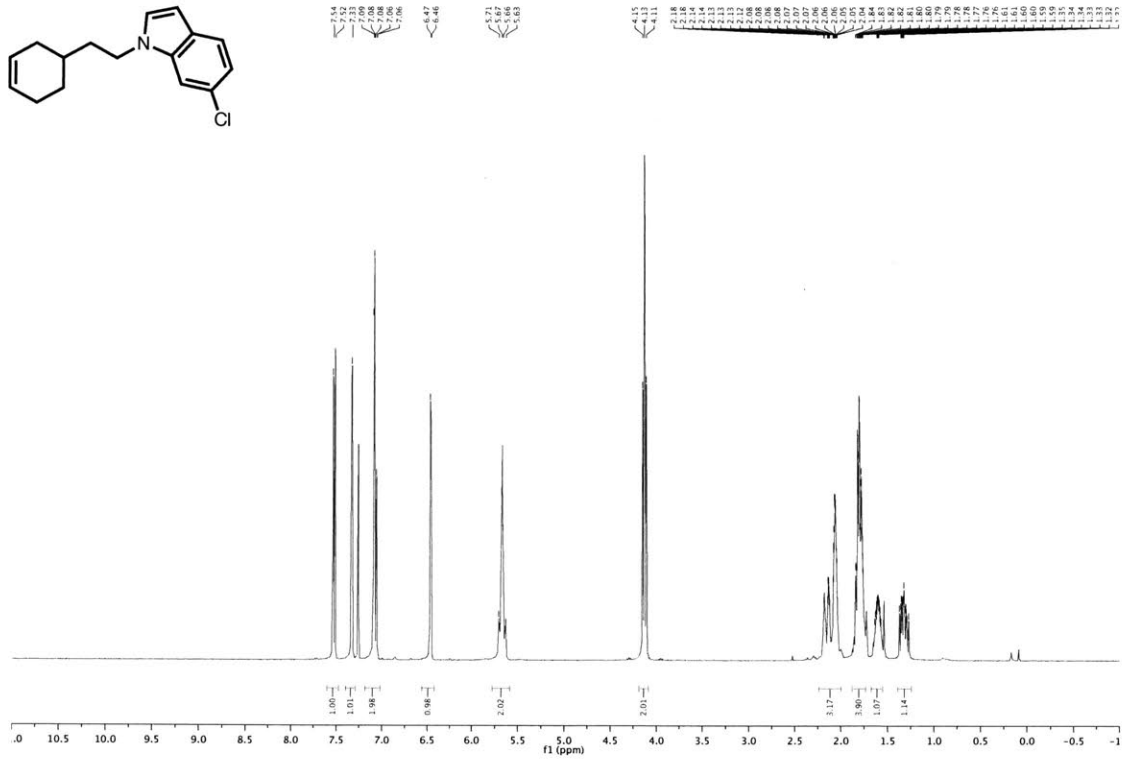

^{13}C NMR, 101 MHz, $CDCl_3$

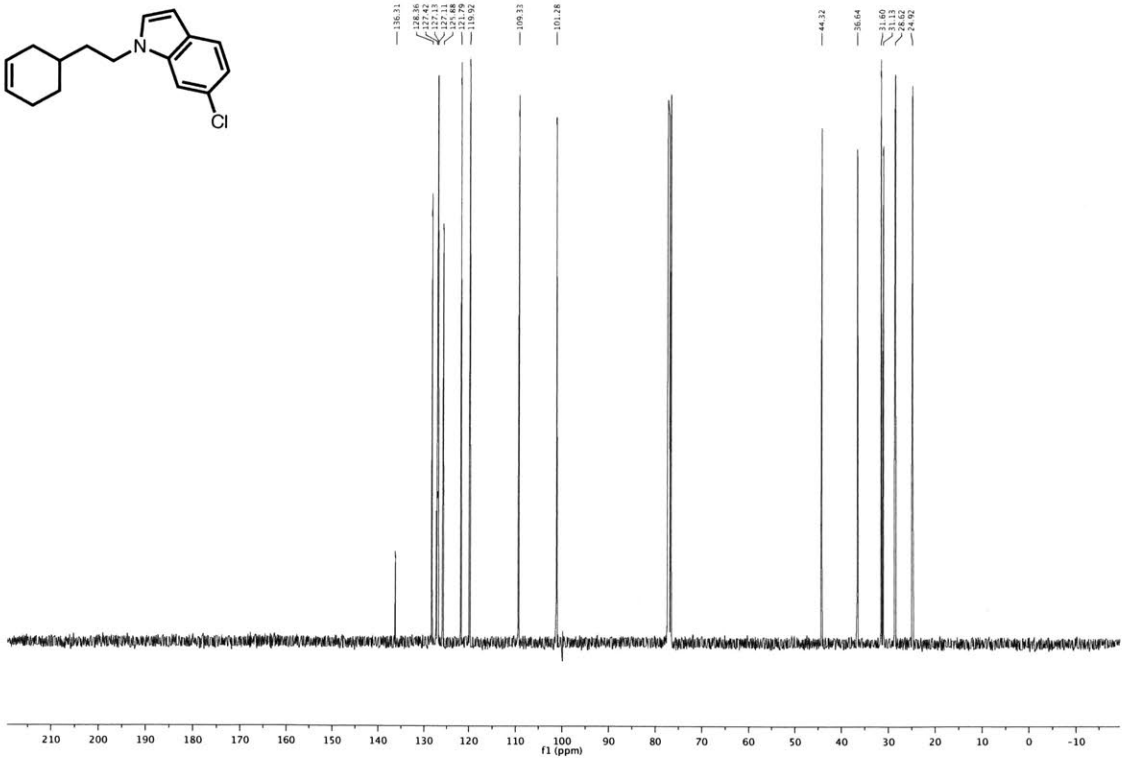

methyl (*S*)-1-(1-phenylethyl)-1*H*-indole-2-carboxylate (3q)

^{1}H NMR, 400 MHz, $CDCl_3$

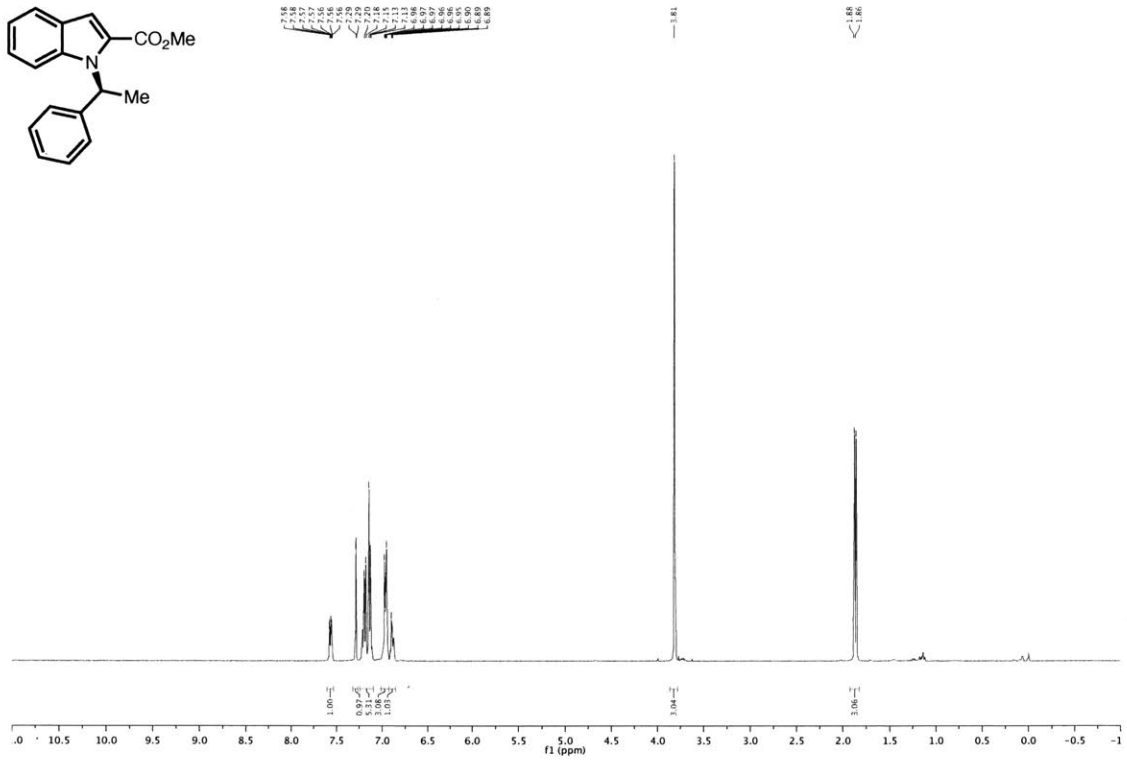

^{13}C NMR, 101 MHz, $CDCl_3$

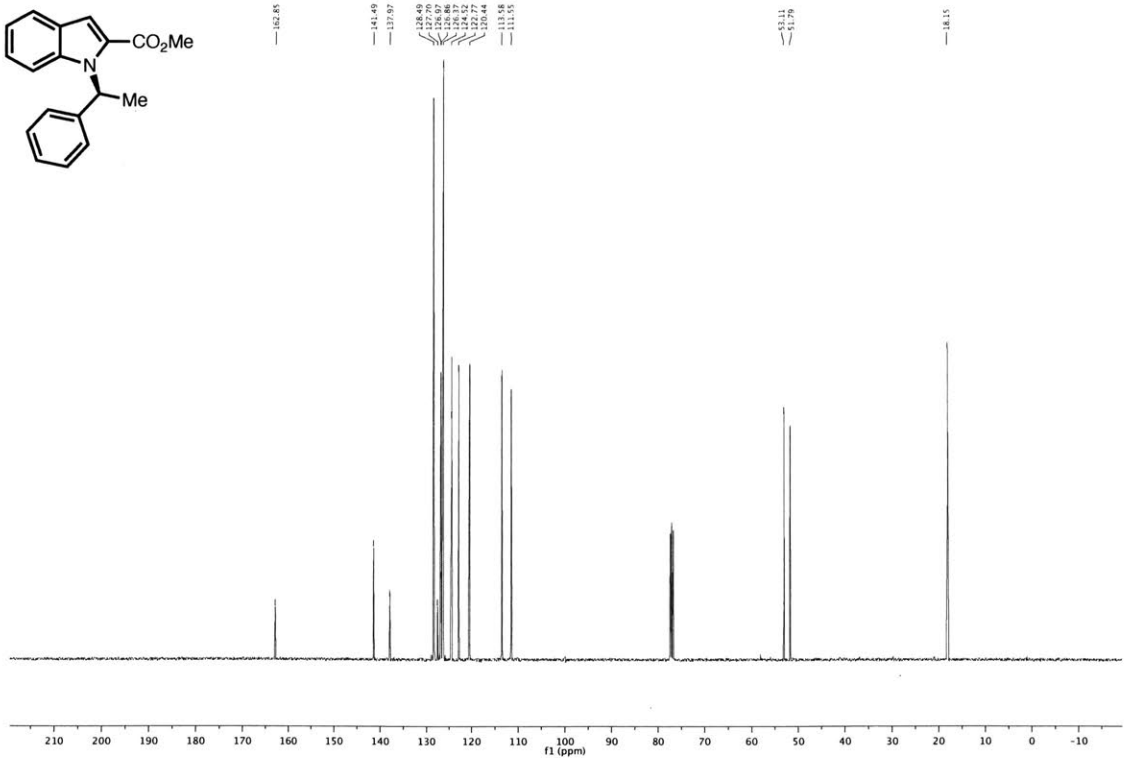

(*S*)-3-(2-methoxyethyl)-1-(1-(4-(trifluoromethyl)phenyl)ethyl)-1*H*-indole (3s)

^{1}H NMR, 400 MHz, $CDCl_3$

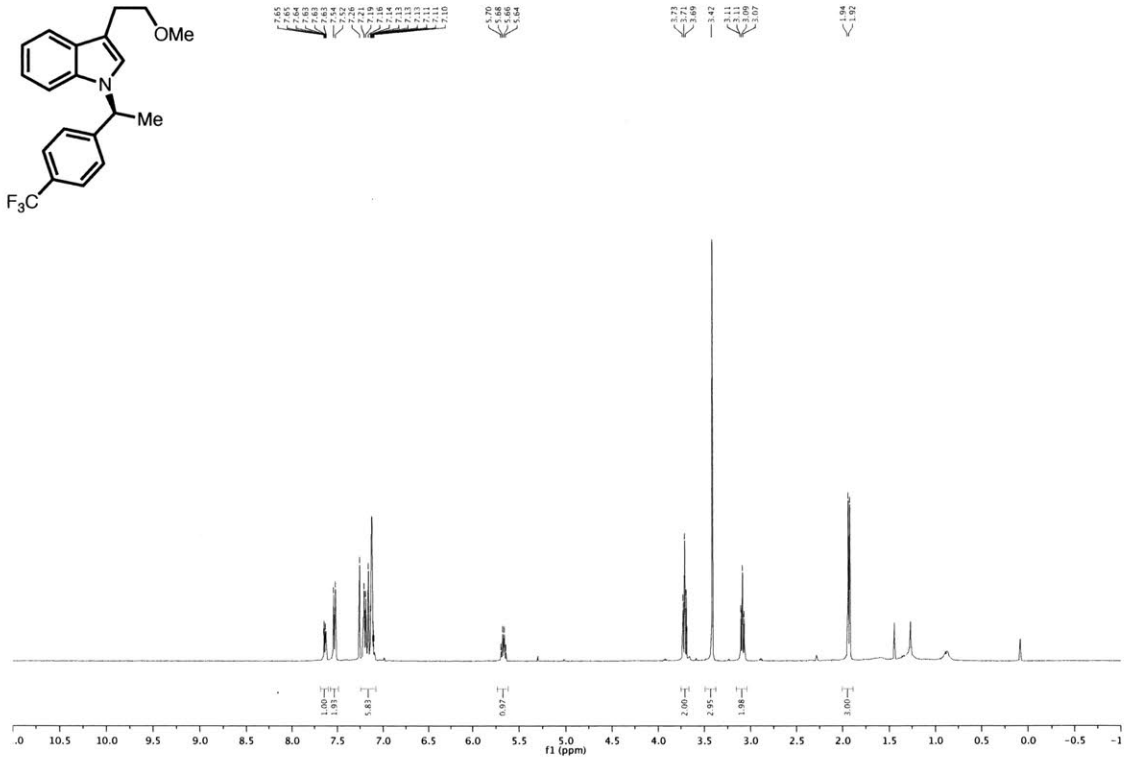

^{13}C NMR, 101 MHz, $CDCl_3$

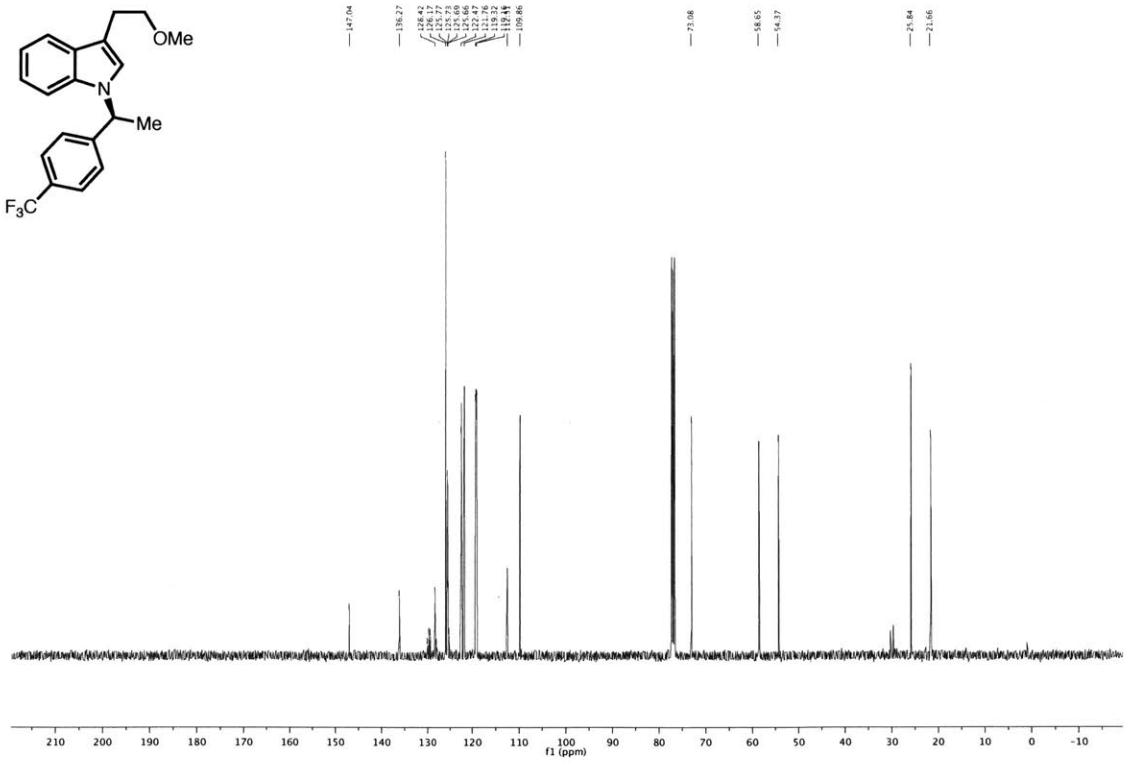

^{19}F NMR, 376 MHz, $CDCl_3$

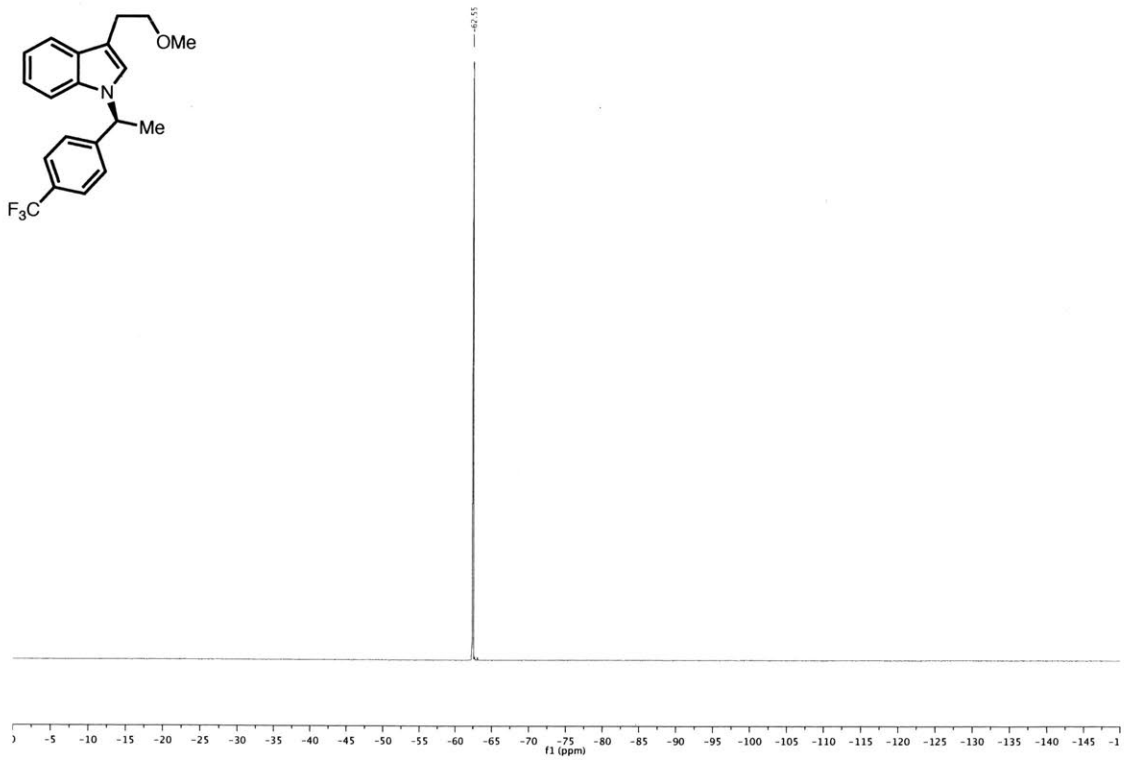

(*S*)-3-(1-phenylethyl)-1*H*-indole (4a)

^{1}H NMR, 400 MHz, $CDCl_3$

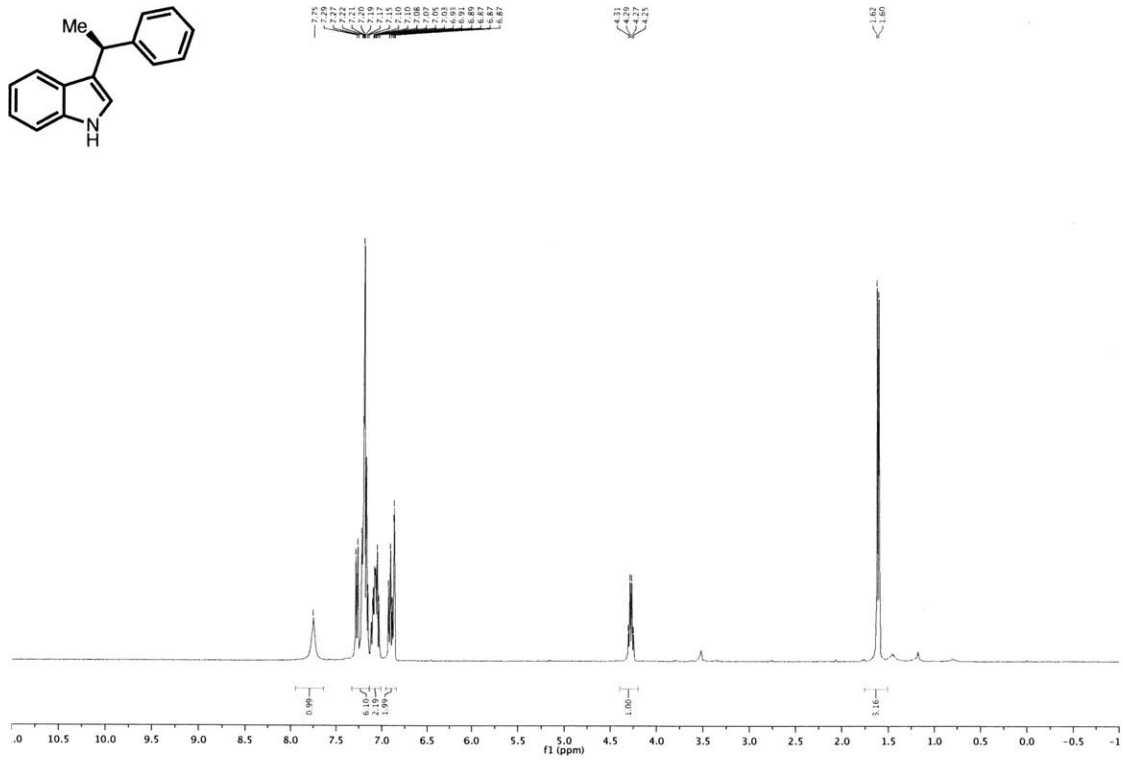

^{13}C NMR, 101 MHz, $CDCl_3$

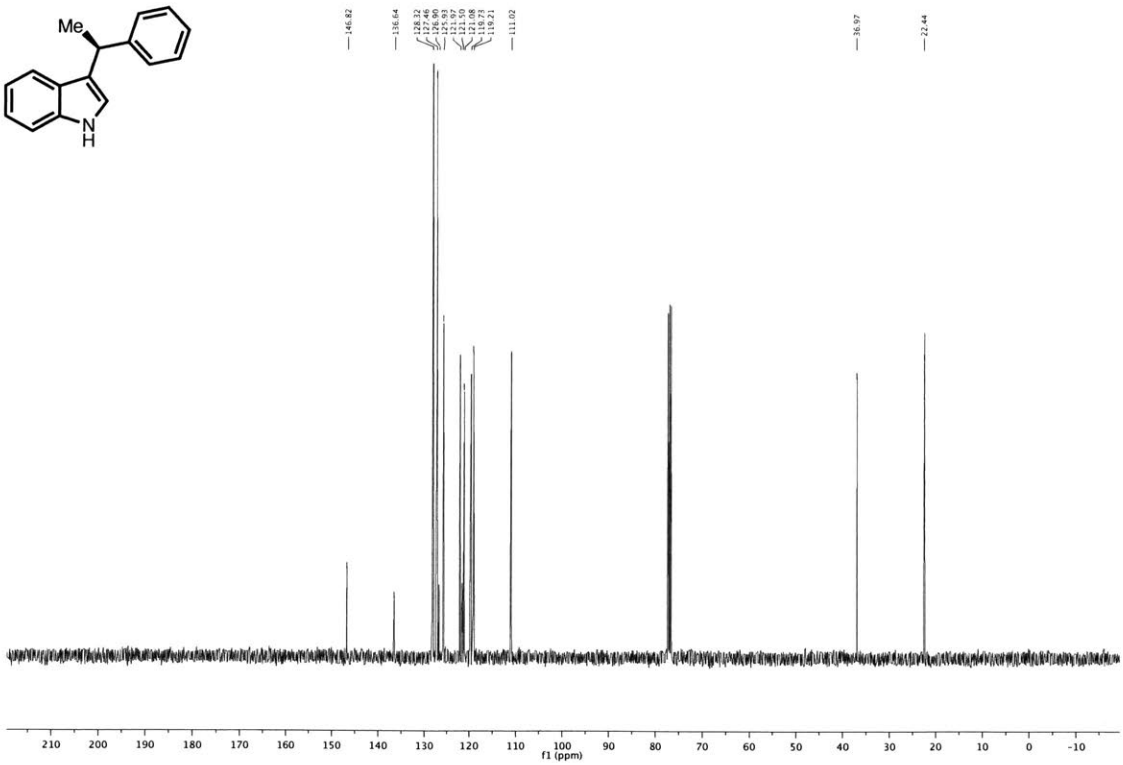

(*S*)-3-(1-(4-(trifluoromethyl)phenyl)ethyl)-1*H*-indole (4b)

^{1}H NMR, 400 MHz, $CDCl_3$

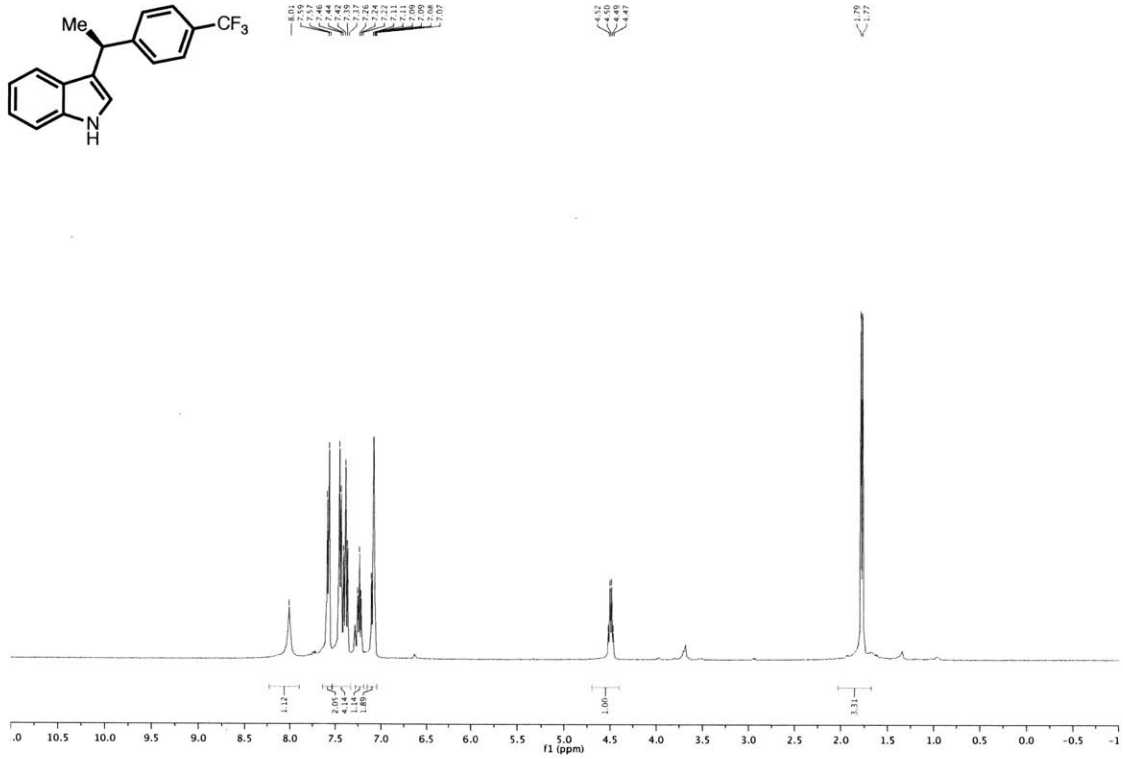

^{13}C NMR, 101 MHz, $CDCl_3$

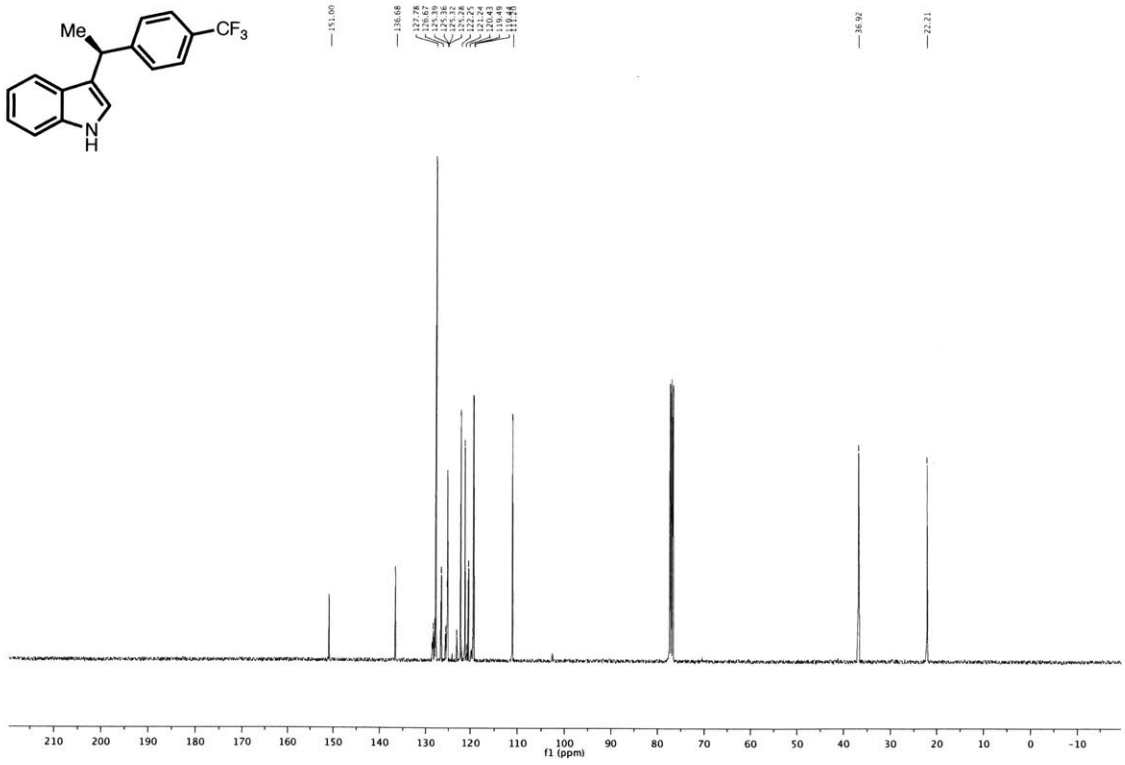

^{19}F NMR, 376 MHz, $CDCl_3$

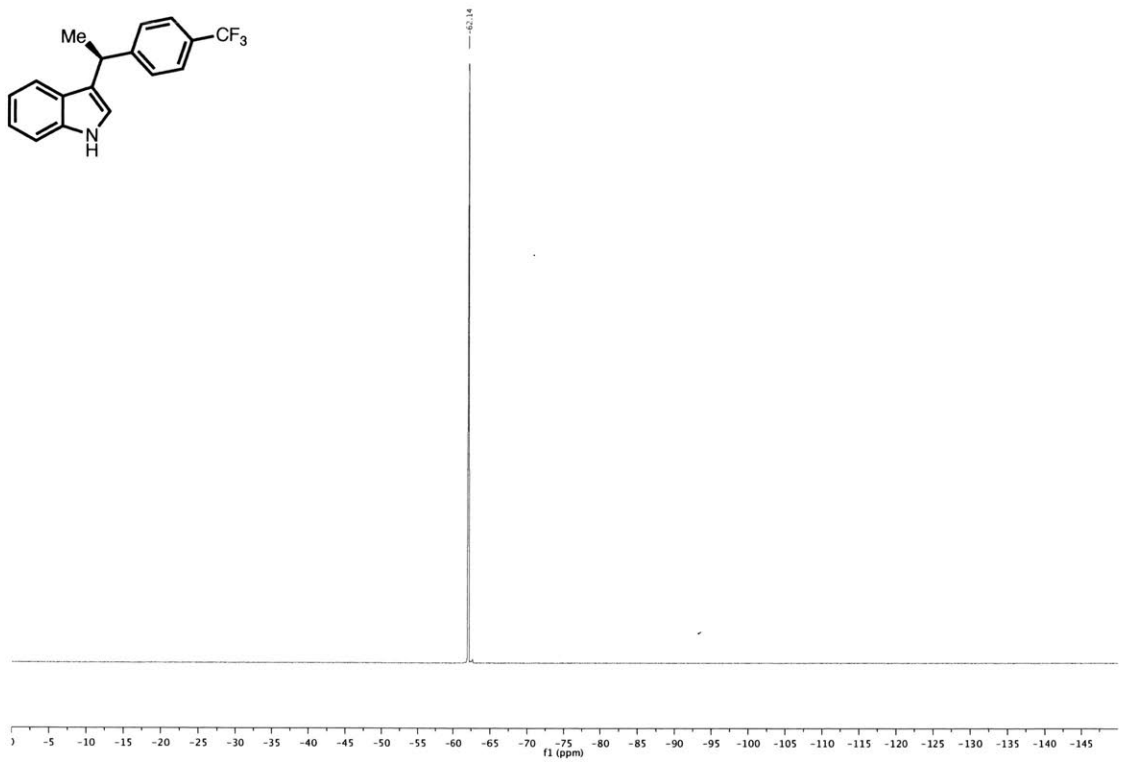

(*S*)-5-(1-(1*H*-indol-3-yl)ethyl)-1-tosyl-1*H*-indole (4c)

^{1}H NMR, 400 MHz, $CDCl_3$

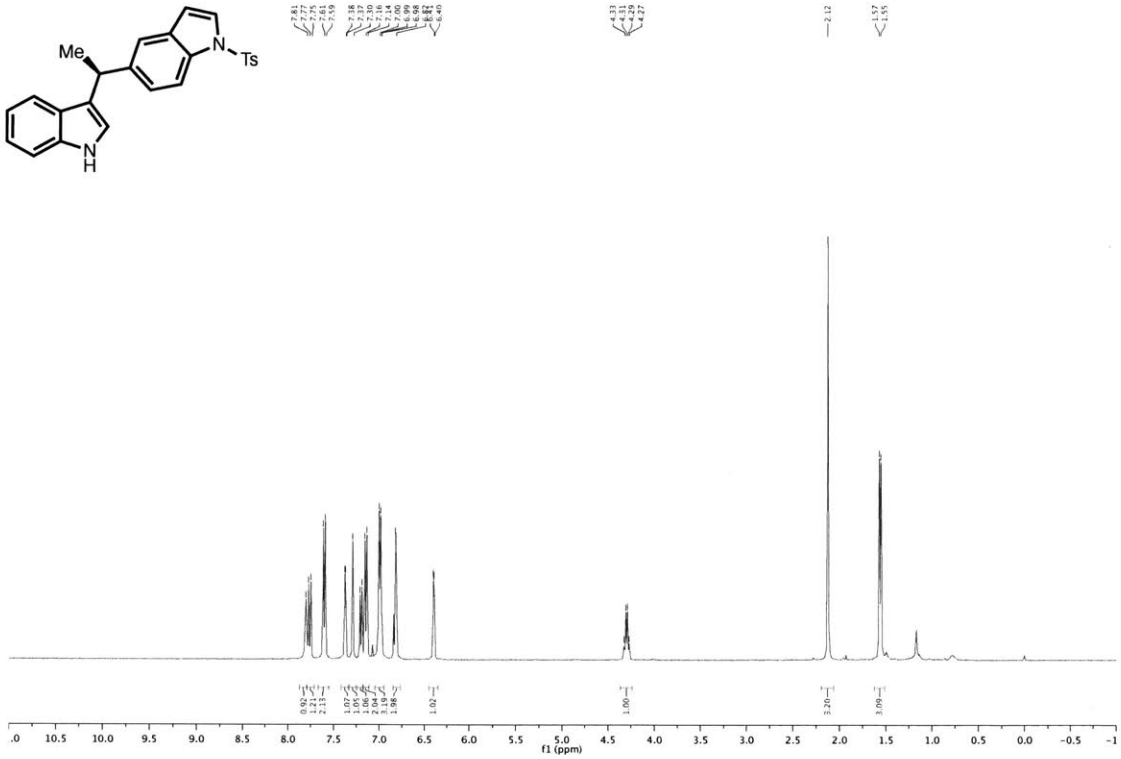

^{13}C NMR, 101 MHz, $CDCl_3$

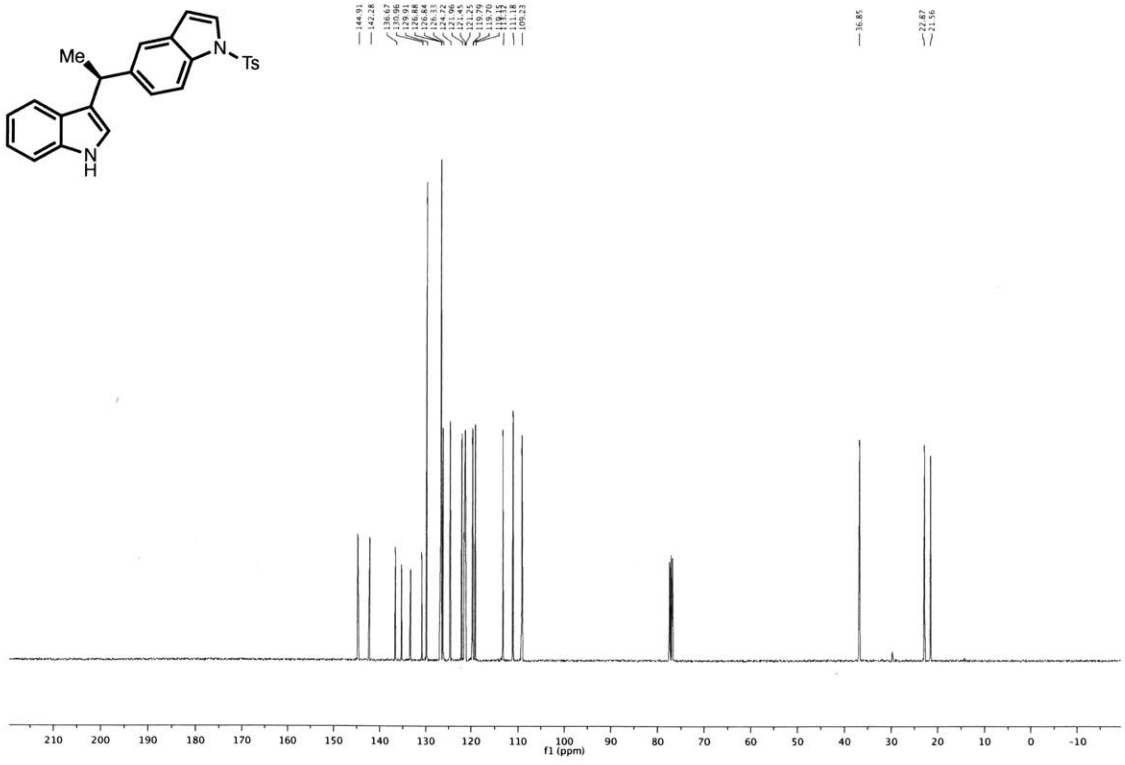

(*S*)-3-(1*H*-indol-3-yl)-*N*-(4-methoxybenzyl)-*N*-methyl-3-phenylpropan-1-amine (4d)

^{1}H NMR, 400 MHz, $CDCl_3$

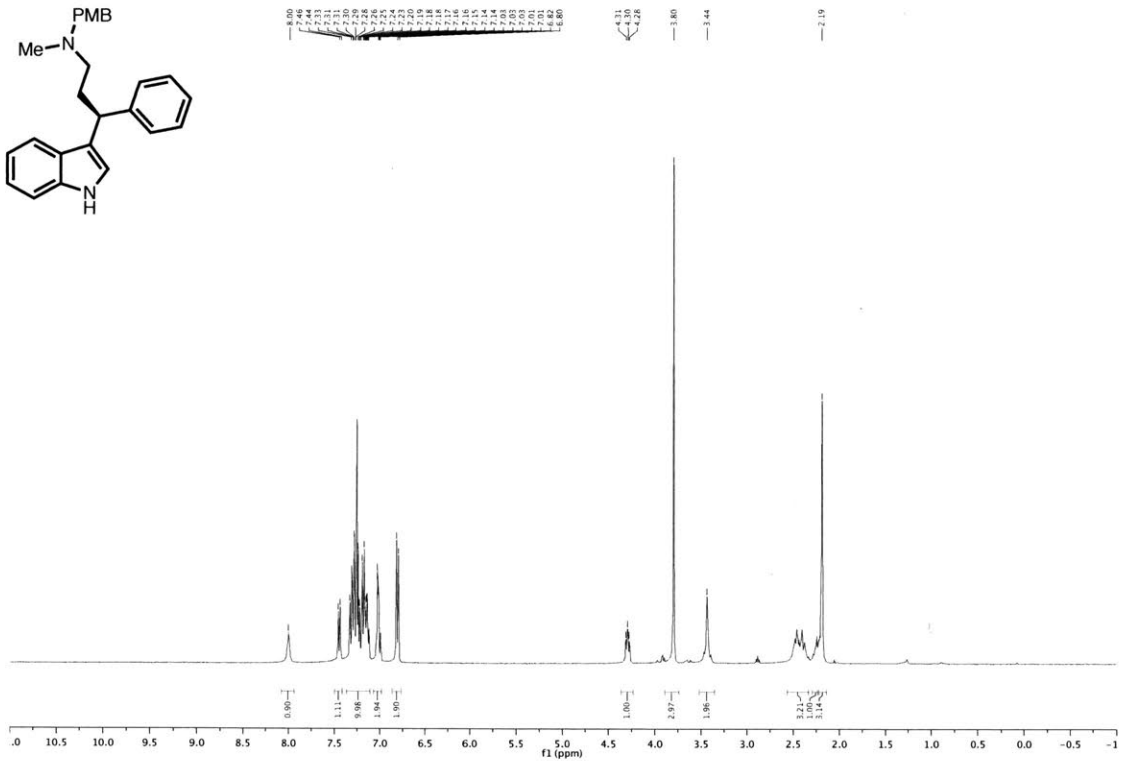

^{13}C NMR, 101 MHz, $CDCl_3$

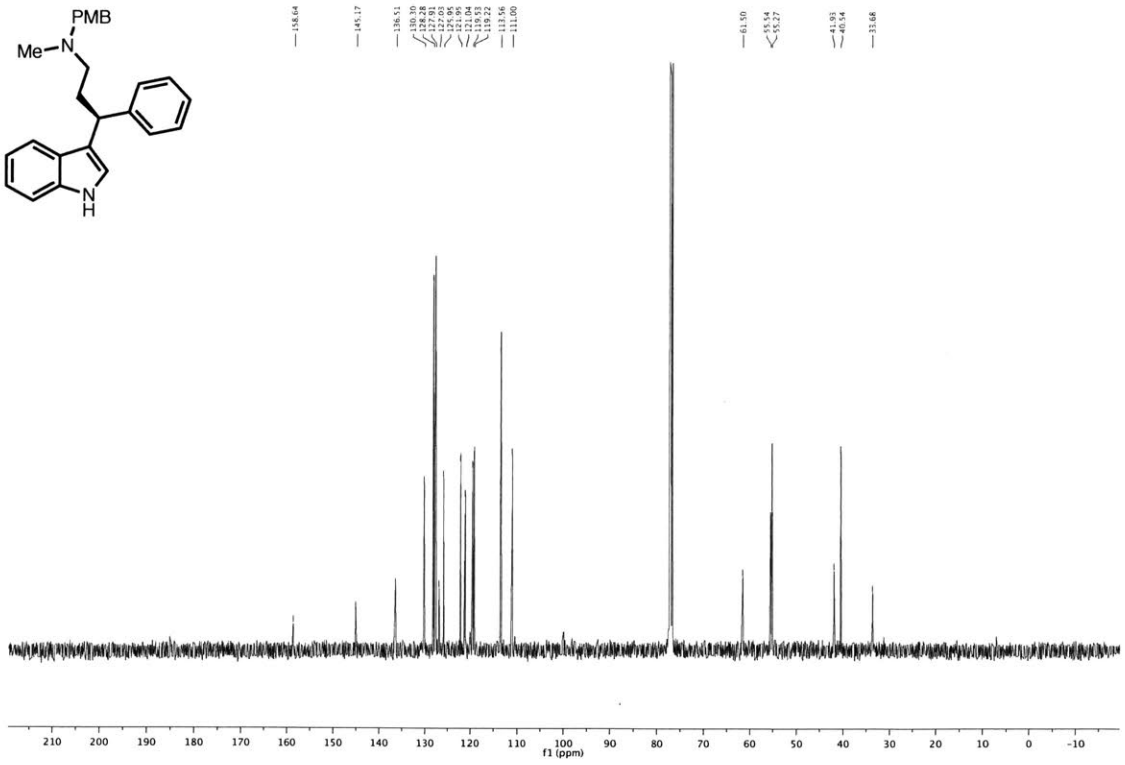

3-((*S*)-1-((8*R*,9*S*,13*S*,14*S*)-13-methyl-6,7,8,9,11,12,13,14,15,16-decahydrospiro[cyclopenta[*a*]phenanthrene-17,2'-[1,3]dioxolan]-2-yl)ethyl)-1*H*-indole (4e)

^{1}H NMR, 400 MHz, $CDCl_3$

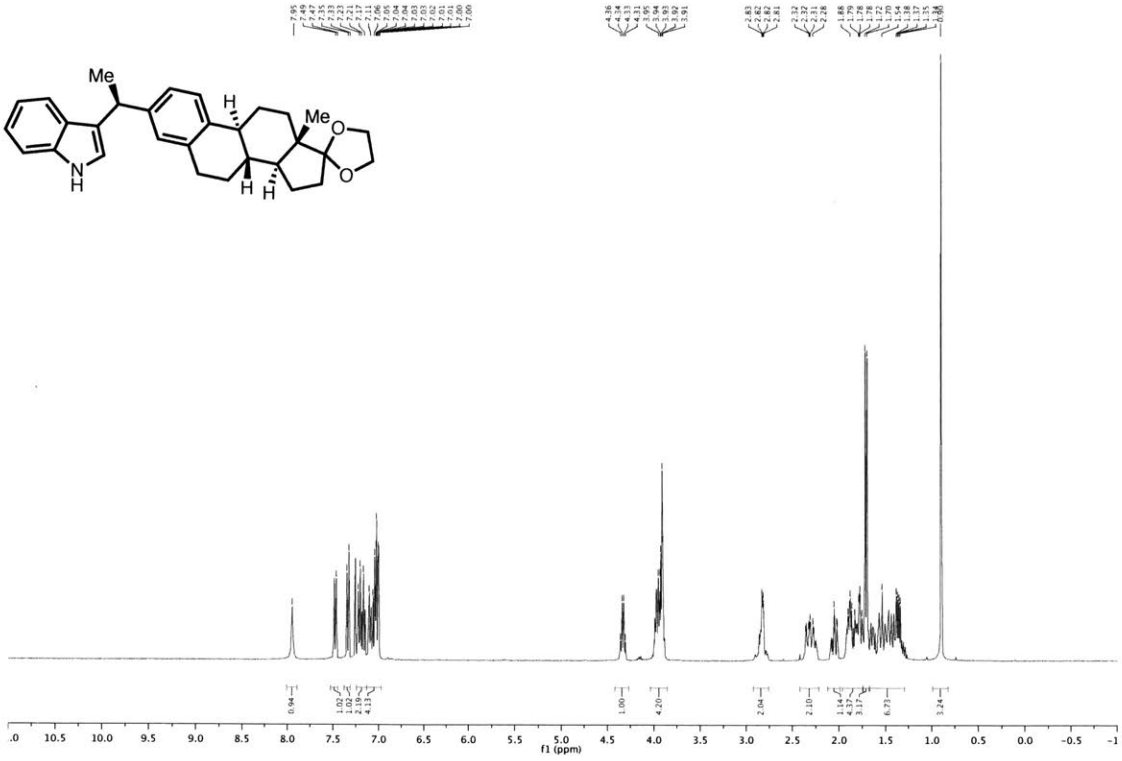

^{13}C NMR, 101 MHz, $CDCl_3$

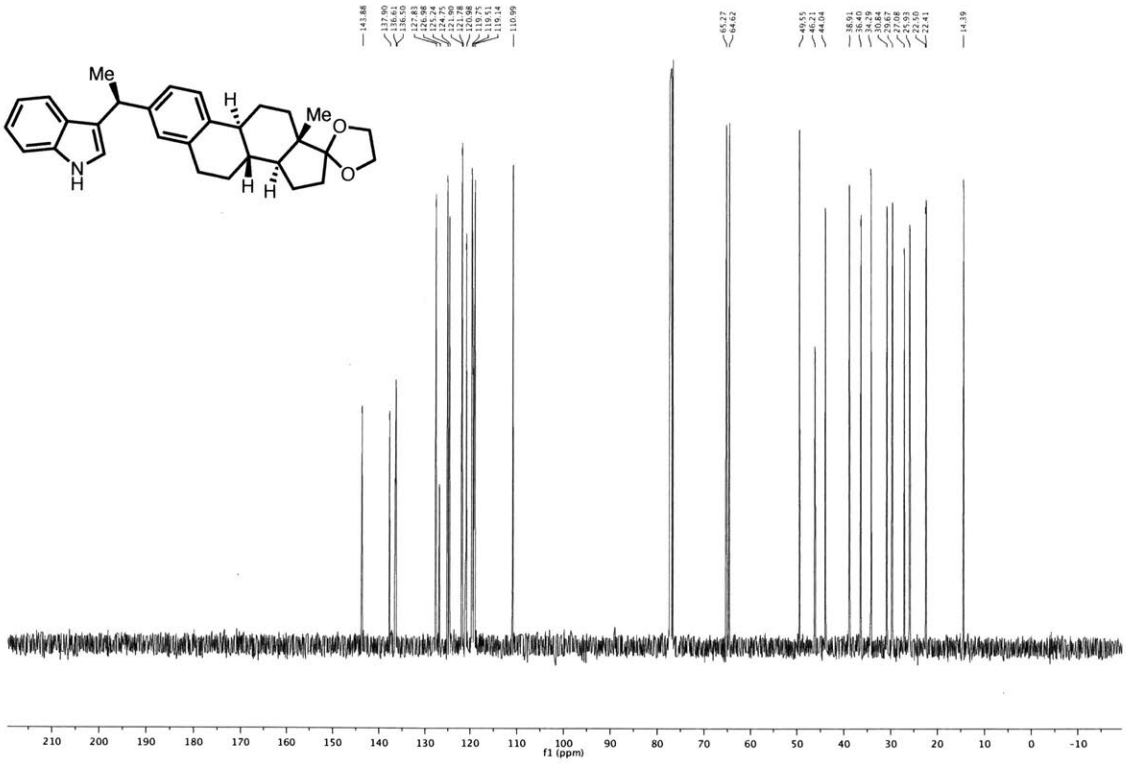

Ethyl (*S*)-4-(8-(1-(1*H*-indol-3-yl)ethyl)-5,6-dihydro-11*H*-benzo[5,6]cyclohepta[1,2-*b*]pyridin-11-ylidene)piperidine-1-carboxylate (4f)

^{1}H NMR, 400 MHz, $CDCl_3$

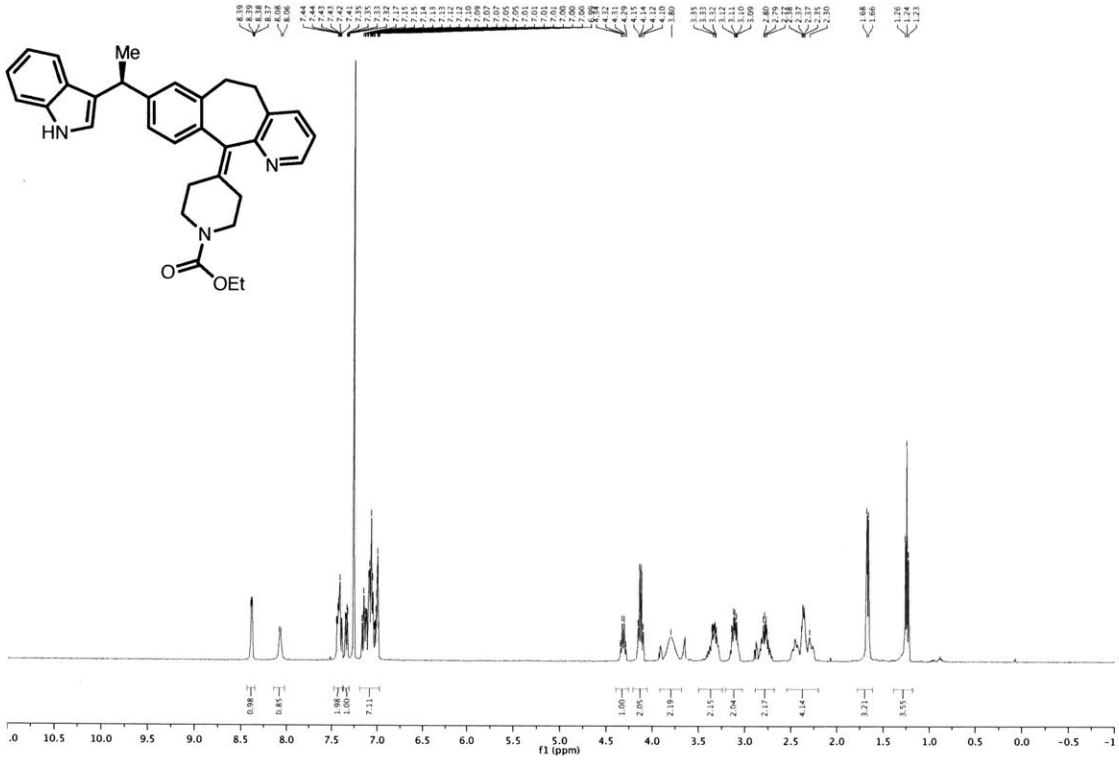

^{13}C NMR, 101 MHz, $CDCl_3$

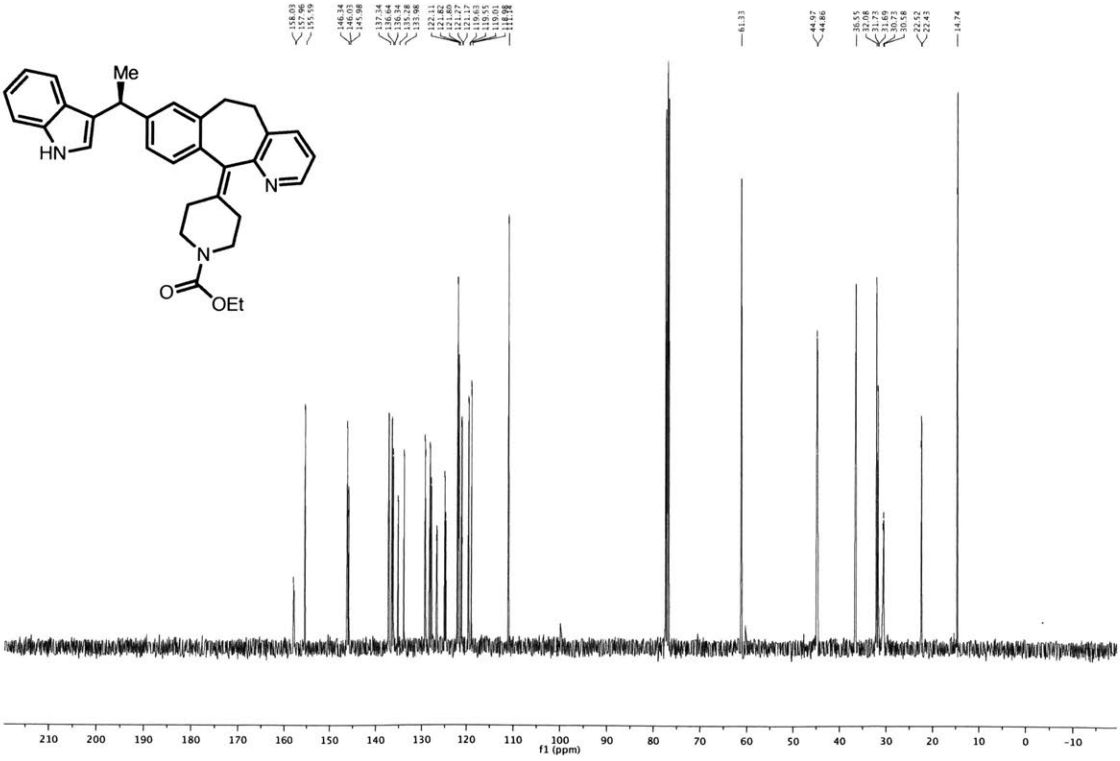

3-(3-(2-fluoro-4-methoxyphenyl)propyl)-1*H*-indole (4g)

^{1}H NMR, 400 MHz, $CDCl_3$

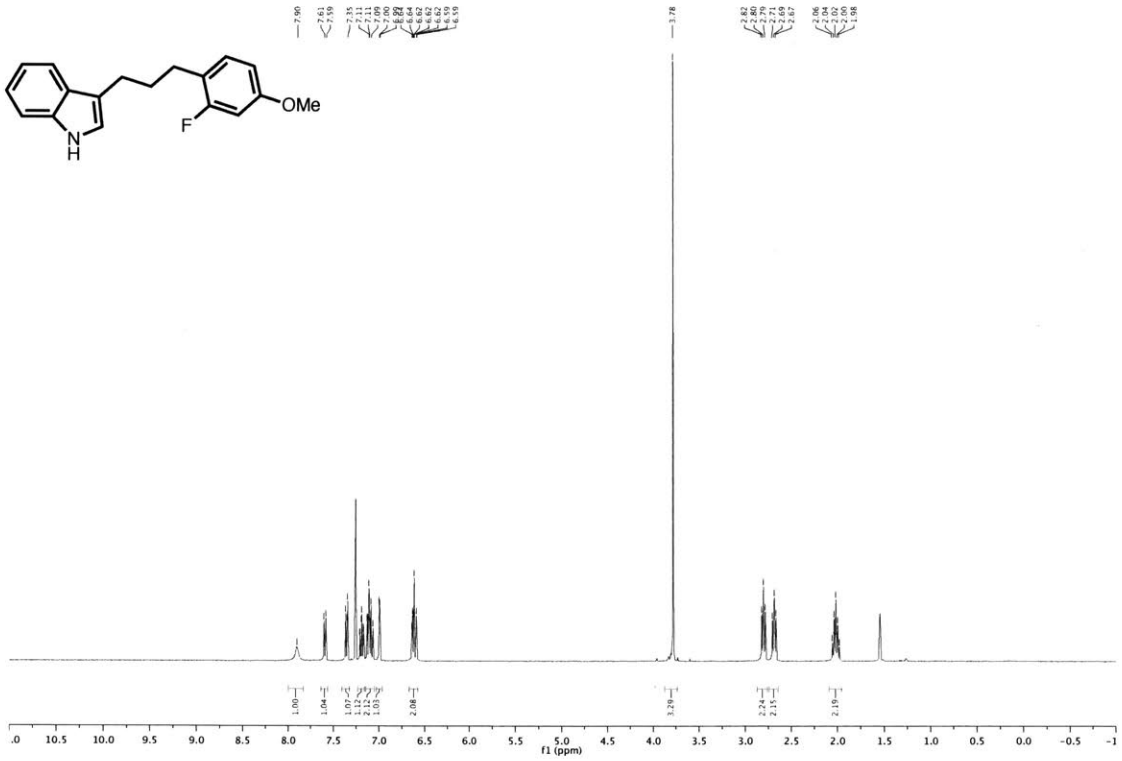

^{13}C NMR, 101 MHz, $CDCl_3$

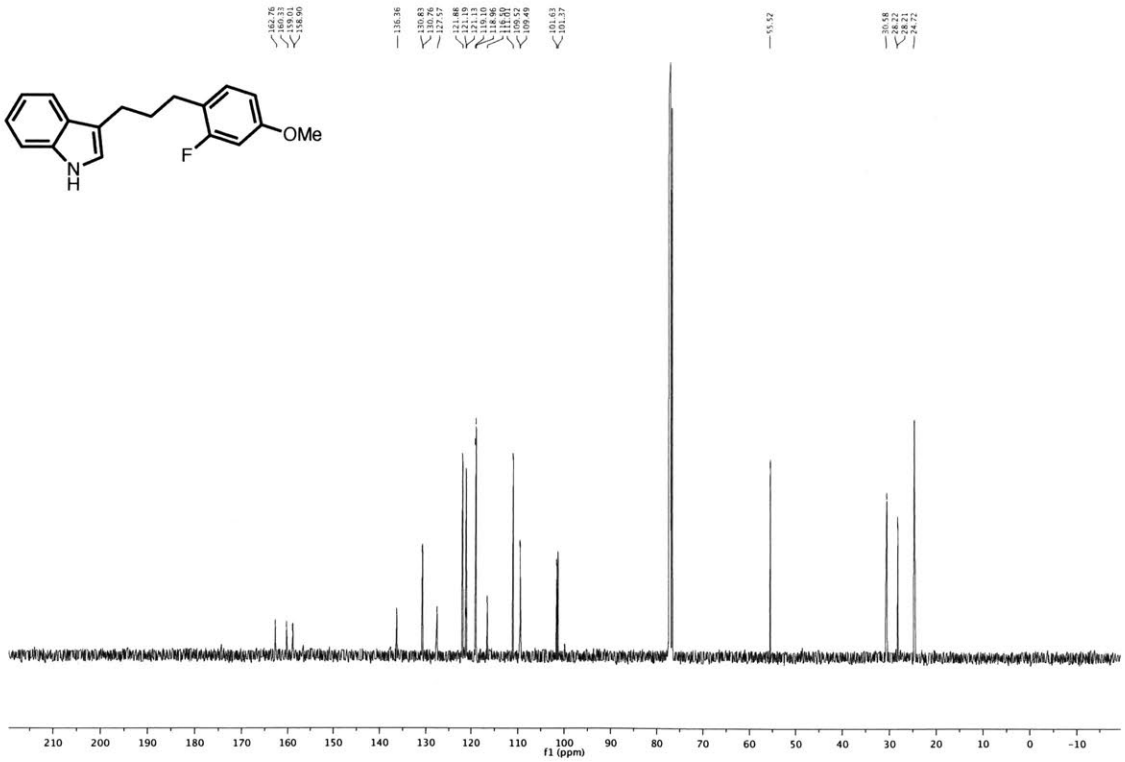

^{19}F NMR, 376 MHz, $CDCl_3$

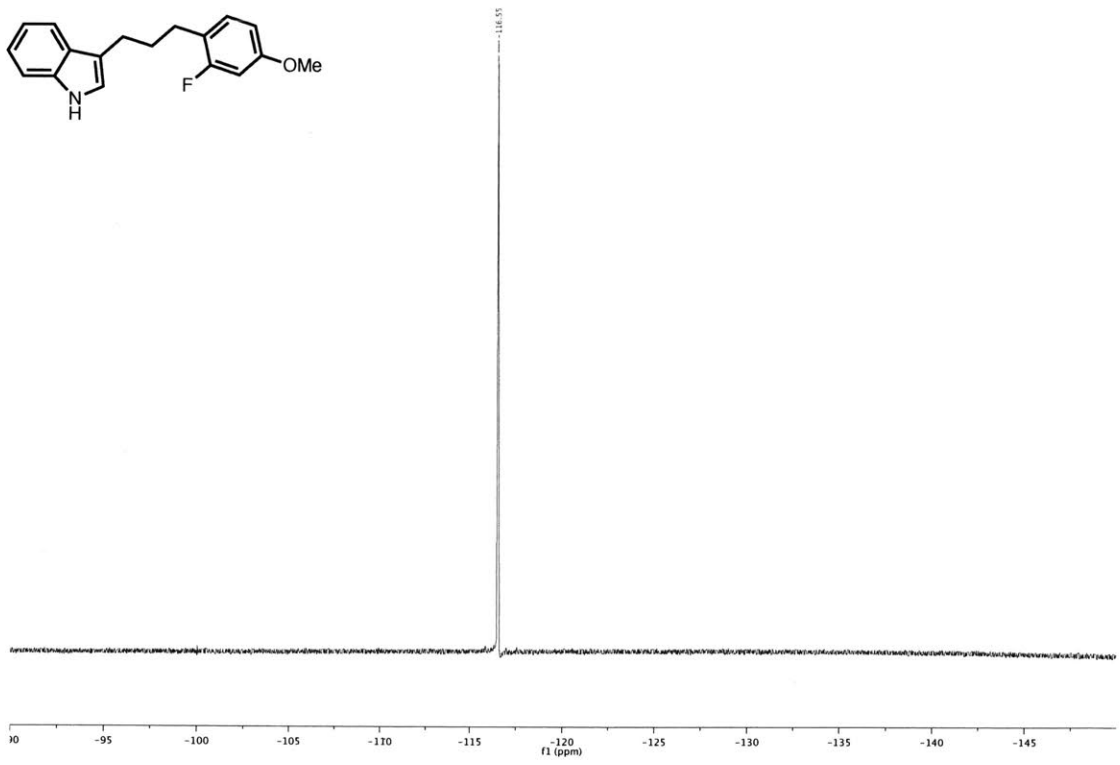

1*H*-indol-1-yl benzoate (2a)

^{1}H NMR, 400 MHz, $CDCl_3$

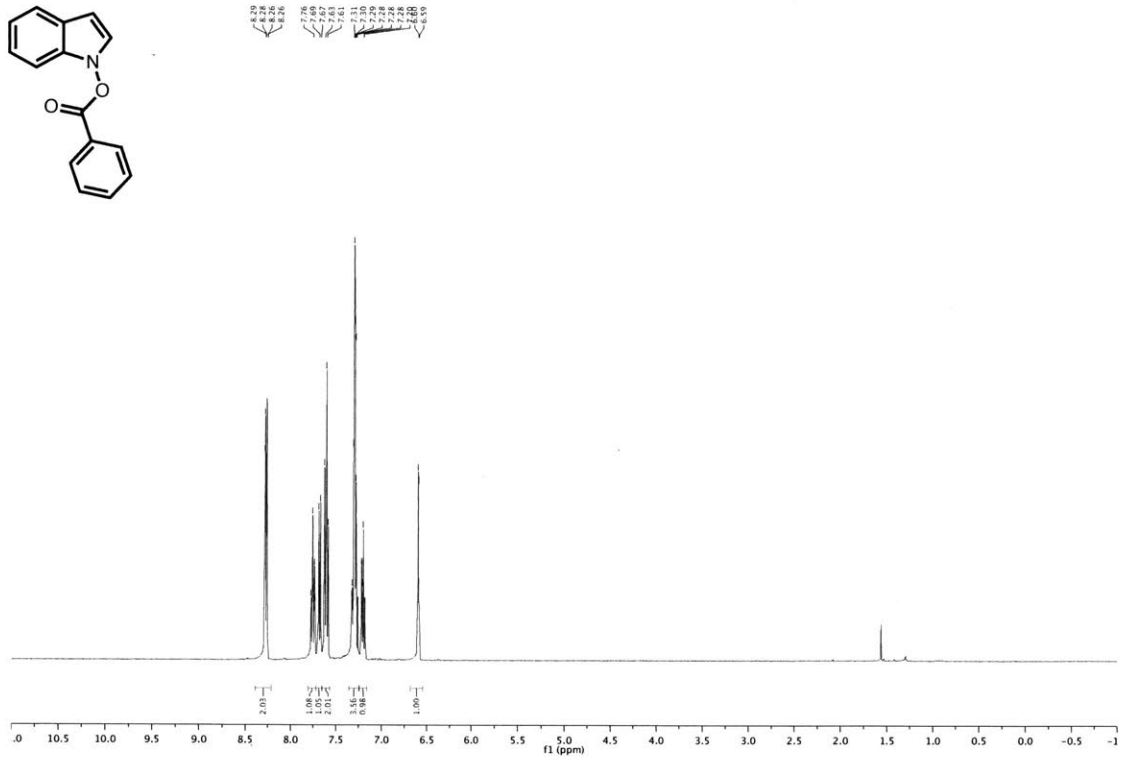

^{13}C NMR, 101 MHz, $CDCl_3$

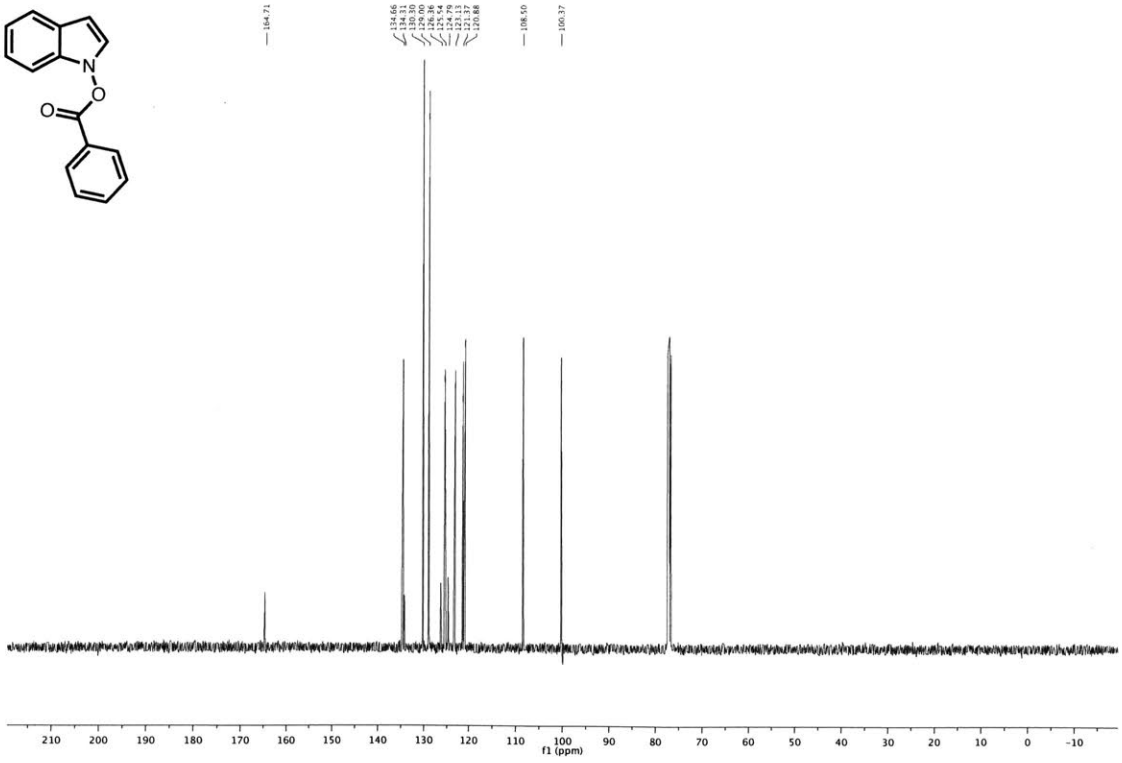

1*H*-indol-1-yl 4-(dimethylamino)benzoate (2b)

^{1}H NMR, 400 MHz, $CDCl_3$

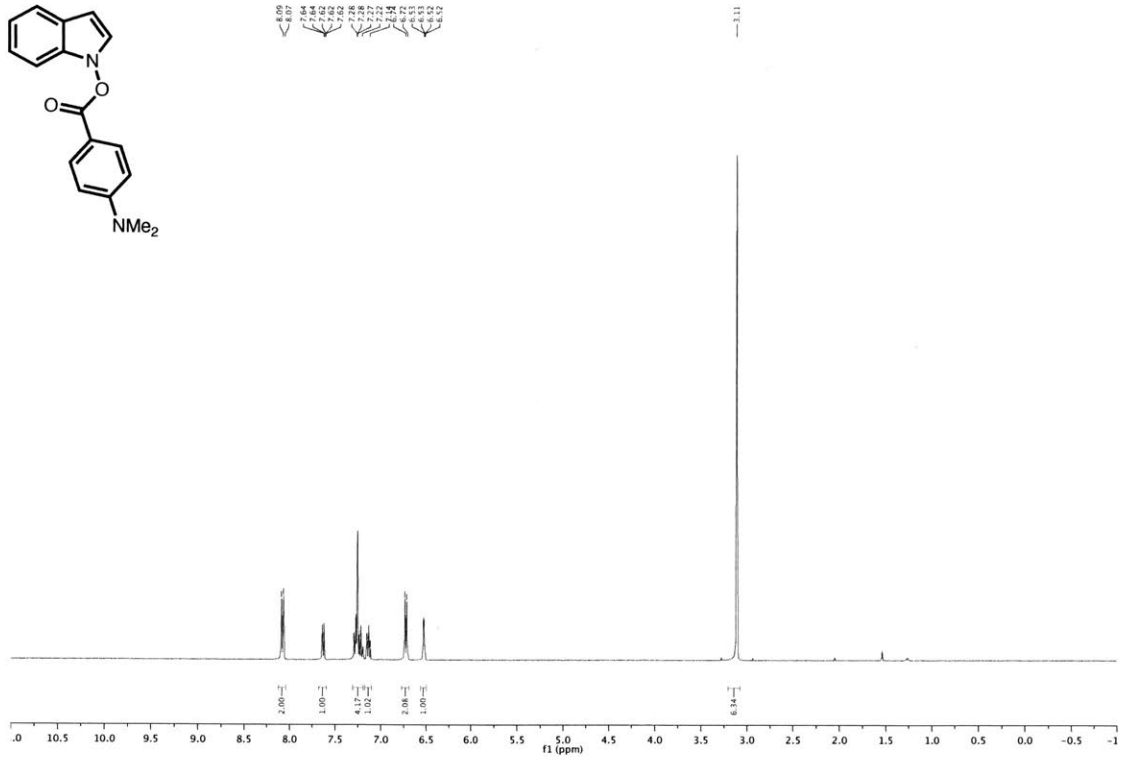

^{13}C NMR, 101 MHz, $CDCl_3$

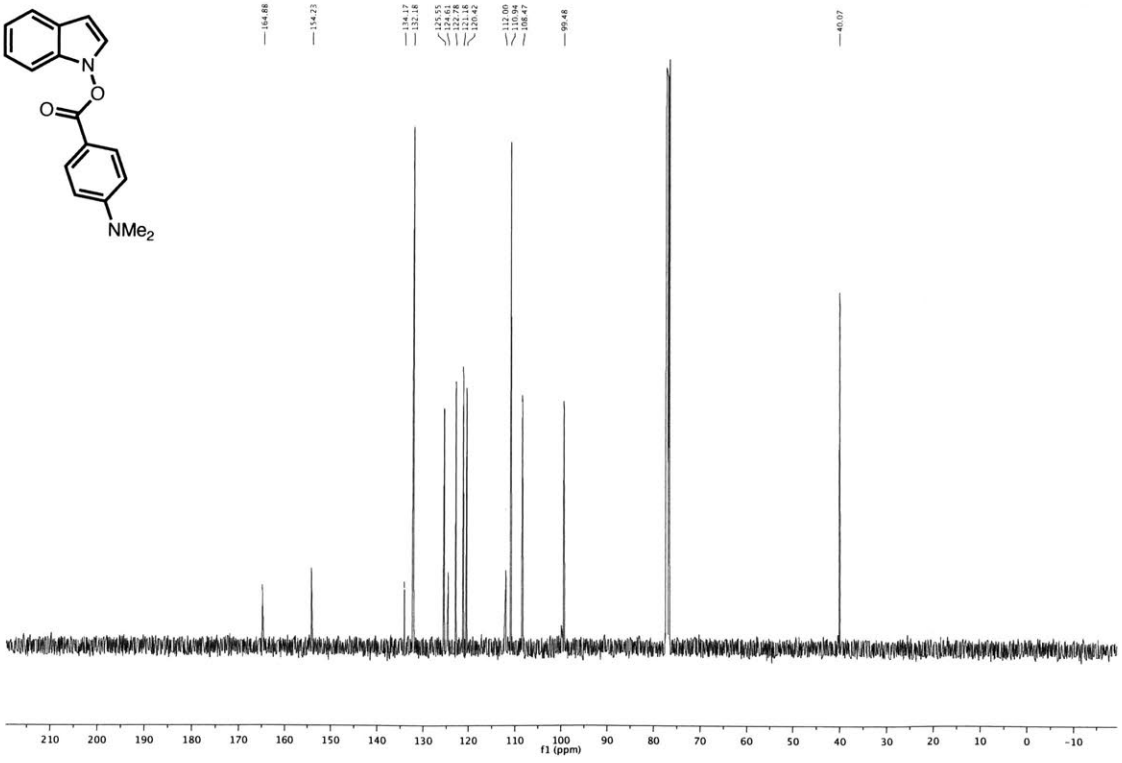

1*H*-indol-1-yl 4-(trifluoromethyl)benzoate (2c)

^{1}H NMR, 400 MHz, $CDCl_3$

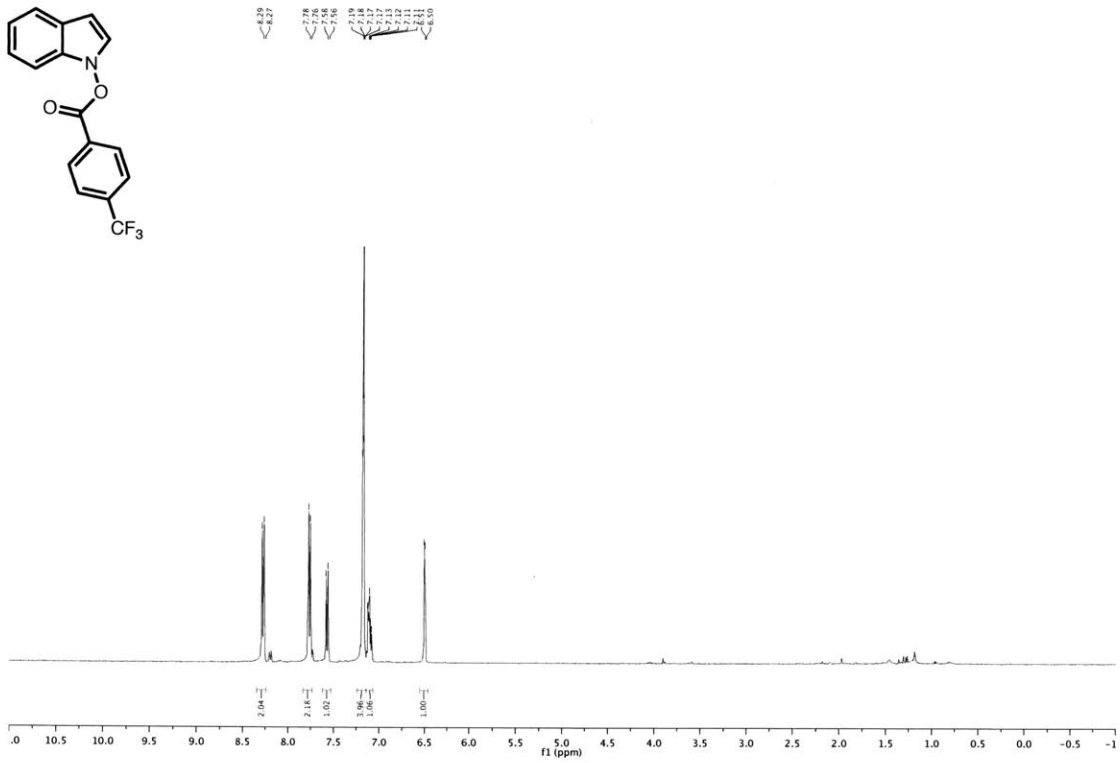

^{13}C NMR, 101 MHz, $CDCl_3$

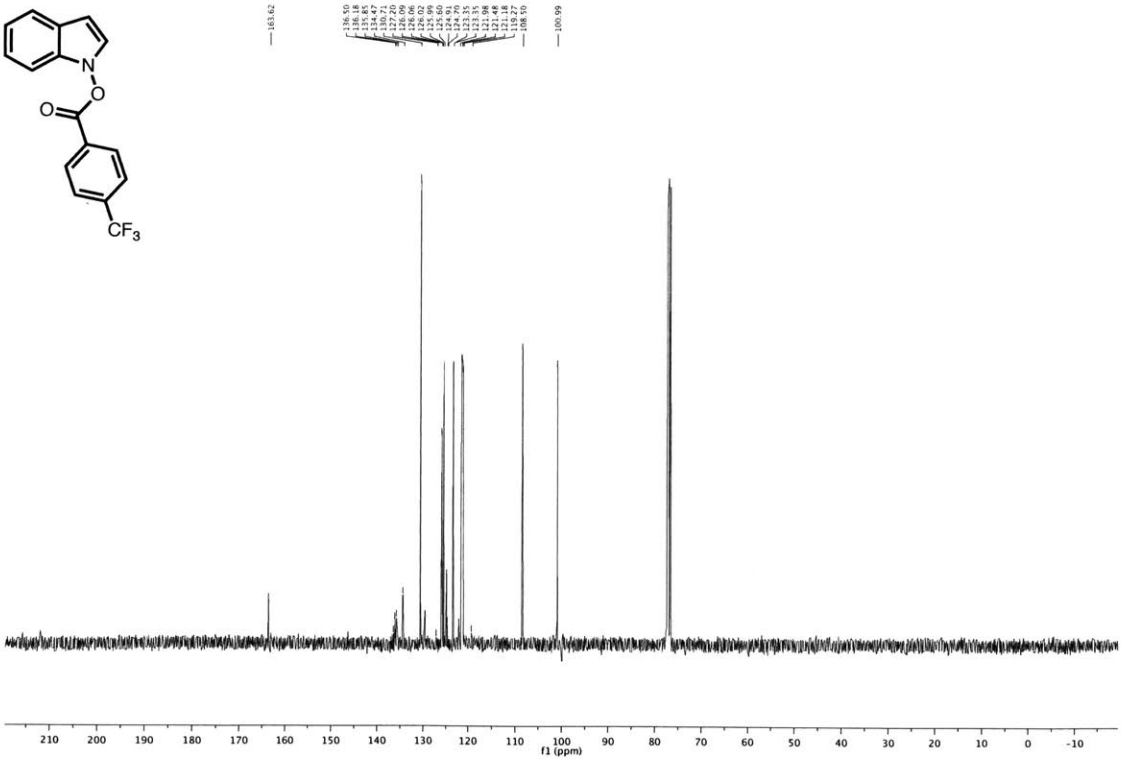

^{19}F NMR, 376 MHz, $CDCl_3$

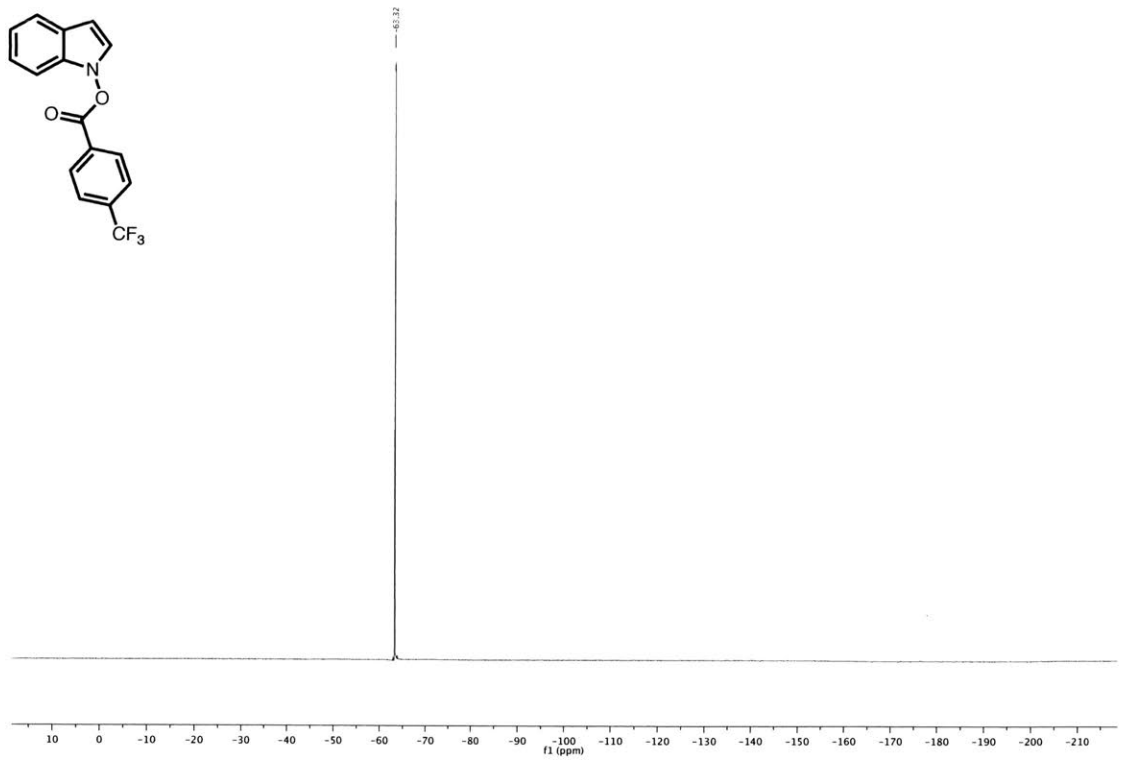

1*H*-indol-1-yl 2,4,6-trimethylbenzoate (2d)

^{1}H NMR, 400 MHz, $CDCl_3$

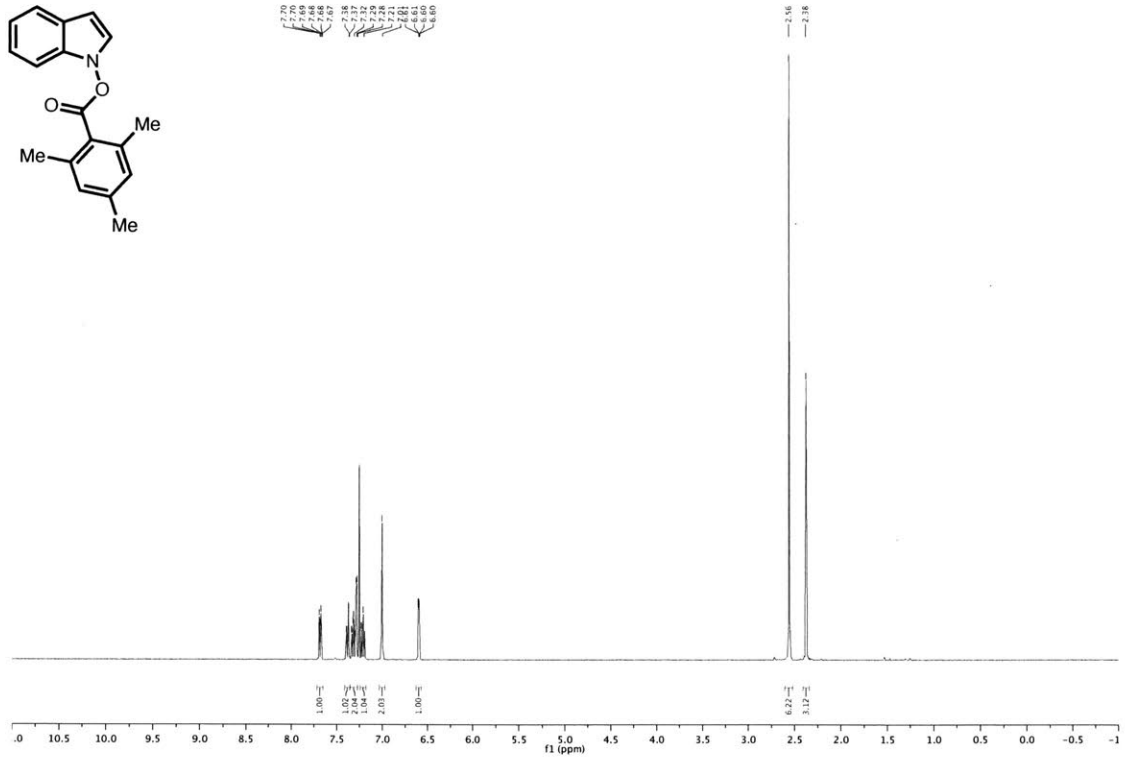

^{13}C NMR, 101 MHz, $CDCl_3$

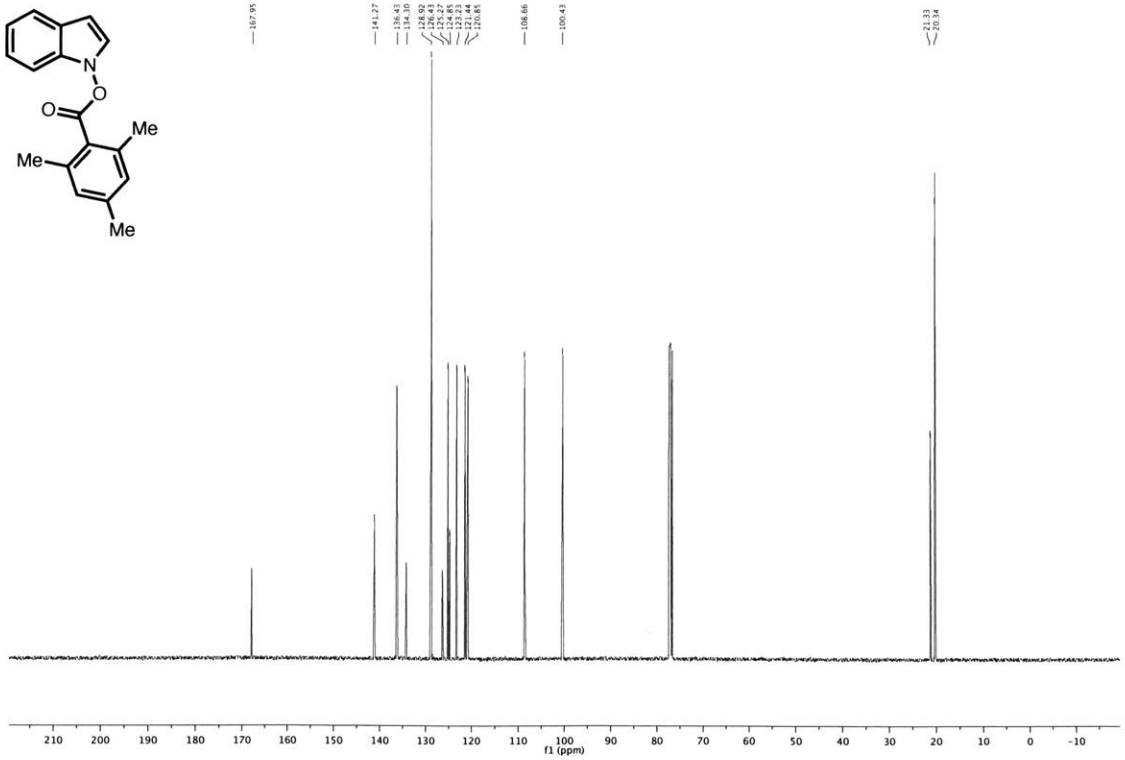

6-(trifluoromethyl)-1*H*-indol-1-yl 2,4,6-trimethylbenzoate (2e)

^{1}H NMR, 400 MHz, $CDCl_3$

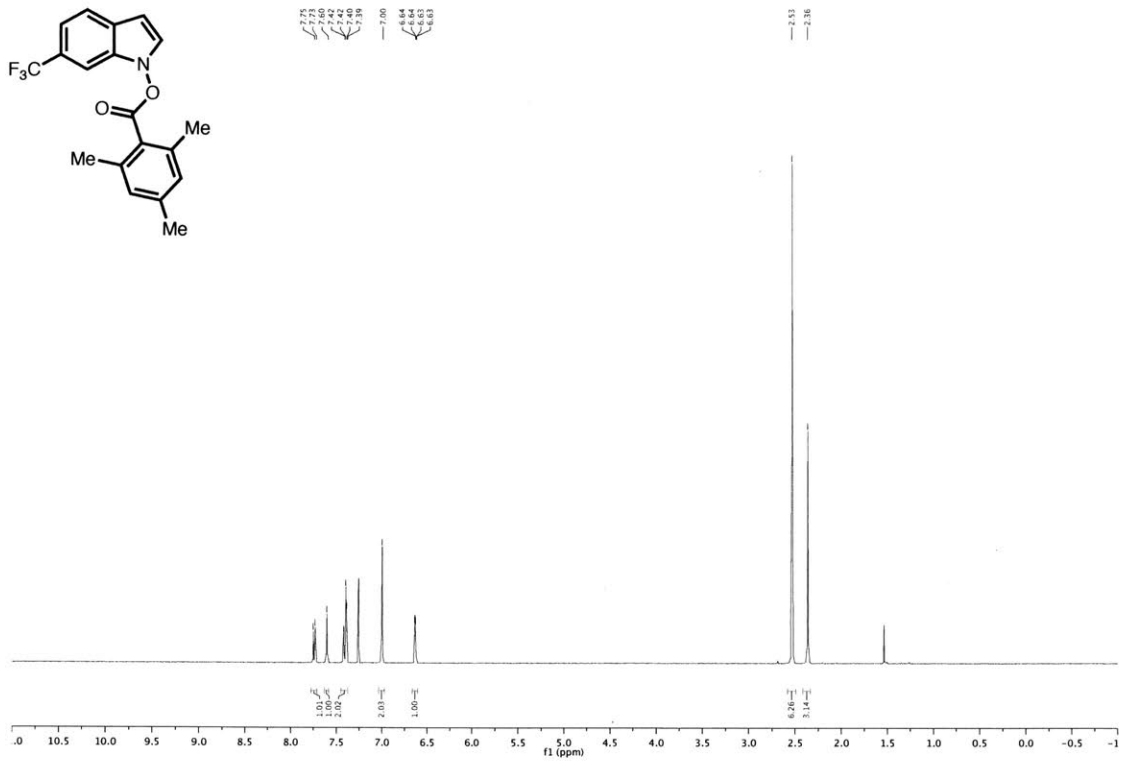

^{13}C NMR, 101 MHz, $CDCl_3$

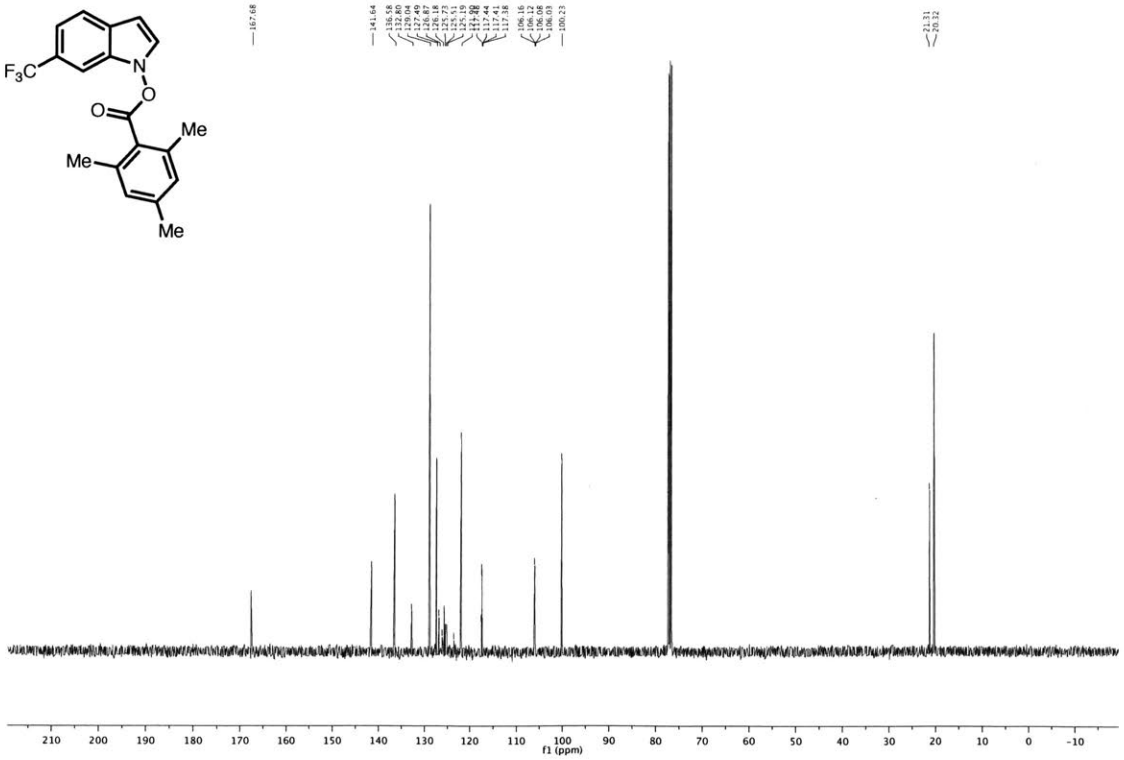

^{19}F NMR, 376 MHz, $CDCl_3$

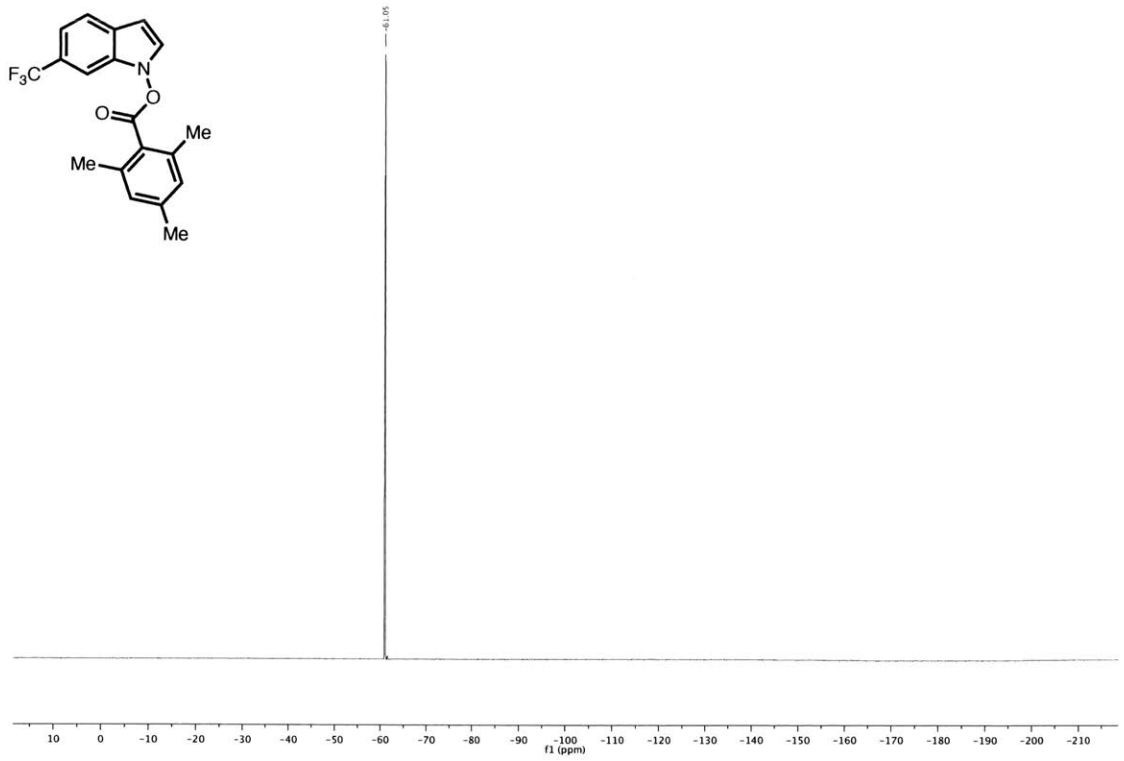

2-methyl-1*H*-indol-1-yl 2,4,6-trimethylbenzoate (2g)

^{1}H NMR, 400 MHz, $CDCl_3$

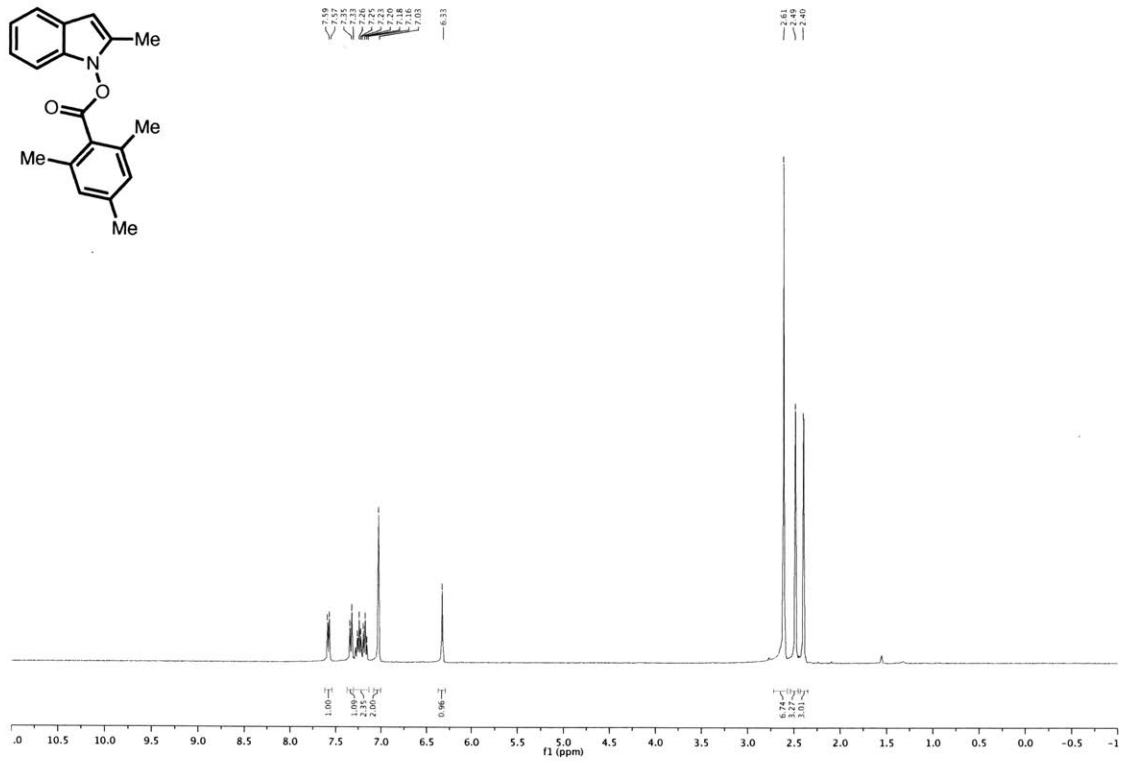

^{13}C NMR, 101 MHz, $CDCl_3$

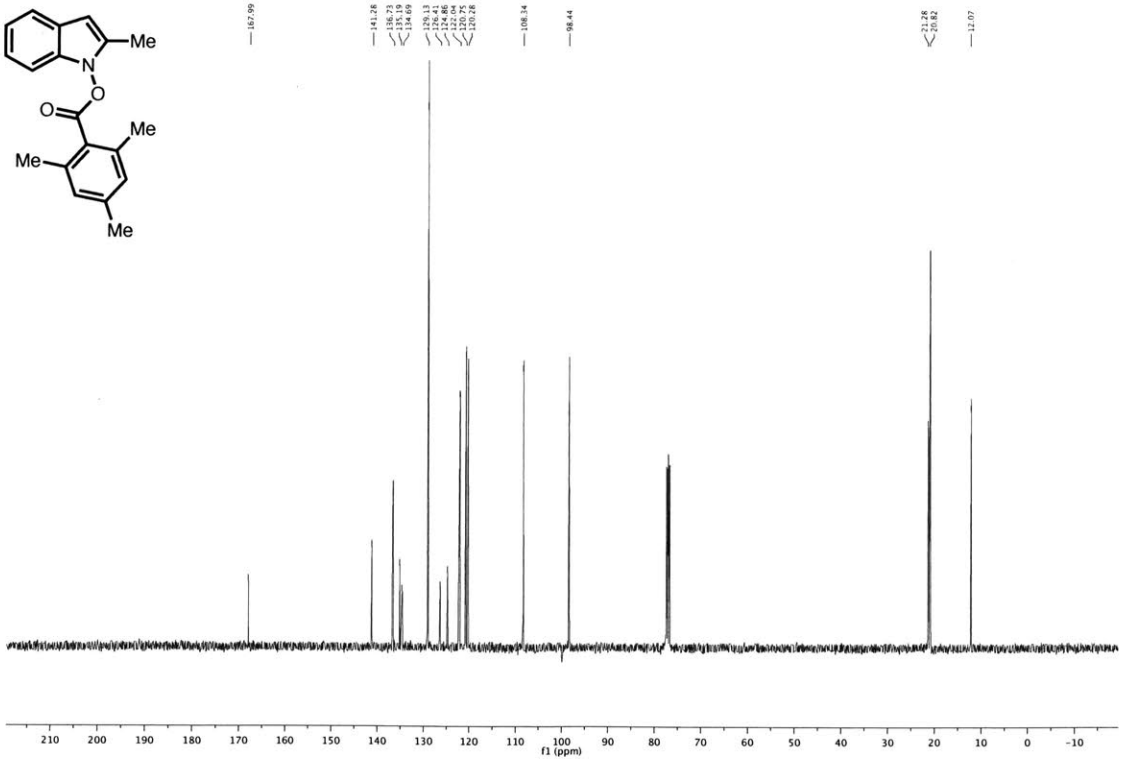

4-methyl-1*H*-indol-1-yl 2,4,6-trimethylbenzoate (2h)

^{1}H NMR, 400 MHz, $CDCl_3$

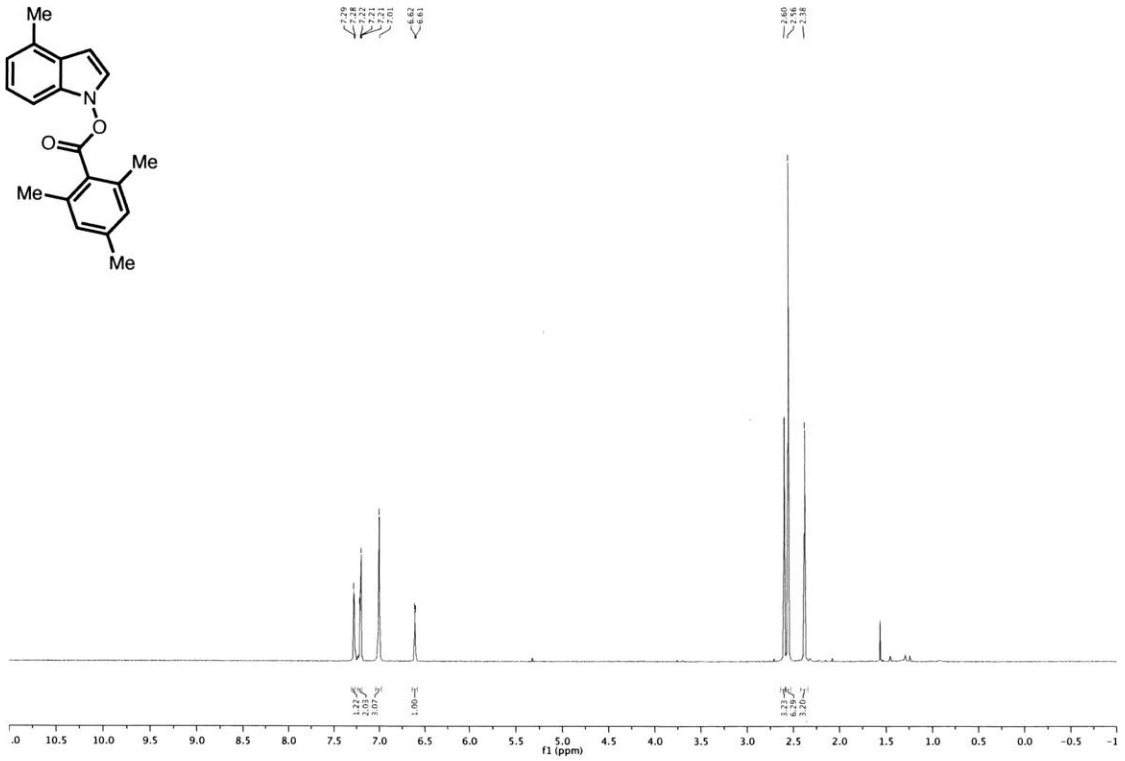

^{13}C NMR, 101 MHz, $CDCl_3$

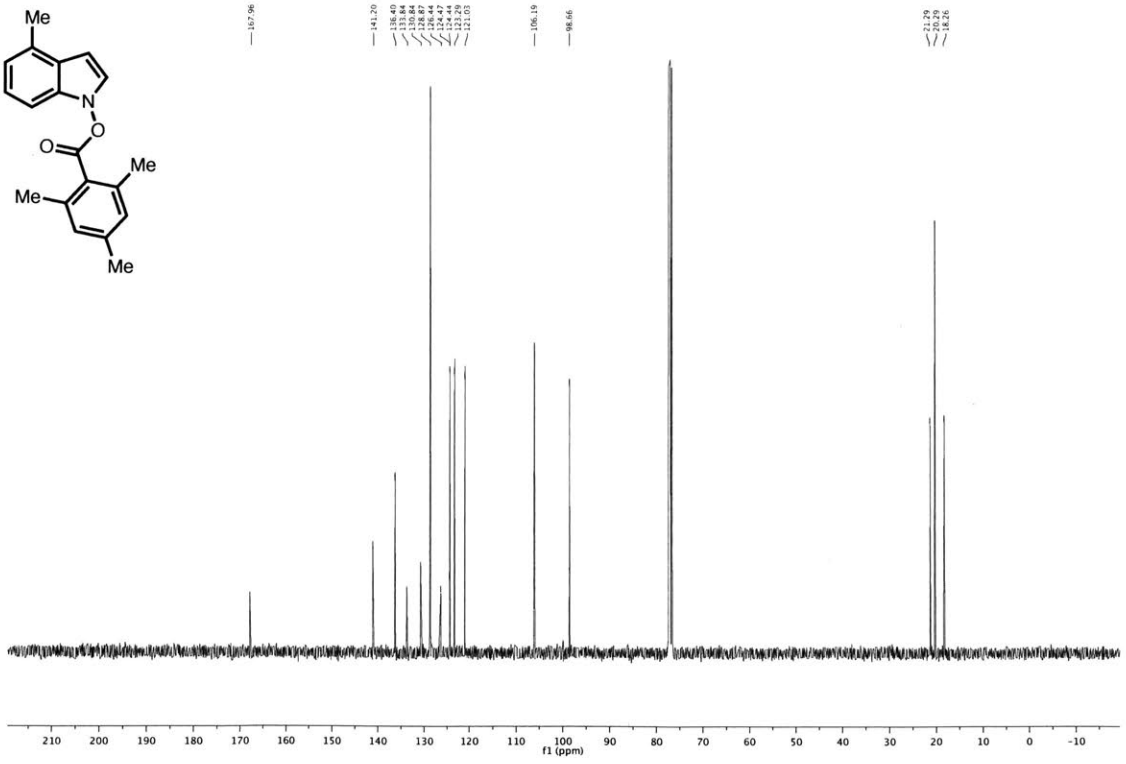

6-chloro-1*H*-indol-1-yl 2,4,6-trimethylbenzoate (2i)

^{1}H NMR, 400 MHz, $CDCl_3$

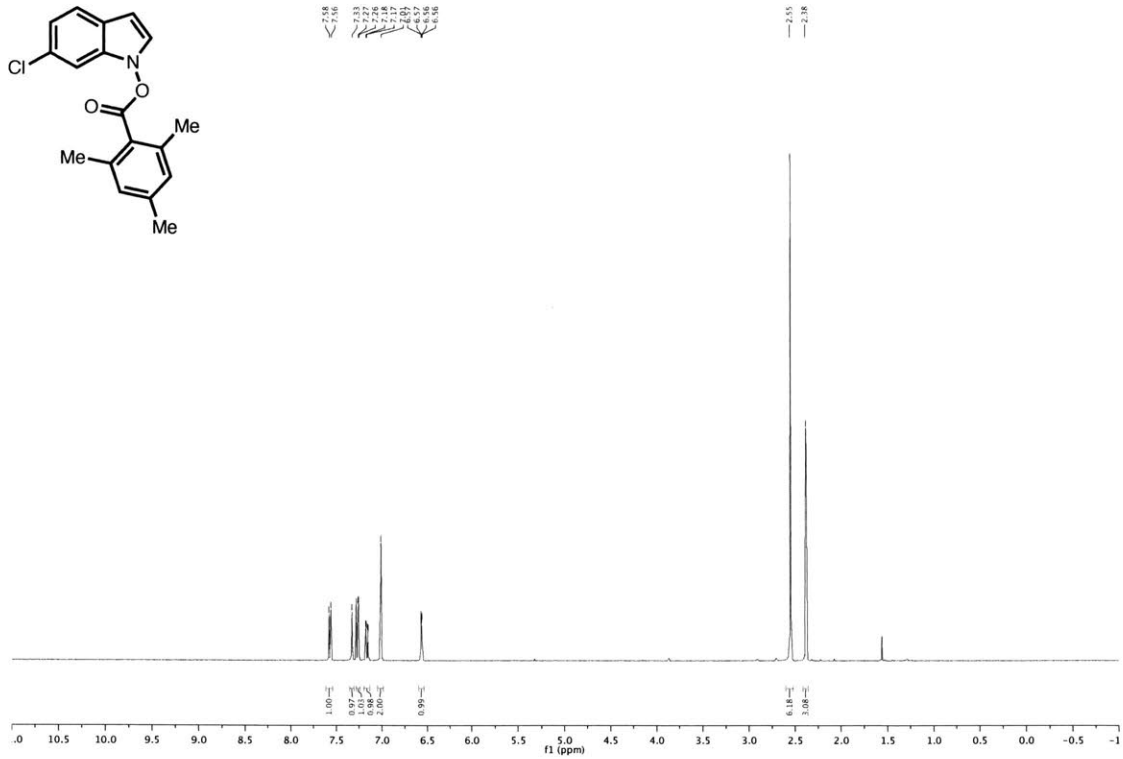

^{13}C NMR, 101 MHz, $CDCl_3$

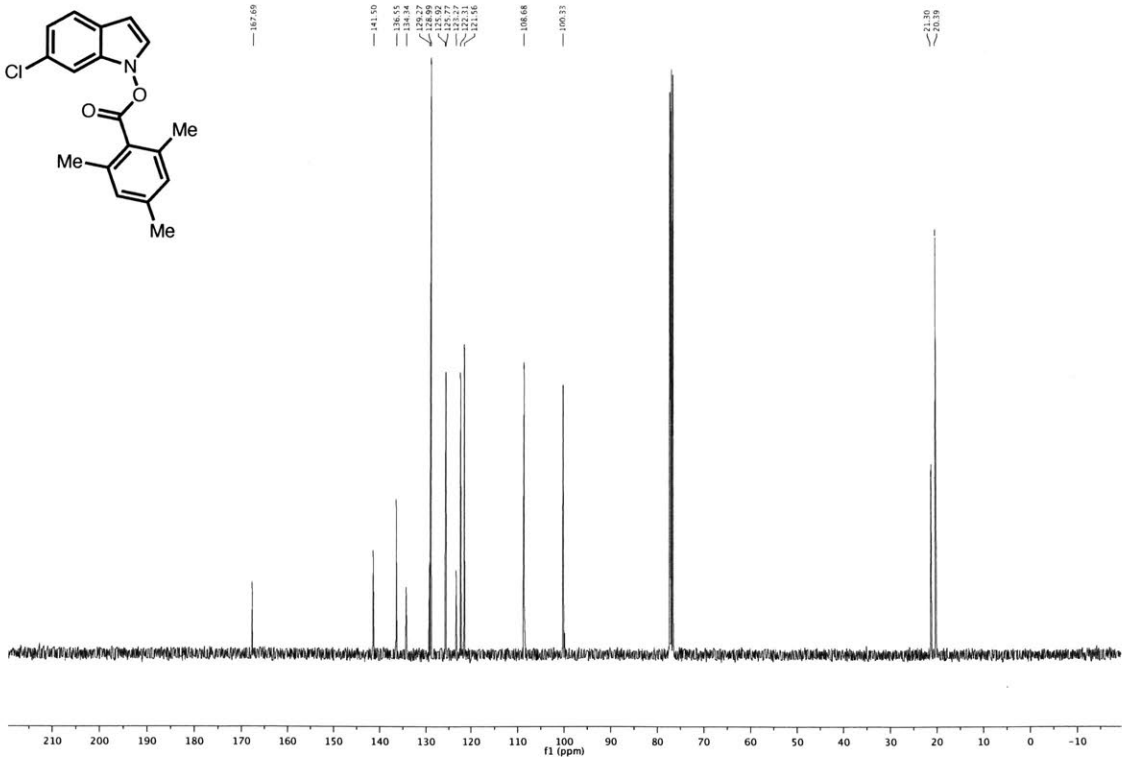

3-(2-methoxyethyl)-1*H*-indol-1-yl 2,4,6-trimethylbenzoate (2k)

^{1}H NMR, 400 MHz, $CDCl_3$

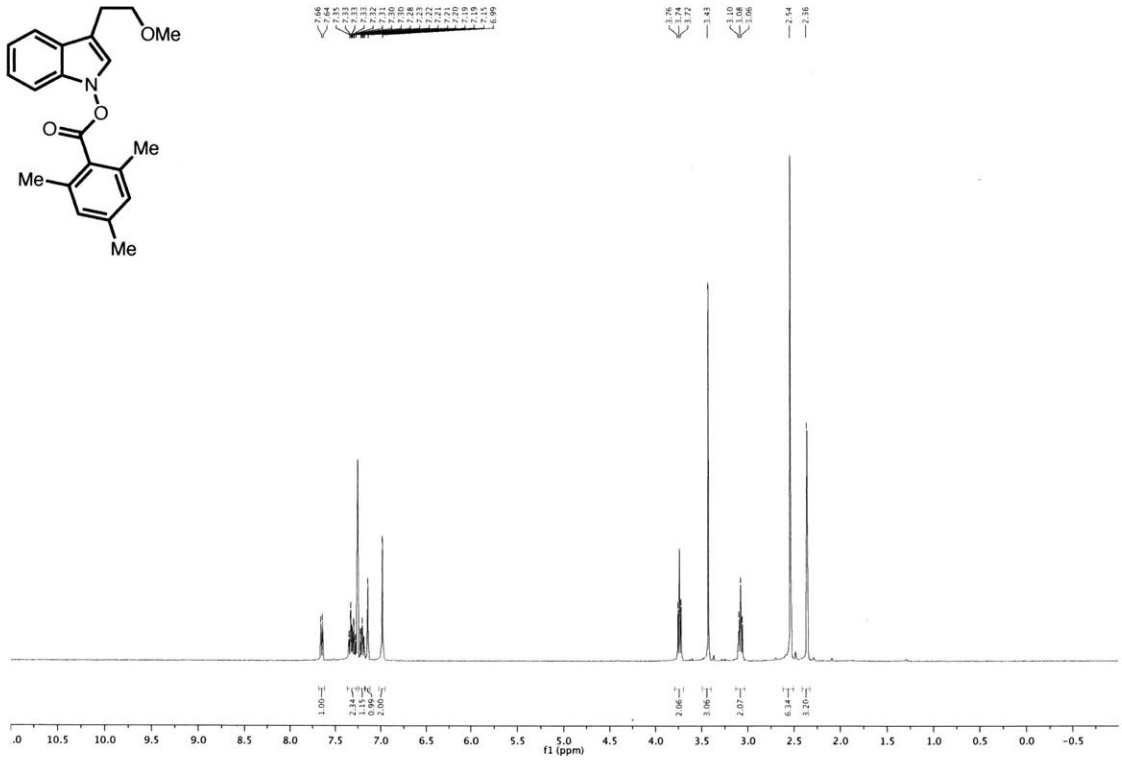

^{13}C NMR, 101 MHz, $CDCl_3$

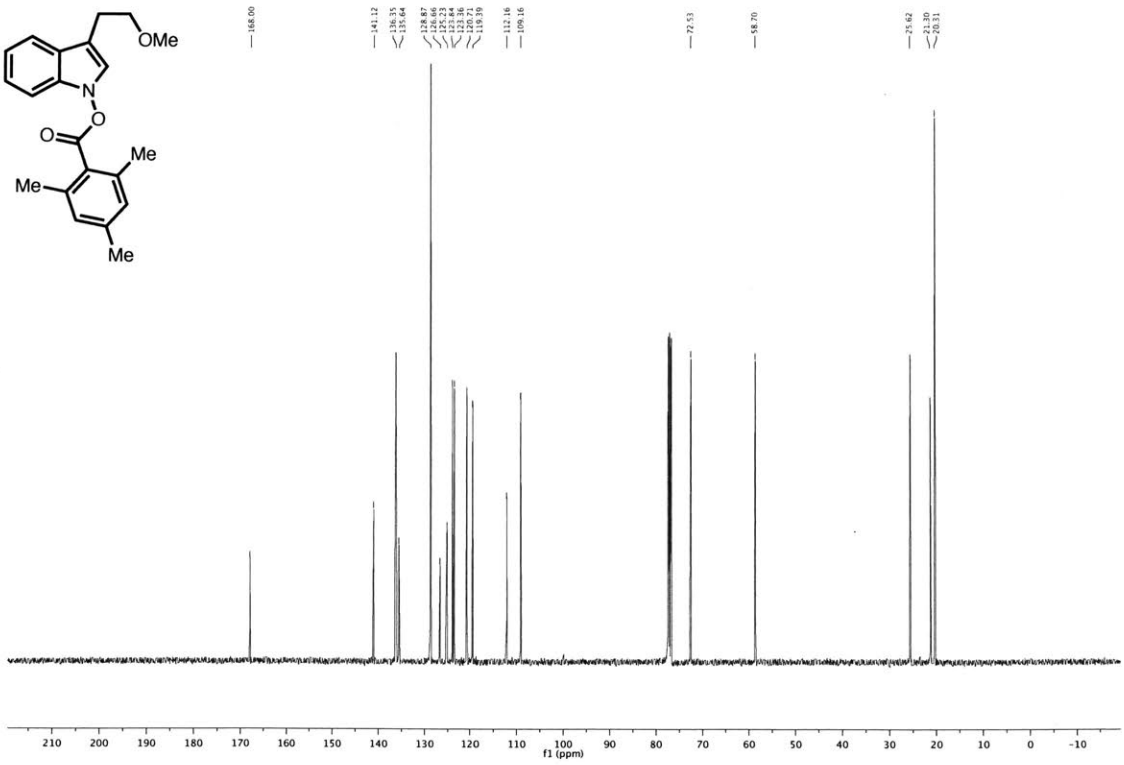

N-cinnamyl-*N*-methylpivalamide (1h)

^{1}H NMR, 400 MHz, $CDCl_3$

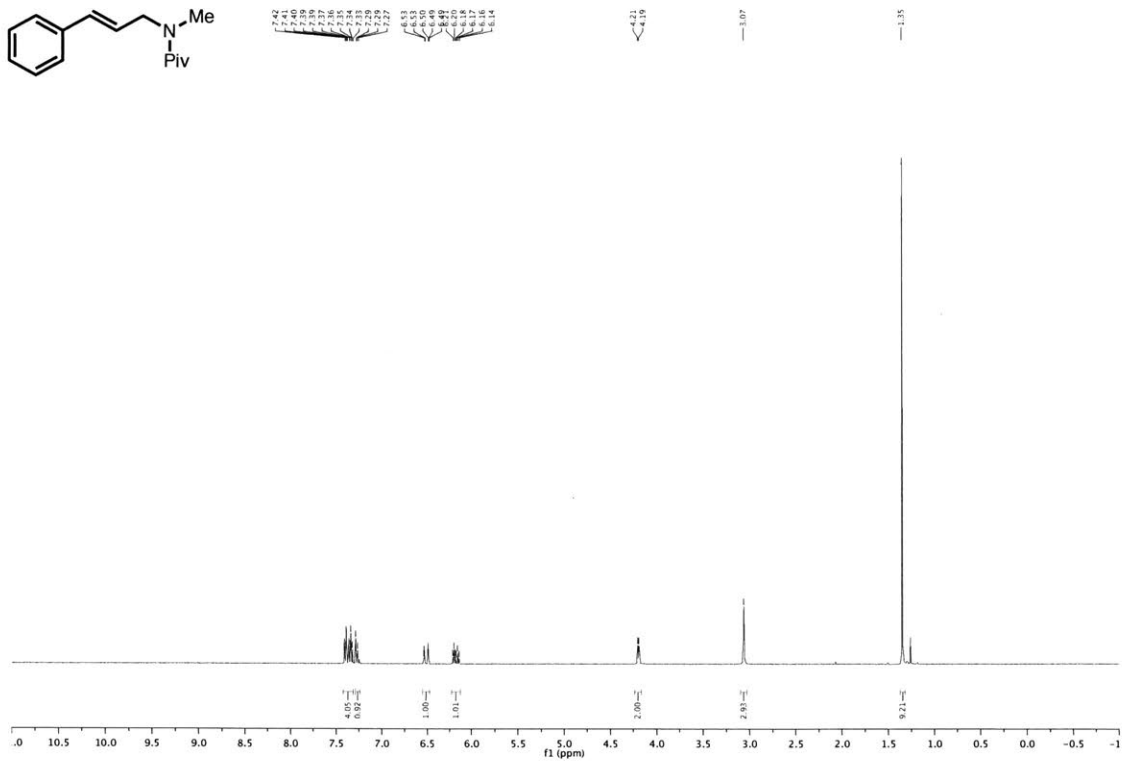

^{13}C NMR, 101 MHz, $CDCl_3$

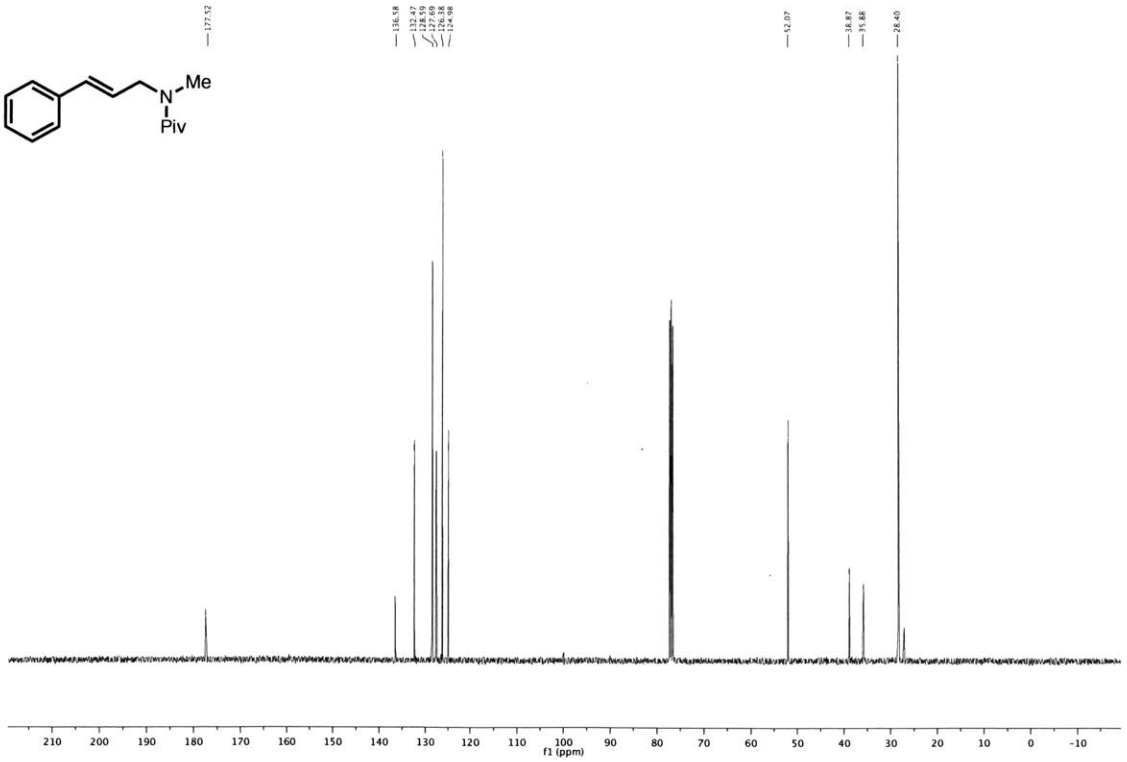

(*E*)-*N*-(4-methoxybenzyl)-*N*-methyl-3-phenylprop-2-en-1-amine (1s)

^{1}H NMR, 400 MHz, $CDCl_3$

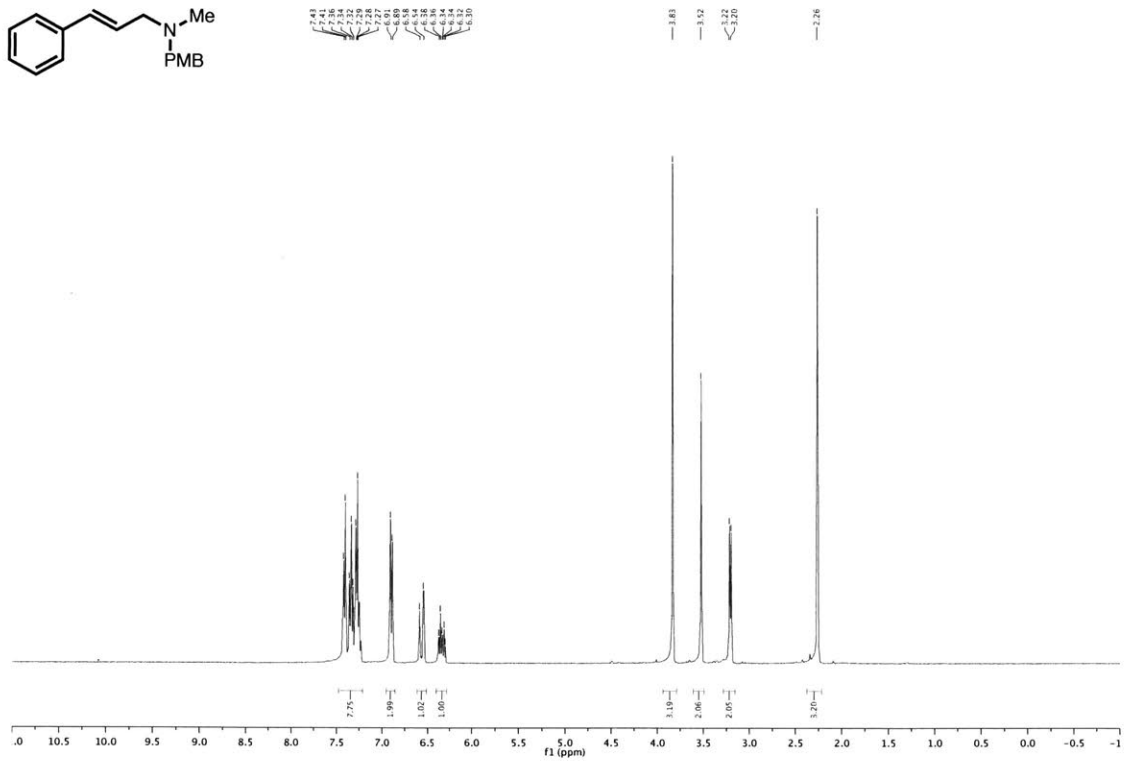

^{13}C NMR, 101 MHz, $CDCl_3$

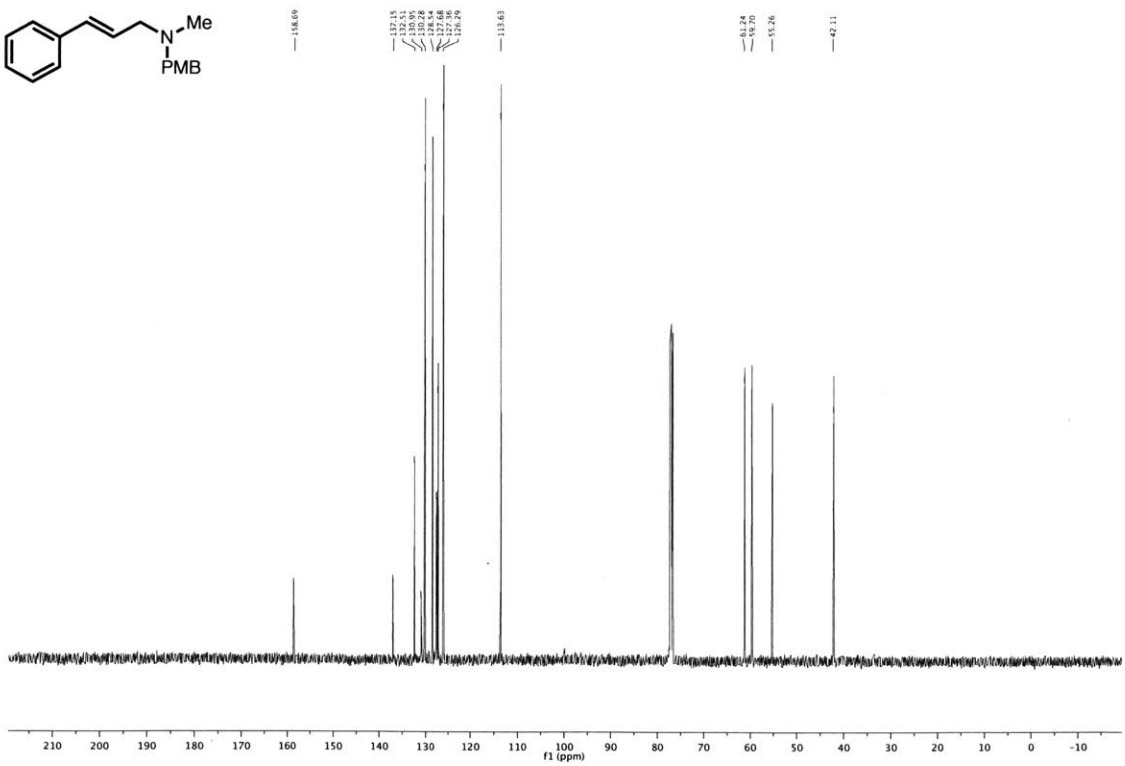

1-allyl-2-fluoro-4-methoxybenzene (1v)

^{1}H NMR, 400 MHz, $CDCl_3$

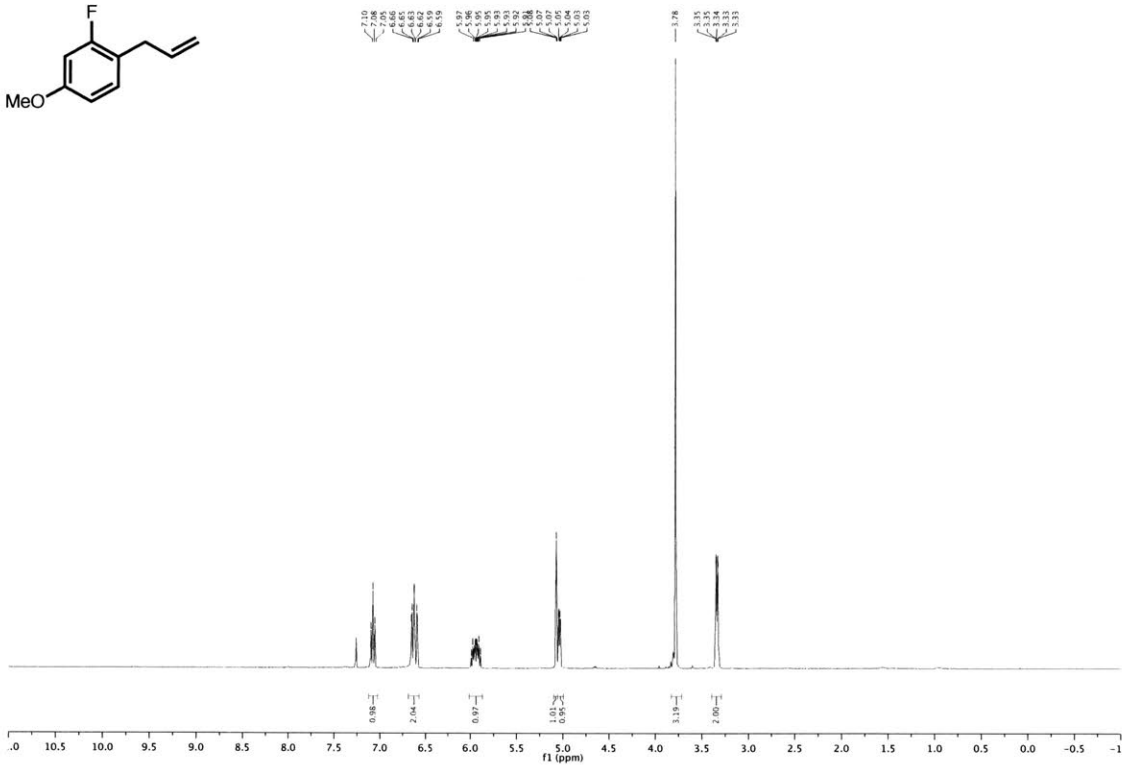

^{13}C NMR, 101 MHz, $CDCl_3$

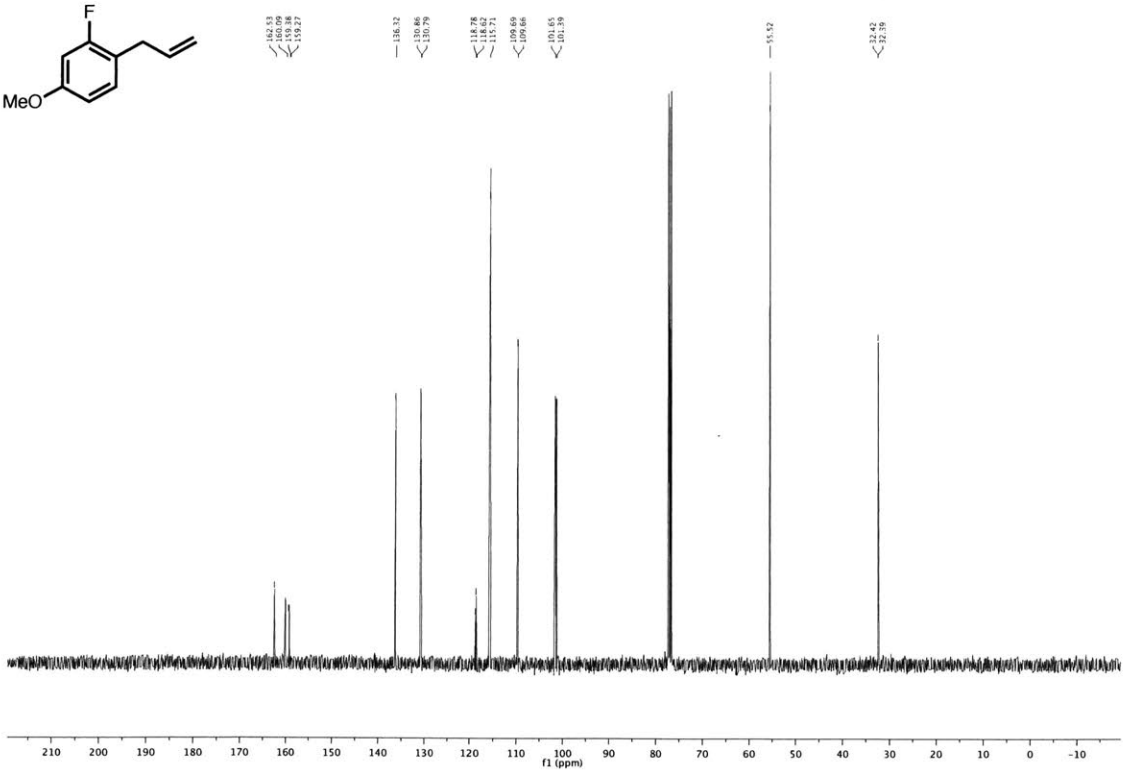

^{19}F NMR, 376 MHz, $CDCl_3$

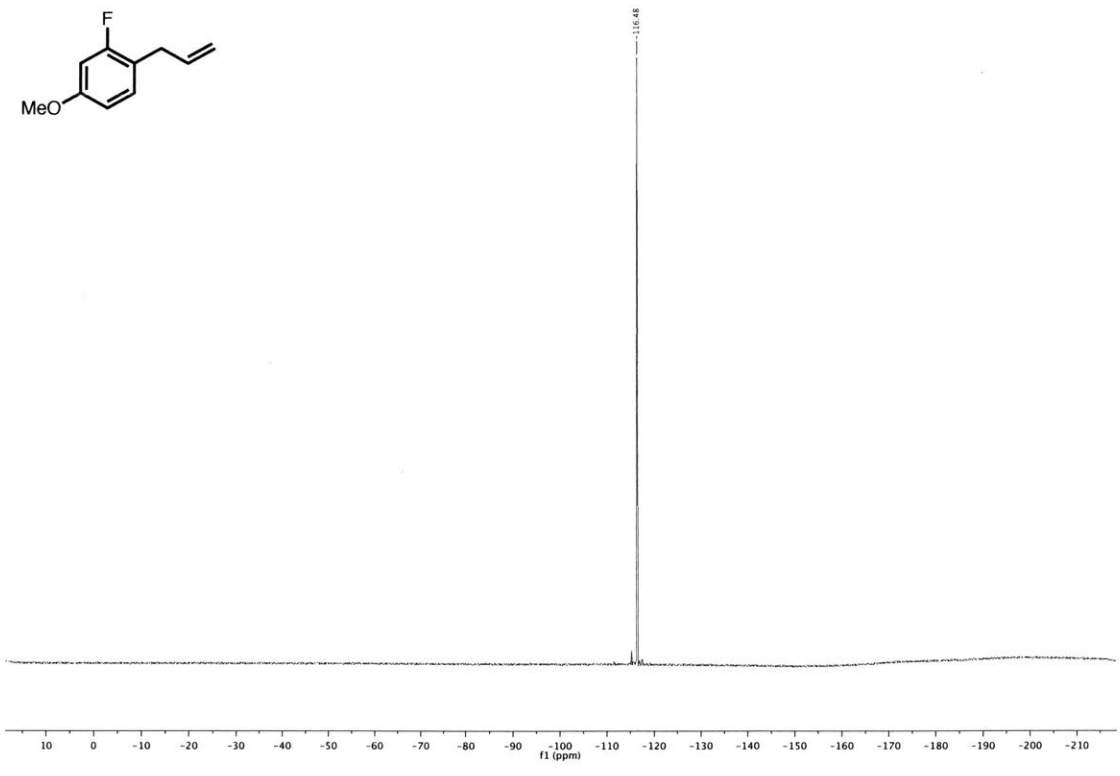
F
MeO
-116.48
10
0
-10
-20
-30
-40
-50
-60
-70
-80
-90
-100
-110
-120
-130
-140
-150
-160
-170
-180
-190
-200
-210
f1 (ppm)

Copies of Chiral SFC/HPLC Traces

(*S*)-1-(1-phenylethyl)-1*H*-indole (3a)

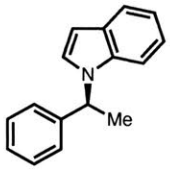

Racemic **3a**:

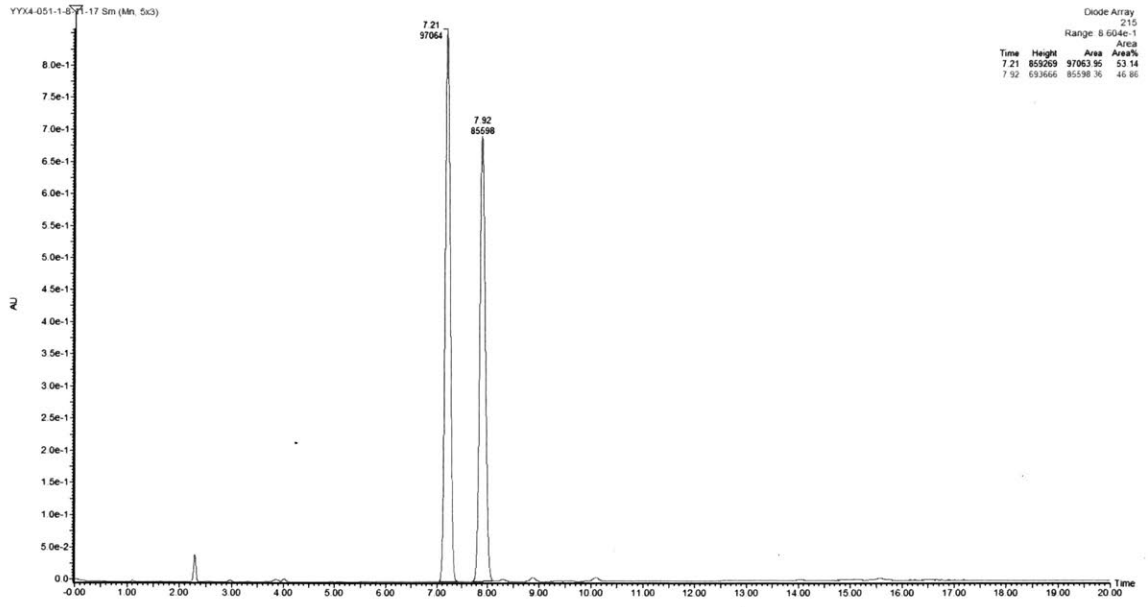

Enantioenriched **3a**:

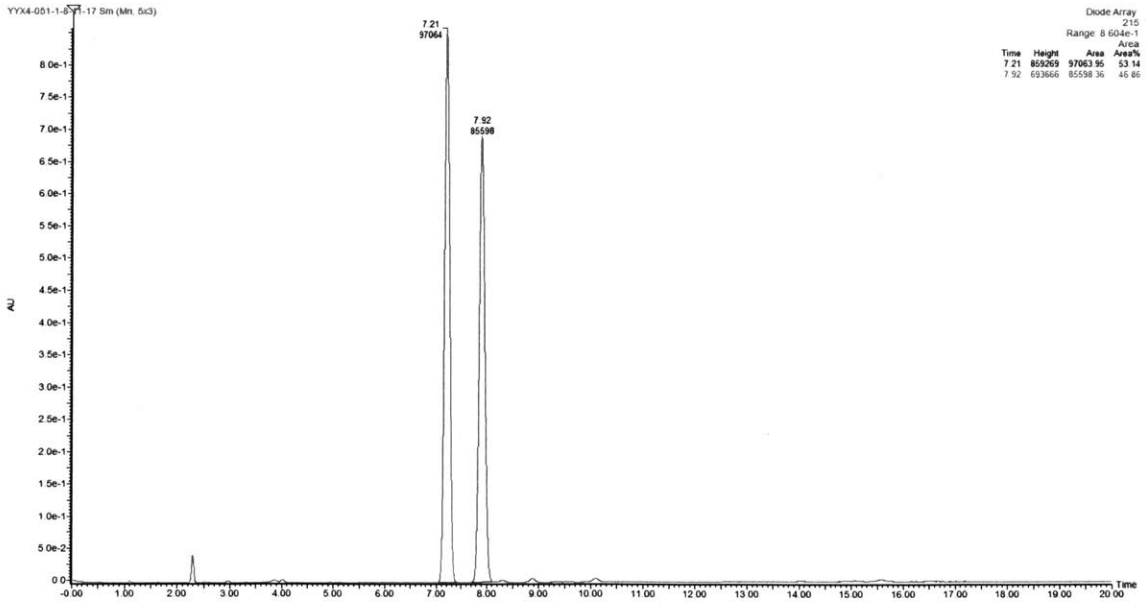

(*S*)-1-(1-(*o*-tolyl)ethyl)-1*H*-indole (3b)

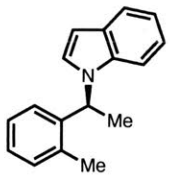

Racemic **3b**:

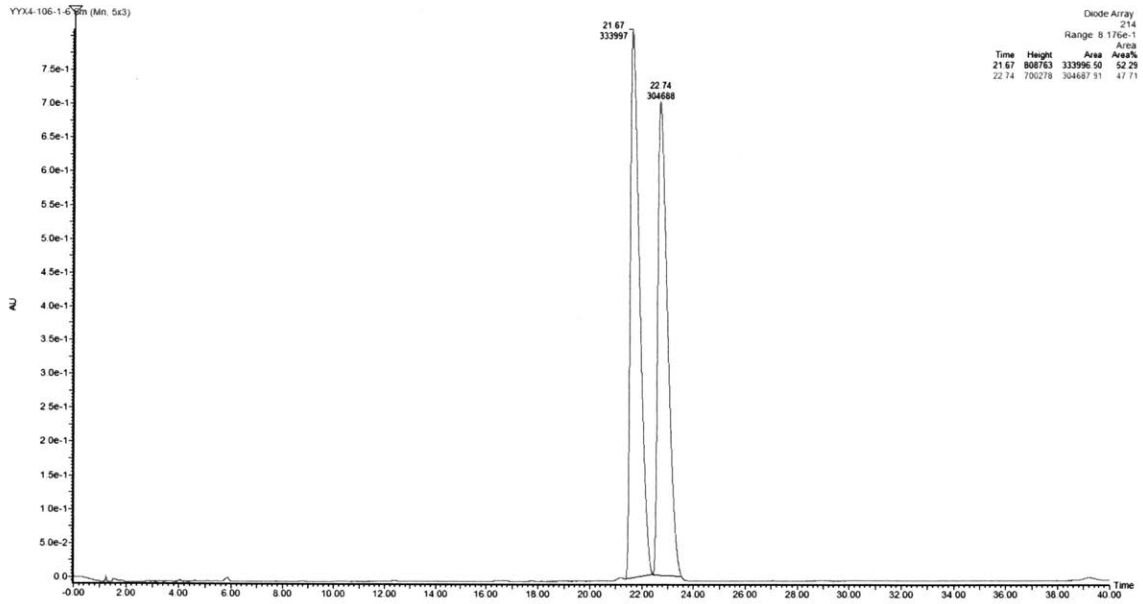

Enantioenriched **3b**:

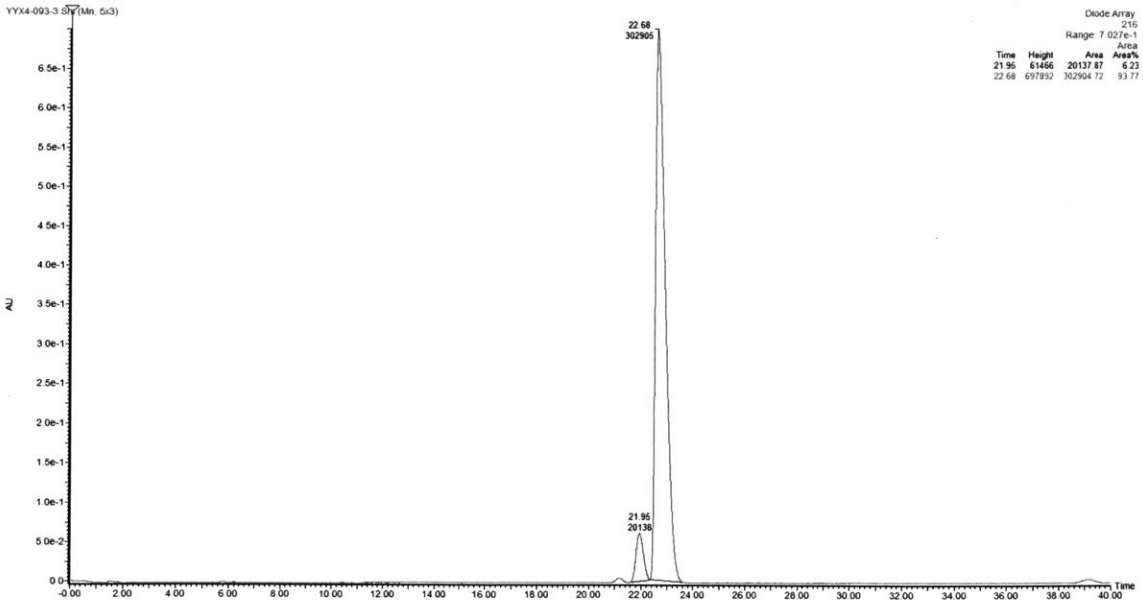

(*S*)-1-(1-(3-methoxyphenyl)ethyl)-1*H*-indole (3c)

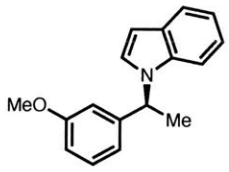

Racemic **3c**:

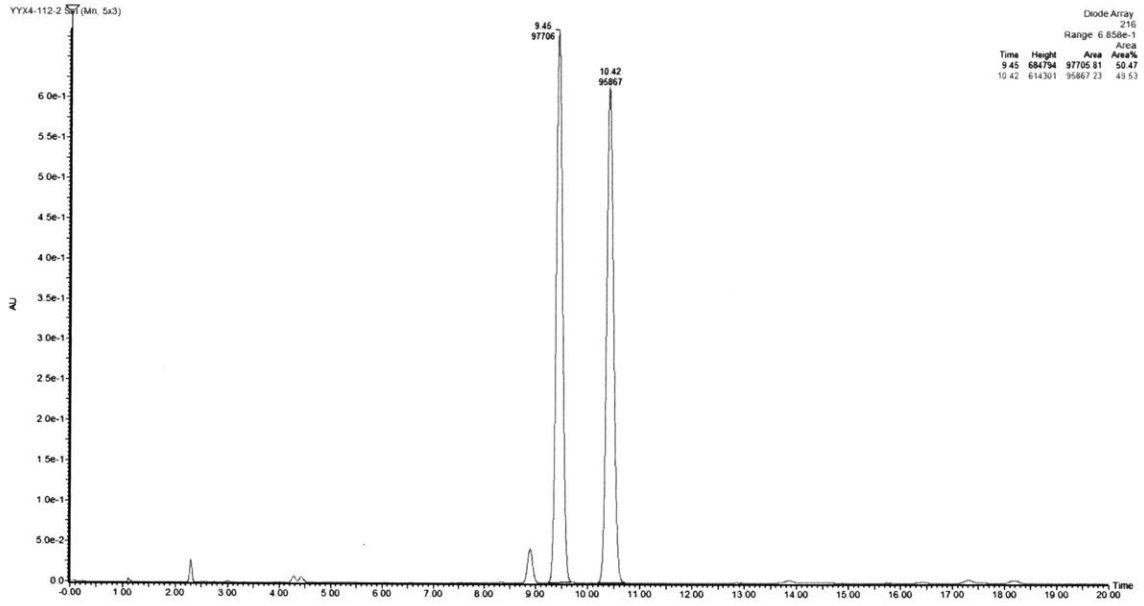

Enantioenriched **3c**:

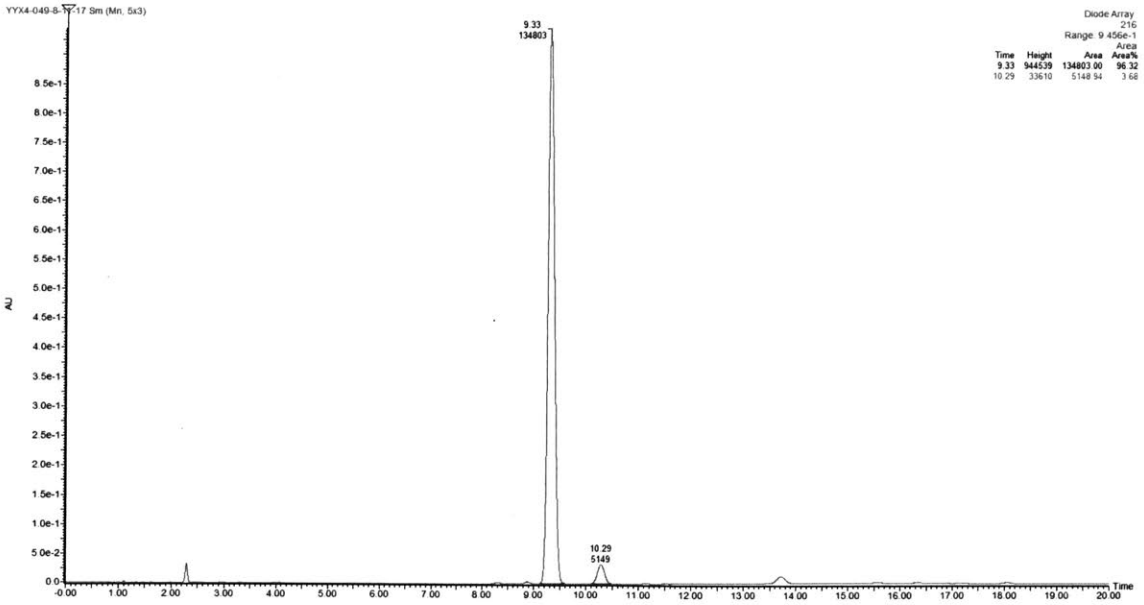

(*S*)-1-(1-(4-fluorophenyl)ethyl)-1*H*-indole (3e)

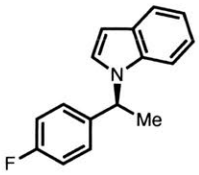

Racemic **3e**:

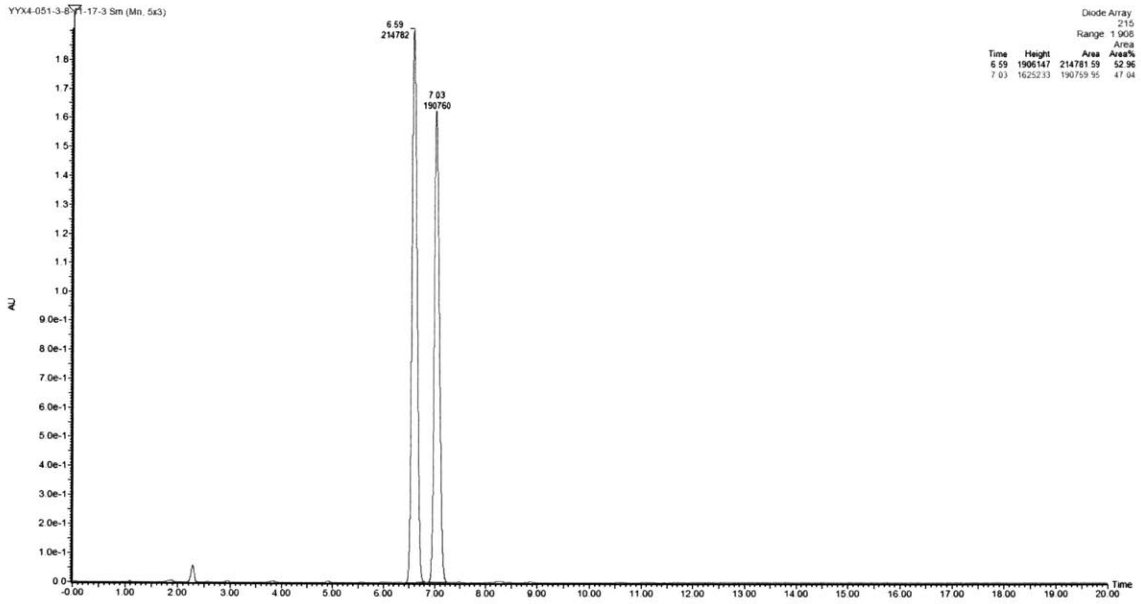

Enantioenriched **3e**:

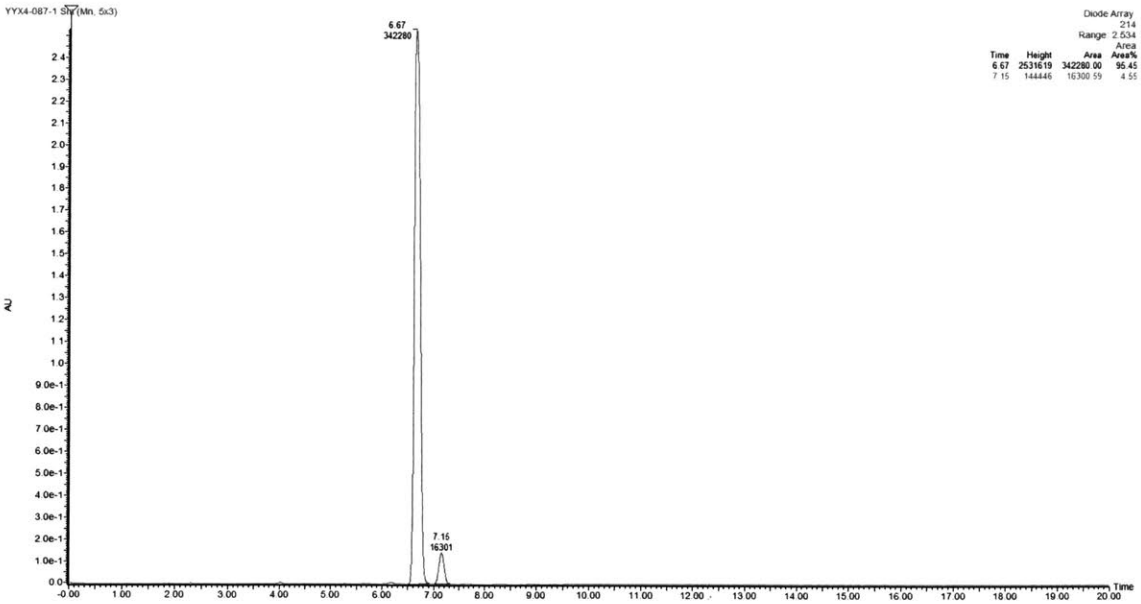

(*S*)-5-(1-(1*H*-indol-1-yl)ethyl)-1-tosyl-1*H*-indole (3f)

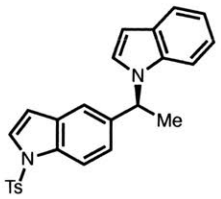

Racemic **3f**:

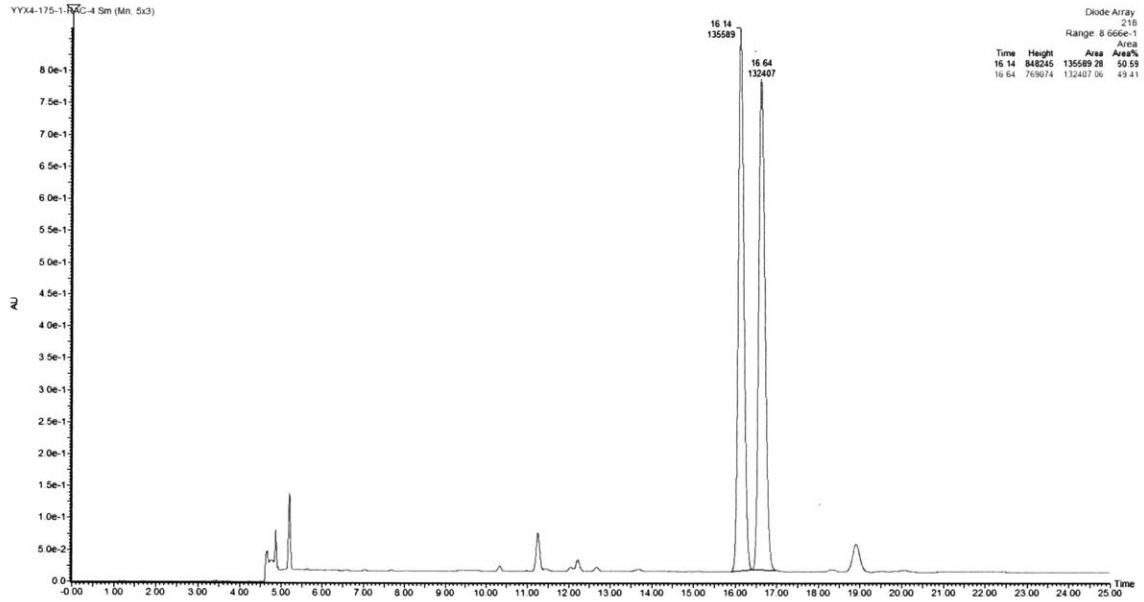

Enantioenriched **3f**:

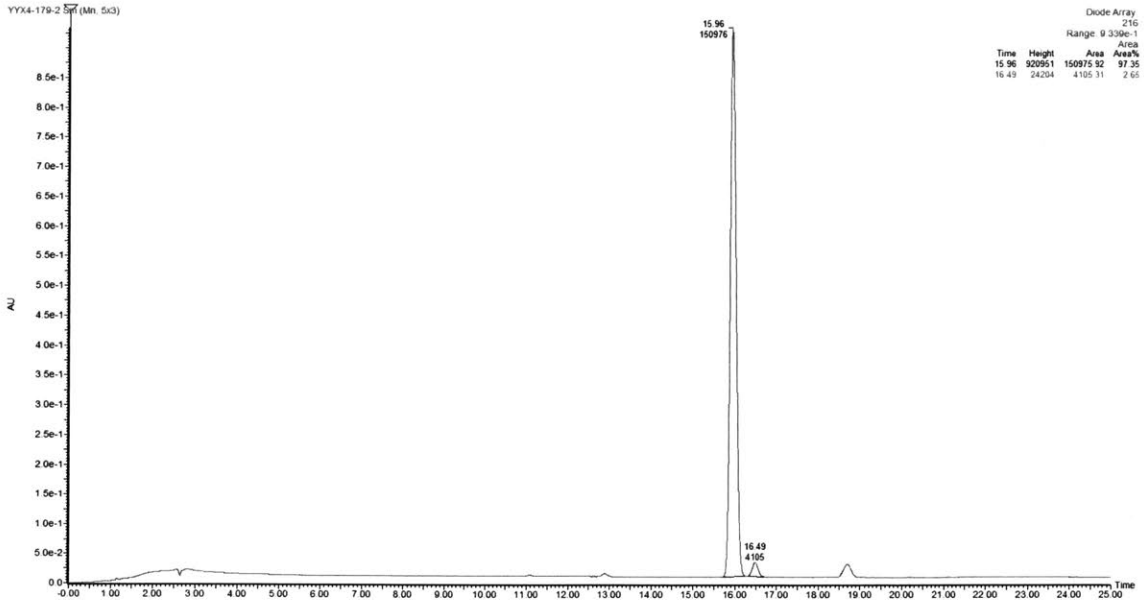

tert-butyl (*S*)-4-(1*H*-indol-1-yl)-4-phenylbutanoate (3g)

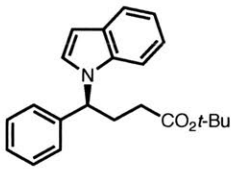

Racemic **3g**:

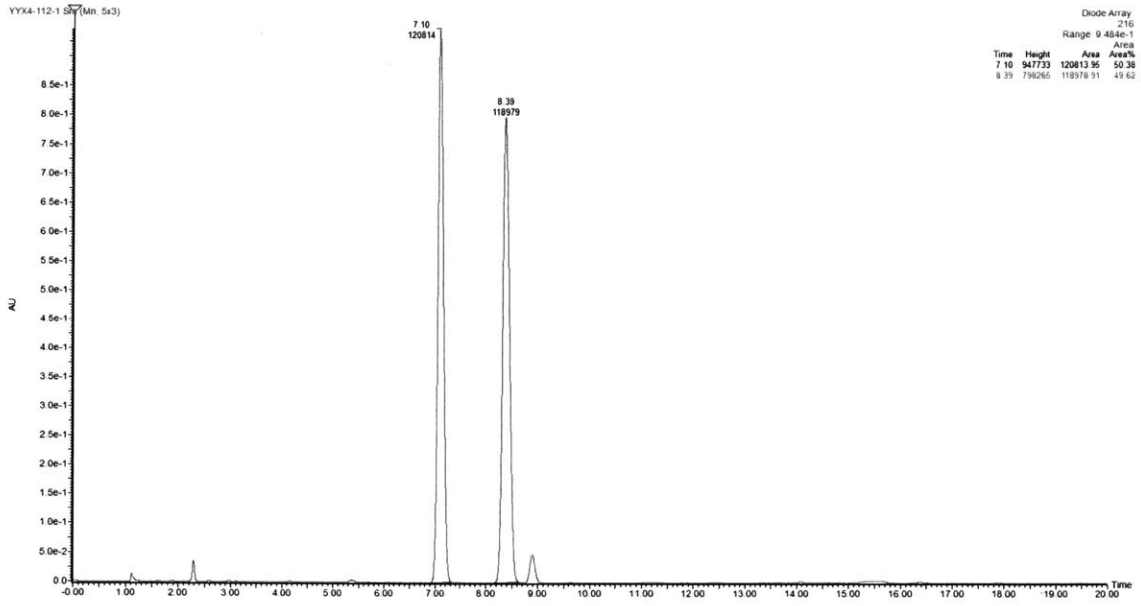

Enantioenriched **3g**:

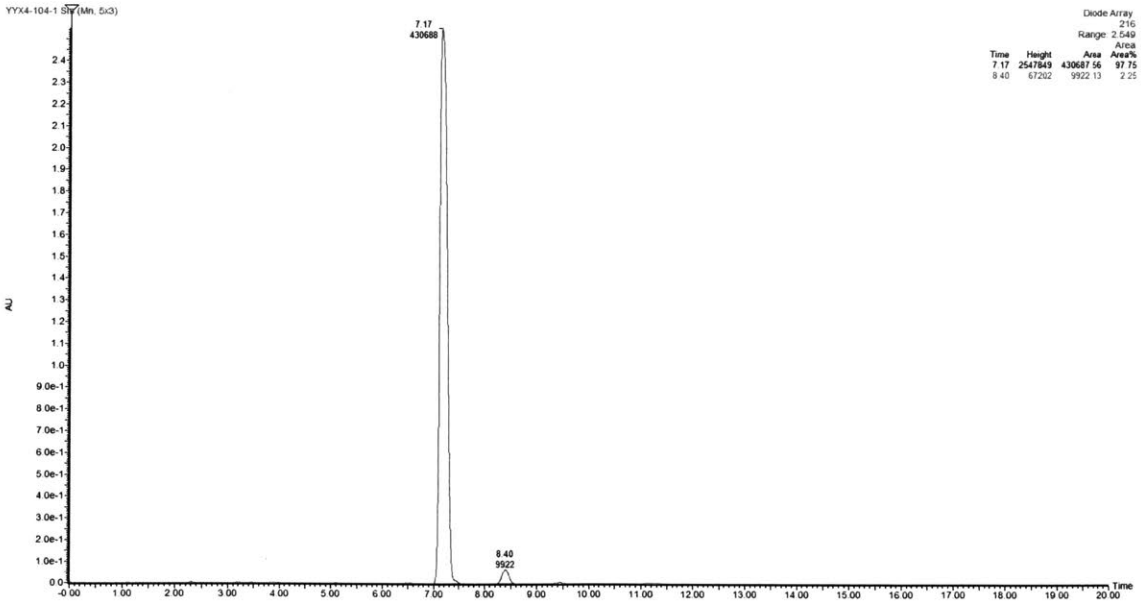

(*S*)-*N*-(3-(1*H*-indol-1-yl)-3-phenylpropyl)-*N*-methylpivalamide (3h)

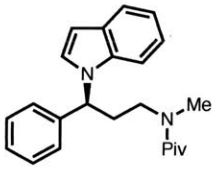

Racemic **3h**:

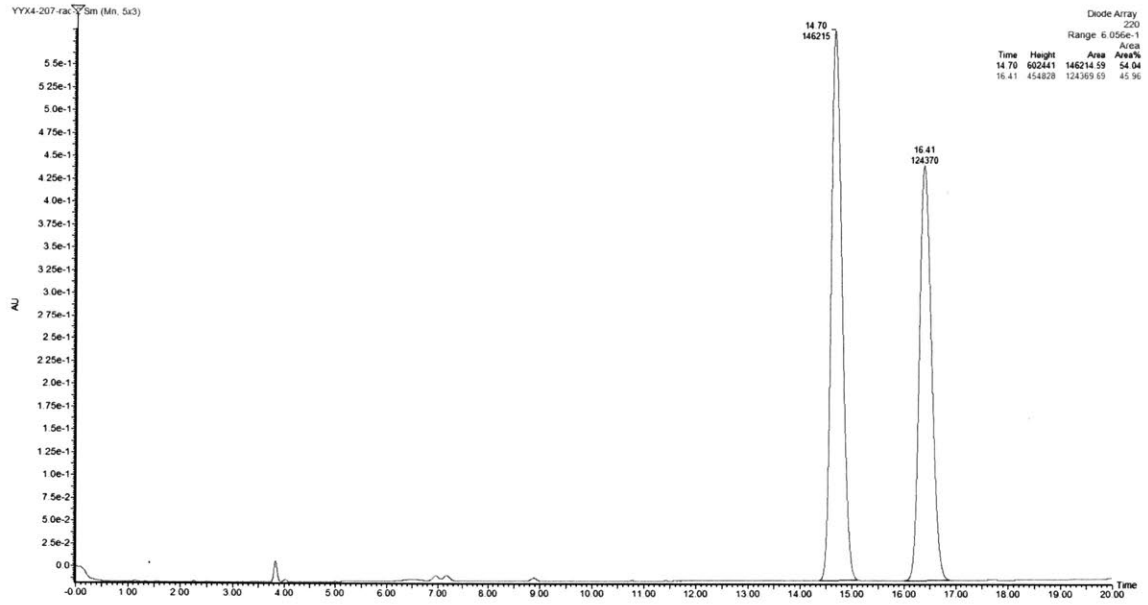

Enantioenriched **3h**:

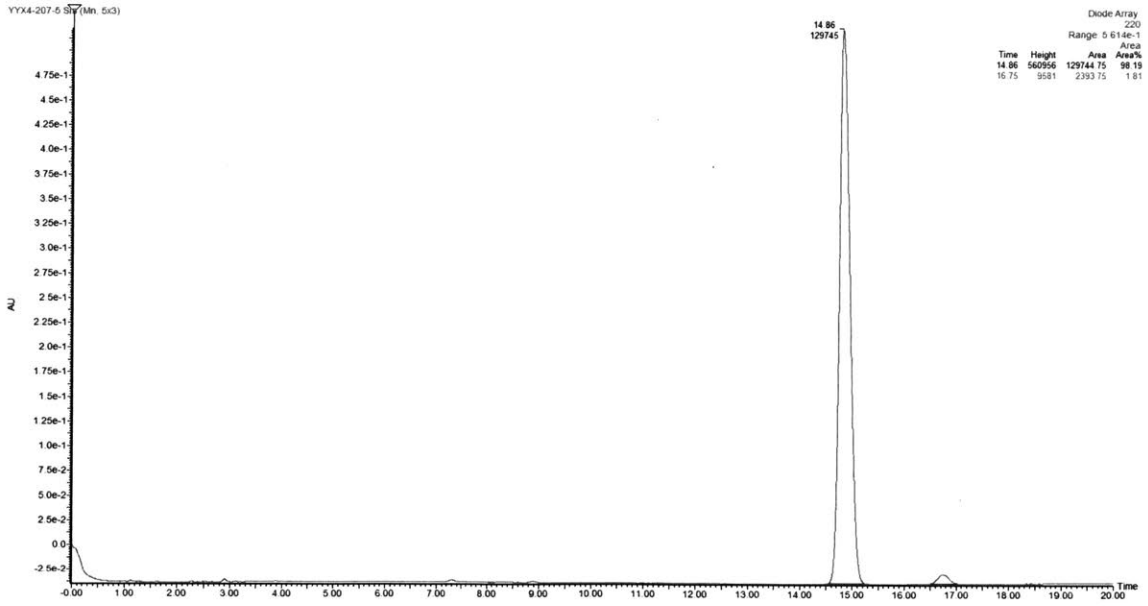

***N*-((2*S*,3*S*)-3-(1*H*-indol-1-yl)-2-methyl-3-phenylpropyl)-*N*,4-dimethylbenzenesulfonamide (3i)**

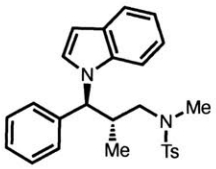

Racemic **3i**:

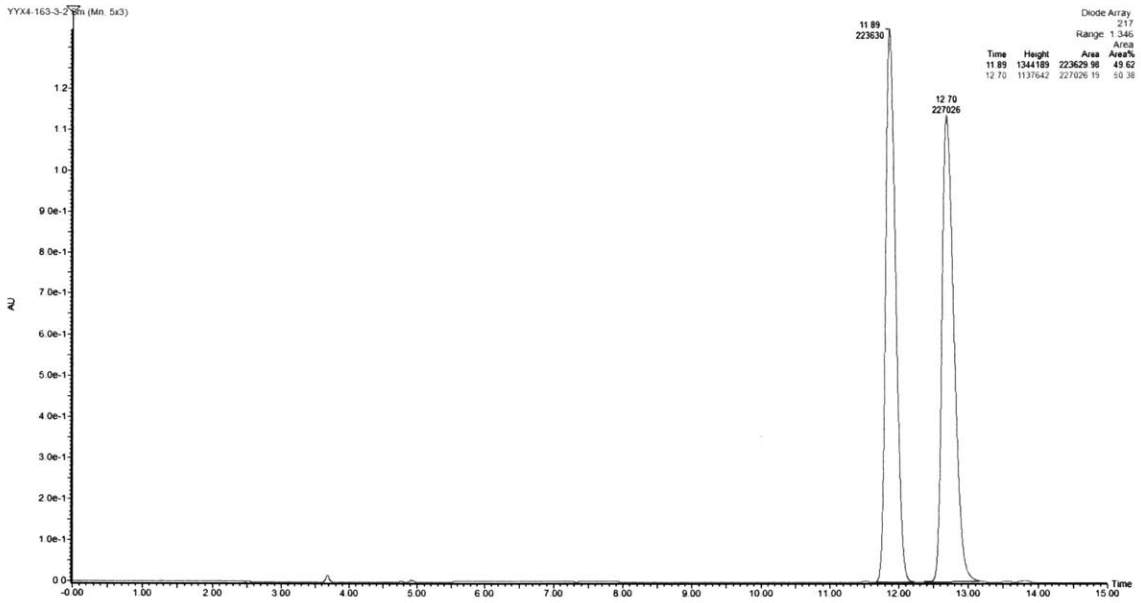

Enantioenriched **3i**:

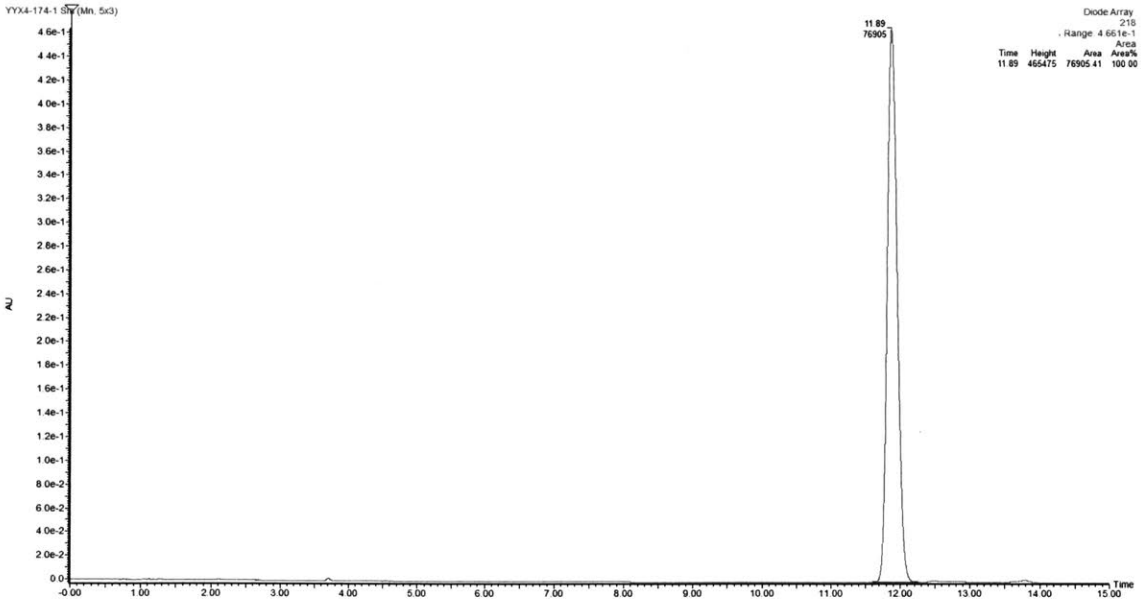

(*S*)-*N*,*N*-diethyl-3-(1-(6-(trifluoromethyl)-1*H*-indol-1-yl)ethyl)benzamide (3m)

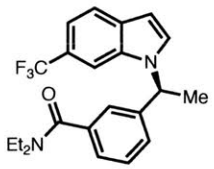

Racemic **3m**:

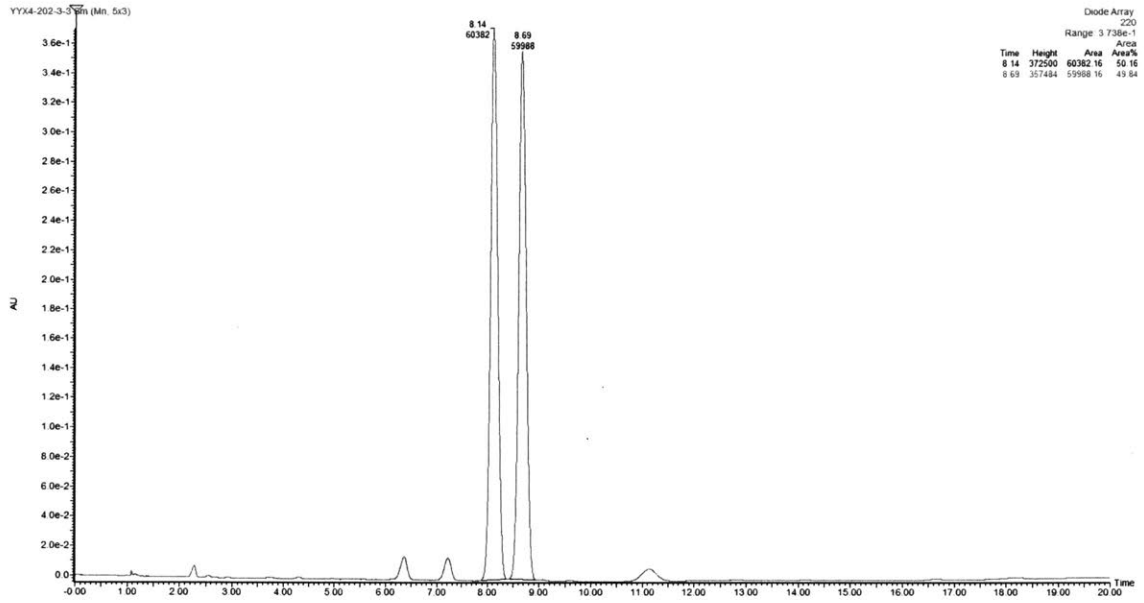

Enantioenriched **3m**:

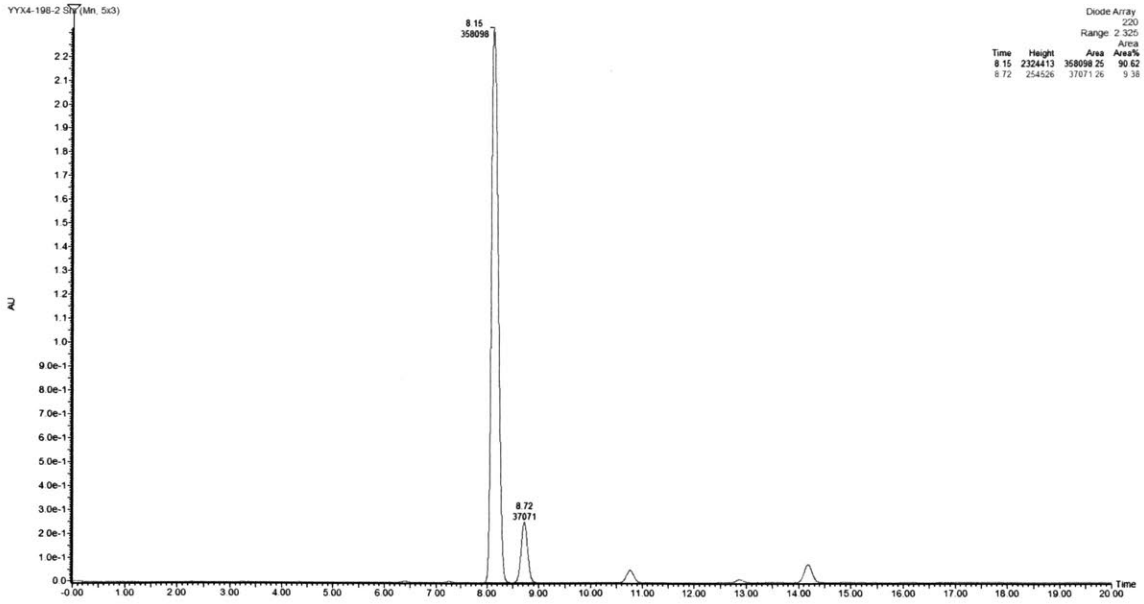

tert-butyl (*S*)-1-(1-(2-(difluoromethoxy)phenyl)ethyl)-1*H*-indole-4-carboxylate (3n)

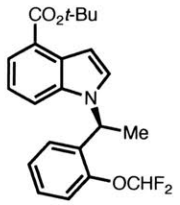

Racemic **3n**:

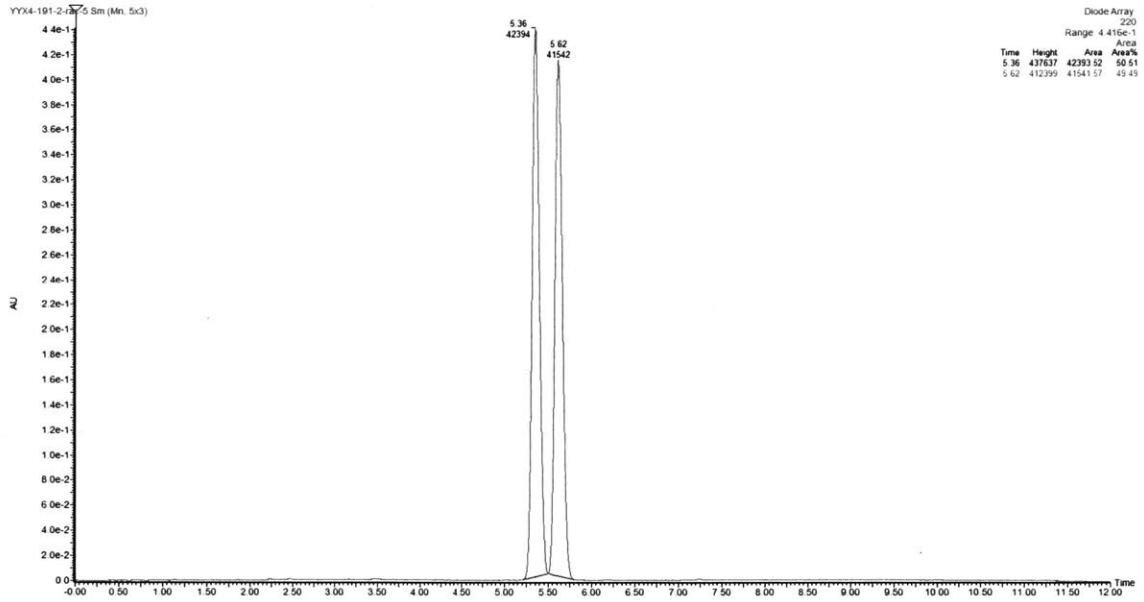

Enantioenriched **3n**:

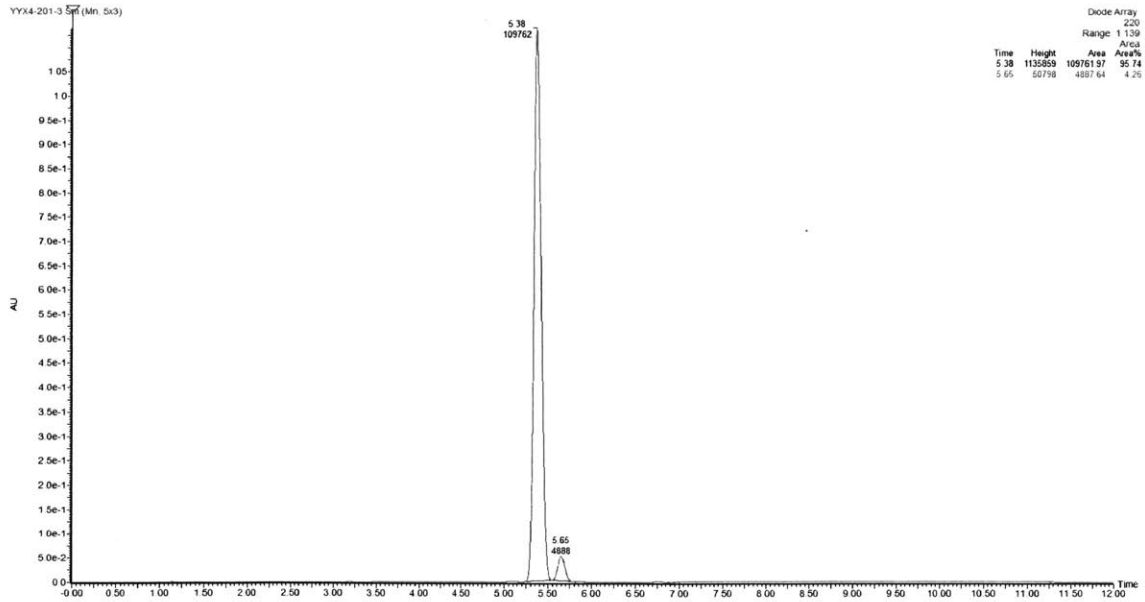

(*S*)-1-(1-(3-chlorophenyl)ethyl)-2-methyl-1*H*-indole (3r)

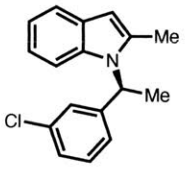

Racemic **3r**:

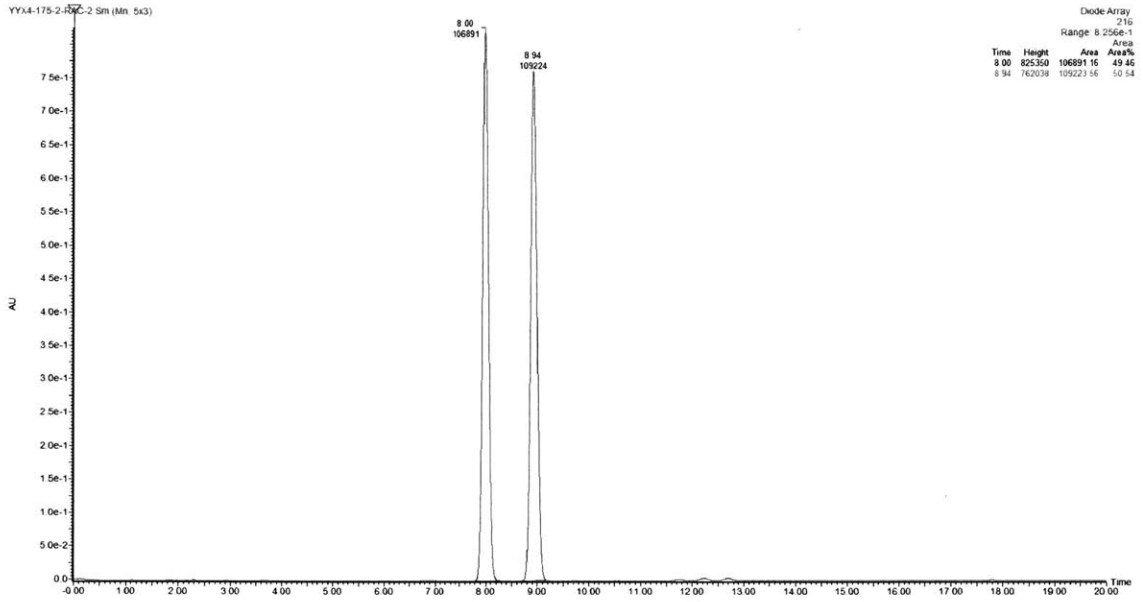

Enantioenriched **3r**:

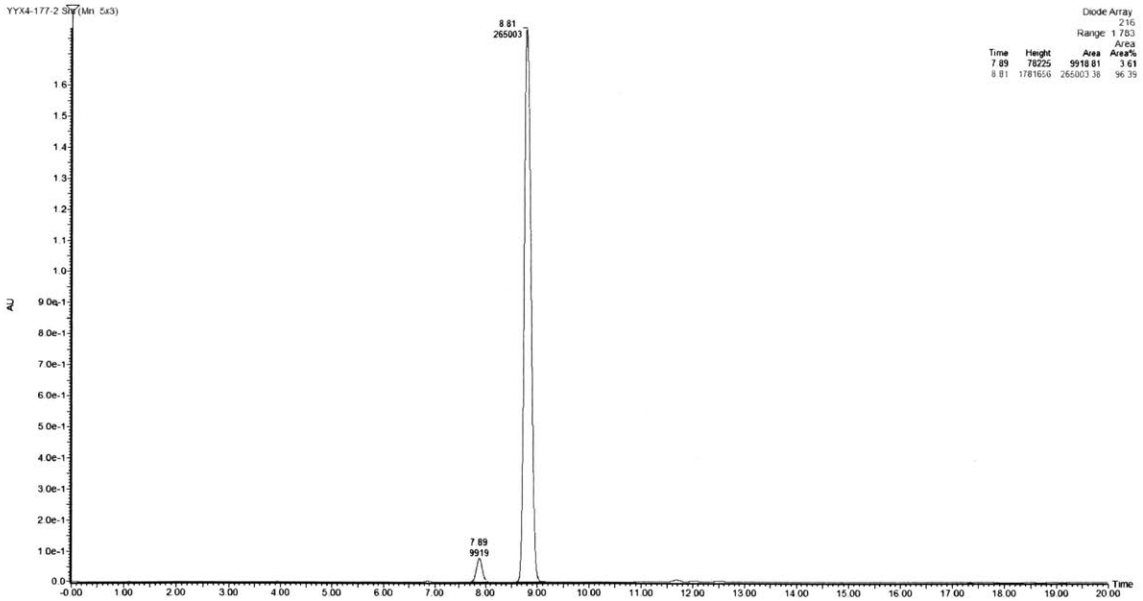

methyl (*S*)-1-(1-phenylethyl)-1*H*-indole-2-carboxylate (3q)

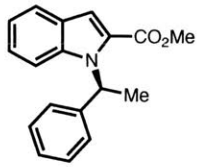

Racemic **3q**:

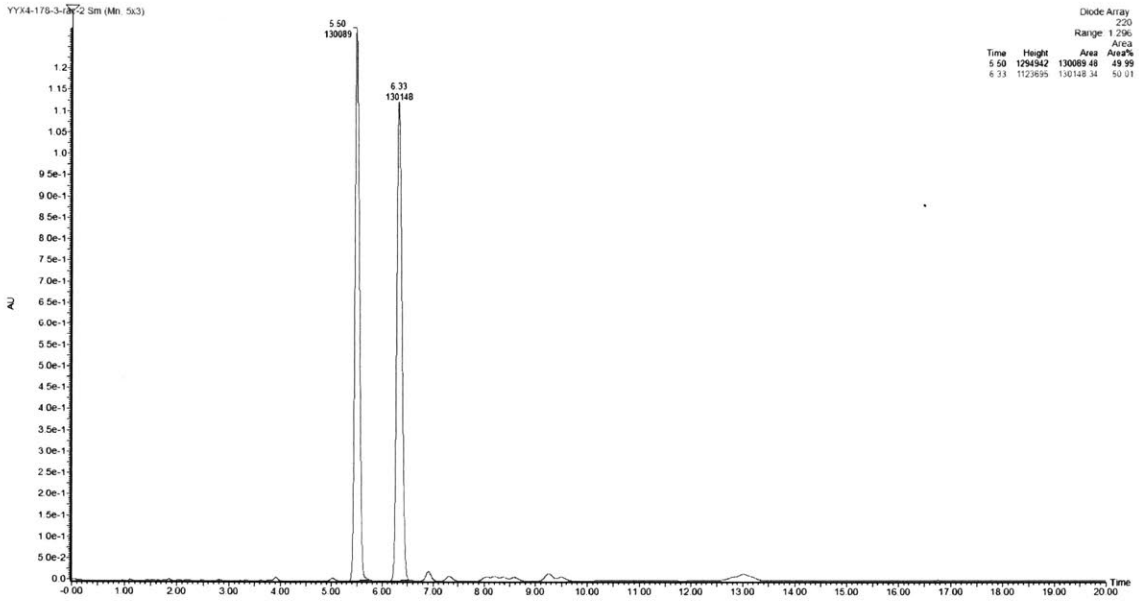

Enantioenriched **3q**:

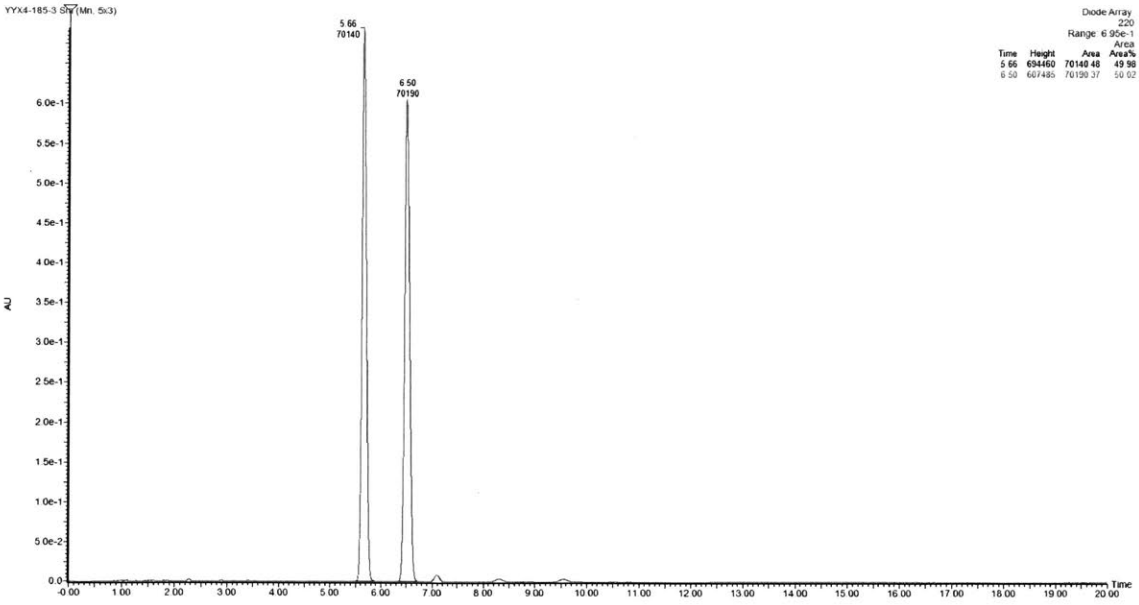

(*S*)-3-(2-methoxyethyl)-1-(1-(4-(trifluoromethyl)phenyl)ethyl)-1*H*-indole (3s)

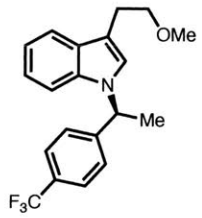

Racemic **3s**:

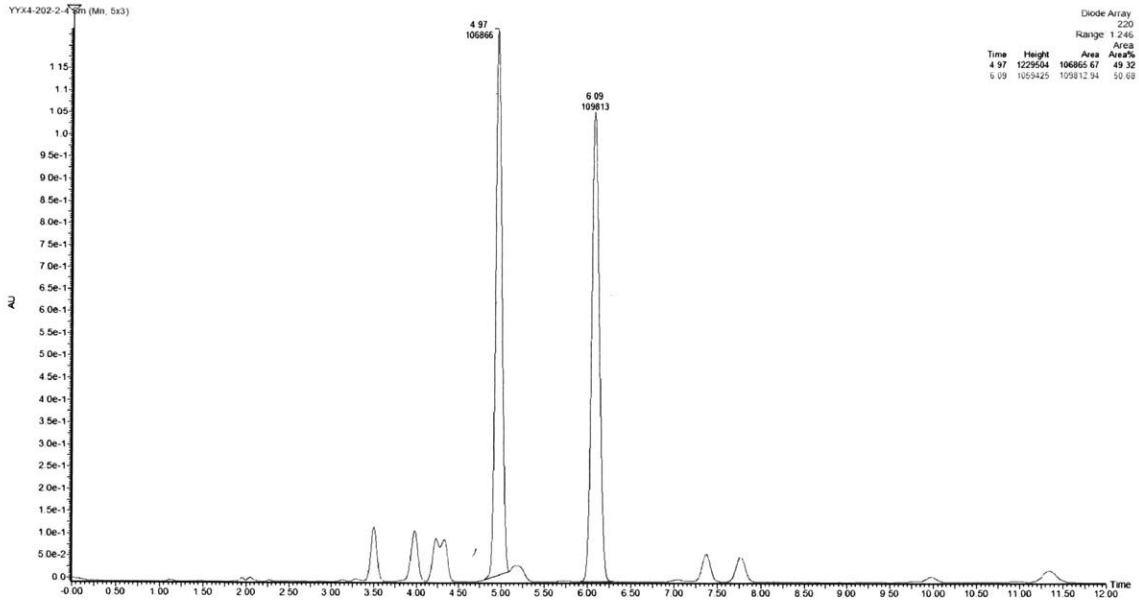

Enantioenriched **3s**:

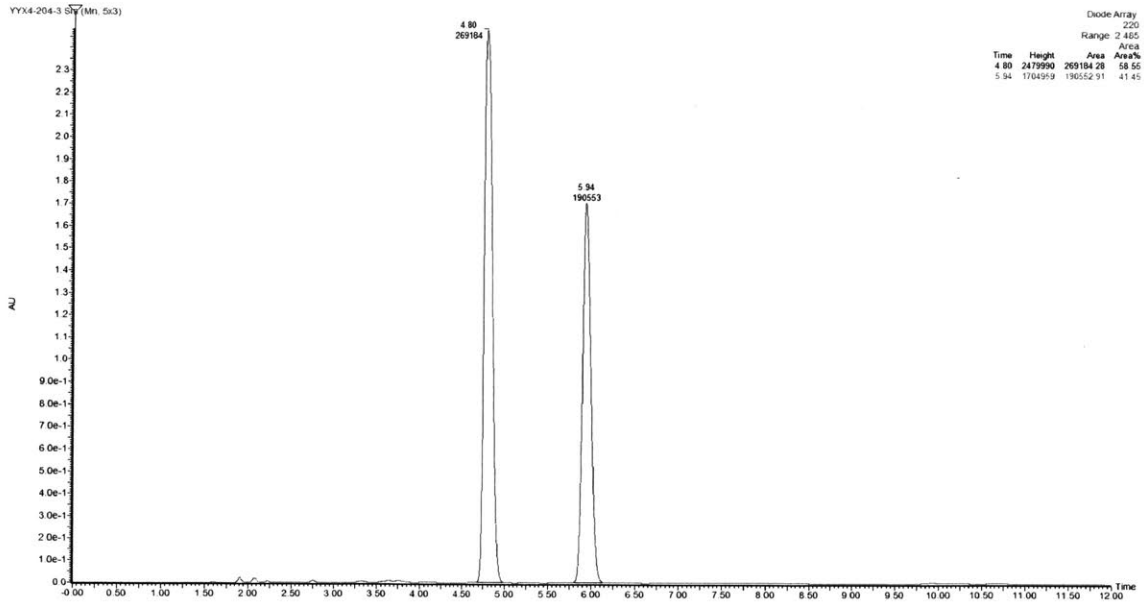

(*S*)-3-(1-phenylethyl)-1*H*-indole (4a)

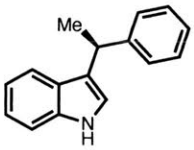

Racemic **4a**:

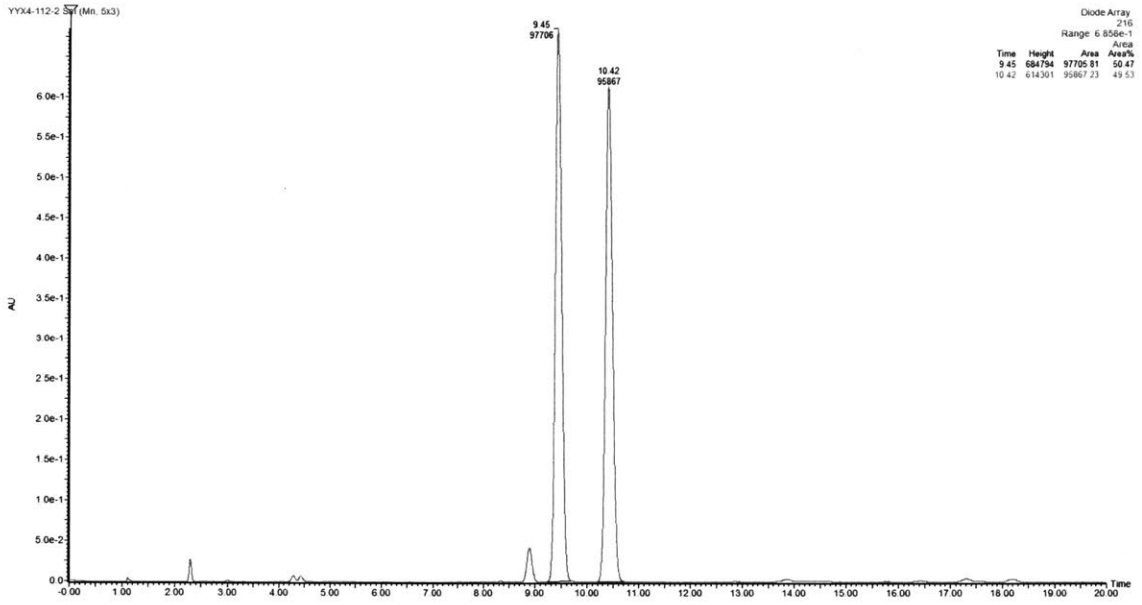

Enantioenriched **4a**:

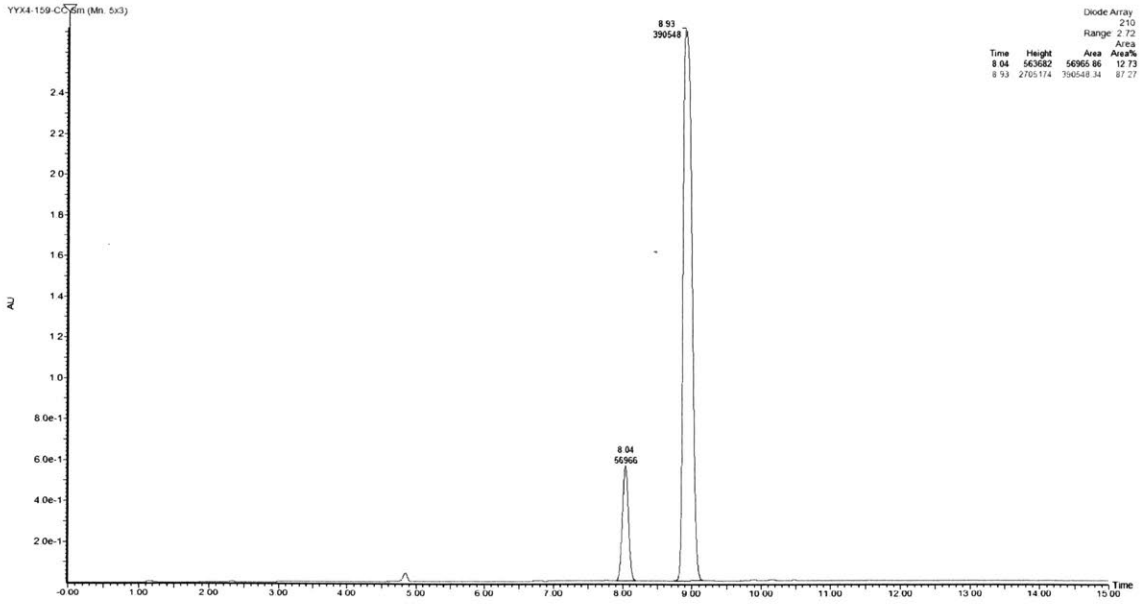

(*S*)-3-(1-(4-(trifluoromethyl)phenyl)ethyl)-1*H*-indole (4b)

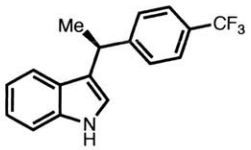

Racemic **4b**:

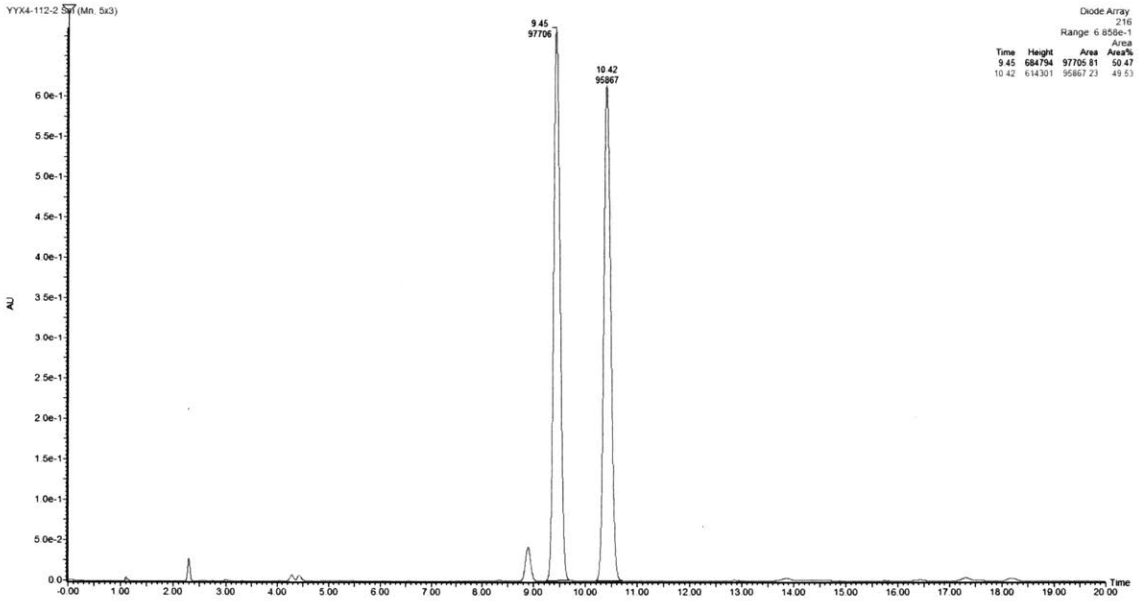

Enantioenriched **4b**:

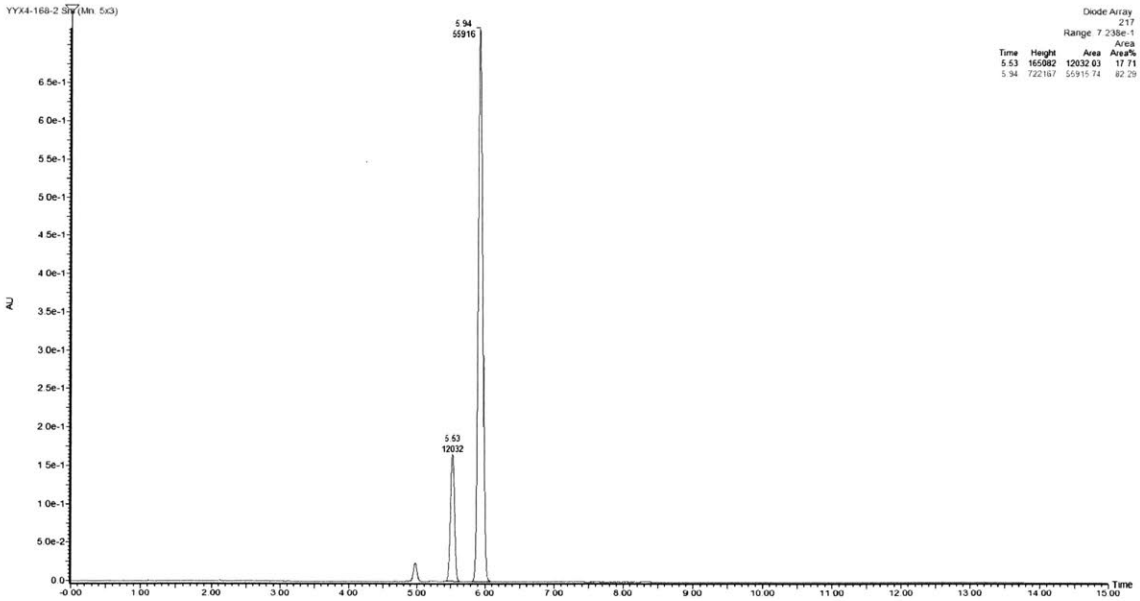

(*S*)-5-(1-(1*H*-indol-3-yl)ethyl)-1-tosyl-1*H*-indole (4c)

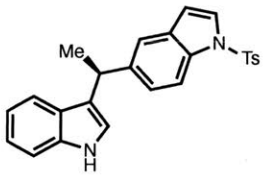

Racemic **4c**:

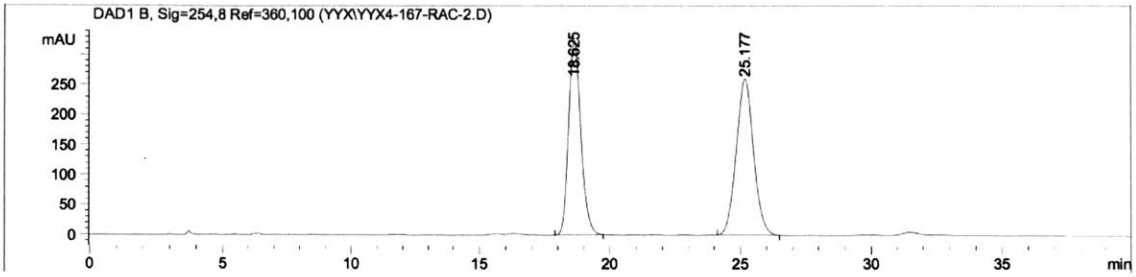

Signal 2: DAD1 B, Sig=254,8 Ref=360,100

Peak #	RetTime [min]	Type	Width [min]	Area [mAU*s]	Height [mAU]	Area %
1	18.625	BB	0.5069	1.06768e4	323.62393	46.8453
2	25.177	BB	0.7078	1.21148e4	260.86627	53.1547
Totals :				2.27916e4	584.49020	

Enantioenriched **4c**:

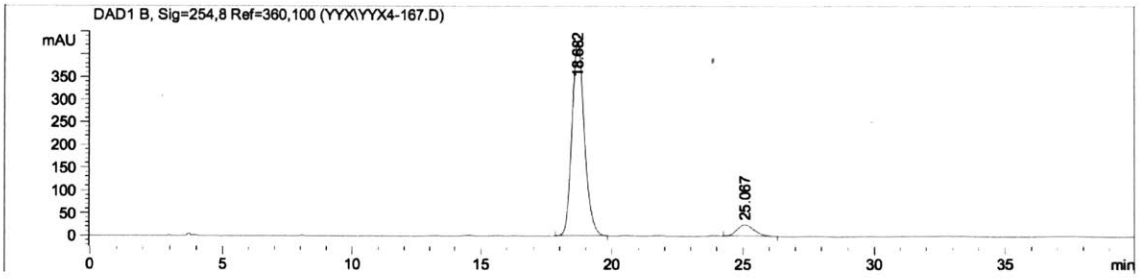

Signal 2: DAD1 B, Sig=254,8 Ref=360,100

Peak #	RetTime [min]	Type	Width [min]	Area [mAU*s]	Height [mAU]	Area %
1	18.682	BB	0.5071	1.42265e4	428.78229	92.3972
2	25.067	BB	0.6924	1170.61060	25.27245	7.6028
Totals :				1.53971e4	454.05474	

(*S*)-3-(1*H*-indol-3-yl)-*N*-(4-methoxybenzyl)-*N*-methyl-3-phenylpropan-1-amine (4d)

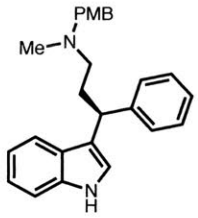

Racemic **4d**:

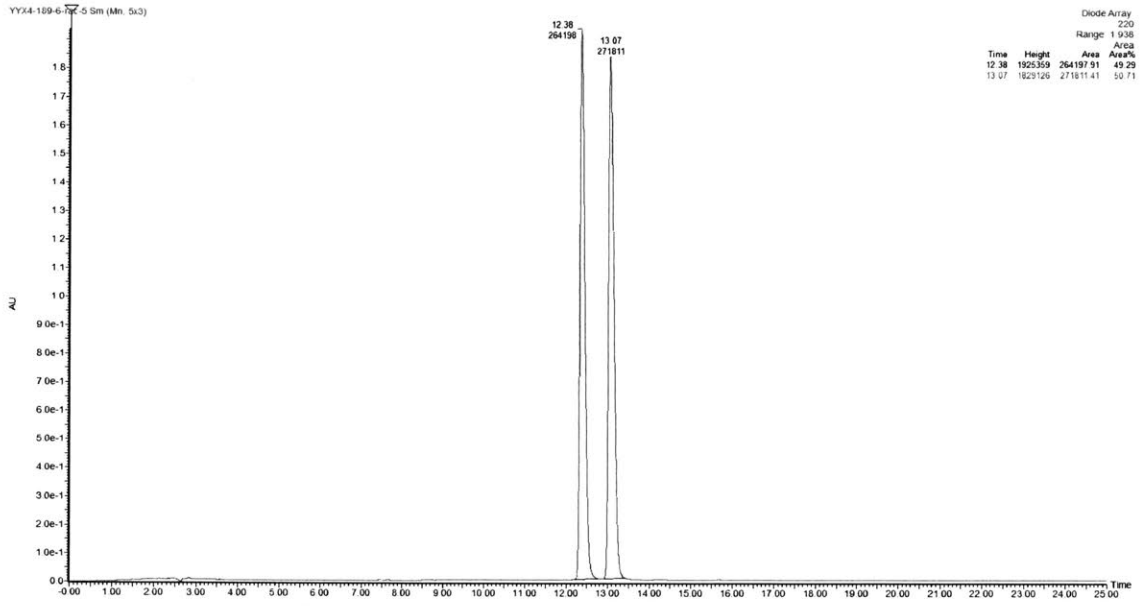

Enantioenriched **4d**:

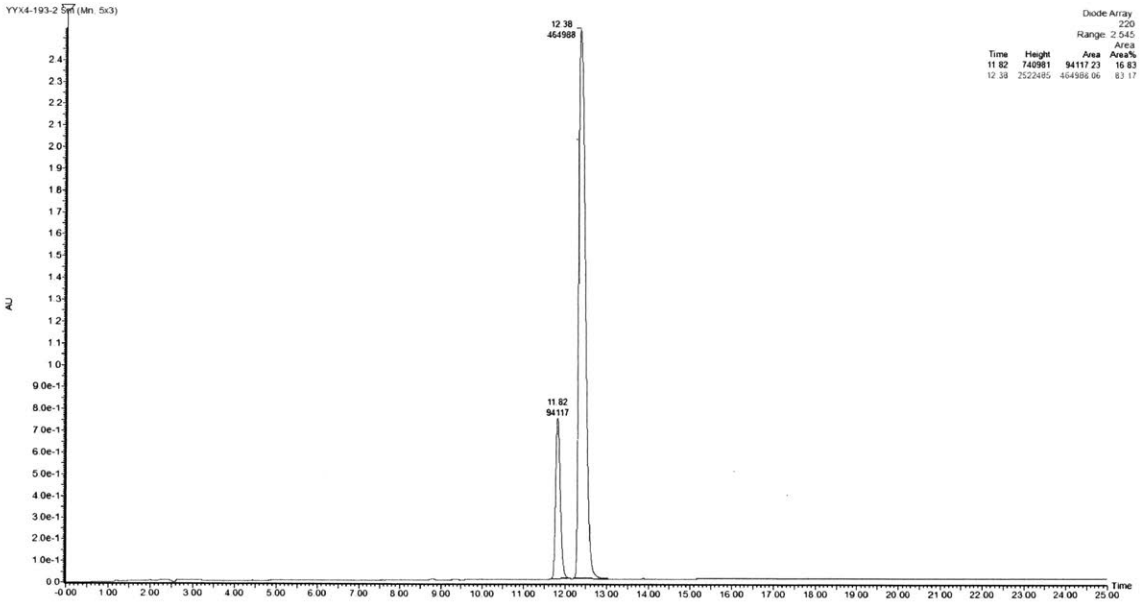

3-((*S*)-1-((8*R*,9*S*,13*S*,14*S*)-13-methyl-6,7,8,9,11,12,13,14,15,16-decahydrospiro[cyclopenta[*a*]phenanthrene-17,2'-[1,3]dioxolan]-2-yl)ethyl)-1*H*-indole (4e)

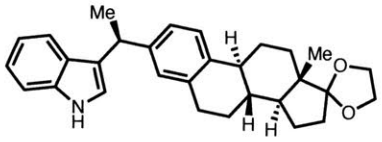

Racemic **4e**:

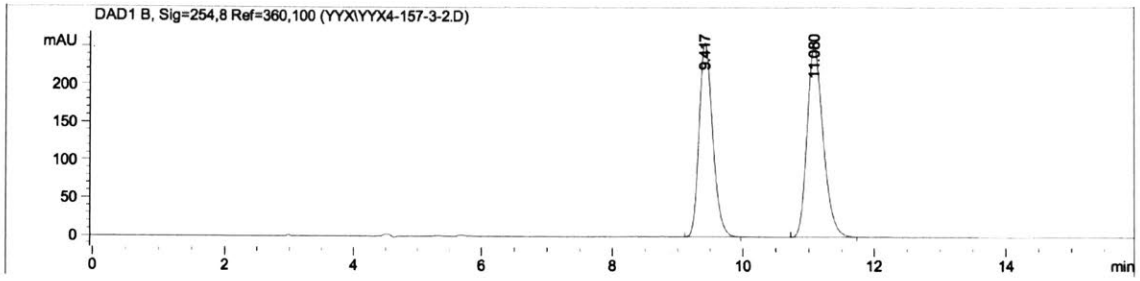

Signal 2: DAD1 B, Sig=254,8 Ref=360,100

Peak #	RetTime [min]	Type	Width [min]	Area [mAU*s]	Height [mAU]	Area %
1	9.417	BB	0.2239	3733.23340	256.35168	46.5545
2	11.080	BB	0.2635	4285.81982	250.66071	53.4455
Totals :				8019.05322	507.01239	

Enantioenriched **4e**:

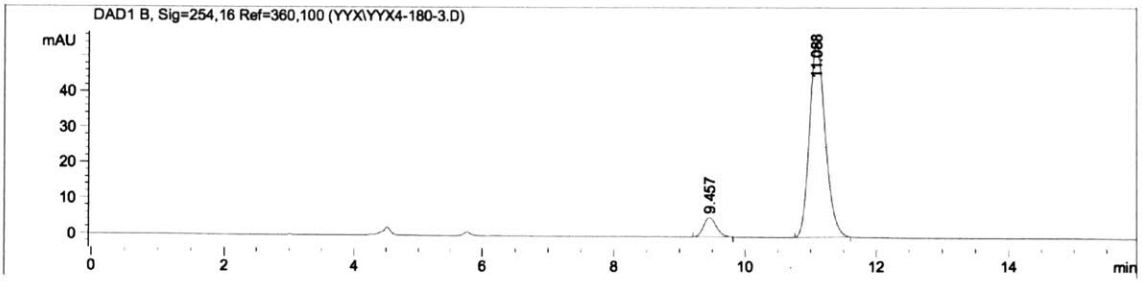

Signal 2: DAD1 B, Sig=254,16 Ref=360,100

Peak #	RetTime [min]	Type	Width [min]	Area [mAU*s]	Height [mAU]	Area %
1	9.457	BB	0.2123	77.20403	5.55072	7.7726
2	11.088	BB	0.2566	916.08411	54.91712	92.2274

Instrument 1 4/12/2018 3:11:02 PM KED Page 2 of 3